THE NATIONAL ACADEMIES PRESS

Reference Guide for Applying Risk and Reliability-Based Approaches for Bridge Scour Prediction

BUY THIS BOOK

FIND RELATED TITLES

AUTHORS

Lagasse, Peter F.; Ghosn, Michel; Johnson, Peggy A.; Zevenbergen, Lyle W.; Clopper, Paul E.

NATIONAL COOPERATIVE HIGHWAY RESEARCH PROGRAM

NCHRP REPORT 761

Reference Guide for Applying Risk and Reliability-Based Approaches for Bridge Scour Prediction

Peter F. Lagasse
AYRES ASSOCIATES
Fort Collins, CO

Michel Ghosn
CCNY/CUNY
New York, NY

Peggy A. Johnson
PENNSYLVANIA STATE UNIVERSITY
University Park, PA

Lyle W. Zevenbergen
AYRES ASSOCIATES
Fort Collins, CO

Paul E. Clopper
AYRES ASSOCIATES
Fort Collins, CO

Subscriber Categories
Bridges and Other Structures • Hydraulics and Hydrology

TRANSPORTATION RESEARCH BOARD

WASHINGTON, D.C.
2013
www.TRB.org

NATIONAL COOPERATIVE HIGHWAY RESEARCH PROGRAM

Systematic, well-designed research provides the most effective approach to the solution of many problems facing highway administrators and engineers. Often, highway problems are of local interest and can best be studied by highway departments individually or in cooperation with their state universities and others. However, the accelerating growth of highway transportation develops increasingly complex problems of wide interest to highway authorities. These problems are best studied through a coordinated program of cooperative research.

In recognition of these needs, the highway administrators of the American Association of State Highway and Transportation Officials initiated in 1962 an objective national highway research program employing modern scientific techniques. This program is supported on a continuing basis by funds from participating member states of the Association and it receives the full cooperation and support of the Federal Highway Administration, United States Department of Transportation.

The Transportation Research Board of the National Academies was requested by the Association to administer the research program because of the Board's recognized objectivity and understanding of modern research practices. The Board is uniquely suited for this purpose as it maintains an extensive committee structure from which authorities on any highway transportation subject may be drawn; it possesses avenues of communications and cooperation with federal, state and local governmental agencies, universities, and industry; its relationship to the National Research Council is an insurance of objectivity; it maintains a full-time research correlation staff of specialists in highway transportation matters to bring the findings of research directly to those who are in a position to use them.

The program is developed on the basis of research needs identified by chief administrators of the highway and transportation departments and by committees of AASHTO. Each year, specific areas of research needs to be included in the program are proposed to the National Research Council and the Board by the American Association of State Highway and Transportation Officials. Research projects to fulfill these needs are defined by the Board, and qualified research agencies are selected from those that have submitted proposals. Administration and surveillance of research contracts are the responsibilities of the National Research Council and the Transportation Research Board.

The needs for highway research are many, and the National Cooperative Highway Research Program can make significant contributions to the solution of highway transportation problems of mutual concern to many responsible groups. The program, however, is intended to complement rather than to substitute for or duplicate other highway research programs.

NOTICE

The project that is the subject of this report was a part of the National Cooperative Highway Research Program, conducted by the Transportation Research Board with the approval of the Governing Board of the National Research Council.

The members of the technical panel selected to monitor this project and to review this report were chosen for their special competencies and with regard for appropriate balance. The report was reviewed by the technical panel and accepted for publication according to procedures established and overseen by the Transportation Research Board and approved by the Governing Board of the National Research Council.

The opinions and conclusions expressed or implied in this report are those of the researchers who performed the research and are not necessarily those of the Transportation Research Board, the National Research Council, or the program sponsors.

The Transportation Research Board of the National Academies, the National Research Council, and the sponsors of the National Cooperative Highway Research Program do not endorse products or manufacturers. Trade or manufacturers' names appear herein solely because they are considered essential to the object of the report.

THE NATIONAL ACADEMIES
Advisers to the Nation on Science, Engineering, and Medicine

The **National Academy of Sciences** is a private, nonprofit, self-perpetuating society of distinguished scholars engaged in scientific and engineering research, dedicated to the furtherance of science and technology and to their use for the general welfare. On the authority of the charter granted to it by the Congress in 1863, the Academy has a mandate that requires it to advise the federal government on scientific and technical matters. Dr. Ralph J. Cicerone is president of the National Academy of Sciences.

The **National Academy of Engineering** was established in 1964, under the charter of the National Academy of Sciences, as a parallel organization of outstanding engineers. It is autonomous in its administration and in the selection of its members, sharing with the National Academy of Sciences the responsibility for advising the federal government. The National Academy of Engineering also sponsors engineering programs aimed at meeting national needs, encourages education and research, and recognizes the superior achievements of engineers. Dr. C. D. Mote, Jr., is president of the National Academy of Engineering.

The **Institute of Medicine** was established in 1970 by the National Academy of Sciences to secure the services of eminent members of appropriate professions in the examination of policy matters pertaining to the health of the public. The Institute acts under the responsibility given to the National Academy of Sciences by its congressional charter to be an adviser to the federal government and, on its own initiative, to identify issues of medical care, research, and education. Dr. Harvey V. Fineberg is president of the Institute of Medicine.

The **National Research Council** was organized by the National Academy of Sciences in 1916 to associate the broad community of science and technology with the Academy's purposes of furthering knowledge and advising the federal government. Functioning in accordance with general policies determined by the Academy, the Council has become the principal operating agency of both the National Academy of Sciences and the National Academy of Engineering in providing services to the government, the public, and the scientific and engineering communities. The Council is administered jointly by both Academies and the Institute of Medicine. Dr. Ralph J. Cicerone and Dr. C. D. Mote, Jr., are chair and vice chair, respectively, of the National Research Council.

The **Transportation Research Board** is one of six major divisions of the National Research Council. The mission of the Transportation Research Board is to provide leadership in transportation innovation and progress through research and information exchange, conducted within a setting that is objective, interdisciplinary, and multimodal. The Board's varied activities annually engage about 7,000 engineers, scientists, and other transportation researchers and practitioners from the public and private sectors and academia, all of whom contribute their expertise in the public interest. The program is supported by state transportation departments, federal agencies including the component administrations of the U.S. Department of Transportation, and other organizations and individuals interested in the development of transportation. **www.TRB.org**

www.national-academies.org

C O O P E R A T I V E   R E S E A R C H   P R O G R A M S

F O R E W O R D

By Waseem Dekelbab
Staff Officer
Transportation Research Board

This report presents a reference guide to identify and evaluate the uncertainties associated with bridge scour prediction including hydrologic, hydraulic, and model/equation uncertainty. Tables of probability values to estimate scour depth with a conditional probability of exceedance when a bridge meets certain criteria for hydrologic uncertainty, bridge size, and pier size are included in the reference guide. For complex foundation systems and channel conditions, a step-by-step procedure is presented to provide scour factors for site-specific conditions. The reference guide also includes a set of detailed illustrative examples to demonstrate the full range of applicability of the procedures. The report will be of immediate interest to hydraulic and bridge engineers.

Current practice for determining the total scour prism at a bridge crossing involves the calculation of the various individual scour components (e.g., pier scour, abutment scour, contraction scour, and long-term channel changes). Then, using the principle of superposition, these individual components are considered to be purely additive and the total scour prism is then drawn as a single cumulative line for various frequency flood events (e.g., 50-year, 100-year, and 500-year flood events). The scour equations are generally understood to be conservative in nature and, with the exception of the contraction scour equations, have been developed as envelope curves for use in design. This approach does not provide an indication of the uncertainty involved in the computation of any of the individual components. Uncertainties in hydrologic and hydraulic models and the resulting uncertainty of relevant inputs (e.g., design discharge, velocity, depth, and flow distribution between the main channel and the floodplain) to the scour calculations will all have a significant influence when evaluating the risk associated with scour prediction.

To develop an overall estimate of confidence in the calculated scour depths, one must use engineering judgment and examine the level of confidence associated with the results of the hydrologic analysis, the level of confidence associated with the hydraulic analysis, and the level of confidence associated with each of the scour components. Scour reliability analysis involves quantification of the uncertainties in each of these steps and then combines them in such a way that the overall estimate of confidence is known for the final prediction of scour.

Research was performed under NCHRP Project 24-34 by Ayres Associates with the assistance of the City College of the City University of New York and the Pennsylvania State University. The objective of NCHRP Project 24-34 was to develop a risk-based methodology that can be used in calculating bridge pier, abutment, and contraction scour at waterway crossings so that scour estimates can be linked to a probability consistent with Load and Resistance Factor Design (LRFD) approaches used by structural and geotechnical engineers.

This Reference Guide is oriented toward the practitioner. The research agency's final report documenting the complete results of the research is not published but is available online at www.trb.org by searching "NCHRP Project 24-34."

C O N T E N T S

Note: Many of the photographs, figures, and tables in this report have been converted from color to grayscale for printing. The electronic version of the report (posted on the Web at www.trb.org) retains the color versions.

S U M M A R Y

Reference Guide for Applying Risk and Reliability-Based Approaches for Bridge Scour Prediction

Overview

NCHRP Report 761: Reference Guide for Applying Risk and Reliability-Based Approaches for Bridge Scour Prediction is based on the results of NCHRP Project 24-34, "Risk-Based Approach for Bridge Scour Prediction." The goals of NCHRP Project 24-34 were (1) to develop a risk and reliability-based methodology that can be used to link scour depth estimates at a river crossing to a probability and (2) to extend this methodology to provide a preliminary approach for determining a target reliability for the service life of the bridge that is consistent with load and resistance factor design (LRFD) approaches used by structural and geotechnical engineers.

The uncertainties associated with bridge scour prediction—including hydrologic, hydraulic, and model/equation uncertainty—are described and evaluated, as is the development of a software tool that links the most widely used 1-dimensional (1-D) hydraulic model (HEC-RAS) with Monte Carlo simulation techniques. Tables of probability values (scour factors) are presented that allow associating an estimate of scour depth with a conditional (single event) probability of exceedance when a bridge meets certain criteria for hydrologic uncertainty, bridge size, and pier size. The tables address pier scour, contraction scour, abutment scour, and total scour.

For complex foundation systems and channel conditions, a step-by-step procedure is presented to provide scour factors for site-specific conditions. An integration technique that incorporates the uncertainties associated with the conditional probability of a limited number of return-period flood events provides a reliability analysis framework for estimating the unconditional probability of exceeding a design scour depth over the service life of a bridge. Detailed illustrative examples demonstrate the full range of applicability of the methodologies.

The research on which this reference guide is based developed probabilistic procedures that are consistent with LRFD approaches used by structural and geotechnical engineers. LRFD incorporates state-of-the-art analysis and design methodologies with load and resistance factors based on the known variability of applied loads and material properties. These load and resistance factors are calibrated from actual bridge statistics to ensure a uniform level of safety over the life of the bridge. LRFD allows a bridge designer to focus on a design objective or limit state, which can lead to a similar probability of failure in each component of the bridge. Bridges designed with the LRFD specifications are intended to have relatively uniform safety levels, which helps ensure superior serviceability and long-term maintainability.

A widespread belief within the bridge engineering community is that unaccounted-for biases, together with input parameter and hydraulic modeling uncertainty, lead to overly

1

conservative estimates of scour depths. The perception is that this results in design and construction of costly and unnecessarily deep foundations. This reference guide is intended to close the gap between perception and reality and provide risk and reliability-based confidence bands for bridge scour estimates that align the hydraulic design approach with the design procedures currently used by structural and geotechnical engineers. Hydraulic engineers now have the option to perform scour calculations that incorporate probabilistic methods into the hydraulic design of bridges.

Research Approach

NCHRP Report 761 is oriented toward the practitioner. The Contractor's Final Report that documents the investigation and results of the research project is available on www.trb.org by searching on "NCHRP Project 24-34."

The research supporting this reference guide involved the following steps:

1. Completion of a literature review and evaluation of current practice in the areas of hydrologic and hydraulic analyses for bridge scour prediction, including the use of probabilistic methods in hydrologic and hydraulic engineering. The review included other disciplines where risk and reliability analyses have been incorporated into engineering design, with emphasis on LRFD approaches used by structural and geotechnical engineers.
2. Investigation of the application of reliability theory to the determination of bridge scour prediction and the quantity and quality of data available to support the objectives of this project.
3. Identification and evaluation of uncertainty associated with the variables and approaches used in bridge scour prediction, including hydrologic, hydraulic, and model/equation uncertainty.
4. Development of a conceptual approach for the implementation phase of the research and production of research-level software that links the most widely used 1-D hydraulic model (HEC-RAS) with Monte Carlo simulation techniques.
5. Development of a set of tables of probability values (scour factors) that can be used to associate an estimate of scour depth with a conditional (single event) probability of exceedance when a bridge meets certain criteria for hydrologic uncertainty, bridge size, and pier size.
6. For complex foundation systems and channel conditions, development of a step-by-step procedure that provides an approach for developing probability-based estimates and scour factors for site-specific conditions.
7. Development of an integration technique that incorporates the uncertainties associated with a conditional probability prediction into a reliability analysis framework to estimate the unconditional probability of exceedance for a selected service life of a bridge.
8. Providing a set of detailed illustrative examples to demonstrate the full range of applicability of the methodologies.
9. Production of this stand-alone reference guide.
10. Identification of additional research that would expand the findings of the project and suggestions for implementing the results of the research.

Appraisal of Research Results

The primary purpose of the research project supporting this reference guide was to analyze the probability of scour depth exceedance, not the probability of bridge failure. The latter requires advanced analyses of the weakened foundation under the effects of the expected applied loads, which was beyond the scope of this project.

The work plan that was developed and implemented for this research project yielded significant results of practical use to practitioners. The goals of the research study were achieved. A methodology is now available that can be used to link scour depth estimates to a probability and determine the risk associated with scour depth exceedance for a given design event. The probability linkage considers the propagation of uncertainties among the parameters that are used to quantify the confidence of scour estimates for a design event (e.g., a 100-year flood) based on uncertainty of input parameters and considering model uncertainty and bias. In addition, this methodology has been extended to provide an initial estimate of target reliability for the design life of a bridge consistent with LRFD approaches used by structural and geotechnical engineers.

The Level 1 approach described in this reference guide consists of a set of tables of probability values or scour factors that can be used to associate an estimated scour depth provided by the hydraulic engineer with a probability of exceedance for simple pier and abutment geometries. For more complex bridge or hydraulic situations, or for different return-period design events, the Level II approach can be used. The Level II approach consists of a step-by-step procedure that hydraulic engineers can follow to provide probability-based estimates of site-specific scour factors. A Level II approach will also be necessary if the unconditional probability of exceeding design scour depths to meet a target reliability over the life of a bridge is desired.

During NCHRP Project 24-34, a research-level software engine called rasTool© also was developed. The rasTool© software was not developed for distribution, nor is it thoroughly documented or supported for general use. It is, however, considered robust and could be applied to a range of bridge and/or open-channel applications.

CHAPTER 1

Introduction and Applications

1.1 Introduction

Load and resistance factor design (LRFD) incorporates state-of-the-art analysis and design methodologies with load and resistance factors based on the known variability of applied loads and material properties. These load and resistance factors are calibrated from actual bridge statistics to ensure a uniform level of safety over the life of the bridge. LRFD allows a bridge designer to focus on a design objective or limit state, which can lead to a similar probability of failure in each component of the bridge. Bridges designed with the LRFD specifications are intended to have relatively uniform safety levels, which should ensure superior serviceability and long-term maintainability.

A widespread belief within the bridge engineering community has been that unaccounted-for biases and input parameter and hydraulic modeling uncertainty lead to overly conservative estimates of scour depths. The perception also has been that this results in design and construction of costly and unnecessarily deep foundations. *NCHRP Report 761: Reference Guide for Applying Risk and Reliability-Based Approaches for Bridge Scour Prediction* is intended to close the gap between perception and reality and provide risk and reliability-based confidence bands for bridge scour estimates that will align the hydraulic design approach with the design procedures currently used by structural and geotechnical engineers. Bridge hydraulic engineers now have the option of and ability to perform scour calculations that incorporate similar probabilistic methods.

This reference guide provides a risk and reliability-based methodology that can be used in calculating bridge pier, abutment, contraction and total scour at waterway crossings so that scour estimates can be linked to a probability. The probabilistic procedures are consistent with LRFD approaches used by structural and geotechnical engineers.

This document provides two approaches to estimating and predicting bridge scour. **The Level I approach uses sets of tables of probability values (scour factors) that associate the estimated scour depth provided by the hydraulic engineer with a probability of exceedance for a given design event.** The Level I approach is illustrated by a series of examples in Chapter 7 of this document.

For complex foundation systems and channel conditions, or for cases requiring special consideration, the site-specific Level II approach is necessary. The Level II approach consists of a step-by-step procedure that hydraulic engineers can follow to develop probability-based estimates of site-specific scour factors. The Level II approach also is described in this document using an illustrative example.

When using the Level I probability-based estimates or scour factor tables for each scour component or applying the Level II approach, the methodology requires an understanding of

4

the uncertainties associated with the prediction of individual scour components. **This reference guide incorporates these uncertainties into a reliability analysis framework to estimate the probability of scour level exceedance for the service life of a bridge.** The service life reliability analysis for scour is consistent with the reliability analysis procedures developed and implemented by AASHTO LRFD/LRFR for calibrating load and resistance factors for bridge structural components and bridge structural systems as well as foundations.

The primary purpose of *NCHRP Report 761* is to enable practitioners to analyze the probability of scour depth exceedance, not the probability of bridge failure. Addressing the probability of bridge failure requires advanced analyses of the weakened foundation under the effects of the expected applied loads, which is beyond the scope of this reference guide.

1.2 Applications

This reference guide is based on the results of NCHRP Project 24-34, "Risk-Based Approach for Bridge Scour Prediction" (Lagasse et al. 2013). The goals of NCHRP Project 24-34 were to develop a methodology that can be used to link scour depth estimates at a river crossing to a probability and extend this methodology to provide a preliminary approach for determining a target reliability for the service life of the bridge consistent with LRFD approaches used by structural and geotechnical engineers. The probability linkage considered the propagation of uncertainties among the parameters used to quantify the confidence of scour estimates for a design event based on uncertainty of input parameters and considering model uncertainty and bias. Although the focus of NCHRP Project 24-34 was refining hydraulic design approaches for bridges, the tools developed also can be applied to other situations for which a more precise evaluation of risk and reliability associated with flooding would improve public safety.

1.2.1 Transportation Facilities

Bridge scour applications are the focus of this reference guide; however, the techniques described in this document can be used to assess potential threat and risk of failure for any existing or proposed transportation facility. These techniques also can be used to evaluate and justify the need for structural solutions or countermeasures to inhibit scour or channel instability in proximity to existing or proposed transportation facilities. Bridge appurtenant structures such as guide banks and roadway approach embankments, flow-control structures such as spurs or bendway weirs, and roadway alignments trending parallel to an active channel or on a floodplain could all benefit from a risk and reliability analysis using the techniques in this document.

As a specific example, accumulations of vegetative debris (or drift) on bridges during flood events constitute a continuing threat to bridges nationally. Debris accumulations can obstruct, constrict, or redirect flow through bridge openings, resulting in flooding, damaging loads, or excessive scour at bridge foundations (see Figure 1.1). *NCHRP Report 653: Effects of Debris on Bridge Pier Scour* provides an approach to computing the increased scour potential at piers with debris (Lagasse et al. 2010). That study also provides an extensive data base from laboratory studies of debris clusters with a range of shapes, geometry, and locations in the water column. The scour equations developed from the debris study are deterministic and essentially provide a transform from a pier with debris to an equivalent wider pier. With these equations and the available data set, it is possible to use the techniques introduced in this reference guide to conduct a detailed probability analysis of the results of the calculation procedures developed for debris loading on bridge piers.

Figure 1.1.   Drift accumulation on a single bridge pier (photo courtesy of Ayres Associates).

1.2.2 Floodplain Risk and Flood Control Facilities

In many areas along larger river systems and in close proximity to large urban areas, flood control facilities such as levees, dikes, and flood-relief structures are used to protect the public from major floods (see Figure 1.2). The U.S. Army Corps of Engineers (USACE) has developed a National Levee Data Base (NLD) to provide a focal point for comprehensive information about the nation's levees. The data base contains information to facilitate and link activities such as flood risk communication, levee system evaluation for the National Flood Insurance Program (NFIP), levee system inspections, flood plain management, and risk assessments (Military Engineer 2012). The techniques developed in this reference guide, particularly the unique linkage between the fundamental hydraulic model supporting the NFIP—the USACE's Hydrologic Engineering Center River Analysis System (HEC-RAS)—and accepted statistical methods to quantify risk through simulation of the hydraulic parameters for a large number of flood events, enable a quantitative evaluation of risk to flood control facilities from a single flood event or over the remaining service life of a facility. Specifically, these techniques can

Figure 1.2.   California State Highway 160 on Sacramento River levee (photo courtesy of Google Earth™).

establish the probability of exceeding design flood elevations or determine the probability of occurrence of critical flow velocities in excess of failure thresholds used as a basis for design.

Nationally, roughly 2,000 federal levees extend over some 13,000 miles; more than 20,000 non-federal levees also exist whose extent has yet to be fully identified. Although an agency such as the USACE has a broad base of highly qualified hydrologists, hydraulic engineers, and scientists to assess the reliability and evaluate risks to federal levees, other levee owners do not have a commensurate level of technical support. For private levee districts, smaller municipalities, and private owners, the risk assessment techniques presented in *NCHRP Report 761* offer an approach to identify, prioritize, evaluate, and counter possible threats to flood control infrastructure within their districts and on critical river reaches.

1.2.3 Channel Restoration and Rehabilitation Works

Many stream bank stabilization and rehabilitation measures have failed because the designer was unable to establish the risk of failure during a design flood or the reliability of the structure over its design life. In addition, there is increasing interest in the use of environmentally sensitive biotechnical approaches to channel restoration and stream bank protection as an alternative to more traditional "hard" engineering techniques (see Figure 1.3). Design of both traditional and biotechnical measures requires accounting for hydrologic, hydraulic, geomorphic, geotechnical, vegetative, construction, and maintenance factors. Many biotechnical measures (e.g., root wads, engineered log jams, and vegetated riprap) have been deployed for channel restoration and have survived for a number of years, but considerable skepticism remains within the engineering community regarding performance of these measures when subjected to flood event magnitudes typically experienced over the design life desired for restoration or rehabilitation projects. In particular, very little information is available regarding the durability and service life expectations and maintenance requirements for biotechnical countermeasures.

The techniques developed in this reference guide for simulating the hydraulic conditions for a large number of flood events would enable a quantitative evaluation of risk to channel restoration installations from a single flood event or over the remaining service life of the structure. These techniques can establish the probability of exceedance (or of non-exceedance) of critical hydraulic design parameters such as flow velocity and shear stress in relation to failure thresholds used as a basis for design. Because many rehabilitation projects require establishing a desired sinuosity and protecting the resulting bendways from erosion (as shown in Figure 1.3), the ability to determine the probability of exceeding the design scour depth at protected meander bends is one obvious application of the techniques presented in this reference guide.

1.3 Organization of the Reference Guide

Chapter 2 of this reference guide provides a discussion of the various types and sources of uncertainty that must be considered in the assessment of bridge scour. Citations from the literature provide relevant background information on the current state of practice. Hydrology and hydraulics both introduce uncertainties in the determination of the variables that are subsequently used as input to the various scour equations. That is, the three components of scour addressed (pier, contraction, and abutment scour) are fundamentally linked to both the hydrologic estimation of the magnitude of a design flood event and the anticipated hydraulic conditions associated with that event. The scour equations themselves involve uncertainty, as evidenced by the fact that even under controlled laboratory conditions the equations do not precisely predict the observed scour. Lastly, the scour problem is framed in the context of

(a) Blunn Creek, Austin, TX, before restoration

(b) During construction

(c) After construction

Figure 1.3.   Typical biotechnical river restoration project protecting an eroding bendway (photo courtesy of City of Austin, TX, Watershed Protection Department).

current guidance from FHWA and AASHTO LRFD statistical methods and procedures used in bridge structural design from the perspective of a hydraulic engineer.

Chapter 3 describes an approach to evaluating the uncertainty of the three scour components. The approach is based on Monte Carlo simulation linked directly with the most common and widely accepted hydraulic model used in current practice, HEC-RAS. For each individual scour component, the parameters that were allowed to vary in the Monte Carlo simulation are discussed along with a matrix of other factors and considerations that were not addressed. The chapter provides a discussion of model uncertainty and the definitions of bias and coefficient of variation (COV) in relation to the scour equations. Chapter 3 also provides a discussion of the linkage between the hydraulic model HEC-RAS and the Monte Carlo simulation software.

Chapter 4 presents a brief summary of the data sets used in developing model bias and COV for each of the three individual scour components. For pier scour, both the HEC-18 and Florida Department of Transportation (Florida DOT) equations are assessed. The equations are from the 5th edition of FHWA's *Hydraulic Engineering Circular* (HEC) *No. 18* (Arneson et al. 2012). The equations are assessed using comprehensive data sets from both laboratory and field studies. Contraction scour uses the HEC-18 equation for clear-water scour with laboratory data only. Abutment scour uses the total scour approach recommended in the most recent edition of HEC-18 with laboratory data only.

Chapter 5 provides two approaches for assessing the conditional probability that the design scour depth will be exceeded for a given design flood event. Either approach can be used to estimate this probability for each of the three individual scour components. The first approach (Level 1) assumes that the practitioner can categorize a bridge based on three general conditions: (1) the size of the bridge, channel, and floodplain (small, medium or large); (2) the size of the piers (small, medium, or large); and (3) the hydrologic uncertainty (low, medium, or high). This Level I approach provides scour factors that can be used to multiply the estimated scour depth to achieve a desired level of confidence based on the reliability index, β, commensurate with standard LRFD practice. Scour factors are provided in tabular format for each of the individual scour components for all 27 combinations of the three category conditions for simple pier and abutment geometries (Appendix B).

When the practitioner cannot match a particular site to the categories described for Level 1, a Level II approach is required. Necessarily site-specific, the Level II approach is illustrated in this reference guide using data from a bridge on the Sacramento River. The discussion includes the results for pier, contraction, abutment, and total scour considering hydrologic uncertainty, hydraulic uncertainty, and scour prediction (model) uncertainty. A step-by-step summary of the Level II procedure is also provided.

Chapter 6 presents a methodology to determine the unconditional probability that a scour estimate will not be exceeded over the remaining service life of an existing bridge or the design life of a new bridge. The proposed methodology uses the conditional probabilities of the design scour depth being exceeded for a limited number of return-period flood events. The conditional probabilities are then integrated to determine the unconditional probability of exceedance over the entire service life. The integration method is implemented for pier scour (both HEC-18 and Florida DOT methods), contraction scour (HEC-18 method), combined pier and contraction scour, and abutment scour using bridge-specific data.

Chapter 7 provides five illustrative examples using the Level I approach to: (1) categorize a bridge site; (2) estimate pier, contraction, abutment, and total scour; and (3) identify the appropriate scour factors for a desired level of confidence using the results provided in Chapter 5 and

the information in Appendix B. Examples are presented for a range of bridge configurations and hydrologic/geomorphic settings where hydraulic input is developed from both 1-D and 2-D models.

Chapter 8 briefly summarizes the procedures and applications and discusses topics beyond the scope of this document that would extend the results and usefulness of these procedures.

A list of the references cited in *NCHRP Report 761* follows Chapter 8.

Appendix A provides a glossary of terms used in the reference guide that will be helpful to the practitioner not completely familiar with the statistical approaches that underpin the procedures of this guidance document.

Appendix B presents a summary of scour factors in tabular and graphical form for use with the Level I approach described in Chapter 5.

Uncertainty in Hydraulic Design

2.1 Introduction

This chapter provides a discussion of the various types and sources of uncertainty that must be considered in the assessment of bridge scour. Citations from the literature provide relevant background information on the current state of practice. Hydrology and hydraulics both introduce uncertainties in the determination of the variables that are subsequently used as input to the various scour equations. That is, the three components of scour (pier, contraction, and abutment scour) are fundamentally linked to both the hydrologic estimation of the magnitude of a design flood event and the anticipated hydraulic conditions associated with that event.

It must also be understood that the scour equations themselves have uncertainty, as evidenced by the fact that even under controlled laboratory conditions the equations do not precisely predict the observed scour. Current guidance from FHWA on incorporating risk in bridge scour analyses is summarized; and the scour problem is framed in the context of AASHTO LRFD statistical methods and procedures used in bridge structural design from the perspective of a hydraulic engineer.

2.2 Hydrologic Uncertainty

2.2.1 Overview

The majority of hydrologic phenomena (e.g., droughts and floods, precipitation, dewpoint, etc.) are stochastic processes, which can be characterized as processes governed by laws of chance. Strictly speaking, no pure deterministic hydrologic processes exist in nature; hydrologic phenomena have traditionally been understood and described using methods of probability theory (Yevjevich 1972).

Scour prediction is typically associated with a design hydrologic event that has a given likelihood of recurrence (e.g., the 100-year flood). Hydraulic conditions from such an event, in terms of the depth and velocity of flow corresponding to the peak rate of flow, are used to predict local and contraction scour at the bridge using methods described in the 5th edition of HEC-18 (Arneson et al. 2012). This scour prediction is in turn used for determining structural stability for the case in which all the soil material in the scour prism is removed. Usually the time rate of scour is ignored and scour is assumed, in effect, to occur instantaneously in response to the peak hydraulic load for the event of interest.

Practitioners understand that the 100-year flood is defined as the discharge rate that has a 1% chance of being equaled or exceeded in any given year; the 50-year flood has a 2% probability of exceedance, and so forth. Typically, the discharge is estimated based on flow records from stream gaging stations upstream or downstream of the bridge, and the discharge estimates are adjusted

11

to the bridge location using area-weighting and other techniques. Where gaging station records on the particular stream or river are unavailable, data are used from stations in nearby watersheds of similar size and nature to the watershed of interest. In many cases, regional regression relationships are available for use, and these typically include watershed area and a rainfall index (such as the 2-year, 24-hour rainfall depth) as input values to the regression equations.

Practitioners understand that the magnitude of any recurrence-interval event is an *estimate,* but the current state of practice in bridge scour prediction places no emphasis on quantifying the *reliability* of that estimate. However, it has been standard practice to report the 95% confidence limits as part of the methodology described in U.S. Geological Survey (USGS) Bulletin 17B for nearly half a century (USGS 1981). As with any probability-based estimate, confidence in the predicted value of the 100-year flood increases with the number of observations from the population of discharges. Regional regression relationships often include a measure of uncertainty about the predicted recurrence-interval values.

NCHRP Report 717: Scour at Bridge Foundations on Rock (Keaton et al. 2012) provides an example to illustrate this issue. In the research for that project, four field sites were investigated where the erodibility of rock at bridge pier foundations was assessed. One site, SR-22 over Mill Creek in western Oregon, has exhibited approximately 7 ft of scour over the period from December 1945 to August 2008. Data are available from the USGS gaging station upstream of the bridge from the station's installation in 1958 until use of the station was discontinued in 1973, so only 15 years of mean daily flows and annual instantaneous peaks are available from that location. The time series was extended by regression analysis using data from stations on the South Yamhill River, located farther downstream. This technique provided additional data necessary to assess the cumulative hydraulic loading experienced by the bridge to the present time. The resulting time series of mean daily flows is shown in Figure 2.1.
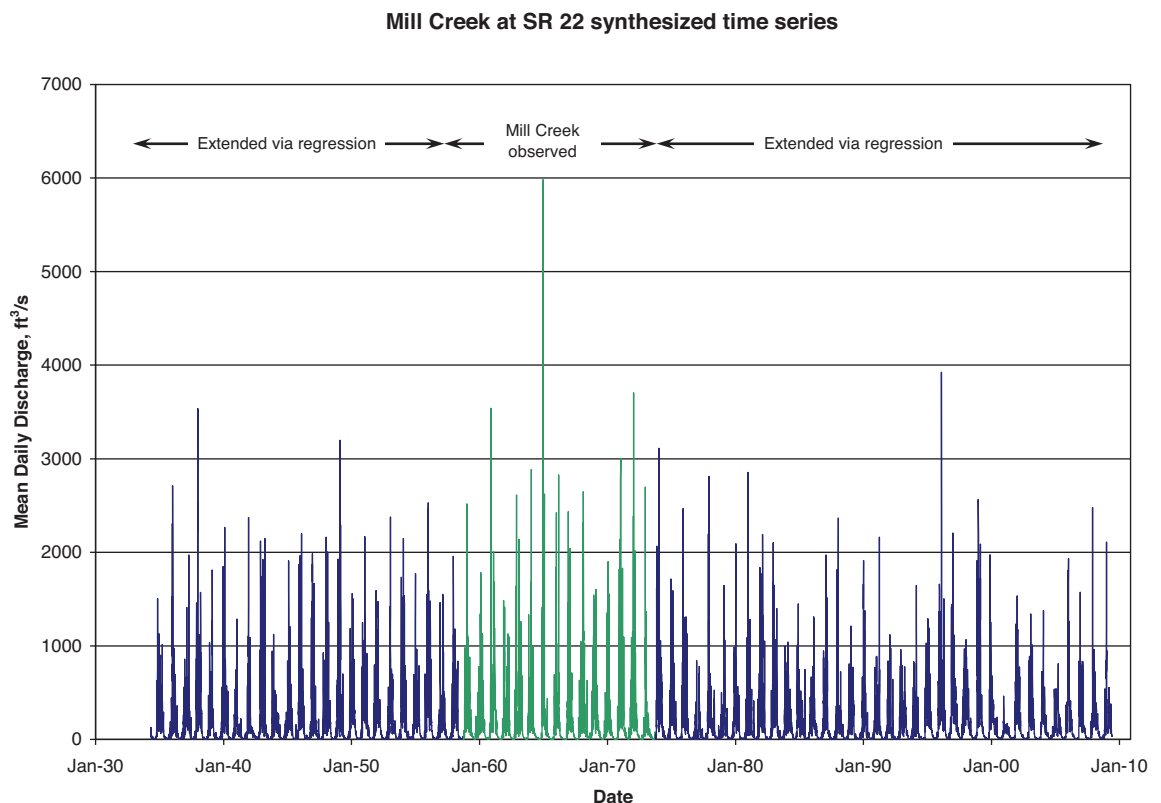
Figure 2.1.   *Mean daily flows, Mill Creek at SR-22 showing observed and extended records.*

Table 2.1.   Flood frequency analyses for SR-22 over Mill Creek, Oregon.

Recurrence Interval (yrs)	15-Year Period Weighted Skew = 0.159			74-Year Period Weighted Skew = 0.253		
	Discharge (ft³/s)	95% Confidence		Discharge (ft³/s)	95% Confidence	
		Lower	Upper		Lower	Upper
1.5	3,142	2,633	3,629	2,806	2,653	2,954
2	3,630	3,116	4,220	3,138	2,981	3,302
5	4,858	4,182	5,995	3,946	3,734	4,205
10	5,686	4,811	7,384	4,472	4,197	4,827
25	6,752	5,562	9,344	5,132	4,761	5,634
50	7,561	6,102	10,940	5,622	5,171	6,247
100	8,384	6,633	12,650	6,113	5,575	6,871
500	10,380	7,860	17,120	7,275	6,514	8,383

The data from other gaging stations allowed the period of record to be extended from 1935 through 2008 (74 years) for purposes of quantifying the cumulative hydraulic loading from the time the bridge was built to the present. Figure 2.1 clearly shows that the single largest flood event in the entire period of record (mean daily flow of 5,980 ft³/s, with an instantaneous peak of 7,320 ft³/s) occurred during the period of time when the Mill Creek gaging station was active. All other mean daily flows recorded for the 74-year period were less than 4,000 ft³/s.

The USGS flood frequency analysis software PKFQWin (Flynn et al. 2006) was used to estimate the magnitudes of various recurrence-interval floods using Bulletin 17B methodology, assuming a Log-Pearson Type III probability distribution. For both the 15- and 74-year periods of record, the generalized skew of 0.086 at this location was combined with the observed station skew to produce a weighted skew for use with this probability distribution. Table 2.1 presents the results of these flood frequency analyses.

Figure 2.2 presents the predicted frequency curves and associated 95% confidence limits for the 15 years of observed annual peaks and for the entire 74-year extended period of record. As seen in Figure 2.2, the estimates of the recurrence-interval flood magnitude and the corresponding confidence limits are quite different for the two periods of record.

Table 2.1 and Figure 2.2 illustrate how the confidence limits associated with a Log-Pearson Type III probability distribution are sensitive to the number of observations, and how the confidence interval becomes wider as the recurrence interval increases. For smaller, more frequent events, the reliability of the discharge estimate is greater than for larger, less frequent floods.

In summary, the characteristics of the probability distribution typically used in flood frequency analyses (Log-Pearson Type III) are well known and described. This result is well suited to LRFD procedures for establishing a probability-based characterization of scour using standard practices in hydrologic analysis. Clearly, an understanding of and ability to characterize sources of hydrologic uncertainty are central to probability-based bridge scour predictions.

2.2.2 Evaluating Hydrologic Uncertainty

2.2.2.1 Flood Frequency Estimates From Gaging Station Data

As discussed in Section 2.2.1, characteristics of the probability distribution typically used in flood frequency analyses (Log-Pearson Type III) are well known and described. Uncertainty in hydrologic estimates can, therefore, be easily incorporated within the framework of existing LRFD procedures to establish a probability-based characterization of scour using standard practices in hydrologic analysis.

FLOOD FREQUENCY ESTIMATES
MILL CREEK AT SR 22, OREGON
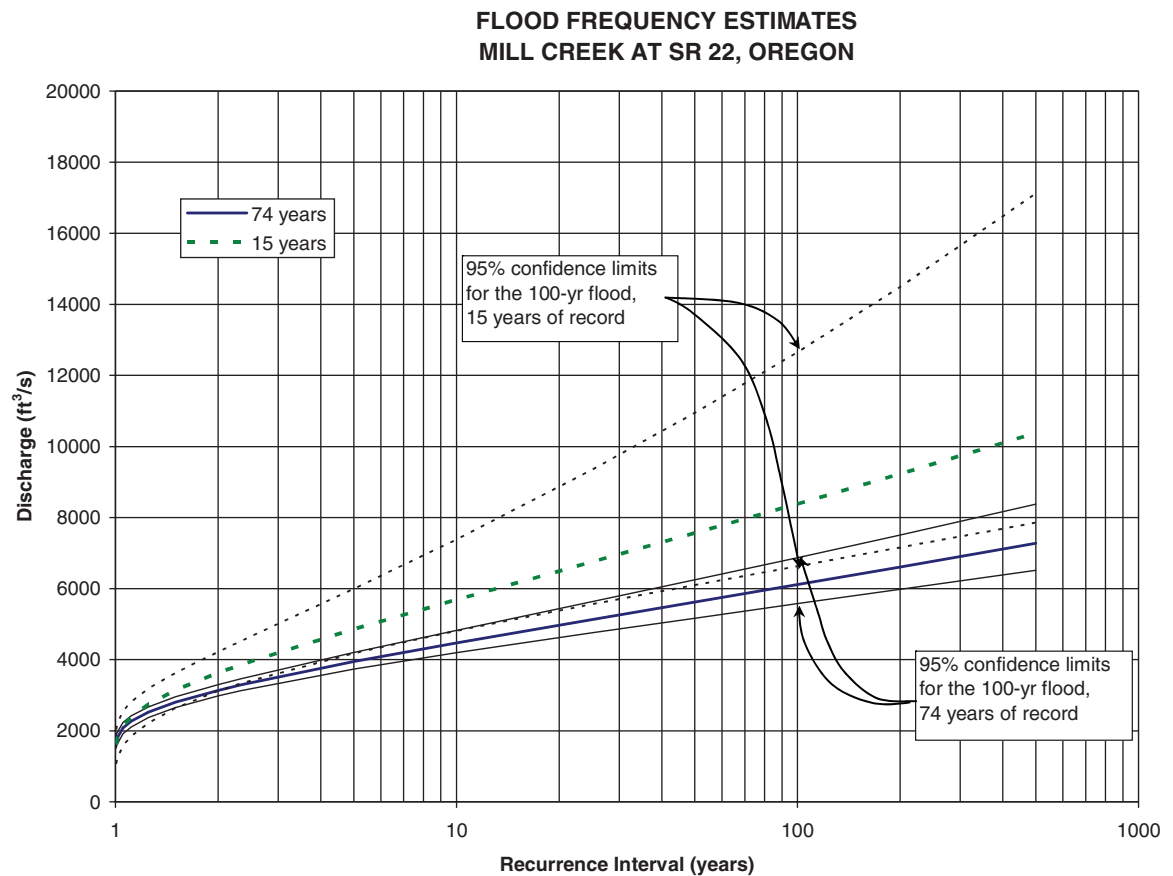
Figure 2.2.   Flood frequency estimates for 15- and 74-year periods of record, SR-22 over Mill Creek, Oregon.

The USGS software package PKFQWin can be used to determine hydrologic uncertainty when dealing with data from gaged sites. The software is a public-domain, Windows-based program that allows the user to access annual peak flow records in standard USGS format. Flood frequency estimates, as well as the 95% confidence limits about the estimated values, are part of the PKFQWin output files. From the USGS gaging station identifier, PKFQWin identifies the generalized skew based on location (latitude and longitude) and computes the actual station skew using the observed record from the site. These values are then used to compute a weighted skew value in accordance with USGS Bulletin 17B procedures.

2.2.2.2 Flood Frequency Estimates From Regional Regression Equations

The USGS has developed and published regression equations for every state, the Commonwealth of Puerto Rico, and a number of metropolitan areas in the United States. The National Streamflow Statistics (NSS) software compiles all current USGS regional regression equations for estimating streamflow statistics at ungaged sites in an easy-to-use interface that operates on computers with Microsoft Windows operating systems. NSS expands on the functionality of the National Flood Frequency program, which it replaces.

The regression equations included in NSS (Ries 2007) are used to transfer streamflow statistics from gaged to ungaged sites through the use of watershed and climatic characteristics as explanatory or predictor variables. Generally, the equations were developed on a statewide or metropolitan-area basis as part of cooperative study programs. NSS output also provides indicators of the accuracy of the estimated streamflow statistics. The indicators may include any

combination of the standard error of estimate, the standard error of prediction, the equivalent years of record, or 90% prediction intervals, depending on what was provided by the authors of the equations.

NSS is a public-domain software program that can be used to:

- Obtain estimates of flood frequencies for sites in rural (non-regulated) ungaged basins.
- Obtain estimates of flood frequencies for sites in urbanized basins.
- Estimate maximum floods based on envelope curves.
- Create hydrographs of estimated floods for sites in rural or urban basins and manipulate the appearance of the graphs.
- Create flood frequency curves for sites in rural or urban basins and manipulate the appearance of the curves.
- Quantify the uncertainty of flood frequency estimates.
- Obtain improved flood frequency estimates for gaging stations by weighting estimates obtained from the systematic flood records for the stations with estimates obtained from regression equations.
- Obtain improved flood frequency estimates for ungaged sites by weighting estimates obtained from the regression equations with estimates obtained by applying the flow per unit area for an upstream or downstream gaging station to the drainage area for the ungaged site.

2.3 Hydraulic Uncertainty

2.3.1 Overview

As discussed in Section 2.2, hydraulic conditions associated with the design event must be determined in order to estimate scour depths. At a particular location, such as a pier, the hydraulic parameters of flow depth and velocity are related through the Manning n resistance factor and the local energy slope. From these basic parameters, other hydraulic variables, such as Froude number, shear stress, shear velocity, stream power, and so forth, are calculated. The distribution of flow and velocity within the main channel or between the main channel and overbank (floodplain) is highly sensitive to the river reach geometry and the choice of Manning n used to characterize these areas.

Figure 2.3 shows a bridge opening approach cross section and the associated velocity distributions from a HEC-RAS model (USACE 2010), which bases flow distribution on conveyance. A change in geometry or in Manning n would result in a different flow distribution between channel and floodplain (impacting the contraction scour) and the magnitudes of the computed velocities (impacting local pier and abutment scour).

However, whether simple models (e.g., Manning's equation) or more sophisticated approaches (e.g., HEC-RAS, FESWMS, etc.) are used to estimate the hydraulic conditions at a particular site and at a particular discharge, such estimates necessarily result from a simplification of the complex physical processes involved with open-channel flow. Several broad categories of uncertainty are common to any design process. These can be described as model uncertainty, parameter uncertainty, randomness, and human error.

2.3.1.1 Model Uncertainty

Model uncertainty results from attempting to describe a complex physical process or phenomenon through the use of a simplified mathematical expression. Model uncertainty in scour analysis is the result of selecting a particular scour equation to estimate scour. Each equation has bias that causes it (on average) to over- or underpredict scour for certain situations.
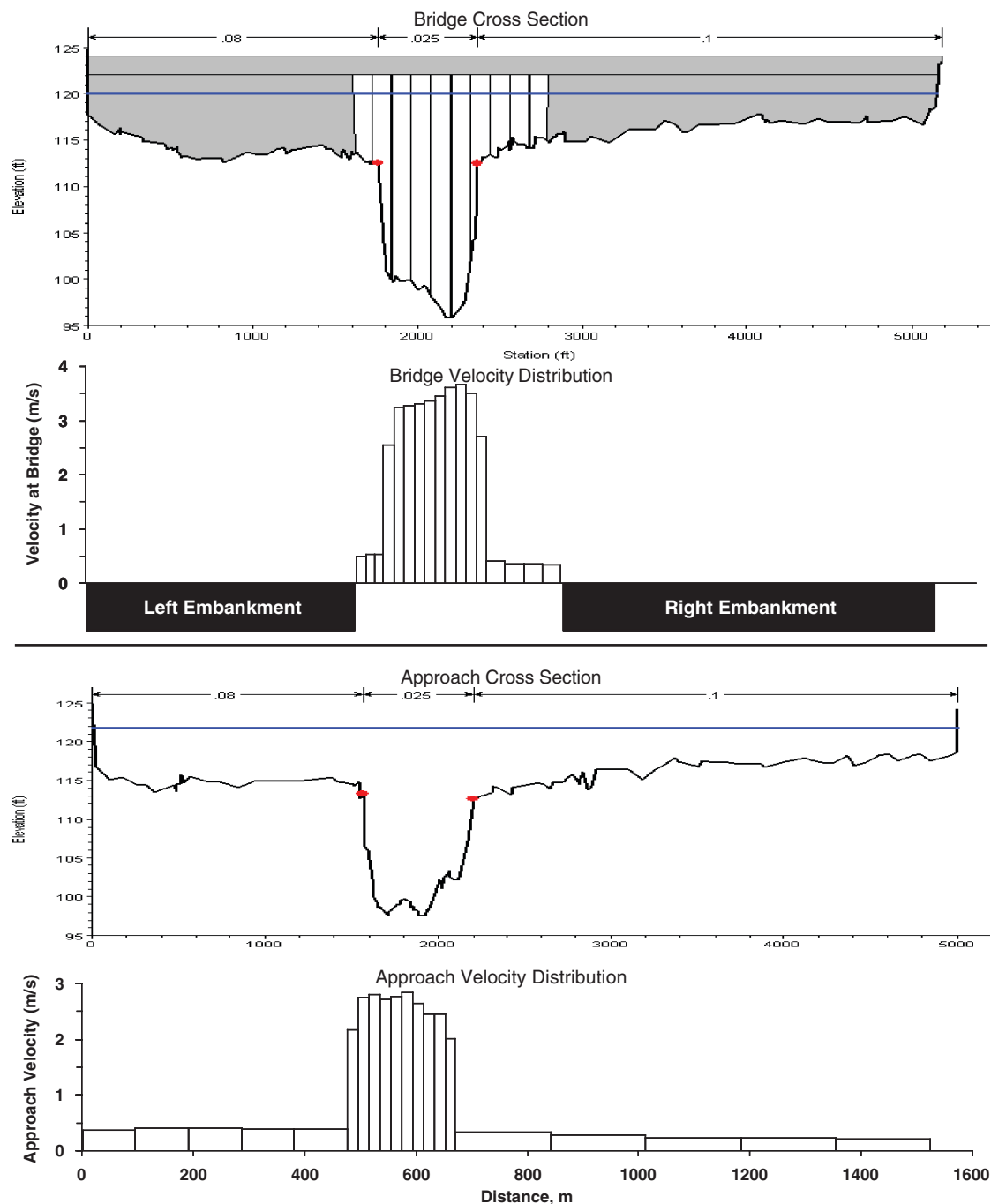
Figure 2.3.   Flow distribution from 1-D hydraulic modeling.

2.3.1.2 Parameter Uncertainty

Parameter uncertainty results from difficulties in estimating model parameters. For example, Manning's roughness coefficient and design discharge are two common parameters that cannot be measured directly; therefore, they must be estimated or assumed. The result is parameter uncertainty. Examples of hydraulic models used in bridge designs include HEC-RAS (USACE 2010) and FESWMS-FST2DH (Froehlich 2003). Each model has strengths and weaknesses that can lead to more or less parameter uncertainty based on the particular bridge, road embankment, and river conditions. Parameter uncertainty can be reduced by using more sophisticated

models (e.g., 2-D models) for more complex situations or by calibrating the model to measured conditions.

2.3.1.3 Randomness

Natural (or inherent) randomness is a source of uncertainty that includes random fluctuation in parameters, such as flow discharges and velocities. Other types of randomness may be changes to floodplain vegetation that occur over time (seasonally or over the life of the bridge).

2.3.1.4 Human Error

Potential always exists for human error in design and in implementation of a design. This type of uncertainty includes calculation and construction errors. Human errors are not usually considered in current reliability-based calculation of load and resistance factors, but their possible occurrence may be considered during the selection of the target reliability levels in the code calibration process.

2.3.2 Evaluating Hydraulic Uncertainty

Hydraulic parameters such as roughness coefficient, channel or energy slope, and critical shear stress, common to many hydraulic engineering problems, are known to contain considerable uncertainty. A common way to express the uncertainty associated with hydraulic parameters is through the coefficients of variation and associated distributions of parameters.

Johnson (1996) quantified uncertainty in common hydraulic parameters based on data from the scientific literature, experiments, and field observations. The Johnson study yielded the data presented in Table 2.2, which provides the COV, distribution, and reference or method by which the data were determined. In Table 2.2, where two values are included, the values represent either a different assumed probability distribution or a different situation. Of course, in a hydraulic model used for bridge design, several Manning n values will be used, including channel, left overbank, and right overbank. Each Manning n value will have its own uncertainty, which may differ from the others. The channel Manning n may be calibrated for frequent bankfull flows and the overbank Manning n values may be selected based on experience

Table 2.2. Uncertainty of hydraulic variables (Johnson 1996).

Variable	Coefficient of Variation (COV)	Distribution	Reference or Method
Manning n	0.1, 0.15	Normal	Cesare 1991
Manning n	0.2, 0.053	Normal	Mays and Tung 1992
Manning n	0.08	Triangular	Yeh and Tung 1993
Manning n	0.10, 0.055	Triangular, gamma	Tung 1990
Manning n	0.20-0.35	Lognormal	HEC 1986
Manning n	0.28, 0.18	Uniform	Johnson 1996
Channel slope	0.3, 0.068	Normal	Mays and Tung 1992
Channel slope	0.12, 0.164	Triangular	Tung 1990
Channel slope	0.25	Lognormal	Johnson 1996
Particle size	0.02	Uniform	Yeh and Tung 1993
Particle size	0.05	Uniform	Johnson and Ayyub 1992
Friction slope	0.17	Uniform	Yeh and Tung 1993
Sediment sp. Weight	0.12	Uniform	Yeh and Tung 1993
Flow velocity[a]	$0.008x^b$	Triangular	Meter manufacturer;
Flow velocity	$0.12x^b$	Uniform	Johnson 1996
[a]Measured using electromagnetic meter [b]x = average velocity			

or by comparison with published values. Since its original publication, this table has been cited numerous times in risk, reliability, and other studies, and it has been the basis for parameter input for bridge scour, levee and dam overtopping, and other hydrodynamic studies.

Hydraulic parameters are typically input to hydraulic models such as HEC-RAS to estimate flood elevations and velocities. Uncertainty in the parameters will propagate through the model to create uncertainty in the resulting calculation. In addition, uncertainty in the model itself will combine with the parameter uncertainty to create additional uncertainty.

Uncertainties in hydraulic conditions can be reduced when measured data are available to calibrate the model. For example, high water marks or other observations of water surface elevation, combined with a discharge measurement, can be extremely valuable in adjusting Manning n values in the main channel and overbank areas so that the hydraulic model matches observed conditions. Discharge measurements made using the velocity-area method also provide useful information on the velocity distribution across the channel.

However, channels and floodplains change through time. These changes include maturing vegetation; land-use change; and channel aggradation, degradation, migration, and width adjustment. Though future conditions often are difficult to estimate, they introduce considerable uncertainty and should not be neglected during the hydraulic analysis. They impact flow velocity and depth directly, and they impact the distribution of flow and velocity, each of which has an impact on scour estimates.

As with hydrologic uncertainty, incorporating hydraulic uncertainty into bridge design is not a trivial matter. Considerable information is available on the subject of hydraulic uncertainty, however, and through the use of hydraulic models the levels of uncertainty in velocity, depth, and flow distribution can be quantified both in general and in any specific application.

2.4 Uncertainty in Bridge Scour Estimates

2.4.1 Background

Scour at bridges is a very complex process. Scour and channel instability processes, including local scour at the piers and abutments, contraction scour, channel bed degradation, channel widening, and lateral migration, can occur simultaneously. The sum and interaction of all of these river processes create a very complex phenomenon that has, so far, eluded definitive mathematical modeling. To further complicate a mathematical solution, countermeasures such as riprap, grout bags, and gabions may be in place to protect abutments and piers from scour. A complete mathematical model would also have to account for these structures.

Considerable uncertainty exists in estimating all components of scour at the piers and abutments. Sources of uncertainty include model, parameter, and data uncertainties. For some bridges, the uncertainty is much greater than for other bridges because of unusual circumstances and difficulties in estimating parameters. For example, Oben-Nyarko and Ettema (2011) point out that scour depth at a pier located close to an abutment is determined predominantly by scour at the abutment and, therefore, may substantially exceed the depth estimated for an isolated pier. When the prototype conditions differ significantly from the conditions under which the model was calibrated, the model uncertainty is increased and may overshadow all other types of uncertainty. A number of studies have been aimed at developing probabilistic estimates of bridge scour, particularly for piers, for the purpose of design and mitigation. This section provides useful background information and summarizes several of these studies.

Jones (1984) compared numerous pier scour equations using laboratory data and limited field data. He found that the HEC-18 equation tended to give reasonable, although conservative, results. Johnson (1991) listed four primary concerns with bridge pier scour prediction methods, including the inability to determine the impact of future storms on the scour depth or on the probability that the bridge will fail or survive.

In an effort to use probabilistic estimates as a tool in decision making, Johnson and Dock (1998) developed a probabilistic framework for estimating scour using deterministic methods given in HEC-18. Uncertainties in the HEC-18 model, in determination of the parameters, and in estimating the hydraulic variables for a large event storm were included in the analysis. The probabilistic framework was then used as the basis for determining the likelihood of achieving various scour depths, probabilities of failure for various foundation designs, the pile depths necessary to achieve a specified probability of failure for a design bridge life span, and for comparing designs based on various storm events.

Johnson and Dock (1998) used the Bonner Bridge in North Carolina as an example. Pile depths appropriate for various design life spans were calculated based on both 100-year and 500-year storm events. The following assumptions were made: (1) the failure event was defined as the point at which the scour reached the base of the piles; (2) the arrival of hurricanes is a Poisson process (see glossary in Appendix A); and (3) the piles can be placed at a depth y_p with a small COV and follow a normal distribution. The first assumption can be readily changed to reflect different design criteria. Figure 2.4 shows the resulting frequency histogram for 1,000 simulated scour depths. Based on this resulting normal distribution, a mean scour depth of 53.2 ft (16.21 m), and a standard deviation of 4.8 ft (1.46 m), the probability that a scour depth of less than 68.9 ft (21 m) will occur is 97.4%. The scour depth at which the probability of non-exceedance is 90% is 63.5 ft (19.36 m).

The uncertainty in a scour estimate can be computed in different ways. One method is to use simulation techniques, such as Monte Carlo simulation or modifications of the Monte Carlo simulation technique. The benefit of using simulation is that the uncertainty in scour can be quantified as a function of the uncertainty in the hydraulic model and its parameters. The result is a probabilistic scour estimate (i.e., one that has a mean, standard deviation, and probability distribution associated with it). The drawback of using Monte Carlo simulations is the large number of calculations that are needed, particularly when dealing with large numbers of random variables and low probabilities.

Johnson and Dock (1998) used Monte Carlo simulation to generate random samples of the parameters in the HEC-18 pier scour equation based on the associated coefficients of variation
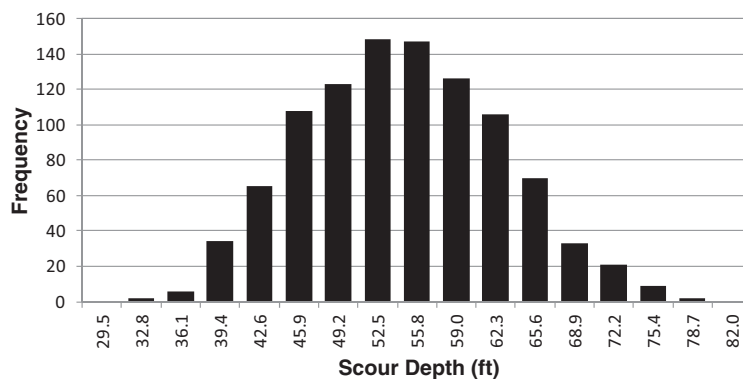
Figure 2.4. **Frequency histogram for 1,000 simulated scour depths.**

and distributions described in Section 2.3.2 and Table 2.2. They also accounted for model uncertainty using a model correction factor and its COV and distribution. Using the example of a 500-year storm at the Bonner Bridge in North Carolina, they generated a scour distribution with a mean scour depth of 53.2 ft (16.21 m), a COV of 0.090, and a normal distribution (Figure 2.4). Following this process, probabilistic statements can be made regarding the likelihood of obtaining a specified scour depth. These types of results, based on the uncertainty in the hydrologic input, hydraulic parameters, and model uncertainty, are the basic input for risk and reliability analyses.

2.4.2 FHWA Guidance—Incorporating Risk in Bridge Scour Analyses

As additional background, this section presents FHWA's latest guidance on risk analysis as applied to bridge scour (see the 5th edition of HEC-18, published in April 2012). To ensure precision, the section presents pertinent excerpts from HEC-18 Chapter 2 and Appendix B verbatim.

Bridge foundations for **new** bridges should be designed to withstand the effects of scour caused by hydraulic conditions from floods larger than the design flood. In 2010, the U.S. Congress recommended that FHWA apply risk-based and data-driven approaches to infrastructure initiatives and other FHWA bridge program goals. This included the FHWA Scour Program. Risk-based approaches factor in the importance of the structure and are defined by the need to provide safe and reliable waterway crossings and consider the economic consequences of failure. For example, principles of economic analysis and experience with actual flood damage indicate that it is almost always cost-effective to provide a foundation that will not fail, even from very large events. However, for smaller bridges designed for lower frequency floods that have lower consequences of failure, it may not be necessary or cost-effective to design the bridge foundation to withstand the effects of extraordinarily large floods. Prior to the use of these risk-based approaches, all bridges would have been designed for scour using the Q_{100} flood magnitude and then checked with the Q_{500} flood magnitude. [Table 2.3] presents recommended **minimum** scour design flood frequencies and scour design check flood frequencies based on hydraulic design flood frequencies (Arneson et al. 2012).

The Hydraulic Design Flood Frequencies outlined in [Table 2.3] assume an inherent level of risk. There is a direct association between the level of risk that is assumed to be acceptable at a structure as defined by an agency's standards and the frequency of the floods they are designed to accommodate.

2.4.2.1 Discussion of Design Flood Frequencies

The Scour Design Flood Frequencies presented in [Table 2.3] are larger than the Hydraulic Design Flood Frequencies because there is a reasonably high likelihood that the hydraulic design flood will be exceeded during the service life of the bridge. For example, using [Table 2.4] . . . it can be seen that during a 50-year design life there is a 39.5% chance that a bridge designed to pass the Q_{100} flood will experience that flood or one that is larger. Similarly, there is a 63.6% chance that a bridge that is designed to pass the Q_{50} flood will experience that or a larger flood during a 50-year design life. Using the larger values for the Scour Design Flood Frequency for the 200-year flood and a 50-year design life reduces the exceedance value to 22.2%. This is considered to be an acceptable level of risk reduction. In other words, a bridge **must** be designed to a higher level for scour than for the hydraulic design because if the hydraulic design flood is exceeded then a greater amount of scour will occur which could lead to bridge failure. Also, designing for a higher level of scour than the hydraulic design flood ensures a level of redundancy after the hydraulic design event occurs.

Table 2.3.   Hydraulic design, scour design, and scour design check flood frequencies (Arneson et al. 2012).

Hydraulic Design Flood Frequency, Q_D	Scour Design Flood Frequency, Q_S	Scour Design Check Flood Frequency, Q_C
Q_{10}	Q_{25}	Q_{50}
Q_{25}	Q_{50}	Q_{100}
Q_{50}	Q_{100}	Q_{200}
Q_{100}	Q_{200}	Q_{500}

Table 2.4.   Probability of flood exceedance of various flood levels (Arneson et al. 2012).

Flood Frequency	Probability of Exceedance in N Years (or Assumed Bridge Design Life)						
Years	N = 1	N = 5	N = 10	N = 25	N = 50	N = 75	N = 100
10	10.0%	41.0%	65.1%	92.8%	99.5%	100.0%	100.0%
25	4.0%	18.5%	33.5%	64.0%	87.0%	95.3%	98.3%
50	2.0%	9.6%	18.3%	39.7%	63.6%	78.0%	86.7%
100	1.0%	4.9%	9.6%	22.2%	39.5%	52.9%	63.4%
200	0.5%	2.5%	4.9%	11.8%	22.2%	31.3%	39.4%
500	0.2%	1.0%	2.0%	4.9%	9.5%	13.9%	18.1%

The Scour Design Check Flood Frequencies are larger than the Scour Design Flood Frequencies using the same logic and for the same reasons as outlined above (Arneson et al. 2012).

If there is a flood event greater than the Hydraulic Design Flood but less than the Scour Design Flood that causes greater stresses on the bridge, e.g., overtopping flood, it should be used as the Scour Design Flood. For this condition there would not be a Scour Design Check Flood since the overtopping flood is the one that causes the greatest stress on the bridge. Similarly, if there is a flood event greater than the Scour Design Flood but less than the Scour Design Check Flood that causes greater stresses on the bridge, it should be used as the Scour Design Check Flood. Balancing the risk of failure from hydraulic and scour events against providing safe, reliable, and economic waterway crossings requires careful evaluation of the hydraulic, structural, and geotechnical aspects of bridge foundation design (Arneson et al. 2012).

2.4.2.2 Flood Exceedance Probabilities

A flood event with a recurrence interval of T years has a 1/T probability of being exceeded in any one year. The 100-year recurrence-interval flood is often used as a hydraulic design value and to establish other types of flooding potential. Regardless of the flood design level, there is a chance, or probability, that it will be exceeded in any one year and the probability increases depending on the life of the structure. The probability that a flood event frequency will be exceeded in N years depends on the annual probability of exceedance as defined by:

$$P_N = 1 - (1 - P_a)^N \qquad (2.1)$$

where:

P_N = Probability of exceedance in N years
P_a = Annual probability of exceedance (1/T)
N = Number of years
T = Flood event frequency of exceedance

The number of years, N, can be assumed to equal the bridge design life or remaining life. [Table 2.4] shows the probability of exceedance of various flood frequencies for time periods (that may be assumed to equal the bridge design life) ranging from 1 to 100 years. For example a 100-year flood has an annual (N = 1) probability of exceedance of 1.0%, but has a 39.5% chance of exceedance in 50 years. A 200-year flood has a 22.2% chance of being exceeded in 50 years and a 31.3% chance of being exceeded in 75 years (Arneson et al. 2012).

FHWA notes that the probability of exceedance may be applied to an individual bridge or for a population of similar bridges. Therefore, if a 200-year design flood condition is used for a population of bridges with expected design lives of 75 years, then that flood condition will be exceeded at approximately 31.3% of the bridges over their lives. Because design flood conditions are exceeded at many bridges during their useful lives, factors of safety, conservative design relationships, and LRFD are used to provide adequate levels of safety and reliability in bridge design.

2.5 LRFD—A Hydraulic Engineering Perspective

2.5.1 Introduction

The LRFD methodologies for bridge design were initially developed using concepts derived from structural engineering procedures. LRFD incorporates state-of-the-art analysis and design methodologies with load and resistance factors based on the known variability of applied loads and material properties. These load and resistance factors are calibrated from actual bridge statistics to ensure a uniform level of reliability. LRFD allows a bridge designer to focus on a design objective or limit state, which can lead to a similar probability of failure in each component of the bridge. Bridges designed with the LRFD specifications should have relatively uniform safety levels, which should ensure superior serviceability and long-term maintainability.

Scour of earth materials from around bridge foundation elements does not represent a load, but a loss of resistance. Hydraulic engineers are tasked with estimating scour depths for different types of scour processes (e.g., pier, contraction, and abutment scour). Scour estimates typically are associated with a design flood event (e.g., a 100-year flood). Structural and geotechnical engineers use this information for developing a bridge design to maintain structural stability that accommodates the loss of resistance due to scour.

2.5.2 Reliability

The aim of reliability theory, as incorporated in LRFD methodology, is to account for the uncertainties encountered while evaluating the safety of structural systems or during the calibration of load and resistance factors for structural design codes. More detailed explanations of the principles discussed in this section can be found in published texts on structural reliability and risk such as those by Thoft-Christensen and Baker (1982); Nowak and Collins (2000); Melchers (1999); Ayyub (2003); and Ayyub and McCuen (2003).

The uncertainties associated with predicting the load-carrying capacity of a structure, the intensities of the loads expected to be applied, and the effects of these loads may be represented by random variables. The value that a random variable can take is described by a probability distribution function. That is, a random variable may take a specific value with a certain probability and the ensemble of these values and their probabilities is described by the probability distribution function.

The most important characteristics of a random variable are its mean (or average) value, and the standard deviation that gives a measure of dispersion (or uncertainty) in estimating the variable. A dimensionless measure of the uncertainty is the coefficient of variation (COV), which is the ratio of standard deviation divided by the mean value. For example, the COV of the random variable R is defined as V_R such that:

$$V_R = \frac{\sigma_R}{\bar{R}} \tag{2.2}$$

where:

σ_R = Standard deviation
$\bar{R}$ = Mean value

Codes often specify nominal values for the variables used in design equations. These nominal values are related to the means through bias values. The bias is defined as the ratio of the mean to the nominal value used in design. For example, if R is the resistance, then the mean of R, expressed as $\bar{R}$, can be related to the nominal (or design) value R_n using a bias factor such that:

$$\bar{R} = b_r R_n \tag{2.3}$$

where:

b_r = Resistance bias
R_n = The nominal value as specified by the design code

For example, A36 steel has a nominal design yield stress of 36 ksi (248,220 kPa), but coupon tests show an actual average value close to 40 ksi (275,800 kPa). Hence, the bias of the yield stress is 40/36 or 1.1. In addition to material properties, the bias and the COV in member resistance account for fabrication errors and modeling uncertainties reflecting the existing lack of precision in the ability to model the actual strength of structural members even when the material properties and dimensions are precisely known.

In structural reliability, safety may be described as the situation in which capacity (e.g., strength, resistance, fatigue life, foundation depth) exceeds demand (e.g., load, moment, stress ranges, scour depth). Probability of failure (i.e., probability that capacity is less than load demand) may be formally calculated; however, its accuracy depends on detailed data on the probability distributions of load and resistance variables. Given that such data are often unavailable, approximate models are often used for calculation.

The reserve margin of safety of a bridge component can be defined as Z, such that:

$$Z = R - S \tag{2.4}$$

where:

R = Capacity
S = Total load demand

The probability of failure, P_f, is the probability that R is less than or equal to the total applied load effect, S, which is equivalent to the probability that Z is less than or equal to zero. This relationship is symbolized by Equation (2.5):

$$P_f = P_r[R \leq S] \tag{2.5}$$

where:

P_r is used to symbolize the term Probability.

If R and S follow independent normal distributions, then:

$$P_f = \Phi\left(\frac{0 - \overline{Z}}{\sigma_Z}\right) = \Phi\left(-\frac{\overline{R} - \overline{S}}{\sqrt{\sigma_R^2 + \sigma_S^2}}\right) \tag{2.6}$$

where:

Φ = Normal probability function that gives the probability that the normalized random variable is below a given value
$\overline{Z}$ = Mean safety margin
σ_Z = Standard deviation of the safety margin

Equation (2.6) gives the probability that Z is less than zero. The reliability index, β, is defined such that:

$$P_f = \Phi(-\beta) \tag{2.7}$$

which for the normal distribution case gives:

$$\beta = \frac{\overline{Z}}{\sigma_Z} = \frac{\overline{R} - \overline{S}}{\sqrt{\sigma_R^2 + \sigma_S^2}} \tag{2.8}$$

Thus, the reliability index, β, which is often used as a measure of structural safety, gives in this instance the number of standard deviations that the mean margin of safety falls on the "safe" side.

The reliability index, β, defined by Equation (2.8), provides an exact evaluation of risk (failure probability) if R and S follow normal distributions. Although β was originally developed for normal distributions, similar calculations can be made if R and S are lognormally distributed (i.e., when the logarithms of the basic variables follow normal distributions). Other methods have been developed to obtain the reliability index, β, for cases when the basic variables are not normally distributed.

More advanced techniques have also been developed to improve the estimates when the failure function is highly nonlinear. On the other hand, Monte Carlo simulations can be used to provide estimates of the probability of failure (e.g., the probability of exceeding a design value). Monte Carlo simulations are suitable for any random variable probability distribution type and failure equation.

In essence, a Monte Carlo simulation involves the creation of a large number of "experiments" through the random generation of sets of resistance and load variables. Estimates of the probability of failure, P_f, are obtained by comparing the number of experiments that produce failure (or exceedance of a design value) to the total number of generated experiments. Given values of the probability of failure, P_f, the reliability index, β, is calculated from Equation (2.7) and used as a measure of structural safety even for non-normal distributions.

2.5.3 LRFD Code Calibration

The reliability index, β, has been used by many groups throughout the world to express structural risk. A value of β in the range of 2 to 4 is usually specified for different structural applications. For example, β = 3.5 was used for the calibration of the Strength I limit state in AASHTO's LRFD specifications for the design of new bridges (AASHTO 2007). The calibration process as described by Nowak (1999) and Kulicki et al. (2007) is based on the reliability of bridge members subject to random truck loads within a 75-year design life. On the other hand, the load and resistance factor rating (LRFR) provisions in the AASHTO *Manual for Bridge Evaluation* (2008) were calibrated to meet a target reliability index of β = 2.5 for checking the safety of existing bridges under random truck loads for a rating period of 5 years (Moses 2001).

The difference between the two return periods and target reliability values in the AASHTO LRFD and LRFR is justified based on a strict inspection process for existing bridges and a qualitative cost-benefit analysis. Although demanding higher reliability levels for new designs will imply a marginal increase of bridge construction costs, the replacement of existing bridges would lead to major construction as well as other tangible and intangible economic and other costs associated with the disruption of traffic.

In structural design and evaluation, the reliability index values used in the AASHTO LRFD and LRFR calibrations correspond to the failure of a single component. If there is adequate redundancy, however, overall system reliability indices will be higher, as indicated by Ghosn and Moses (1998) and Liu et al. (2001), who proposed the application of system factors calibrated to meet system reliability criteria rather than component criteria. A slightly different approach taken in ASCE 7-10 (2010) recommends the use of different member reliability targets based on the consequences of a member's failure. Thus, the target reliability, β_{target}, to be used for the design of a connection must be higher than that of a beam in bending.

Generally speaking, the reliability index, β, is not used in practice for making decisions regarding the safety of a particular design or an existing structure, but instead is used by

code-writing groups for recommending appropriate load and resistance safety factors for new structural design or evaluation specifications. One commonly used calibration approach is based on the principle that each type of structure should have uniform or consistent reliability levels over the full range of applications. For example, in the calibration of the AASHTO LRFD and LRFR codes, load and resistance factors were chosen to produce β values that uniformly match a target reliability level, β_{target}, for bridges of different span lengths, number of lanes, simple or continuous spans, roadway categories, strength, and so forth. Ideally, a single target β is achieved for all applications.

Current reliability models do not account for the effects of material degradation under environmental factors or the expected changes in truck loading conditions over time. A significant amount of theoretical research work has been ongoing over the last 2 decades to develop time-dependent reliability models to account for the deterioration of concrete beams and the corrosion of steel bridge girders and their influence on member, as well as system strength. These efforts, however, have not yet matured to a level at which they can be applied in the LRFD specifications to help extend the useful life of the next generation of bridges and obtain good estimates of the safety and reliability of existing bridges subjected to harsh environments.

The same is true with regard to the design for extreme events other than live loads. A probabilistic model for the consideration of ship collisions is based on calculating a nominal annual probability of failure that should not exceed 0.001 (see AASHTO 2009). However, the design criteria for limit states associated with other types of extreme events are based on previous generations of codes that were not based on reliability principles. In these cases, emphasis was placed on the hazard analysis of the load events without explicitly considering the uncertainties in the response of the bridge to these events and the ability of the bridge to withstand their effects. For example, recent proposals recommend using for design the earthquakes corresponding to a 1,000-year return period without explicitly accounting for the uncertainties associated with estimating the dynamic bridge response or the ability of a bridge system to resist the applied seismic ground motions (Imbsen 2007). Threats from floods are based on probabilistic models of flood occurrence without considering other modeling uncertainties (e.g., the bias and COV of scour prediction equations) and the parametric uncertainties associated with estimating discharge, flow depth, flow velocity, and so forth as discussed in Sections 2.2 and 2.3.

Furthermore, existing bridge design codes propose different return periods—and consequently various levels of conservatism (or safety factors)—for different hazards. For example, the calibration of the live load factors in the AASHTO LRFD is based on the 75-year maximum load effect, the wind maps use 50-year maximum wind speeds, and a 1,000-year return period has been proposed for seismic hazards, whereas scour predictions are based on flood events having various return periods based on bridge size and level of service (see Table 2.3).

Given that structural safety is related to both the magnitude of the hazard and the vulnerability of the bridge elements to that hazard, the discrepancies in the current methods may not lead to consistent levels of reliability for the different hazards that a bridge may be subjected to. To account for many of these uncertainties, some specification writers have recommended the design of bridges for hazard levels corresponding to very high return periods. For example a 2,500-year return period was recommended for seismic hazards when using the traditional force-based design methods, whereas recent proposals have suggested the use of a 1,000-year return period in conjunction with a performance-based design approach (ATC/MCEER 2002, Imbsen 2007). Although the use of different return periods to account for the different levels of conservatism and uncertainties associated with the analysis and design approaches is a valid approach for developing design codes, the determination of the code-specified design return period must be supported using probabilistic analyses of the overall safety of the structure.

During the calibration of a new design code, the average reliability index from typical "safe" designs is used as the target reliability value for the new code. That is, a set of load and resistance factors as well as the nominal loads (or return periods for the design loads) are chosen for the new code such that bridges designed with these factors will provide reliability index values (β values) equal to the target value as closely as possible. For example, Nowak (1999) used a reliability index of $\beta = 3.5$ for the design of new bridge members. On the other hand, Moses (2001) used a reliability index of $\beta = 2.5$ for the evaluation of load capacity of existing bridges.

Both targets are based on a generic set of load- and member-capacity statistical data bases that are believed to represent the most typical loading conditions and material properties. The differences between $\beta = 3.5$ (new bridges) and $\beta = 2.5$ (existing bridges) have been justified based on cost implications, given that the design of new bridges to higher safety standards would only marginally increase the cost of construction, whereas increasing the load capacity criteria for an existing bridge may require its replacement and lead to considerable costs. The lower safety criteria for existing bridges are, however, associated with strict requirements for regular inspection. Ghosn et al. (2003) found that existing design criteria for extreme events (other than scour) are associated with reliability index values that typically vary between $\beta = 2.0$ and $\beta = 3.5$.

The calibration process discussed in this section does not contain any pre-assigned numerical values for the target reliability index. This traditional approach to the calibration of LRFD criteria (e.g., AISC, AASHTO) has led code writers to choose different target reliabilities for different types of structural elements or for different types of loading conditions. For example, in the AISC LRFD, a target β equal to 3.5 was chosen for the reliability of beams in bending under the effect of dead and live loads, whereas a target β equal to 4.0 was chosen for the connections of steel frames under dead and live loads, and a target β equal to 2.5 may be chosen for the main members of a structure that is subject to earthquakes. A reliability index of $\beta = 3.5$ corresponds to a probability of limit state exceedance equal to 2.3×10^{-4}, whereas a reliability index of $\beta = 2.5$ corresponds to a probability of exceedance equal to 6.2×10^{-3}.

Similarly, the USACE (1992) determined that probabilities of unsatisfactory conditions greater than 0.001 for inland navigation structures suggest that frequent outages for repair may occur and at a probability of 0.07 a need for extensive rehabilitation may be required. For structures with even greater probabilities of limit state exceedance, emergency action is required to alleviate risks. Such differences in the target reliability index and associated probabilities clearly reflect the economic costs associated with the selection of the target β and the consequences of exceeding a limit state.

Much progress has been made over the last 3 decades to apply reliability methods during the development of bridge design and evaluation specifications. However, current bridge design specifications and the equations used to model bridge behavior and member/system capacities under various threats are inconsistent and are presented in a format that blurs the implicit levels of conservatism to the end users. Existing discrepancies in the design return periods and the methods used by the specifications to treat the different types of hazards, including scour, have to be overcome in order to address issues related to multi-hazard risk management and life cycle engineering principles (Ghosn et al. 2003).

Evaluating Uncertainty Associated with Scour Prediction

3.1 Introduction

Bridge scour processes, including pier, abutment, and contraction scour, have been well researched over the past several decades and equations have been developed to estimate scour depths for each of the scour components. The vulnerability of a bridge to scour is due to the existence of a weakness or a design that can lead to an unexpected, undesirable event compromising the bridge safety. By assessing and quantifying all sources of uncertainty in the parameters and equations used in the design estimation for scour, the reliability of a bridge scour estimate and the probability that the design estimate will be exceeded over the design life of the bridge can be determined, thus reducing the vulnerability to an undesirable event.

This chapter describes an approach to evaluating the uncertainty of the three scour components. The approach is based on Monte Carlo simulation linked directly with the most common and widely accepted hydraulic model used in current practice, HEC-RAS. For each individual scour component, the parameters that were allowed to vary in the Monte Carlo simulations are discussed along with a matrix of other factors and/or considerations that were not addressed. The chapter provides a discussion of model uncertainty and the definitions of bias and the COV in relation to the scour equations. The chapter concludes with a discussion of the linkage between the hydraulic model HEC-RAS and the Monte Carlo simulation software, and the implementation and testing of the software.

3.2 Determining Individual Scour Component Uncertainty

The current practice for determining the total scour prism at a bridge crossing generally involves summing individually calculated scour components. The scour components include local scour (pier and abutment), contraction scour (live-bed or clear-water), and long-term channel change (degradation, lateral migration, and channel widening). Uncertainty is not directly addressed in the determination of any of the scour components, so current practice establishes a design amount of scour that is generally recognized as conservative, although the level of conservatism is undefined. For scour at bridge abutments, HEC-18 (Arneson et al. 2012) now recommends a methodology developed under NCHRP Project 24-20 (Ettema et al. 2010), which provides an estimate of abutment and contraction scour combined. Chapter 4 provides a summary of the individual scour equations.

Pier, abutment, and contraction scour each involve two types of uncertainty; parameter (aleatory) uncertainty and model (epistemic) uncertainty. This is because each type of scour is defined by an equation (model) that includes variables (parameters) that must be estimated. In the research that produced this reference guide, Monte Carlo simulation was used

27

to assess parameter uncertainty and observed data (laboratory and field) was used to assess model uncertainty. Each of the variables (discharge, velocity, flow depth, particle size, etc.) used in scour calculations possesses a probability density function defined by the distribution type (normal, lognormal, etc.), and distribution properties (mean, standard deviation [SD], skew, etc.).

Monte Carlo simulation was used to address the parameter uncertainty for the local and contraction scour equations or in the case of abutment scour, local scour and contraction scour combined. The Monte Carlo simulation included a hydraulic modeling step in which a hydraulic model was run for a large number of scenarios to develop the input variables for the scour computations. HEC-RAS was used for this step (see USACE 2010). Each run provided data to be used to compute both local and contraction scour. The HEC-RAS input parameters that were varied are discharge, boundary condition (energy slope), channel Manning n, and floodplain Manning n. HEC-RAS produced the hydraulic variables for the scour components, which are velocity, flow depth, and flow distribution between the channel and the overbank areas.

3.3 Parameter and Model Uncertainty

3.3.1 Parameter Uncertainty

The Monte Carlo simulations included the following random variables:

- Hydraulic modeling
  - Hydrologic uncertainty (Log-Pearson Type III)
  - Channel Manning n
  - Floodplain Manning n
  - Boundary condition (energy slope)
- Pier scour
  - Equation (HEC-18 and Florida DOT [Sheppard et al. 2011])
  - Velocity and flow depth
- Abutment scour
  - Equation and methodology for total scour (NCHRP Project 24-20 [Ettema et al. 2010])
  - Obstructed flow area, discharge, velocity, and depth
- Contraction scour
  - Upstream flow distribution (Q_1)
  - Bridge flow distribution (Q_2, Q_{left}, Q_{right})
  - Flow depths (Y_1, Y_o)

Two categories of factors were not included in the Monte Carlo simulation (see Table 3.1). One category is composed of parameters that would be known in a bridge design, such as pier dimensions or road elevation. Therefore, these parameters would be constants and thus be considered deterministic instead of random. The other category that was excluded from the Monte Carlo simulation includes factors that would overly complicate the analysis. As shown in Table 3.1, examples of these types of variables are multiple bridge openings and time rate of scour.

3.3.2 Model Uncertainty

Model (equation) uncertainty depends on how well a given scour equation predicts scour. It can be evaluated by comparing observed scour to predicted scour, comparing simulated scour to predicted scour, or by expert knowledge. **For this study, model uncertainty is represented by the statistical properties of the ratio of observed scour to predicted scour for a given scour equation. The mean of the ratios is the bias (λ), and the standard deviation of the ratios divided by the bias is the coefficient of variation (COV).**

Table 3.1. Deterministic variables and overcomplicating factors not considered in the Monte Carlo simulations.

Topic	Deterministic Variables	Overcomplicating Factors
Hydraulic modeling	• Bridge or embankment skew • Pier size, shape, and skew • Varying road elevation • Abutment shape	• Non-stationary aspects of hydrologic uncertainty (climate change, sea level rise/fall) • Multiple bridge openings • 2-D modeling or complex hydraulic situations
Pier scour	• Pier shape • Pier width • Pier length • Skew angle	• Material erodibility (clay, rock) • Complex pier geometry • Debris or ice • Time rate of scour • Armoring
Abutment scour	• Abutment shape • Embankment skew	• Material erodibility (clay, rock) • Time rate of scour • Change in abutment shape during scour
Contraction scour	• Embankment length • Abutment setback • Approach channel width • Contracted channel width	• Material erodibility (clay, rock) • Relief bridge scour • Time rate of scour • Pressure scour (vertical contraction scour) • Channel bed forms for live-bed conditions
Scour interaction	NA	• Overlapping scour holes (pier-to-pier or abutment-to-pier)
Long-term channel changes	NA	• Aggradation, degradation, or headcuts • Lateral migration • Channel width adjustments

As discussed in Chapter 4, the bias and COV for each of the scour equations were evaluated based on available laboratory and field data, and the reliability index, β, was determined for each scour equation. Because the determination of bias and COV requires observed data, the limitations of each data source need to be addressed. Laboratory data have the disadvantages of small scale, inconsistent length scales (geometric and sediment), and a predominance of clear-water conditions. Field data have the disadvantages of being uncontrolled, large parameter uncertainty, difficulties associated with measuring scour, difficulties in separating types of scour, unmeasured scour-hole refill, highly variable bed materials, and non-ultimate scour levels.

Contraction scour is widely accepted as a sediment transport problem. However, finding reliable laboratory and field contraction scour data was a problem (see Section 4.3). Ultimate live-bed contraction scour is reached when the rate of sediment transport in the bridge opening matches the supply of sediment from the upstream channel. Ultimate clear-water contraction scour is reached when the flow can no longer erode the bed. Most bridge waterway openings are, in reality, short contractions. However, the HEC-18 contraction scour equations were derived using a long contraction, thus introducing additional uncertainty.

Long-term channel changes are components of total scour that need to be considered in bridge design, although they cannot be addressed in the same manner as local and contraction scour. Degradation and lateral migration often contribute significantly to total scour at bridges, although aggradation and channel widening may also cause problems. Future degradation and aggradation may be estimated in several ways, including bridge inspection profiles, rating curve shifts, equilibrium slope, sediment continuity, sediment transport modeling, and headcut analysis. Future amounts of channel migration can be estimated by comparing historic

aerial photos as described in *NCHRP Report 533: Handbook for Predicting Stream Meander Migration* (Lagasse et al. 2004).

Rather than developing uncertainty parameters related to long-term vertical and lateral channel change, standard design approaches were used. The standard approach currently used in bridge design is to establish a conservative estimate of future channel change (Arneson et al. 2012, Lagasse et al. 2012). Uncertainty and reliability approaches for predicting long-term channel change were not considered in this study.

3.4 Development of Supporting Software

3.4.1 HEC-RAS

For each bridge type analyzed, a representative HEC-RAS model was developed to assess the hydraulic conditions at the bridge given the hydrologic and other input variable uncertainties.

Models were developed representing small, medium, and large bridges to support the Level I and Level II analyses (see Chapter 5). Each model consists of:

- A single reach of four cross sections plus the (automatically-generated by HEC-RAS) bridge upstream and bridge downstream sections. These cross sections include ineffective flow areas and flow transition reach lengths, determined using standard engineering methods, appropriate to capture the full effect of flow contraction and expansion at the bridge.
- Manning roughness (n) values assigned with a channel Manning n value and a single over-bank Manning n value for all four cross sections for each realization.
- Design discharge (100-year) set for each bridge.
- The downstream boundary condition, determined by HEC-RAS using a normal depth computation, driven by friction slope. No supercritical simulations were performed; consequently, no upstream water surface elevation computation was required.

Neither overtopping (relief) nor internal pier geometry was directly represented in the models. All flow was forced through the bridge opening. Pier and abutment geometry was considered in the (post-process) scour computations.

3.4.2 Integration of HEC-RAS and Monte Carlo

To analyze the probability of scour depth exceedance, it was necessary to perform a large number of Monte Carlo realizations (cycles) using the HEC-RAS model. This precluded the use of HEC-RAS through its standard graphical user interface (GUI). Consequently, the HEC-RAS application programming interface (API) was used to integrate HEC-RAS simulations with the Monte Carlo simulation software.

Research software (the rasTool©) was developed to automate the running of HEC-RAS. This software included specifying input variables for HEC-RAS geometric and flow files. Results from each run were then appended to a summary output file. This section provides a description of the final rasTool© software and its application to scour risk analysis.

The rasTool© was developed using Microsoft Visual Studio 2010, using the VB.NET language. The program is compatible with Windows XP or Windows 7. **The rasTool© software is a research-level software engine requiring considerable insight on the part of the user for application. The application process used in this study is described in the following paragraphs.**

When rasTool© is started, rasTool© initializes a double-precision random-number generator (RNG), seeded with the computer clock time, to generate a large (~10^{55}), uniformly distributed pseudo-random number string. The uniformly distributed pseudo-random number string values generated by the RNG are transformed as necessary during the Monte Carlo realizations into Gaussian-distributed Z-values using the polar form of the Box-Muller transform and used for all subsequent random numbers required by the simulation (eight per realization). Four of the random numbers are used in the HEC-RAS modeling (discharge, channel Manning n, floodplain Manning n, and energy slope) and four are used in computing scour (HEC-18 pier scour, Florida DOT pier scour, contraction scour, and abutment scour).

Once the Monte Carlo realizations are launched, the rasTool© performs Monte Carlo realizations using the following steps:

Step 1. Randomized input variables are determined for a realization using the input probability density function type, summary statistics, and generated randomized Z-values for each input variable.

Step 2. These input variables are assigned to the HEC-RAS model using the Interop.RAS41 API for geometric variables and direct assignment to input text files for flow and boundary condition variables. The direct assignment of flow variables proved necessary as the Interop.RAS41 API allowed asynchronous updates of flow variables, geometric variables, and simulations, resulting in interleaved updates and inconsistent hydraulic simulation of the desired input variables. Direct assignment of flow and boundary condition variables eliminated this conflict and ensured fully synchronous simulations.

Step 3. HEC-RAS is run for the given geometric, flow, and boundary condition variables assigned.

Step 4. Input variables and detailed hydraulic results are retrieved from the completed HEC-RAS model using the Interop.RAS41.dll API and stored in a results matrix. These results are sufficiently detailed to support contraction scour, abutment scour, and pier scour computations.

Step 5. Steps 1 through 4 are iterated until the user-assigned number of realizations has been performed. From testing, it was determined that 10,000 realizations were sufficient to generate a fully-descriptive data set.

Step 6. The Monte Carlo hydraulic results matrix is written to a text file (OutputMC.txt), along with four standard-normal (Gaussian) random variables per realization to support randomization of the scour results. For this study, scour computations (using HEC-18 and Florida DOT pier methods, contraction, and abutment scour) were performed as a post-processing step in a spreadsheet.

A 10,000-realization simulation requires between 1 and 2 hours of computer time, depending on the machine used.

The rasTool© requires input data from the user to perform its simulation. For each independent input variable, summary statistics and assumed distributions about an expected value are required. This effort randomized discharge, channel Manning n, overbank Manning n, and friction slope for normal depth boundary condition computation. The rasTool© supports normal and lognormal distributions. The rasTool© requires a representative HEC-RAS model of the bridge simulated. Simulation parameters (number of realizations, Z limit) also are required.

Four assumed-independent random geometric and hydraulic variables for each bridge type analyzed were considered for this effort. They were discharge, Manning roughness (overbanks and main channel), and friction slope. The application of these variables is described in Sections 3.4.3, 3.4.4, and 3.4.5.

Table 3.2.   100-year discharge parameters for lognormal distribution (natural log space).

Bridge	A μ[ln (Q)]	B σ[ln (Q)] Hydrologic Uncertainty		
		Low	Medium	High
Large	11.8791	0.1282	0.1865	0.2448
Medium	10.3015	0.1111	0.1617	0.2123
Small	7.5175	0.0811	0.1180	0.1549

Table 3.3.   Illustrative example: low hydrologic uncertainty; A and B based on gage analysis (N = 49 years).

Event		A	B
p(X > x)	T (yrs)	μ[ln (Q)]	σ[ln (Q)]
0.04	25	11.64920308	0.115282339
0.02	50	11.77682701	0.125057456
0.01	100	11.88793137	0.133901695
0.002	500	12.10459348	0.151400894

3.4.3 Discharge

A lognormal discharge distribution about its expected value (mean in logarithm transform) was assumed. The expected value discharge was constant for all hydrologic uncertainty scenarios for a given annual exceedance probability and bridge type (small, medium, or large) as presented in Table 3.2 and Table 3.3 (see also Section 5.2.3). The expected value discharge parameter (in natural logarithm space, A) was determined for each bridge type using Bulletin 17B methods for the relevant period of record and normalized to a N=50-year period of record (see Section 2.2). Notice that the Bulletin 17B predicted discharge for a given exceedance probability represents the mode in linear space, not the mean (expected) value in logarithmic space. The expected value discharge (in natural logarithmic space) is the statistical mean discharge parameter of interest for the Monte Carlo realizations.

COV values for a given hydrologic uncertainty scenario were based on a qualitative review of Bulletin 17B flood frequency analyses performed at eight USGS gaged sites to assess the observed range of discharge COV as a function of period of record and regional variation. COV was constant for a given hydrologic uncertainty and annual exceedance probability, as presented in Table 3.4.

Table 3.4.   Hydrologic uncertainty as a function of annual exceedance probability.

Annual Exceedance		Discharge COV (lognormal)		
p(X > x)	T (yrs)	Low	Medium	High
0.04	25	0.009	0.014	0.018
0.02	50	0.010	0.015	0.019
0.01	100	0.011	0.016	0.021
0.005	200	0.012	0.017	0.022
0.002	500	0.013	0.018	0.023

Table 3.5.   Manning roughness coefficients assuming lognormal distribution.

Linear		Natural Log Space	
Manning n	COV	A $\mu[\ln(n)]$	B $\sigma[\ln(n)]$
0.025	0.015	-3.690411607	0.055356174
0.035	0.015	-3.353672518	0.050305088
0.045	0.015	-3.102175432	0.046532631
0.09	0.015	-2.40859826	0.036128974
0.1	0.015	-2.303181866	0.034547728
0.12	0.015	-2.120769523	0.031811543

The COV values in Table 3.4 were multiplied by the expected value discharge in natural logarithm space to determine discharge lognormal standard deviation values for each bridge type (small, medium, or large) and hydrologic uncertainty scenario (low, medium, or high). Natural log space expected value discharge (A) and standard deviation (B) were input to the Monte Carlo realizations. Input parameters to the Monte Carlo simulation were constant for each bridge type and hydrologic uncertainty scenario, and are presented in Table 3.2.

3.4.4 Manning Roughness Coefficient

Manning roughness values were randomized assuming a lognormal distribution. Overbank roughness and main channel roughness were considered independent random variables for this analysis. They were held constant for a given Monte Carlo realization (e.g., all cross sections were assigned the same, independently randomized, overbank roughness and main channel roughness). The linear space mean values were estimated for each bridge type using standard engineering methods for estimating Manning roughness coefficients and were converted into natural logarithmic input variables using the variable transforms presented in Equation (3.10) and Equation (3.11). A constant COV was assumed for all bridge types and hydrologic scenarios. The final natural log space variables are presented in Table 3.5. (See Section 3.5.3 for a discussion of initial estimates, testing, and refinement of these variables.)

3.4.5 Downstream Boundary Friction Slope

The downstream boundary friction slope was assumed to be normally distributed about the expected (mean) value. Expected values were estimated in the field for each bridge type (see Section 5.2.3). Standard deviation values were determined using COV values developed as shown in Table 3.6. The final values of downstream boundary friction slopes for each of three bridge types (small, medium, or large) as defined in Table 5.1 are presented in Table 3.6. (Section 3.5.3 provides a discussion of initial estimates, testing, and refinement of these variables.)

Table 3.6.   Friction slopes assuming normal distribution.

Linear		
μ	COV	σ
0.0048	0.1	0.00048
0.0024	0.1	0.00024
0.005	0.1	0.0005

3.4.6 Summary

Each Monte Carlo realization generated a set of randomized input variables based on the underlying input variables and summary statistics discussed in this section. These variables were assigned to the HEC-RAS model and a HEC-RAS model run was performed for each realization. Once this run was complete, input variables and hydraulic results for the realization to support pier scour (HEC-18 and Florida DOT methods), contraction scour (HEC-18 methods), and abutment scour (NCHRP Project 24-20 method as presented in HEC-18) were accessed using the rasTool© software and exported in a tab-delimited text file for post-processing. Four additional double-precision, normally distributed, random variable values were recorded for each realization to support randomization of the (post-processed) scour predictions based on the scour prediction component bias and COV from the data analysis in Chapter 4.

3.5 Implementing the Software

3.5.1 Approach

A four cross-section HEC-RAS bridge hydraulic model was developed for each Monte Carlo simulation. The base-model input parameters, including discharge, Manning n (channel and overbank), and downstream energy slope and the corresponding uncertainties in these parameters were specified in the input file of the rasTool© program. The rasTool© output included hydraulic results for the base condition (expected values) and output for each of the randomly generated input parameter values. RasTool© does not make scour calculations but does create a table of output. This output table is then copied and pasted into an Excel spreadsheet that performs the scour calculations. For each simulation, pier (HEC-18 and Florida DOT), contraction (HEC-18), and abutment scour (NCHRP Project 24-20 method) are computed from the Monte Carlo simulation output. The rasTool© software also includes four normally distributed random numbers ($\mu = 0.0$ and $\sigma = 1.0$) for each simulation. The model (equation) bias and COV from the data analysis in Chapter 4 are then applied to each of the computed scour values to compute the expected distribution of each scour component for the specified event.

3.5.2 Hydraulic Parameter Uncertainty

The HEC-RAS Monte Carlo analysis requires that uncertainty in the input parameters be quantified to compute the range of hydraulic conditions and scour that can occur at a bridge. The input parameters selected for HEC-RAS simulations were discharge, channel Manning n, overbank Manning n, and the energy slope downstream boundary condition. Each of these parameters has a value that is either determined or selected during the bridge hydraulic design process, which then results in the design value of scour. By incorporating the hydraulic parameter uncertainty and the model (scour equation) uncertainty, the statistical characteristics of the individual scour components (pier, contraction, and abutment) and total scour can be evaluated.

3.5.2.1 Hydrologic Uncertainty (Discharge)

Flood frequency analysis provides estimates of discharge versus exceedance probability. The Bulletin 17B procedure uses the Log-Pearson Type III distribution to develop the "Bulletin 17B estimate" over the range of annual exceedance probabilities ranging from 0.95 to 0.002, which are the recommended discharges for flood mapping, hydraulic structure design, and other types of analysis (see Section 2.2). The results of the Bulletin 17B procedure also include 95%

confidence limits and an "expected probability" estimate of discharge. As defined by Bulletin 17B, the confidence limits are one-sided, meaning that 95% of the estimates of discharge are greater than the lower bound and 95% less than the upper bound.

The probability distribution of a discharge estimate is established by the expected probability value and the two confidence limits of the log-transformed values. Therefore:

$$\ln(Q_{p\text{-ex},0.95}) = \mu + 1.645\sigma \tag{3.1}$$

$$\ln(Q_{p\text{-ex},0.05}) = \mu - 1.645\sigma \tag{3.2}$$

$$\sigma = \frac{1}{3.29}\ln\left(\frac{Q_{p-ex,0.95}}{Q_{p-ex,0.05}}\right) \tag{3.3}$$

$$\mu = 0.5\ln\left(Q_{p-ex,0.95}\, Q_{p-ex,0.05}\right) \tag{3.4}$$

$$COV_{\ln} = \sigma/\mu \tag{3.5}$$

where $Q_{p-ex,0.05}$ and $Q_{p-ex,0.95}$ are the lower and upper one-sided 95% confidence limits for a particular exceedance probability (p−ex), μ is the log-transformed expected probability discharge value, and σ is the standard deviation of the normally distributed probability density function of the particular exceedance probability.

For example, the 100-year Bulletin 17B flow estimate (p-ex = 0.01) for the test Monte Carlo/HEC-RAS analysis of the Sacramento River bridge (see Section 3.5.3) is 140,000 cfs with expected probability flow of 145,500 cfs and 95% confidence limits of 115,800 cfs and 179,900 cfs. These values result in $\sigma = 0.134$ and $\mu = 11.888$, which are entered as the discharge values for the Monte Carlo simulation flagged as a log-transformed variable.

3.5.2.2 Regional Regression Equations

Where gaging station data is unavailable, the use of regression relationships is a common method for estimating flood magnitudes for various return-period events. These relationships utilize watershed and climatologic characteristics specific to a physiographic region to estimate the 2-year up to the 500-year peak discharge at any location within the region of interest. Typical relationships often take the form $Q_i = A(X_1)^b(X_2)^c, \ldots, (X_n)^n$. In these equations, Q_i is the estimated discharge for an i-year flood, A is a region-specific coefficient, $X_1, X_2, \ldots, X_n$ are watershed and climatologic characteristics such as drainage area, mean annual precipitation, percent forest cover, mean basin elevation, and so forth, and $b, c, \ldots, n$ are region-specific exponents.

The standard error of prediction (SE) in percent is typically reported for each equation and is a measure of the predictive accuracy of the equation for each return period $Q_2, Q_5, \ldots, Q_{500}$ as compared to actual streamflow measurements and gaging station data in that physiographic region. Approximately two-thirds of the estimates obtained from a regression equation for ungaged sites will have errors less than the standard error of prediction (Helsel and Hirsch, 1992).

For purposes of assigning a level of hydrologic uncertainty to ungaged sites where regional regression equations are used to estimate flood magnitudes, the following standard error limits are suggested for the applications in this document:

- **Low hydrologic uncertainty:**   **SE < 15%**
- **Moderate hydrologic uncertainty:**   **15% < SE < 30%**
- **High hydrologic uncertainty:**   **30% < SE**

3.5.2.3 Manning n Uncertainty

As described in Johnson (1996), numerous methods have been used to describe the uncertainty in Manning n estimates. The "data" provided in USACE (1986) are the most comprehensive and are used in this study. The USACE study included nine natural channels with a wide range of conditions in locations throughout the United States. A group of 77 engineers were shown pictures of the channels and asked to estimate the Manning n for a 100-year flow at each location. The engineers could base their estimates on experience, tables, or pictures found in the scientific literature. Outliers were removed from the estimates so that the individual number of estimates ranged from 71 to 77 at each site for a total of 675 estimates and an average of 75 estimates per site. The USACE concluded that the distribution of Manning n was lognormal but did not provide the statistical properties of the log-transformed data.

For this study the USACE estimates were normalized by dividing by the mean estimate for each site and grouping the data into a single data set. The 675 normalized data were then log-transformed to evaluate the suitability of using a lognormal distribution. The results are shown in Figure 3.1 and indicate the suitability of using the lognormal distribution on Manning n for these data.

Figure 3.2 shows the complete probability distribution function (PDF) and cumulative distribution function (CDF) of the normalized Manning n data. With this distribution, 93% of the Manning n values fall between 0.5 and 1.5 of the expected Manning n. The assumption for applying the results in the HEC-RAS Monte Carlo simulation is that the mean estimate of
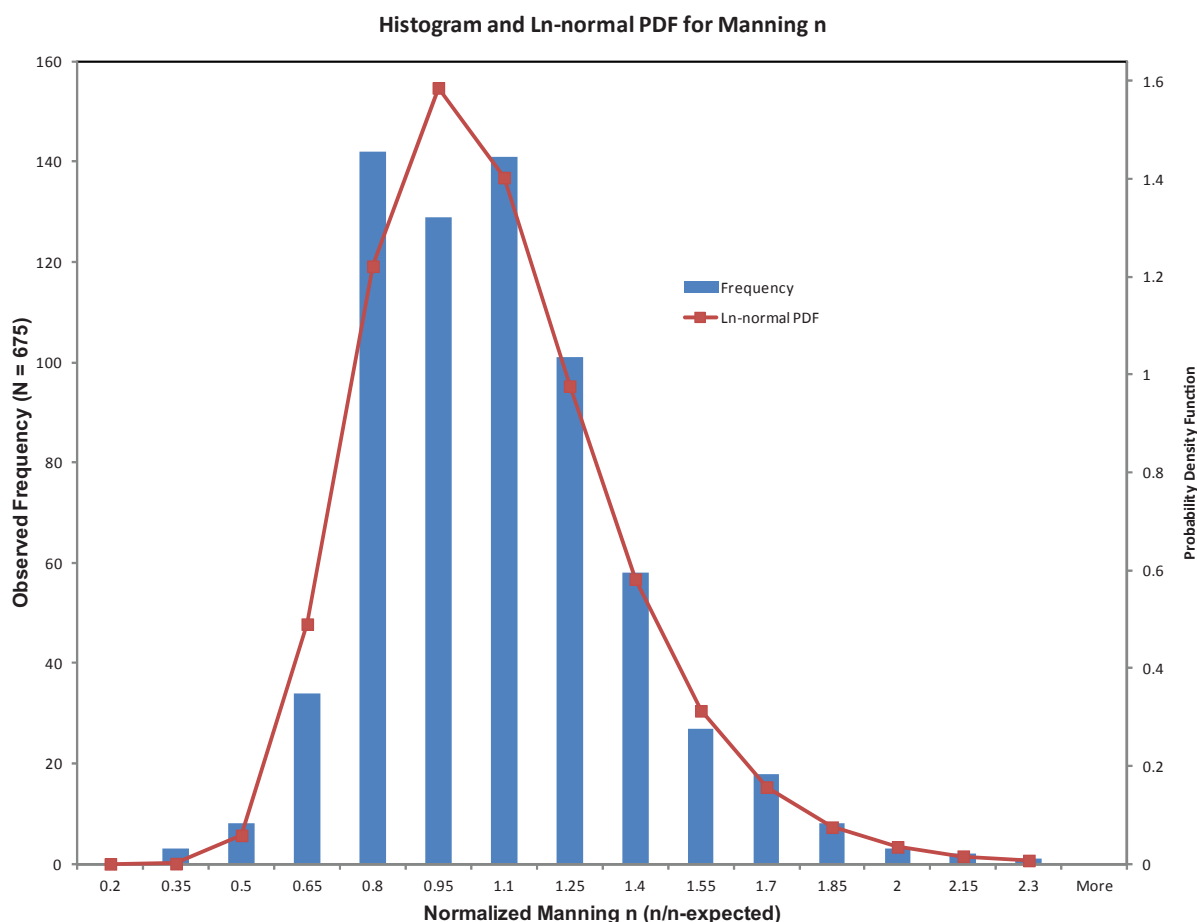
Figure 3.1.   USACE (1986) Manning n data.
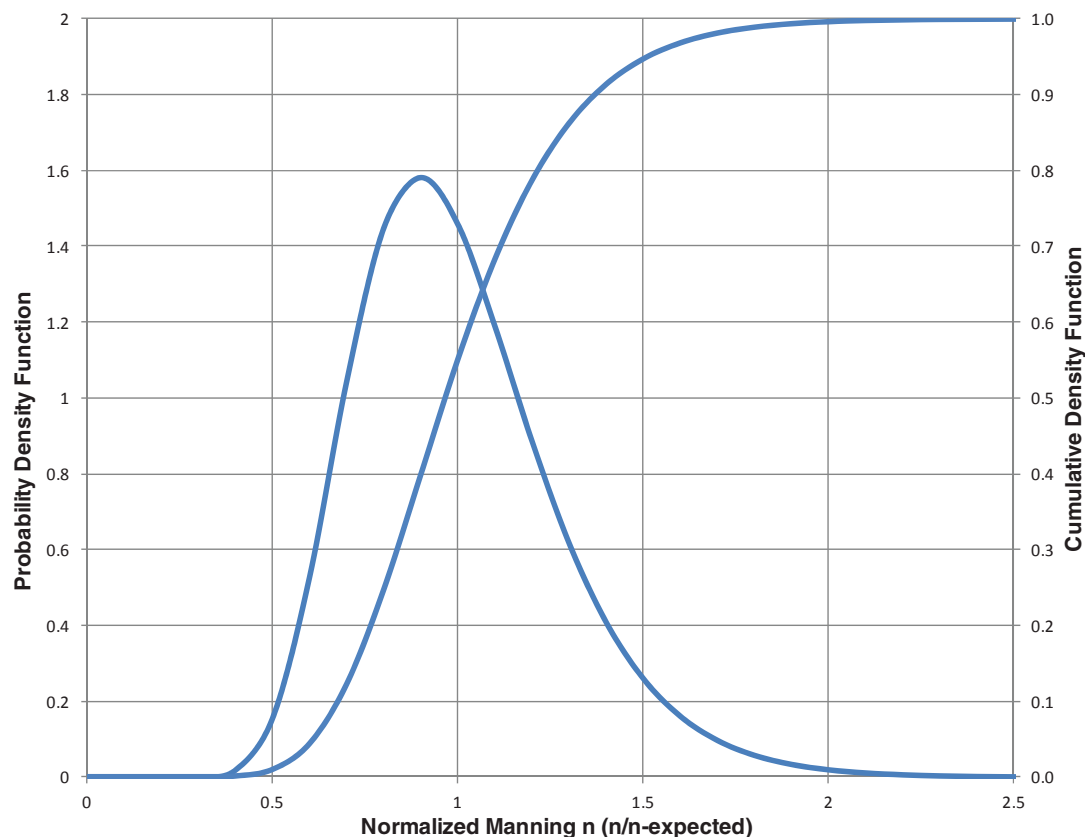
Figure 3.2. *Normalized Manning n probability distribution function and cumulative distribution function.*

the 77 engineers corresponds well to the expected Manning n for the nine rivers at 100-year flood stage.

The COV of the log-transformed data was 0.082. Therefore, an estimate of a channel (or overbank) Manning n (n used in design) can be used to estimate μ and σ of the log-transformed variable using the following equations:

$$n = \exp(\mu + 0.5\sigma^2) = \exp\left[\mu + 0.5(\mu COV)^2\right] \qquad (3.6)$$

$$\mu = \frac{-1 + \sqrt{1 + 2\ln(n)COV^2}}{COV^2} = \frac{-1 + \sqrt{1 + 2\ln(n)0.082^2}}{0.082^2} \qquad (3.7)$$

$$\sigma = \mu COV = \mu 0.082 \qquad (3.8)$$

The values of σ and μ are entered for the Monte Carlo simulation flagged as a log-transformed variable. Because the value of COV of the log-transformed data is 0.082, only the expected channel or overbank Manning n value is required to develop the input for the HEC-RAS/Monte Carlo simulation (see Section 3.5.3).

3.5.2.4 Energy Slope Uncertainty

Although energy slope and channel slope appear to be relatively simple parameters to estimate, Johnson (1996) found this variable to have relatively significant uncertainty that should

not be ignored. Johnson found that several types of distributions have been used to describe channel and friction slope, including uniform, normal, triangular, and lognormal. For this study, a normal distribution with COV = 0.17 was used initially (see Section 3.5.3). This distribution and value was selected such that plus or minus three standard deviations would result in 99.8% of the starting energy slope values between 0.5 and 1.5 times the expected value.

3.5.3 Testing and Adjusting the Software

The Sacramento River bridge (Example Bridge No. 3 in Chapter 7) was used to refine the HEC-RAS/Monte Carlo software. For the initial runs, the hydraulic parameter uncertainty values for discharge, Manning n (channel and overbank), and energy slope as discussed in Section 3.4 were used. The Monte Carlo analysis was compared with data from a gage near the Sacramento River bridge site for flows in the range of the discharges in the Monte Carlo analysis. The comparison was done to test the reasonableness of the Monte Carlo runs. It was determined that the HEC-RAS modeling compared well with the discharge variation at the gage, and that the recommended energy slope parameter uncertainty (normal distribution and COV = 0.17) produced slightly greater variation in water surface and depth as compared to the gage data. The recommended Manning n parameter uncertainty produced extreme variability in water surface. Therefore, the energy slope and Manning n parameter uncertainties were reduced until the combined effects of Manning n and energy slope produced variability similar to that of the water surface measurements at the gage.

Given the large range in discharge as represented by the 5% and 95% confidence limits (see the discussion of hydrologic uncertainty in Section 3.4.3), a large range in water surface elevation and flow depth was expected at the bridge in the Monte Carlo simulation. The Monte Carlo simulation includes flows much further out on the tails of the distribution, so the smallest and largest simulated flows for the 100-year discharge were well under 100,000 cfs to well over 200,000 cfs. Over this range of flows, the HEC-RAS model computed water surface varied by nearly 7 ft when Manning n and energy slope were held constant. Figure 3.3 shows gage heights for extreme flows at the Butte City gage (11389000) on the Sacramento River, which is approximately 11 miles downstream of the bridge site. For flows in the range of 100,000 cfs to 144,000 cfs, the gage water surface varies by approximately 3.0 ft and the HEC-RAS water surface varies by 3.3 ft. Therefore, the variations in water surface and flow depth with changing discharge in the HEC-RAS model are reasonable.
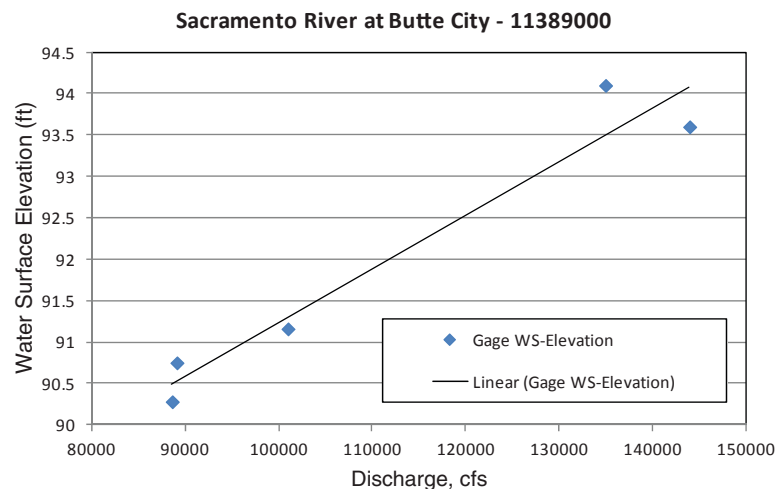
Figure 3.3.   Gage heights versus discharge at Sacramento River, Butte City gage.

The data in Figure 3.3 also illustrate the variability in water surface measurements at the Butte City gage. The standard deviation of the differences in the observed values versus the trend line is 0.49 ft. Therefore, this value was used to assess the reasonableness of the parameter uncertainties of Manning n and energy slope because these parameters will create variability in water surface for a given discharge.

3.5.3.1 Energy Slope Uncertainty

As noted in Section 3.5.2, Johnson (1996) found that several types of distributions have been used to describe channel and friction slope, including uniform, normal, triangular, and lognormal. Initially, a normal distribution with COV = 0.17 was used for this study. This produced a standard deviation in water surface of 0.66 ft, which is greater than the observed value of 0.49 ft at Butte City gage. Therefore, COV was reduced to 0.10, which resulted in a water surface standard deviation of 0.37 ft.

3.5.3.2 Manning n Uncertainty

When the 675 data points of the USACE (1986) study were evaluated, a COV of 0.082 for the log-transformed data fit the data well (see Section 3.5.2). However, when this COV was used in the HEC-RAS Monte Carlo simulation, the standard deviation in water surface was 2.5 ft, which was twice the standard deviation created by discharge uncertainty and much greater than the observed variability in water surface for a given discharge. Therefore, the COV was adjusted until the variability in water surface was more consistent with observed amounts. The COV of the log-transformed Manning n variable of 0.015 yielded a standard deviation in water surface of 0.47. Therefore, an estimate of a channel (or overbank) Manning n can be used to estimate μ and σ of the log-transformed variable using the following equations:

$$n = \exp(\mu + 0.5\sigma^2) = \exp\left[\mu + 0.5(\mu COV)^2\right] \tag{3.9}$$

$$\mu = \frac{-1 + \sqrt{1 + 2\ln(n)COV^2}}{COV^2} = \frac{-1 + \sqrt{1 + 2\ln(n)0.015^2}}{0.015^2} \tag{3.10}$$

$$\sigma = \mu \times COV = \mu \times 0.015 \tag{3.11}$$

The large difference in COV (0.082 based on selection of Manning n versus 0.015 based on impacts on water surface variability) indicates that Manning n is an important parameter that may often be difficult to reliably estimate. Therefore, calibration of Manning n to observed conditions is an important practice whenever possible.

3.6 Summary and Preview of Applications

This chapter provided an approach to evaluating the uncertainty of the three scour components: pier, contraction, and abutment scour. The methodology is based on software, referred to as the rasTool©, developed specifically for the purpose of linking the most widely accepted 1-D hydraulic model, HEC-RAS, with Monte Carlo simulation techniques. To reduce the complexity of the model runs (which will require on the order of 10,000 Monte Carlo realizations per run), only a limited number of hydraulic parameters can be allowed to vary. Other factors are identified as either deterministic or overcomplicating; that is, they are user-defined bridge characteristics and scour variables that would be determined during design, or they are secondary considerations in the analysis of bridge scour that, if allowed to vary, would complicate the Monte Carlo simulations to the point that application of the rasTool© would become impractical.

The statistical properties describing model uncertainty, bias and COV, were defined. In addition, model uncertainty in relation to the key hydraulic parameters of discharge (hydrologic uncertainty), Manning roughness, and downstream boundary friction slope were defined, and an approach to using regional regression equations to define hydrologic uncertainty was developed. An application of the HEC-RAS/Monte Carlo linkage to a bridge on the Sacramento River was used to test and refine the software and provide a reality check on the assumptions driving the uncertainty statistics for the key hydraulic parameters.

With the supporting software in place, tested, and adjusted to reflect typical hydraulic conditions in the field, the bias and COV for the equations used to estimate pier, contraction, and abutment scour can now be investigated. Chapter 4 accomplishes this using, primarily, carefully screened hydraulic laboratory data for each of the scour components. Chapter 4 also summarizes the fundamental equations for the three scour components as presented in the current edition of HEC-18 (Arneson et al. 2012).

Based on more than 300,000 HEC-RAS/Monte Carlo simulations, Chapter 5 presents two different approaches to assessing the conditional probability that the design scour depth will be exceeded for a given design flood event. The first (Level I) approach assumes that the practitioner can categorize a bridge based on (1) the size of the bridge, channel, and floodplain; (2) the size of the bridge piers; and (3) the hydrologic uncertainty. If so, a 27-element matrix is used to determine scour factors that can be used to multiply the estimated scour depth to achieve a desired level of confidence for pier, contraction, abutment, and total scour based on a reliability index that is commensurate with standard LRFD practice

When the practitioner cannot match a bridge to the categories established in the 27-element matrix, a site-specific (Level II) approach to the probability evaluation is required. For complex foundation systems and channel conditions, or for cases requiring special consideration, the Level II approach involves the application of HEC-RAS/Monte Carlo analyses for the site-specific conditions. A step-by-step procedure for developing probability-based estimates of scour factors for site-specific conditions is outlined in Chapter 5 and illustrated by application to the Sacramento River bridge (see Section 3.5.3).

In some cases it may be necessary to determine the unconditional probability that a scour estimate will not be exceeded over the remaining service life of an existing bridge or the design life of a new bridge. To estimate this unconditional probability of scour depth exceedance, Chapter 6 provides an abbreviated LRFD approach using the conditional probabilities for a limited number of return period flood events. This approach integrates the conditional probabilities of three or more flood events to determine the unconditional probability of exceedance over the entire service life of a bridge.

Chapter 7 provides illustrative examples that demonstrate the application of the 27-element matrix to determine the conditional probability of exceedance of estimated scour depths for a 100-year event at a bridge that fits one of the categories established in the matrix. For five bridges, representing a range of bridge configurations and physiographic regions across the continental United States, the examples guide the practitioner through the steps required to identify appropriate scour factors for a desired level of confidence using the results of Chapter 5 and the matrix presented in Appendix B. Analysis of the Sacramento River bridge is included in this section. The user of this reference guide is strongly encouraged to cross reference the material presented in Chapters 4 and 5 with the illustrative examples of Chapter 7.

CHAPTER 4

Bridge Scour Equations and Data Screening

4.1 Introduction

This chapter includes a brief summary of the data sets used in developing model bias and COV for each of the three individual scour components. For pier scour, both the HEC-18 and Florida DOT equations are assessed using comprehensive data sets from both laboratory and field studies. Contraction scour uses the HEC-18 equation for clear-water scour using laboratory data only. Abutment scour uses the NCHRP Project 24-20 total scour approach (Ettema et al. 2010), which is recommended in the most recent edition of HEC-18 (Arneson et al. 2012), using laboratory data only.

4.2 Pier Scour Data

4.2.1 Pier Scour Laboratory Data—Compilation, Screening, and Analysis

Pier scour data obtained under controlled laboratory conditions were assembled from 22 sources, yielding 699 independent measurements of pier scour in cohesionless soils. All data sets consisted of studies where the following information was documented: (1) scour depth, y_s, (2) approach flow depth, y, (3) approach flow velocity, V, (4) median sediment size, d_{50}, (5) pier width, a, and (6) pier shape (e.g., cylindrical, square, rectangular, etc.). Seventeen of the 22 data sources were obtained from *NCHRP Report 682* (Sheppard et al. 2011), which provided 569 data points. Data also were acquired from five additional studies, contributing another 130 data points.

To determine whether an individual test run was conducted under clear-water or live-bed conditions, the procedure presented in the 5th edition of HEC-18 (Arneson et al. 2012) uses the critical velocity for particle motion given by the following relationship (in U.S. customary units):

$$V_c = \frac{1.486 \, y^{1/6} \sqrt{K_s (S_s - 1) d_{50}}}{n} \tag{4.1}$$

where:

V_c = Critical velocity for particle motion, ft/s
y = Approach flow depth, ft
K_s = Dimensionless shields parameter for sediment motion (0.03 for gravel, 0.047 for sand)
S_s = Specific gravity of particle (assumed equal to 2.65 unless otherwise indicated)
d_{50} = Median particle diameter, ft
n = Manning resistance coefficient, estimated as $n = 0.034(d_{50})^{1/6}$ (d_{50} in ft)

41

Nearly all of the laboratory tests involved cylindrical piers; only 36 tests (about 5% of the data points) used square, rectangular, or multiple-column piers. The 36 tests with non-cylindrical piers all used an orientation aligned with the flow such that a skew angle was not introduced.

4.2.1.1 HEC-18 Pier Scour Equation—Laboratory Data

Using the laboratory data, pier scour for each test was predicted using the HEC-18 equation as presented in HEC-18 5th Ed. (Arneson et al. 2012). The HEC-18 equation, normalized to pier width, is:

$$\frac{y_s}{a} = 2.0\, K_1 K_2 K_3 K_w \left(\frac{y}{a}\right)^{0.35} (Fr)^{0.43} \qquad \text{subject to the following limits:} \qquad (4.2)$$

$$\frac{y_s}{a} = 2.4 \qquad \text{for } Fr < 0.8$$

$$\frac{y_s}{a} = 3.0 \qquad \text{for } Fr > 0.8$$

The coefficients and variables of the HEC-18 equation are:

y_s = Scour depth, ft or m
  a = Pier width normal to flow, ft or m
K_1 = Correction factor for shape of pier nose
K_2 = Correction factor for skew angle (= 1.0 for piers aligned with the flow)
K_3 = Correction factor for bed forms
K_w = Correction factor for very wide piers
  y = Depth of approach flow, ft or m
Fr = Froude number of the approach flow

The correction factor K_w for very wide piers is:

$$K_w = 2.58\left(\frac{y}{a}\right)^{0.34} Fr^{0.65} \qquad \text{for } V/V_c < 1.0 \qquad (4.3)$$

$$K_w = 1.0\left(\frac{y}{a}\right)^{0.13} Fr^{0.25} \qquad \text{for } V/V_c \geq 1.0$$

$$K_w \leq 1.0$$

The correction factor K_w is only applied when *all* of the following conditions are met:

$y/a < 0.8$

$a/d_{50} > 50$, and

$Fr < 1.0$

Based on the estimated critical velocity using the HEC-18 procedure described in this section, 495 data tests were conducted under clear-water scour conditions; the remaining 204 tests were conducted with live-bed conditions. The evolution of scour depth over time was not investigated in many of the studies; therefore, the data collection required introducing assumptions regarding the maturity of the scour hole at the end of each test.

Following an initial analysis of all 699 data points from the 22 data sources, a method was developed and used to identify and remove outliers. The data quality assessment method developed for this purpose relied only on variables that were directly measured during each
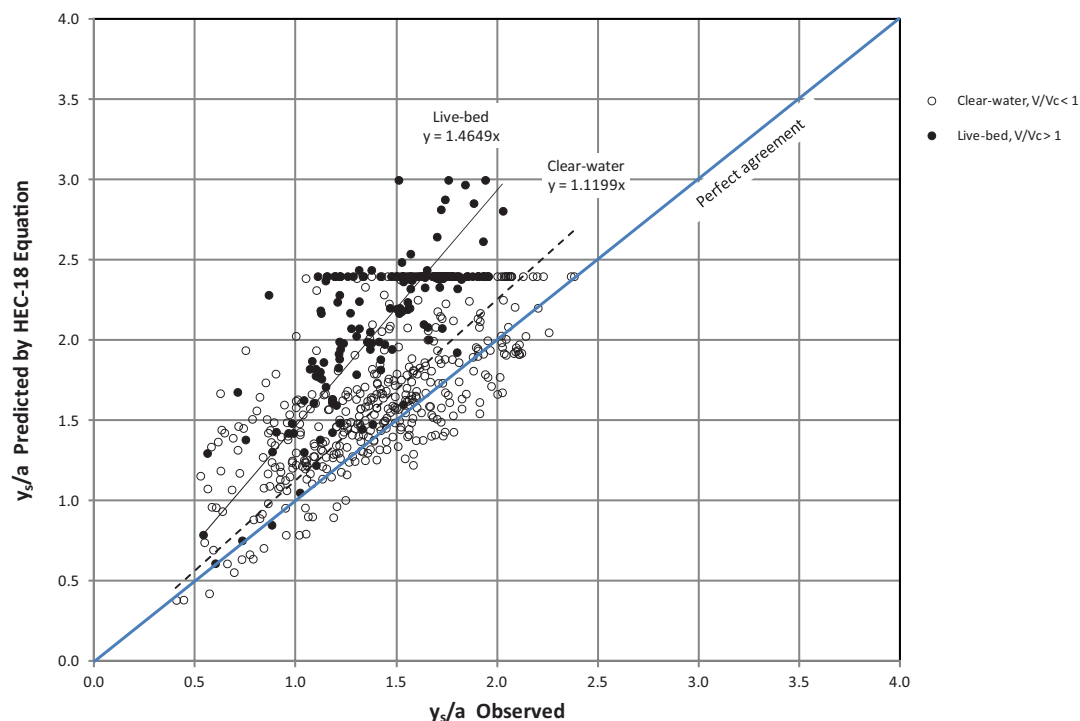
Figure 4.1.   HEC-18 pier scour prediction vs. observed scour for clear-water and live-bed conditions, final laboratory data set (outliers removed).

test; no predictive techniques were used to discriminate among data points. Of the original 699 data points, 119 were identified as outliers (approximately 17% of the total data points), resulting in a final data set of 580 points for analysis. A detailed description of the outlier identification method is provided in the Contractor's Final Report for NCHRP Project 24-34 (Lagasse et al. 2013), which is available at www.trb.org.

With the outliers removed, the final data set was plotted and used to analyze the bias and COV of the HEC-18 pier scour prediction equation. Figure 4.1 presents the final data graphically. Table 4.1 provides the final results of the analysis (see Section 2.5.2 for a discussion of the reliability index, β, as a measure of structural safety).

4.2.1.2 Florida DOT Pier Scour Equation—Laboratory Data

The pier scour approach in *NCHRP Report 682* (Sheppard et al. 2011) is referenced as the Florida DOT (FDOT) Pier Scour Methodology in the 5th edition of HEC-18. The method is referred to as the Florida DOT pier scour equation in this document.

As with the HEC-18 equation, the Florida DOT pier scour equation includes flow velocity, depth and angle of attack, pier geometry and shape, but also includes particle size. The Florida

Table 4.1.   Bias and coefficient of variation of the HEC-18 pier scour equation with laboratory data (all data with outliers removed).

Data Set	No. Data Points	Bias	COV	Percent Under-predicted	Reliability (β)	
					Normal	Lognormal
All data	580	0.82	0.23	17.2%	0.97	1.00
Clear-water subset	402	0.88	0.21	24.6%	0.66	0.73
Live-bed subset	178	0.68	0.16	0.6%	2.92	2.49

DOT equation combines pier geometry, shape, and angle of attack to compute an effective pier width, a*. In contrast to the HEC-18 equation, the Florida DOT pier scour equation also distinguishes between clear-water and live-bed flow conditions.

The critical velocity equation as given in *NCHRP Report 682* (Sheppard et al. 2011), is:

$$V_c = (u_{*c})5.75 \log\left(1685\frac{y}{d_{50}}\right) \tag{4.4}$$

where:

V_c = Critical velocity for particle motion, ft/s
u_{*c} = Shear velocity for 0.1 mm < d_{50} < 1 mm given by: $0.0377 + 0.0410(d_{50})^{1.4}$, ft/s
u_{*c} = Shear velocity for 1 mm < d_{50} < 100 mm given by: $0.1(d_{50})^{0.5} - 0.0213(d_{50})^{-1}$, ft/s
y = Approach flow depth, ft
d_{50} = Median grain diameter, mm

Although the HEC-18 equation provides good results for most applications, the Florida DOT equation should be considered as an alternative, particularly for wide piers (y/a < 0.2) (Arneson et al. 2012). The Florida DOT methodology includes the following equations:

$$\frac{y_s}{a^*} = 2.5f_1f_2f_3 \qquad\qquad \text{for } 0.4 \leq \frac{V_1}{V_c} < 1.0 \tag{4.5}$$

$$\frac{y_s}{a^*} = f_1\left[2.2\left(\frac{\frac{V_1}{V_c}-1}{\frac{V_{lp}}{V_c}-1}\right) + 2.5f_3\left(\frac{\frac{V_{lp}}{V_c}-\frac{V_1}{V_c}}{\frac{V_{lp}}{V_c}-1}\right)\right] \qquad \text{for } 1.0 \leq \frac{V_1}{V_c} \leq \frac{V_{lp}}{V_c} \tag{4.6}$$

$$\frac{y_s}{a^*} = 2.2f_1 \qquad\qquad \text{for } \frac{V_1}{V_c} > \frac{V_{lp}}{V_c} \tag{4.7}$$

$$f_1 = \tanh\left[\left(\frac{y_1}{a^*}\right)^{0.4}\right] \tag{4.8}$$

$$f_2 = \left\{1 - 1.2\left[\ln\left(\frac{V_1}{V_c}\right)\right]^2\right\} \tag{4.9}$$

$$f_3 = \left[\frac{\left(\frac{a^*}{D_{50}}\right)^{1.13}}{10.6 + 0.4\left(\frac{a^*}{D_{50}}\right)^{1.33}}\right] \tag{4.10}$$

where:

y_s = Pier scour depth, ft or m
a^* = Effective pier width, ft or m
V_1 = Mean velocity of flow directly upstream of the pier, ft/s or m/s
V_{lp} = Velocity of the live-bed peak scour, ft/s or m/s
V_c = Critical velocity for movement of D_{50} as defined in Equation (4.4), ft/s or m/s
D_{50} = Median particle size of bed material, ft or m

$$V_{lp} = 5V_c \text{ or } 0.6\sqrt{gy_1} \qquad \text{(whichever is greater)} \tag{4.11}$$

where V_c is computed using Equation (4.4).

The effective pier width, a^*, is the projected width of the pier times the shape factor, K_{sf}.

$$a^* = K_{sf} a_{proj} \tag{4.12}$$

The shape factor for a circular or round-nosed pier is 1.0; the shape factor for a square-end pier depends on the angle of attack.

$$K_{sf} = 1.0 \qquad\qquad \text{for circular or round-nosed piers} \tag{4.13}$$

$$K_{sf} = 0.86 + 0.97 \left(\left| \frac{\pi\theta}{180} - \frac{\pi}{4} \right| \right)^4 \qquad \text{for square-nosed piers} \tag{4.14}$$

where:

  θ = flow angle of attack in degrees

The projected width of the pier is:

$$a_{proj} = a \cos \theta + L \sin \theta \tag{4.15}$$

where:

  a_{proj} = Projected pier width in direction of flow, ft or m
  a = Pier width, ft or m
  L = Pier length, ft or m

The methodology can be accessed through a spreadsheet available at the Florida DOT website. It can also be computed from the equations presented in this chapter or by following the following steps.

Step 1. Calculate V_c using Equation (4.4)
Step 2. Calculate V_{lp} using Equation (4.11)
Step 3. Calculate a^* using Equation (4.12)
Step 4. Calculate f_1 using Equation (4.8)
Step 5. Calculate f_3 using Equation (4.10)
Step 6. Calculate $\frac{y_{s-c}}{a^*}$ and y_{s-c} (see Note below Equation [4.16])
Step 7. Calculate $\frac{y_{s-lp}}{a^*}$ and y_{s-lp} (see Note below Equation [4.16])
Step 8. If $V_1 < 0.4V_c$, then $y_s = 0.0$
Step 9. If $0.4V_c < V_1 \leq V_c$, then calculate f_2 using Equation (4.9) and $y_s = f_2 y_{s-c}$
Step 10. If $V_1 \geq V_{lp}$, then $y_s = y_{s-lp}$
Step 11. If $V_c < V_1 < V_{lp}$, then calculate y_s from:

$$y_s = y_{s-c} + \frac{(V_1 - V_c)}{(V_{lp} - V_c)} (y_{s-lp} - y_{s-c}) \tag{4.16}$$

Note: Equation (4.16) is an equivalent but simplified version of Equation (4.6); y_{s-c} is the scour at critical velocity for bed material movement (V_c) and is equal to $2.5 f_1 f_3 a^*$; and y_{s-lp} is the scour at live-bed peak velocity (V_{lp}) and is equal to $2.2 f_1 a^*$. The Florida DOT spreadsheet uses y_{s-c} as the design scour value when it is greater than y_{s-lp}.

The Florida DOT methodology for pier scour includes four regions as shown in Figure 4.2.

- Scour Region I (see Step 8) is for clear-water conditions with velocity too low to produce scour, which occurs for velocities less than $0.4V_c$. However, field data in *NCHRP Report 682* include observed scour for this condition, although it was only observed on one occasion for laboratory data.
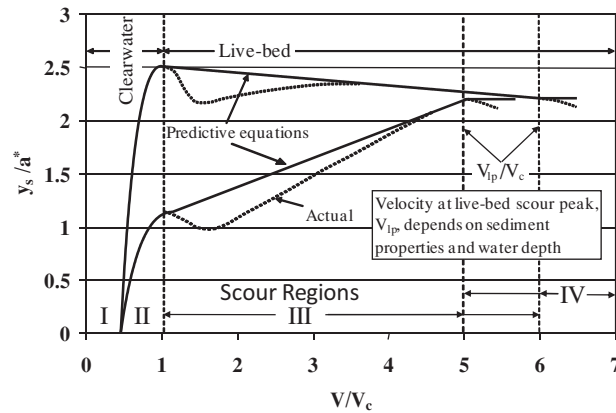
Figure 4.2.   Scour regions for Florida DOT pier scour methodology (from NCHRP Report 683*).*

- Scour Region II is for clear-water conditions with flow velocity large enough to produce pier scour ($V_c > V_1 > 0.4V_c$) as defined by Step 9.
- Scour Region IV is defined by the live-bed peak velocity (V_{lp}), where the maximum live-bed scour occurs at $5V_c$ or greater. Any velocity greater than V_{lp} is assigned the scour, y_{s-lp}, computed for V_{lp} (Step 10).
- Live-bed scour that occurs for flow velocities between critical velocity and the live-bed peak velocity ($V_c < V_1 < V_{lp}$) occurs in Scour Region III as defined by Step 11 and Equation (4.16).

Pier scour was predicted using the Florida DOT methodology on the same 580 laboratory data points previously analyzed with the HEC-18 equation. Figure 4.3 presents the final data
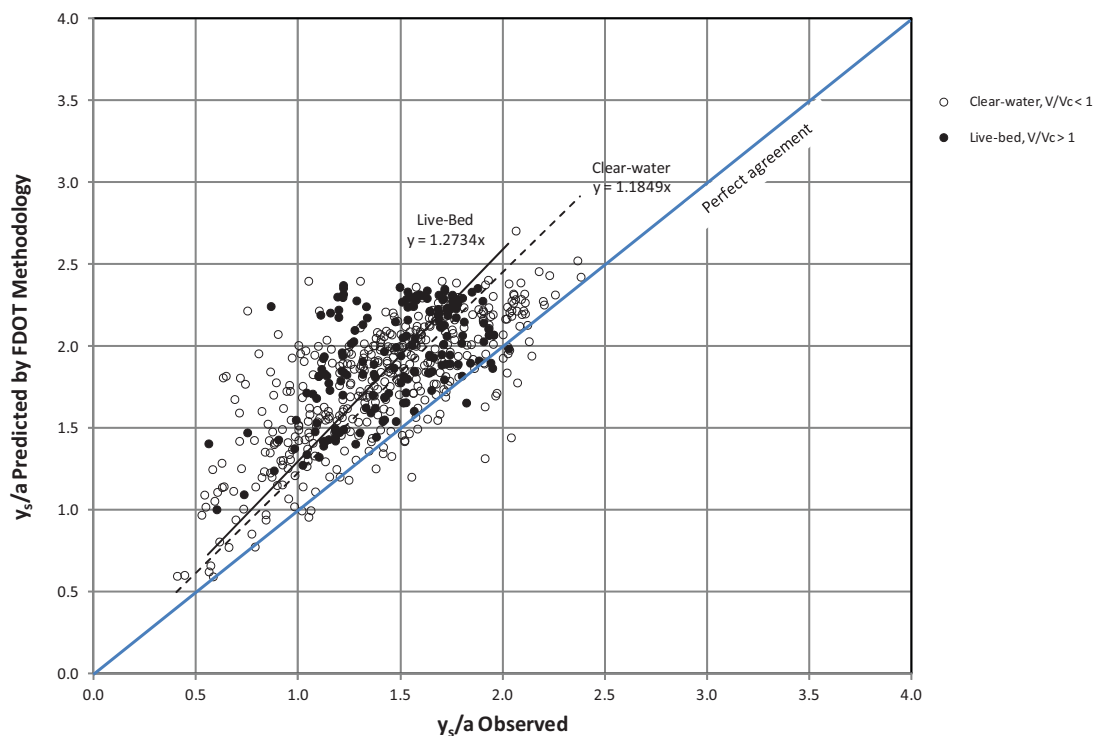
Figure 4.3.   Florida DOT pier scour prediction vs. observed scour for clear-water and live-bed conditions, final laboratory data set (outliers removed).

Table 4.2.   Bias and coefficient of variation of the Florida DOT pier scour methodology with laboratory data (all data with outliers removed).

Data Set	No. Data Points	Bias	COV	Percent Under-predicted	Reliability (β)	
					Normal	Lognormal
All data	580	0.78	0.20	6.7%	1.42	1.29
Clear-water subset	359	0.80	0.20	9.5%	1.26	1.55
Live-bed subset	221	0.75	0.18	2.3%	1.78	1.58

graphically. Table 4.2 provides the final results of the pier scour prediction for the laboratory data using the Florida DOT methodology.

4.2.2 Pier Scour Field Data—Compilation and Analysis

Pier scour data from field studies were obtained from *NCHRP Report 682* (Sheppard et al. 2011), which provided 943 data points from four sources. From that study, 183 data points were identified as outliers, leaving 760 data points for analysis. The COVs for both the HEC-18 and Florida DOT pier scour equations were significantly higher compared to the laboratory data sets due to the difficulty in estimating the hydraulic conditions associated with the event causing the scour, as well as the uncertainty in determining the maturity of the scour-hole depths. Both equations resulted in substantial overprediction of the observed scour depths.

For these reasons, the laboratory data sets were considered much more reliable for purposes of assessing the model uncertainty of the two pier scour equations. The reader is referred to the NCHRP Project 24-34 Contractor's Final Report (Lagasse et al. 2013), available at www.trb.org, for a detailed discussion of the analyses associated with the pier scour field data.

4.3 Contraction Scour

4.3.1 Clear-Water Contraction Scour Laboratory Data—Compilation and Screening

The HEC-18 clear-water contraction scour equation was not developed from laboratory or field data, but instead was derived from sediment transport concepts and theory (Richardson et al. 2001). The HEC-18 clear-water contraction scour equation is:

$$y_2 = \left[\frac{K_u Q^2}{D_m^{2/3} W^2} \right]^{3/7} \tag{4.17}$$

$$y_s = y_2 - y_0 \tag{4.18}$$

where:

y_2 = Depth of flow in contracted section after scour has occurred, ft or m
K_u = Conversion factor equal to 0.0077 for U.S. customary units (0.025 for SI units)
Q = Discharge in contracted section, ft^3/s or m^3/s
D_m = Representative particle size equal to 1.25 times d_{50}, ft or m
W = Width of contracted section, ft or m
y_s = Depth of scour in contracted section, ft or m
y_0 = Depth of flow in contracted section before scour occurs, ft or m

A definition sketch showing these variables is provided as Figure 4.4.
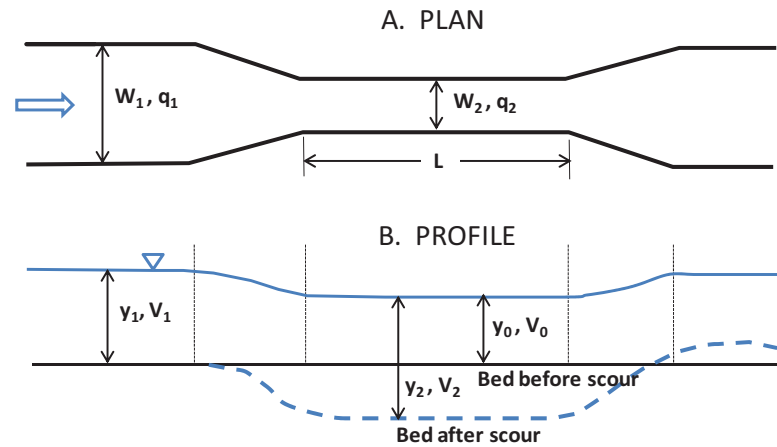
Figure 4.4.   Definition sketch for HEC-18 clear-water contraction scour equation.

Contraction scour data obtained under controlled laboratory conditions were assembled from eight sources, yielding 182 independent measurements of contraction scour in cohesionless soils. Only long contractions were considered, because short contractions include an abutment scour effect in addition to the contraction scour. A contraction is considered to be long if the length, L, of the contracted section is greater than the width, W_1, of the approach section as shown in Figure 4.4 (Raikar 2004). However, comprehensive studies by Webby (1984) suggest that a long contraction is defined when the length, L, is twice the width of the approach section, W_1.

All data sets considered in this study consisted of laboratory experiments in which the following information was documented:

- Scour depth, y_s;
- Approach flow depth, y_1;
- Approach flow velocity, V_1;
- Median sediment size, d_{50};
- Approach width, W_1;
- Width of contracted section, W_2; and
- Length of contracted section, L.

Data from 182 test runs are summarized in Dey and Raikar (2005) and were obtained from that reference. In that publication, data from other researchers (Komura 1966, Gill 1981, Webby 1984, and Lim 1993) were included along with data from the tests performed by Dey and Raikar.

All 182 tests involved clear-water conditions in the approach flow ($V_1/V_c < 1.0$), where V_c is the critical velocity for each test as determined using Equation (4.1).

4.3.1.1 Assessment of Data Quality

Because of questions regarding the accuracy of some of the data provided in the Dey and Raikar (2005) table, the original work from all the previous studies was obtained and reviewed during the screening and assessment of the contraction scour data.

A detailed review of previous studies found that Dey and Raikar (2005) incorrectly interpreted the results of the tests conducted by Komura (1966), Gill (1981), and Lim (1993). Specifically, those studies did not actually measure the depth of scour in the contracted

section, but instead assumed that the depth of scour was equal to the difference in flow depths, $y_2 - y_1$.

Dey and Raikar reported those results as "observed scour"; however, their assumption is not valid because the drawdown effect on the water surface in the contracted section is not accounted for. Therefore, it was concluded in the review that the scour "measurements" from the studies by Komura (1966), Gill (1981), and Lim (1993) are unreliable, and those data points were discarded from further analysis.

The Dey and Raikar tests that utilized well-graded bed materials also were re-examined. Although Dey and Raikar do not provide the grain size curves for the materials, they do provide the d_{50} grain size and the geometric standard deviation, σ_g, defined as

$$\sigma_g = \sqrt{\frac{d_{84}}{d_{16}}} \tag{4.19}$$

For the Dey and Raikar tests using well-graded bed materials, σ_g ranged from 1.46 to 3.60. Further investigation revealed that when σ_g is greater than 1.9, a sufficient number of larger particles are present in the bed material to create a self-armoring condition that limits the depth of scour. Therefore, the Dey and Raikar tests that used well-graded bed material for which σ_g was greater than 1.9 were eliminated.

After screening the 182 data points as discussed in this section, 119 data points remained with which to assess the HEC-18 clear-water scour equation.

4.3.2 Clear-Water Contraction Scour Laboratory Data—Analysis

In practice, at a bridge the depth of flow, y_0, in the contracted section before scour occurs is routinely determined by use of a water surface profile model such as HEC-RAS. However, because the laboratory data did not include a direct measurement of this flow depth (presumably because, in the laboratory, scour occurs before the target flow conditions are established), y_0 must be estimated from available data. As a first approximation, the velocity, V_0, and flow depth, y_0, in the contracted section before scour occurs are estimated as:

From continuity,

$$V_0 = \frac{Q}{A} \approx \frac{Q}{y_1 W_2} \tag{4.20}$$

Assuming no energy losses, the specific energy in the contracted section is equal to that in the approach section, so:

$$y_0 = y_1 + \frac{V_1^2}{2g} - \frac{V_0^2}{2g} \tag{4.21}$$

V_0 is then recalculated as:

$$V_0 = \frac{Q}{A} = \frac{Q}{y_0 W_2} \tag{4.22}$$

For the laboratory data, this approach yielded estimates of y_0 which in many cases were unreasonably small and, for a significant number of data points, negative values of y_0 were obtained using this first approximation. Further investigation revealed that the contraction ratios W_2/W_1 in the laboratory tests were severe enough to create a "choked" condition at the

entrance to the contraction. The threshold of choking occurs when the actual contraction ratio is less than the critical ratio σ, defined as follows by Wu and Molinas (2005):

$$\sigma = \left(\frac{3}{\left(2 + F_1^2\right)} \right)^{3/2} F_1^2 \tag{4.23}$$

It was found that 113 of the 119 tests were conducted with some degree of choking. Figure 4.5 presents the dimensionless choking ratio $\sigma W_2/W_1$ plotted versus the unit discharge in the contracted section. To resolve this issue, the estimate of y_0 was refined by comparing the initial depth ratio, y_0/y_1, to the contraction ratio, W_2/W_1. If the depth ratio from the initial approximation was less than the contraction ratio, the depth y_0 was re-estimated as y_1 times the contraction ratio as a limiting condition. This second iteration yielded more reasonable values for assessing the HEC-18 clear-water contraction scour prediction. During this process, three additional data points were identified as outliers, leaving a final data set of 116 data points for analysis.

Figure 4.6 shows the results of the analysis with the final data set. The bias of the HEC-18 clear-water contraction scour equation was determined to be 0.92 as the mean value of the ratio y_s (observed) to y_s (predicted). The COV of the data is the standard deviation divided by the mean, determined to be 0.21 for this data set. The clear-water scour equation underpredicted the observed scour for 23.3% of the data points (27 tests out of 116).

The reliability index, β, for the clear-water contraction scour equation was determined to be 0.44 and 0.52 for normal and lognormal distributions, respectively. These relatively low values of β are not surprising, considering that the HEC-18 clear-water contraction scour equation was not developed from laboratory or field data, but instead was derived from sediment transport concepts and theory. It is therefore a predictive equation, not a design equation, and as such does not have built-in conservatism. Values of β near zero indicate that, on average, observed
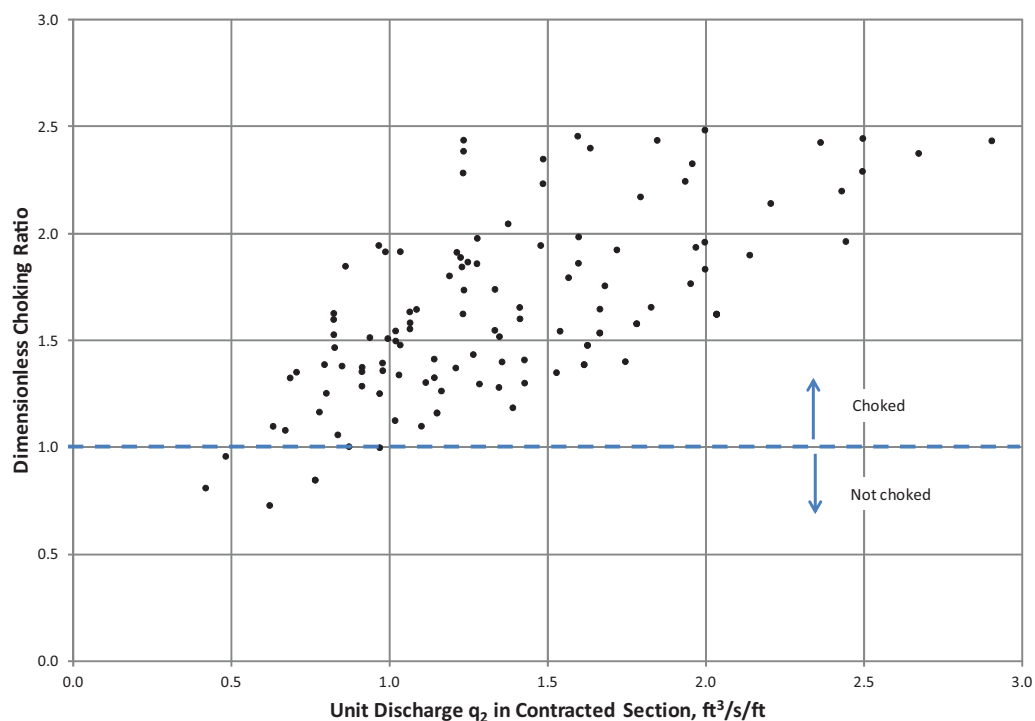
Figure 4.5.   Dimensionless choking ratio vs. unit discharge in the contracted section.
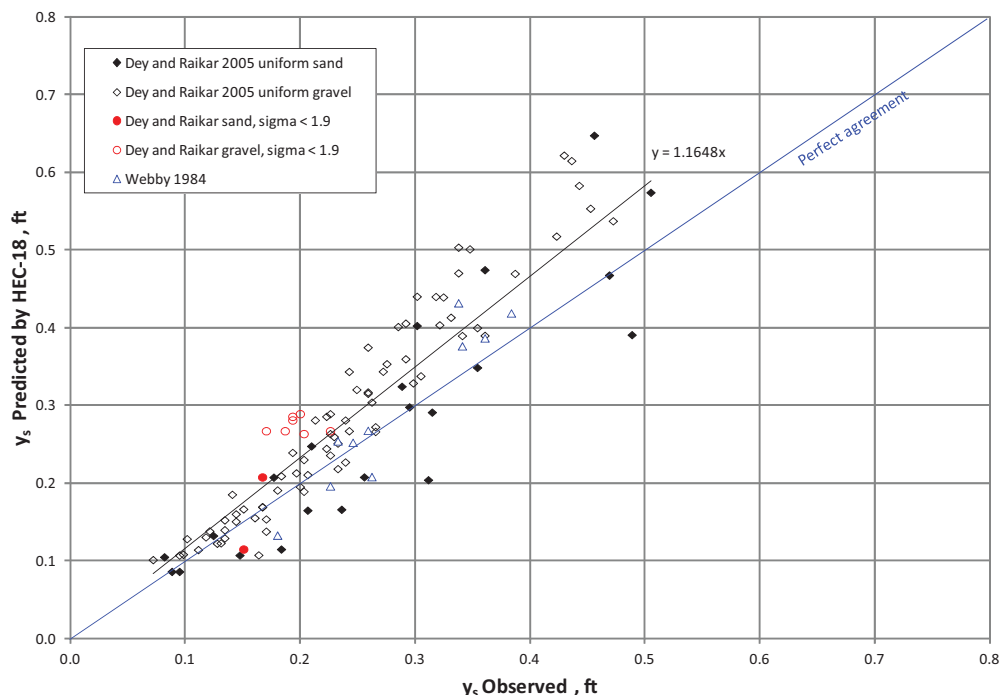
Figure 4.6. Predicted vs. observed clear-water contraction scour.

scour is underpredicted by about the same magnitude and frequency as it is overpredicted. Table 4.3 provides a summary of the prediction statistics for the HEC-18 clear-water contraction scour equation.

4.4 Abutment Scour Data

4.4.1 Abutment Scour Laboratory Data—Compilation

The analyses in this section reflect information from the final reports of NCHRP Project 24-20 (Ettema et al. 2010) and NCHRP Project 24-27(02) (Sturm et al. 2011).

Both NCHRP project reports were reviewed and all laboratory data from the NCHRP Project 24-20 study were acquired. This study combines contraction and abutment scour processes to provide an estimate of the total scour at an abutment. This section presents the results of the screening and analysis of the NCHRP Project 24-20 data and includes a similar abutment scour data set (Ballio et al. 2009).

Rather than analyzing abutment scour data using the Froehlich and HIRE equations (local scour only at an abutment) and developing scour factors for equations that now appear to be outdated, the predictive capability of the approach taken by NCHRP Project 24-20 and

Table 4.3. Bias and coefficient of variation of the HEC-18 clear-water contraction scour equation with laboratory data (outliers removed).

Data Set	No. Data Points	Bias	COV	Percent Under-predicted	Reliability (β)	
					Normal	Lognormal
All data (clear-water)	116	0.92	0.21	23.3%	0.44	0.52

subsequently endorsed by NCHRP Project 24-27(02) was investigated. Although the Froehlich and HIRE equations still appear in the 5th edition of HEC-18 (Arneson et al. 2012), FHWA guidance suggests that the NCHRP Project 24-20 methodology will provide a better estimate of the combined effects of contraction scour and local scour at an abutment.

NCHRP Project 24-20 developed abutment scour equations considering a range of abutment types, abutment locations, flow conditions, and sediment transport conditions. These equations use contraction scour as the starting calculation for abutment scour and apply an amplification factor to account for large-scale turbulence that develops in the vicinity of the abutment tip.

One important distinction regarding the contraction scour calculation is that the abutment creates a non-uniform flow distribution in the contracted section. The flow is more concentrated in the vicinity of the abutment and the contraction scour component is greater than for average conditions in the constricted opening. NCHRP Project 24-20 defines three abutment scour conditions:

Scour Condition A: Scour that occurs when the abutment is in, or close to, the main channel.
Scour Condition B: Scour that occurs when the abutment is on the floodplain and set well back from the main channel.
Scour Condition C: Scour that occurs when the embankment breaches and the abutment foundation acts as a pier. NCHRP Project 24-20 concluded that there is a limiting depth of abutment scour when the geotechnical stability of the roadway embankment or channel bank is reached.

Abutment scour conditions A, B, and C are illustrated in Figure 4.7. For purposes of this research project, Scour Condition C (in which the approach embankment is breached) is a special case and is not considered here. Notice that the abutment scour computed from the NCHRP Project 24-20 approach is *total* scour at the abutment; it is not added to contraction scour because it already includes contraction scour.

4.4.2 NCHRP Project 24-20 Abutment Scour Approach

The NCHRP Project 24-20 approach for calculating the depth of scour at abutments uses contraction scour as the starting calculation for abutment scour and applies an amplification factor to account for large-scale turbulence that develops in the vicinity of the abutment. One important distinction regarding the contraction scour calculation is that the abutment creates a non-uniform flow distribution in the contracted section. The flow is more concentrated in the vicinity of the abutment, and the contraction scour component is greater than for average conditions in the constricted opening.

The scour equations for Scour Condition A and Scour Condition B are:

$$y_{max} = \alpha_A y_c \text{ or } y_{max} = \alpha_B y_c \tag{4.24}$$

$$y_s = y_{max} - y_0 \tag{4.25}$$

where:

y_{max} = Maximum flow depth resulting from abutment scour, ft or m
y_c = Flow depth including live-bed or clear-water contraction scour, ft or m
α_A = Amplification factor for live-bed conditions
α_B = Amplification factor for clear-water conditions
y_s = Total scour depth at abutment, ft or m
y_0 = Flow depth prior to scour, ft or m
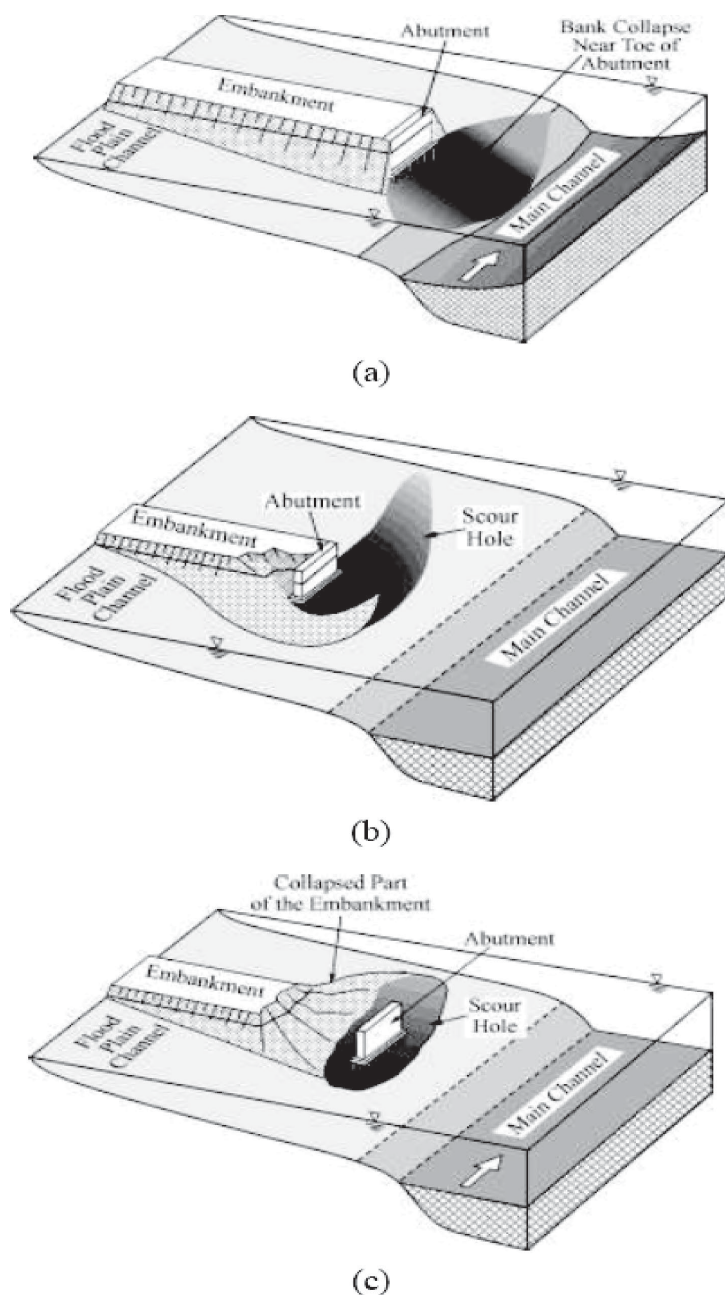
Figure 4.7.   Abutment scour conditions A, B, and C from NCHRP Project 24-20 (Ettema et al. 2010).

4.4.2.1 Scour Condition A

If the projected length of the embankment, L, is 75% or greater than the width of the floodplain (B_f), Scour Condition A in Figure 4.7 is assumed to occur and the contraction scour calculation is performed using a live-bed scour calculation. The contraction scour equation presented in NCHRP Project 24-20 is a simplified version of the HEC-18 live-bed contraction scour equation. The equation combines the discharge and width ratios due to the similarity of the exponents because other uncertainties are more significant. By combining the discharge and width, the live-bed contraction scour equation simplifies to the ratio of two unit discharges. Unit discharge, q, can be estimated either by discharge divided by

width or by the product of velocity and depth. The contraction scour equation for Scour Condition A is:

$$y_c = y_1 \left(\frac{q_2}{q_1} \right)^{6/7} \tag{4.26}$$

where:

y_c = Flow depth including live-bed contraction scour, ft or m
y_1 = Upstream flow depth, ft or m
q_1 = Upstream unit discharge, ft²/s or m²/s
q_2 = Unit discharge in the constricted opening accounting for non-uniform flow distribution, ft²/s or m²/s

The value of q_2 can be estimated as the total discharge in the bridge opening divided by the width of the bridge opening. The value of y_c is then used in Equation (4.24) to compute the total flow depth at the abutment. The value of α_A is selected from Figure 4.8 for spill-through abutments and Figure 4.9 for wingwall abutments. The solid curves should be used for design. The dashed curves represent theoretical conditions that have yet to be proven experimentally.

For low values of q_2/q_1, contraction scour is small, but the amplification factor is large because flow separation and turbulence dominate the abutment scour process. For large values of q_2/q_1, contraction scour dominates the abutment scour process and the amplification factor is small.

4.4.2.2 Scour Condition B

If the projected length of the embankment, L, is less than 75% of the width of the floodplain, B_f, Scour Condition B in Figure 4.7 occurs and the contraction scour calculation is performed using a clear-water scour calculation. The clear-water contraction scour equation also uses unit discharge, q, which can be estimated either by discharge divided by width or by the product
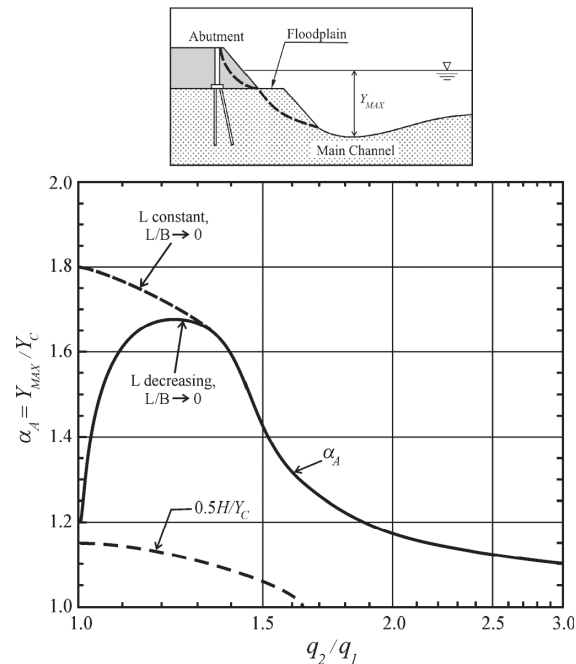
Figure 4.8.   Scour amplification factor for spill-through abutments and live-bed conditions (Ettema et al. 2010).
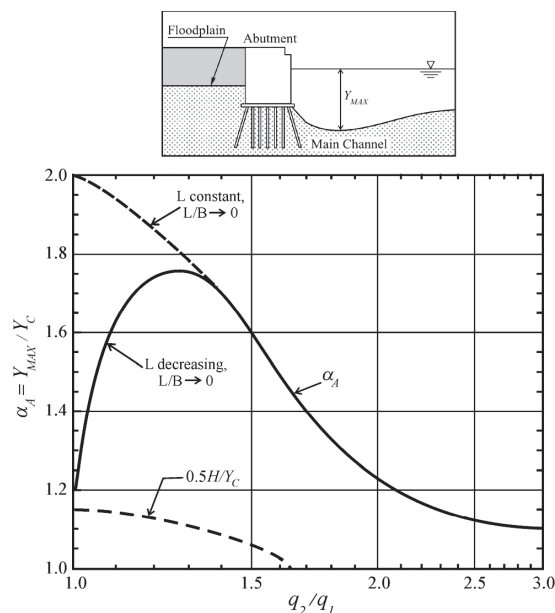
Figure 4.9. Scour amplification factor for wingwall abutments and live-bed conditions (Ettema et al. 2010).

of velocity and depth. Two clear-water contraction scour equations may be applied. The first equation is the standard equation based on particle size:

$$y_c = \left(\frac{q_{2f}}{K_u d_{50}^{1/3}} \right)^{6/7}$$

(4.27)

where:

y_c = Flow depth including clear-water contraction scour, ft or m
q_{2f} = Unit discharge in the constricted opening accounting for non-uniform flow distribution, ft²/s or m²/s
K_u = 11.17 English units
K_u = 6.19 SI
d_{50} = Median particle diameter with 50% finer, ft or m

A lower limit of particle size of 0.2 mm is a reasonable limitation on the use of Equation (4.27) because cohesive properties increase the critical velocity and shear stress for cohesive soils that have finer grain sizes. If the critical shear stress is known for a floodplain soil, then an alternative clear-water scour equation can be used:

$$y_c = \left(\frac{\gamma}{\tau_c} \right)^{3/7} \left(\frac{n q_{2f}}{K_u} \right)^{6/7}$$

(4.28)

where:

n = Manning n of the floodplain surface material under the bridge
τ_c = Critical shear stress for the floodplain surface material, lb/ft² or Pa
γ = Unit weight of water, lb/ft³ or N/m³
K_u = 1.486 English units
K_u = 1.0 SI
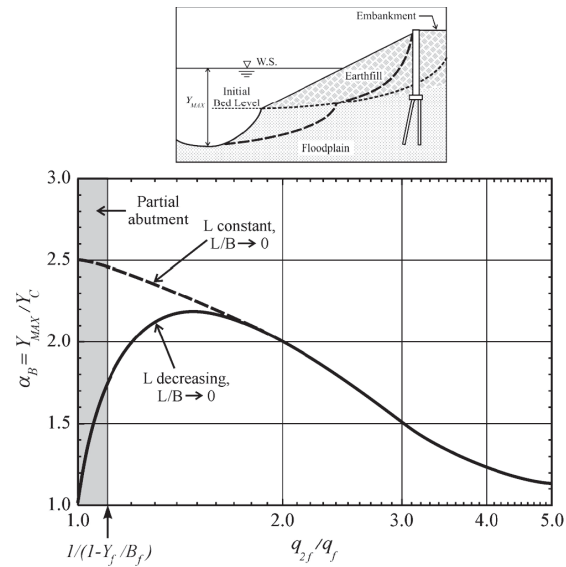
Figure 4.10.   Scour amplification factor for spill-through abutments and clear-water conditions (Ettema et al. 2010).

The value of q_{2f} should be estimated including local concentration of flow at the bridge abutment. The value of q_f is the floodplain flow upstream of the bridge. The value of y_c is then used in Equation (4.24) to compute the total flow depth at the abutment. The value of α_B is selected from Figure 4.10 for spill-through abutments and from Figure 4.11 for wingwall abutments. The solid curves should be used for design. The dashed curves represent theoretical conditions that have yet to be proven experimentally. For low values of q_{2f}/q_f, contraction scour is small, but the amplification factor is large because flow separation and turbulence dominate the
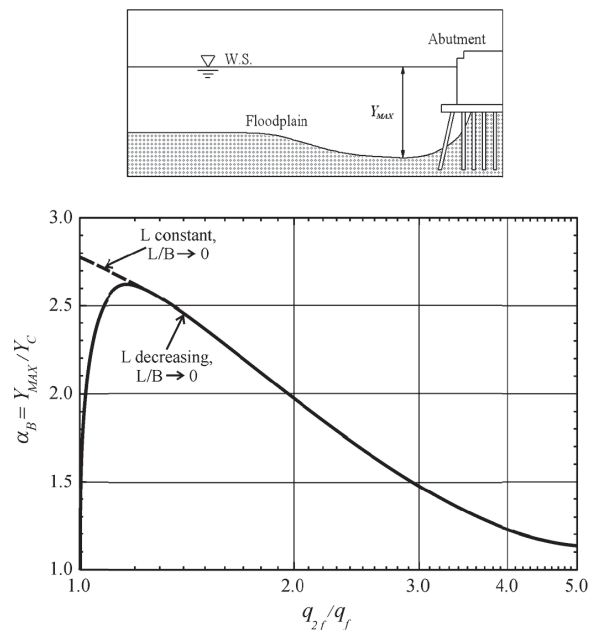
Figure 4.11.   Scour amplification factor for wingwall abutments and clear-water conditions (Ettema et al. 2010).

abutment scour process. For large values of q_{2f}/q_f, contraction scour dominates the abutment scour process and the amplification factor is small.

Unit discharge can be calculated at any point in the 2-D flow field by multiplying velocity and depth. Although 2-D modeling is strongly recommended for bridge hydraulic design, HEC-18 (Arneson et al. 2012) includes a method for estimating the velocity at an abutment. This method is used to size abutment riprap, but can also be used to determine the unit discharge at an abutment.

4.4.3 Abutment Scour Data Screening and Analysis

Fifty tests of abutment scour under live-bed conditions (Scour Condition A) and 12 clear-water tests (Scour Condition B) were conducted under NCHRP Project 24-20. An additional 19 clear-water tests were conducted by Ballio et al. (2009). Of the 50 live-bed tests, 6 were considered outliers for which the ratio q_2/q_1 was less than 1.05 and the scour amplification factor was ambiguous. Of the 31 clear-water tests, 5 tests from the Ballio 2009 data set (Ballio's Test Series D) also were considered outliers because they were conducted in a different flume and used very small particle sizes ($d_{50} < 0.2$ mm) near the silt size range, causing severe underprediction. After this screening, 70 data points remained for analysis using the NCHRP Project 24-20 abutment scour method.

Figure 4.12 shows the results of the analysis. The bias of the NCHRP Project 24-20 abutment scour equation was determined to be 0.74 as the mean value of the ratio y_s (observed) to y_s (predicted). The COV of the data is the standard deviation divided by the mean, determined to be 0.23 for this data set. The NCHRP Project 24-20 abutment scour equation underpredicted the observed scour for 2.9% of the data points (2 tests out of 70).
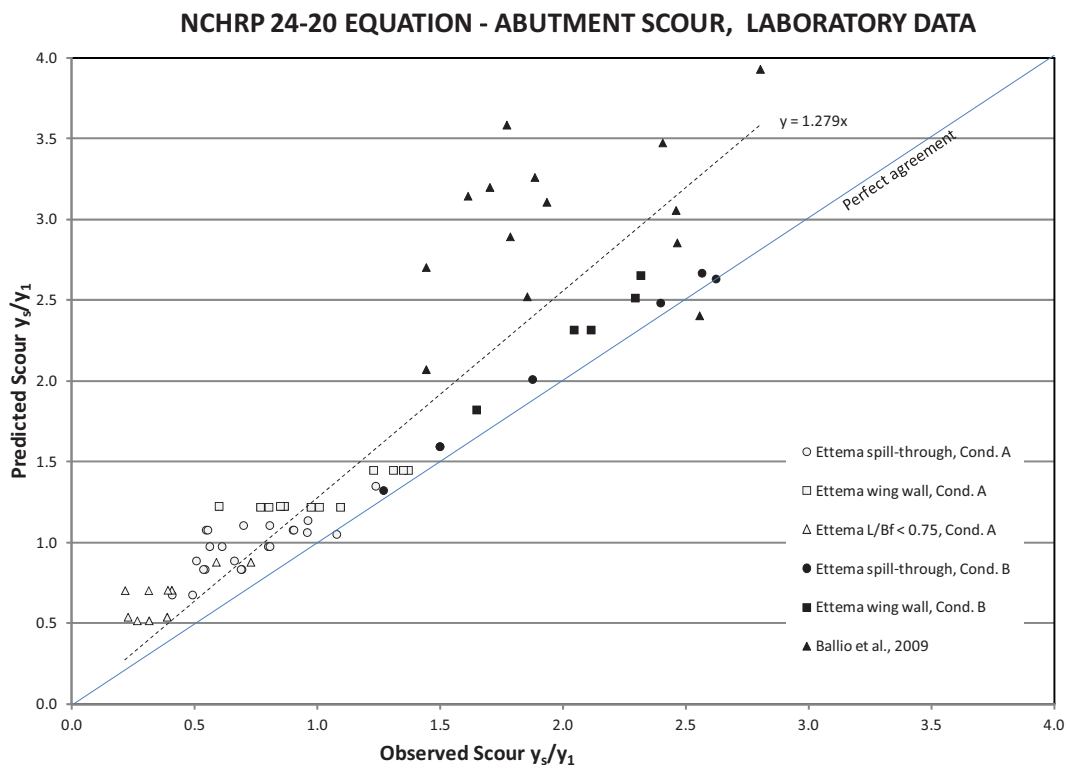
Figure 4.12.   Predicted vs. observed abutment scour, 70 laboratory tests (outliers removed).

Table 4.4.   Bias and coefficient of variation of the NCHRP Project 24-20 abutment scour equations with laboratory data (outliers removed).

Data Set	No. Data Points	Bias	COV	Percent Under-predicted	Reliability (β)	
					Normal	Lognormal
All data	70	0.74	0.23	2.9%	1.53	1.44

The reliability index, β, for the NCHRP Project 24-20 abutment scour equation was determined to be 1.53 and 1.44 for normal and lognormal distributions, respectively. These relatively high values of β reflect the fact that the curves for the amplification factors α_A and α_B for both spill-through and wingwall abutments (Figures 4-8 through 4-11) were developed by Ettema et al. (2010) as envelope curves for design. Although the Ballio data tend to be overpredicted by the NCHRP Project 24-20 method, it was important to include an independent data set and not rely solely on Ettema's data. Table 4.4 provides a summary of the prediction statistics for the NCHRP Project 24-20 abutment scour procedure.

CHAPTER 5

Probability-Based Scour Estimates

5.1 Introduction

Chapter 5 provides two approaches for assessing the conditional probability that the design scour depth will be exceeded for a given design flood event. Either approach can be used to estimate this probability for each of the three individual scour components. The first approach (Level I) assumes that the practitioner can categorize a bridge based on three general conditions: (1) the size of the bridge, channel, and floodplain; (2) the size of the piers; and (3) the hydrologic uncertainty. This Level I approach provides scour factors which can be used to multiply the estimated scour depth to achieve a desired level of confidence based on the reliability index, commensurate with standard LRFD practice.

When the practitioner cannot match a particular site to a category based on the general conditions described in the preceding paragraph, a Level II approach is necessary. The Level II approach is necessarily site-specific and is illustrated using data from a bridge on the Sacramento River. The discussion includes the results for pier, contraction, abutment, and total scour considering hydrologic uncertainty, hydraulic uncertainty, and scour prediction (model) uncertainty. A step-by-step summary of the Level II procedure is also provided.

5.2 Approach

5.2.1 Background

The primary objective of NCHRP Project 24-34 (Lagasse et al. 2013) was to develop a methodology that can be used to estimate the probability that the design scour level will be exceeded. The goal was to check whether the probability of design scour exceedance will meet an acceptable level of risk. The developed probabilistic procedures were to be consistent with LRFD approaches used by structural and geotechnical engineers.

This objective was achieved by providing a set of tables of probability values and scour factors for a given design event that can be used to associate the estimated scour depth with a conditional probability of exceedance (i.e., **that probability is conditional based on the hydrologic design event selected**). The probability values and scour factors were calibrated for typical bridge foundations and river channel geometries and conditions. A 100-year return period was used as the design event.

This approach is identified as Level I analysis. For complex foundation systems and channel conditions, or for cases requiring special consideration, a Level II approach that consists of a step-by-step procedure that hydraulic engineers can follow to provide site-specific probability estimates was developed. Providing the Level II option is similar to what the AASHTO *Guide Manual for Condition Evaluation and Load and Resistance Factor Rating (LRFR) of Highway Bridges* (2005) proposes when a refined evaluation is deemed necessary.

5.2.2 Calibration of Level I Statistical Parameters

The Level I approach provides an easy-to-apply method to allow the engineer to control the level of safety to use when designing a foundation for scour. The calibration of the probability values and scour factors requires knowledge of the appropriate bias and COV values, which may depend on the bridge foundation and channel geometric and site conditions. These two parameters must account for all the levels of uncertainties and conservative assumptions that are intentionally or unintentionally embedded in the scour estimation process.

Two types of uncertainties need to be accounted for:

1. Aleatory uncertainties (natural uncertainties due to inherent parameter variability and randomness), and
2. Epistemic uncertainties (modeling uncertainties).

Aleatory uncertainties are due to random variations in the variables that control the parameter being estimated. For example, a 100-year river discharge rate used for design is only an estimated value that is calculated from previous discharge rates. Such estimates are associated with various levels of uncertainties. Similarly, even when measured in laboratory tests, estimated values of soil properties are associated with various levels of uncertainties that are due to local spatial variations in the soil profile and uncertainties in the accuracy of the test devices.

The calibration of the probability values and scour factors accounts for the uncertainties inherent in the scour analysis process. These include modeling (epistemic) uncertainties as well as parametric (aleatory) uncertainties as described in the preceding paragraph. The availability of probability values and scour factors that represent typical (standard) conditions provides an engineer with the flexibility of selecting the level of scour risk appropriate for the particular bridge being analyzed for a given design event. That level of risk is represented by a reliability index, β. (See Section 2.5.2 for a discussion of the reliability index as a measure of structural safety.)

Section 5.2.3 and Section 5.3 outline the development of the scour factor tables, describe a representative table, and summarize the bias and COV values for the individual scour components. Chapter 7 provides illustrative examples applying the Level I approach to determine the conditional probability of exceedance for estimated scour depths for bridges selected from different physiographic regions of the United States.

5.2.3 Level I Applications for Typical Site Conditions

The Level I approach to providing probability values and scour factors for typical or standard bridge configurations is shown in Table 5.1. A 3 x 3 matrix based on bridge size (bridge length) and pier size is considered as shown in the table. The analysis includes a small, medium, and large bridge each with small, medium, and large piers. The size of the piers increases proportionately with each bridge.

Bridge, channel, and floodplain size scale together and each must be represented by a Monte Carlo simulation. In addition, the typical bridge matrix was expanded by including three levels

Table 5.1.   Bridge and pier geometry for typical bridges.

Bridge Size	Bridge Length (ft)		Pier Size (ft)		
	Range	Monte Carlo	Small	Medium	Large
Small	< 100	50	1	2	3
Medium	100–300	180	1.5	3	4.5
Large	> 300	1200	3	6	9

Table 5.2.   Bridge discharges for typical bridges.

Bridge Size	Q_{100} (cfs)	Hydrologic Uncertainty					
		Low		Medium		High	
		5%	95%	5%	95%	5%	95%
Small	1,840	1,610	2,100	1,520	2,230	1,430	2,370
Medium	29,800	24,800	35,700	22,800	38,900	21,000	42,200
Large	144,000	117,000	178,000	106,000	196,000	96,400	216,000

of hydrologic uncertainty. The values in Table 5.2 show the 100-year discharges used for the typical bridges and correspond to the values shown in Table 3.2 and Table 3.4. Thus, a total of 27 scour permutations were considered for the Level I analysis.

5.3 Level I Analysis and Results

The results of each of the 27 Monte Carlo scour simulations (3 bridge sizes × 3 pier sizes × 3 hydrologic uncertainties) were analyzed to compute pier scour (HEC-18 and Florida DOT), contraction scour (HEC-18), and abutment scour (NCHRP 24-20) for representative 100-year design events (see Table 5.2). Total scour, the sum of pier and contraction scour, was also computed using each of the pier scour equations. Each simulation included a computation of design scour for the base condition. With every Monte Carlo realization, the computed amounts of each scour component were adjusted with the laboratory bias and COV applied as normally distributed random numbers. This produced data sets of 10,000 scour values that included model (equation) uncertainty and hydraulic uncertainty, where hydraulic uncertainty is the combination of hydrologic, Manning n, and boundary condition uncertainties. From each Monte Carlo simulation (10,000 runs), the expected scour (mean of the data set), bias (expected/design), standard deviation (SD), and COV (standard deviation/expected) were computed.

In total, more than 300,000 HEC-RAS/Monte Carlo simulations were required to produce the statistics on which the 27 tables in Appendix B are based. In addition, more than 300,000 scour calculations for each of the scour equations (i.e., more than 1.2 million off-line scour calculations) were completed off-line.

For each of the types of scour, the bias from the Monte Carlo simulation was essentially equal to the model bias. This was expected because the hydraulic uncertainties result in scour conditions more and less severe than the base hydraulic condition. For pier scour (both HEC-18 and Florida DOT), the COV from the Monte Carlo simulations was also essentially the same as the model COV. This indicates that the model bias and COV are the primary factors for the extreme conditions represented by the Monte Carlo simulations, which were computed for 100-year events. For contraction and abutment scour, although the bias from the Monte Carlo simulations was essentially equal to the model bias from the laboratory data, COV was greater in the Monte Carlo simulations. Although the hydraulic conditions were both more and less severe than the base condition, the variability of hydraulic conditions produced highly variable contraction scour results. Because abutment scour depends on contraction scour, the increased variability was also seen in the abutment scour results.

Table 5.3 shows the summary table from one Monte Carlo simulation. Appendix B presents 27 summary tables from the Monte Carlo simulations (see also Table 5.1 and Table 5.2). Table 5.3 represents a medium bridge with a medium pier size and medium hydrologic uncertainty, and corresponds to Table B.14 in the Appendix. Each of the types of scour is shown. For pier scour, the HEC-18 equation results in design scour of 7.20 ft. Design contraction scour is 8.02 ft, for

Table 5.3.   Medium bridge, medium hydrologic uncertainty, medium pier (3 ft).

	Pier Scour (HEC-18)	Pier Scour (FDOT)	Contraction Scour	Total Scour (HEC-18)	Total Scour (FDOT)	Abutment Scour
Design scour (ft)	7.20	5.94	8.02	15.22	13.95	15.12
Expected scour (ft)	4.89	4.45	7.42	12.31	11.87	11.35
Bias	0.68	0.75	0.93	0.81	0.85	0.75
Std. dev. (ft)	0.77	0.79	2.74	2.86	2.89	3.18
COV	0.16	0.18	0.37	0.23	0.24	0.28
Design scour β	2.99	1.89	0.22	1.01	0.72	1.18
Non-exceedance	0.9986	0.9706	0.5857	0.8444	0.7648	0.8818
Scour Non-exceedance (ft) Based on Monte Carlo Results						
$\beta = 0.5$ (0.6915)	5.29	4.85	8.60	13.58	13.13	12.77
$\beta = 1.0$ (0.8413)	5.68	5.24	10.17	15.18	14.76	14.55
$\beta = 1.5$ (0.9332)	6.05	5.63	11.89	16.90	16.47	16.38
$\beta = 2.0$ (0.9772)	6.44	6.01	13.56	18.69	18.28	18.21
$\beta = 2.5$ (0.9938)	6.73	6.37	15.50	20.73	20.21	20.54
$\beta = 3.0$ (0.9987)	6.96	6.62	17.24	22.54	22.19	22.31
Scour Factors Based on Monte Carlo Results						
$\beta = 0.5$ (0.6915)	0.73	0.82	1.07	0.89	0.94	0.84
$\beta = 1.0$ (0.8413)	0.79	0.88	1.27	1.00	1.06	0.96
$\beta = 1.5$ (0.9332)	0.84	0.95	1.48	1.11	1.18	1.08
$\beta = 2.0$ (0.9772)	0.89	1.01	1.69	1.23	1.31	1.20
$\beta = 2.5$ (0.9938)	0.94	1.07	1.93	1.36	1.45	1.36
$\beta = 3.0$ (0.9987)	0.97	1.11	2.15	1.48	1.59	1.48
Scour Non-exceedance (ft) Based on Scour Mean and Standard Deviation						
$\beta = 0.5$ (0.6915)	5.28	4.84	8.79	13.75	13.31	12.94
$\beta = 1.0$ (0.8413)	5.66	5.23	10.16	15.18	14.75	14.53
$\beta = 1.5$ (0.9332)	6.05	5.63	11.53	16.61	16.20	16.12
$\beta = 2.0$ (0.9772)	6.43	6.02	12.91	18.04	17.64	17.72
$\beta = 2.5$ (0.9938)	6.82	6.42	14.28	19.48	19.08	19.31
$\beta = 3.0$ (0.9987)	7.20	6.81	15.65	20.91	20.53	20.90
Scour Factors Based on Scour Mean and Standard Deviation						
$\beta = 0.5$ (0.6915)	0.73	0.82	1.10	0.90	0.95	0.86
$\beta = 1.0$ (0.8413)	0.79	0.88	1.27	1.00	1.06	0.96
$\beta = 1.5$ (0.9332)	0.84	0.95	1.44	1.09	1.16	1.07
$\beta = 2.0$ (0.9772)	0.89	1.01	1.61	1.19	1.26	1.17
$\beta = 2.5$ (0.9938)	0.95	1.08	1.78	1.28	1.37	1.28
$\beta = 3.0$ (0.9987)	1.00	1.15	1.95	1.37	1.47	1.38

a total design scour of 15.22 ft. Considering the bias in the scour equations, the results of the Monte Carlo simulation indicate expected scour of 4.89 ft of pier scour, 7.42 ft of contraction scour, and 12.31 ft of total scour. Although the sum of the expected component scour values equals the total expected scour, the expected total scour was actually calculated as the average of the 10,000 computed total scour amounts. This very consistent result indicates that the expected total scour can be computed from the expected values of pier and contraction scour.

Looking in Table 5.3 and using Equation (2.8), the HEC-18 pier scour equation reliability index, β, is calculated as $(7.20 - 4.89)/0.77 = 3.0$, which compares to the table's value of 2.99. The difference is due to the number of significant figures displayed in the table. Contraction scour has a very low reliability based on the expected scour being only slightly less than the design

scour and a very large value of COV, which was 0.21 from the model (equation) and increased to 0.37 for this bridge associated with hydraulic uncertainty.

Also included in Table 5.3 is an estimate of the design-equation non-exceedance β value and percentile computed from the design scour, expected scour, and scour standard deviation assuming a normal distribution. As indicated in Table 5.3, a β value of 0.5 (for example) results in a probability of scour depth non-exceedance of 69.15%, or conversely, an exceedance probability of 30.85% for this bridge during a 100-year event. Notice that Table 5.3 provides scour non-exceedance depths and corresponding scour factors derived directly from the Monte Carlo simulation (based on Monte Carlo results), and also with the assumption that the 10,000 predicted scour depths are normally distributed (based on scour mean and standard deviation). The fact that the scour depths and scour factors are similar but not identical indicates that the probability distribution based on Monte Carlo results is not precisely normal.

The pier scour standard deviation for this simulation was 0.77 ft (COV = 0.16). Contraction scour was much more variable with a standard deviation of 2.74 ft (COV = 0.37). The total scour standard deviation from the Monte Carlo results was 2.86 ft (COV = 0.23) and can be estimated from the pier and contraction component values as the square root of the sum of the squares $(0.77^2 + 2.74^2)^{0.5} = 2.85$ ft (Equation [2.8]).

As shown in Table 5.3, HEC-18 and Florida DOT pier scour results have the highest level of reliability, contraction scour has the lowest level of reliability, and abutment scour has an intermediate level of reliability. Because total scour is used in design at a pier, the high reliability of the pier scour compensates for the lower level of reliability in the contraction scour value. This cannot, however, be considered a general result because of cases where there is small pier scour and large contraction scour.

Table 5.3 also shows non-exceedance scour amounts for β ranging from 0.5 to 3.0. These amounts are computed in two ways for comparison. The first method is to take the amount directly from the Monte Carlo results and the second method is to calculate the amount based on the expected scour and standard deviation. The results of the two methods generally fall within plus or minus 5% for all scour components; however, the contraction scour amounts tend to be greater with the Monte Carlo results than from the statistics for β of 2.0 to 3.0.

From the non-exeedance scour values, the scour factors for each scour component are also shown. For this bridge, pier size, and hydrologic uncertainty, the Monte Carlo results show that the HEC-18 pier scour equation provides a β of 3.0 without any increase whereas the Florida DOT equation would require a small scour factor (1.11) to achieve a β of 3.0. Based on the Monte Carlo results, the current design values of contraction and abutment scour would have to be increased by factors of 2.15 and 1.48 to achieve this level of reliability.

The scour factors for each component can be used for that component individually but cannot be combined individually to arrive at the scour factor for total scour. Abutment scour is total scour based on the development of the NCHRP Project 24-20 equation. Total scour at a pier includes pier and contraction scour. Although the scour factors for total scour (pier plus contraction) are shown, they depend on the relative amounts of the two types of scour.

Therefore, the β value for total scour should include calculation of the design scour components and total scour, expected scour components and total scour, and the standard deviation of the scour components and total scour. Simply adding the scour components for a specific β value would be overly conservative. For example, using a β of 2.5 and the statistical results in Table 5.3, Florida DOT pier scour is 6.42 ft and contraction scour is 14.28 ft, which combines to 20.70 ft. The total scour for β = 2.5 is 19.08 ft. Using the expected scour and standard deviations of the scour components, the total scour for β = 2.5 is 19.0 ft, which is very close to the desired result. The value of 19.0 ft comes from expected scour of 11.87 ft (4.45 ft pier + 7.42 ft

contraction) and standard deviation of 2.85 ft $(0.79^2 + 2.74^2)^{0.5}$, with a 2.5 multiplier for β (11.87 $+ 2.5 \times 2.85 = 19.00$ ft). This approach is general in that it accounts for any relative range of pier and contraction scour.

Figure 5.1 shows the scour factors for HEC-18 pier scour for all 27 bridge, pier, and hydrologic uncertainty combinations presented in Appendix B (see Figure B.1). In the legend SB, MB, and LB represent small, medium, and large bridges; LH, MH, and HH represent low, medium, and high hydrologic uncertainty; and SP, MP, and LP represent small, medium, and large piers.

Figure 5.1(a) shows the scour factors obtained directly from the results of the Monte Carlo simulations and Figure 5.1(b) shows the scour factors obtained from the bias and COV of each

(a)

(b)
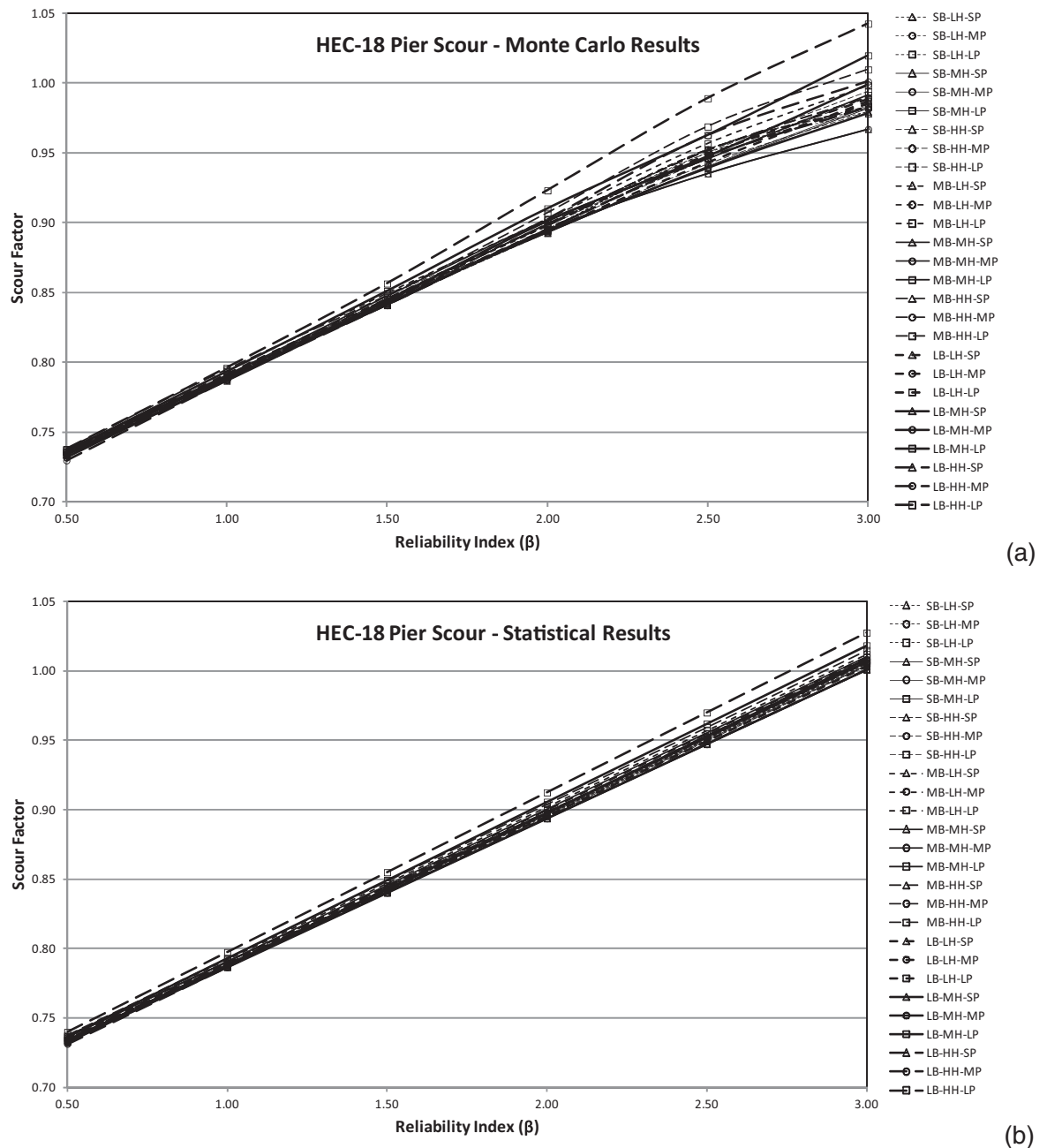
Figure 5.1. Scour factors for HEC-18 pier scour equation.

of the simulations. For pier scour, whether the HEC-18 or Florida DOT equation is used, there is very little difference in the scour factors among the 27 simulations. At a β of 3, the range obtained from the Monte Carlo results is 0.97 to 1.04 with an average of 0.99. From the statistical results, the range is 1.00 to 1.03 with an average of 1.01. The two highest scour factors were computed for the large bridge, large pier, medium and high hydrologic uncertainty runs. Although the bias for these runs was consistent with the other runs, the COV for these runs was 0.17, compared with 0.16 for all the other runs.

Figure 5.2 shows the scour factors for the Florida DOT equation. There is very little difference in the scour factors among the 27 runs and very little difference between the Monte Carlo

(a)

(b)
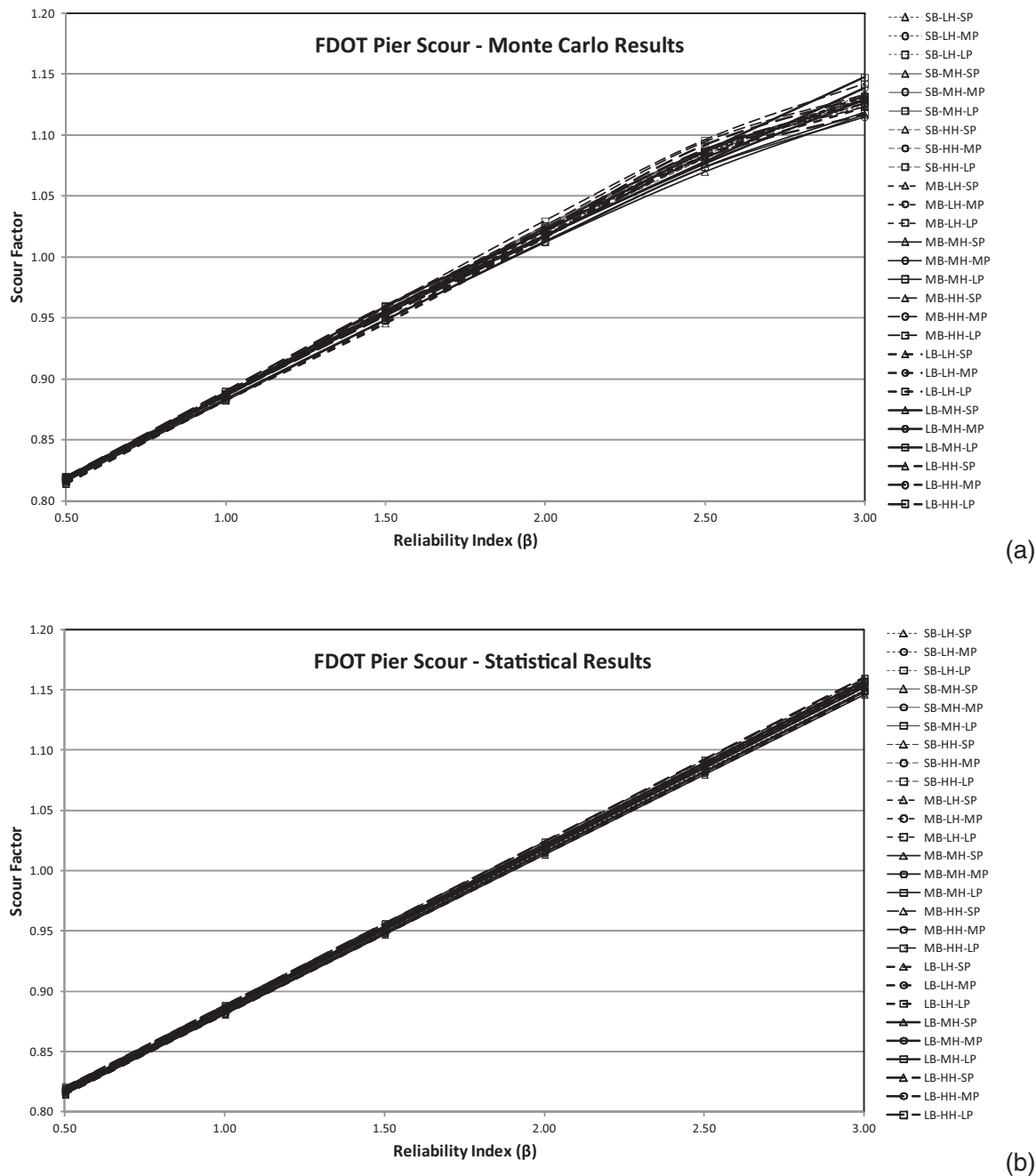
Figure 5.2.   Scour factors for Florida DOT (FDOT) pier scour equation.

results shown in Figure 5.2(a) and the statistics shown in Figure 5.2(b). The scour factors for the Florida DOT method are slightly higher than those for the HEC-18 equation, indicating slightly lower conservatism in the Florida DOT design equation. For a β of 2.5, the Florida DOT equation would require a scour factor of only 1.09.

Table 5.4 and Table 5.5 show the bias and COV for HEC-18 and Florida DOT pier scour equations and all 27 Monte Carlo simulations. These tables demonstrate that three significant figures are required to discern any difference in these statistics, except for COV of the large bridge, large pier, medium and high hydrologic uncertainty conditions for the HEC-18 equation. Therefore, the pier scour bias and COV can be summarized and were applied as shown in Table 5.6, which shows the same values as the laboratory data values.

Table 5.4.   HEC-18 pier scour bias and COV from Monte Carlo analysis.

		Pier Scour Bias (HEC-18)								
		Small Bridge			Medium Bridge			Large Bridge		
		S-Pier	M-Pier	L-Pier	S-Pier	M-Pier	L-Pier	S-Pier	M-Pier	L-Pier
Hydrologic uncertainty	Low	0.680	0.679	0.679	0.680	0.680	0.682	0.680	0.679	0.680
	Medium	0.680	0.679	0.680	0.680	0.680	0.681	0.679	0.677	0.680
	High	0.679	0.678	0.679	0.682	0.682	0.682	0.680	0.676	0.682
		Pier Scour COV (HEC-18)								
		Small Bridge			Medium Bridge			Large Bridge		
		S-Pier	M-Pier	L-Pier	S-Pier	M-Pier	L-Pier	S-Pier	M-Pier	L-Pier
Hydrologic uncertainty	Low	0.159	0.160	0.160	0.159	0.159	0.162	0.158	0.161	0.162
	Medium	0.159	0.160	0.160	0.157	0.157	0.161	0.158	0.163	0.166
	High	0.158	0.160	0.161	0.159	0.159	0.163	0.157	0.164	0.169

Table 5.5.   Florida DOT pier scour bias and COV from Monte Carlo analysis.

		Pier Scour Bias (Florida DOT)								
		Small Bridge			Medium Bridge			Large Bridge		
		S-Pier	M-Pier	L-Pier	S-Pier	M-Pier	L-Pier	S-Pier	M-Pier	L-Pier
Hydrologic uncertainty	Low	0.751	0.751	0.751	0.750	0.750	0.750	0.748	0.748	0.748
	Medium	0.751	0.751	0.751	0.748	0.749	0.749	0.750	0.750	0.750
	High	0.750	0.750	0.750	0.752	0.753	0.754	0.751	0.752	0.752
		Pier Scour COV (Florida DOT)								
		Small Bridge			Medium Bridge			Large Bridge		
		S-Pier	M-Pier	L-Pier	S-Pier	M-Pier	L-Pier	S-Pier	M-Pier	L-Pier
Hydrologic uncertainty	Low	0.177	0.177	0.177	0.181	0.181	0.181	0.178	0.178	0.179
	Medium	0.180	0.180	0.180	0.177	0.177	0.178	0.179	0.180	0.181
	High	0.179	0.179	0.179	0.178	0.179	0.180	0.178	0.180	0.181

Table 5.6.   Pier scour equation bias and COV from Monte Carlo analysis.

Equation	Pier Scour	
	Bias	COV
HEC-18	0.68	0.16
Florida DOT	0.75	0.18

Figure 5.3 shows the scour factors for contraction scour. Pier size was considered a secondary influence with contraction scour; therefore, the nine conditions represent bridge size and hydrologic uncertainty. Because the contraction scour equation is a predictive equation and is significantly influenced by the variability of flow distribution resulting from hydraulic uncertainty, the scour factors are significantly greater than for pier scour. Figure 5.3(a) shows the scour factors obtained directly from the Monte Carlo results and Figure 5.3(b) shows the scour factors calculated from the statistics (bias and COV).

Up to β of 1.5 there is little difference in the two plots, but the curves diverge for higher levels of β. This indicates that there is positive skew in the distribution, as is shown in Figure 5.9 (see

(a)

(b)
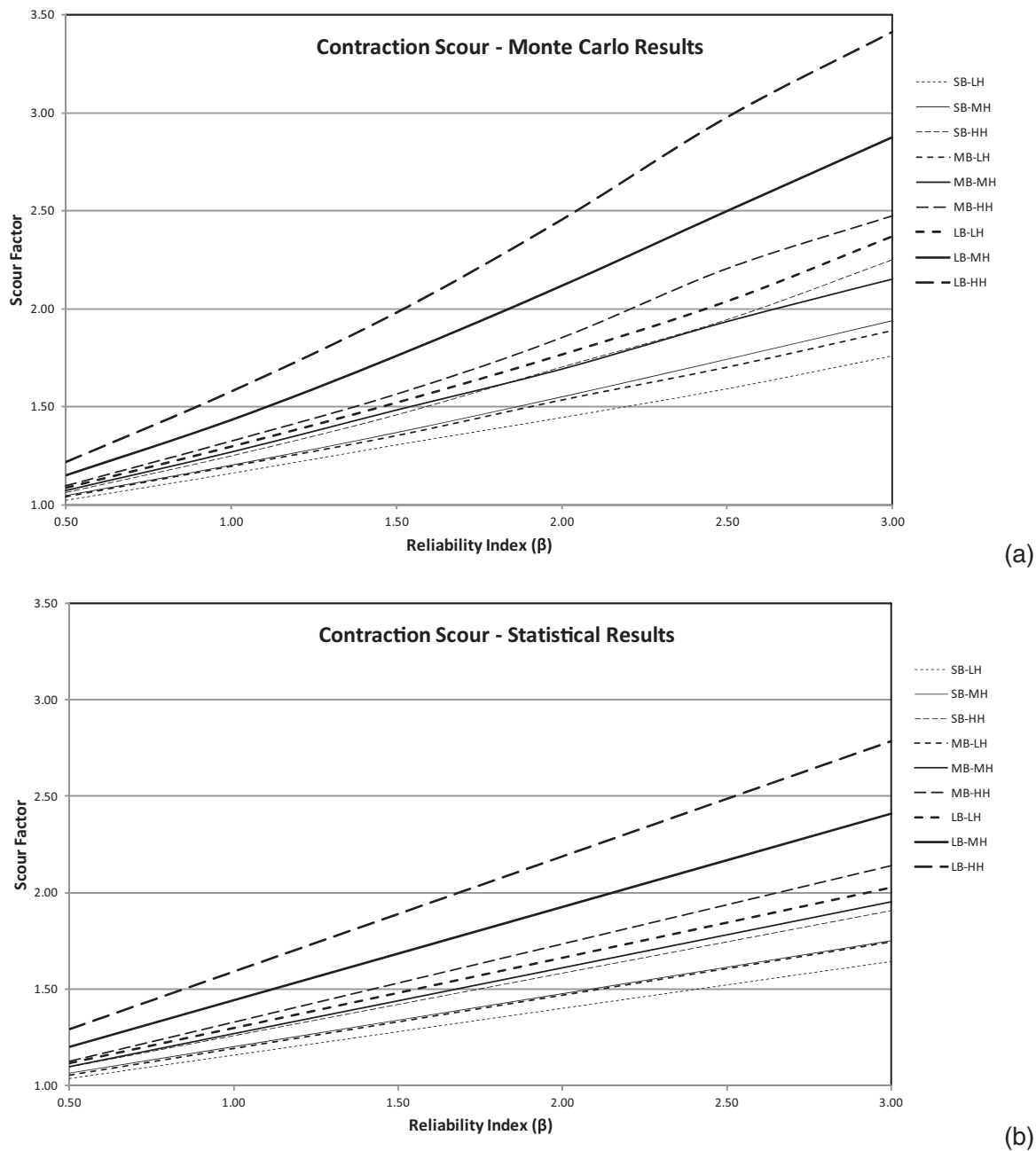
Figure 5.3.   Scour factors for contraction scour.

Table 5.7.   Contraction scour bias and COV.

		Contraction Scour Bias Bridge Size			Contraction Scour COV Bridge Size		
		Small	Medium	Large	Small	Medium	Large
Hydrologic uncertainty	Low	0.92	0.92	0.93	0.26	0.30	0.39
	Medium	0.93	0.93	0.96	0.29	0.37	0.50
	High	0.93	0.92	0.99	0.35	0.44	0.60
Laboratory data		0.92			0.21		

Section 5.4.3). Had a lognormal distribution been used, the degree of curvature would have exceeded what is shown in Figure 5.3(a). Also shown in Figure 5.9 is an example of the reduced extreme values of contraction scour when relief from road overtopping is included. Extreme flows are most likely to create overtopping, but also produce the greatest contraction scour in the Monte Carlo simulation (which excludes overtopping).

Table 5.7 shows the bias and COV for contraction scour Monte Carlo runs and the laboratory results. The bias is very consistent and similar to the laboratory results with the exception of the large bridge with medium to high hydrologic uncertainty, where the bias ranges from 0.96 to 0.99. A value of 0.93 is reasonable for all other cases. COV increases with bridge size and hydrologic uncertainty and is considerably greater than the laboratory value.

Abutment scour results are very similar to the contraction scour results. Figure 5.4 shows the scour factors, which are less than those for contraction scour but greater than those for pier scour. Table 5.8 shows that the bias is similar to that of the laboratory results, with increased values for the large bridge. COV also increases with bridge size and hydrologic uncertainty. The level of bias is lower for abutment scour because the amplification factors developed for abutment scour in the NCHRP Project 24-20 method enveloped the data (see Section 4.4.2).

5.4 Level II Analysis and Results

The application of the 27 tables calibrated for the Level I approach can be executed on a regular basis for probability-based analyses of typical or standard scour site conditions. However, the calibration of the Level I statistical parameters will average the model biases for pier, abutment, and contraction scour (λ_p, λ_a, and λ_c) and associated COV values and distributions for random variables at similar sites (see Section 3.3.2).

When a bridge site does not fit any of the categories identified, or when the bridge is unique or is classified as being critically important for economic, societal, or security reasons, it may be necessary to execute site-specific probabilistic or reliability analyses of scour depths using site-specific statistical data for each variable that is used as input in the scour model. Site-specific (Level II) analysis may also be required if the hydraulic uncertainty parameters exceed the values used in Level I or if other parameters not considered in Level I are deemed to be significant in the design.

The process described in detail in Section 5.4.1 would need to be followed to perform a Level II analysis. This process includes performing a Monte Carlo analysis using a hydraulic model with valid uncertainty parameters including, but not necessarily limited to, hydrologic uncertainty, flow resistance uncertainty, and boundary condition uncertainty. The scour equation bias and COV from the laboratory data as described in Chapter 4 would be used in conjunction with the hydraulic modeling results to develop the distribution of scour components and total scour. If other scour equations are used, then the individual bias and COV of these equations would also need to be determined.
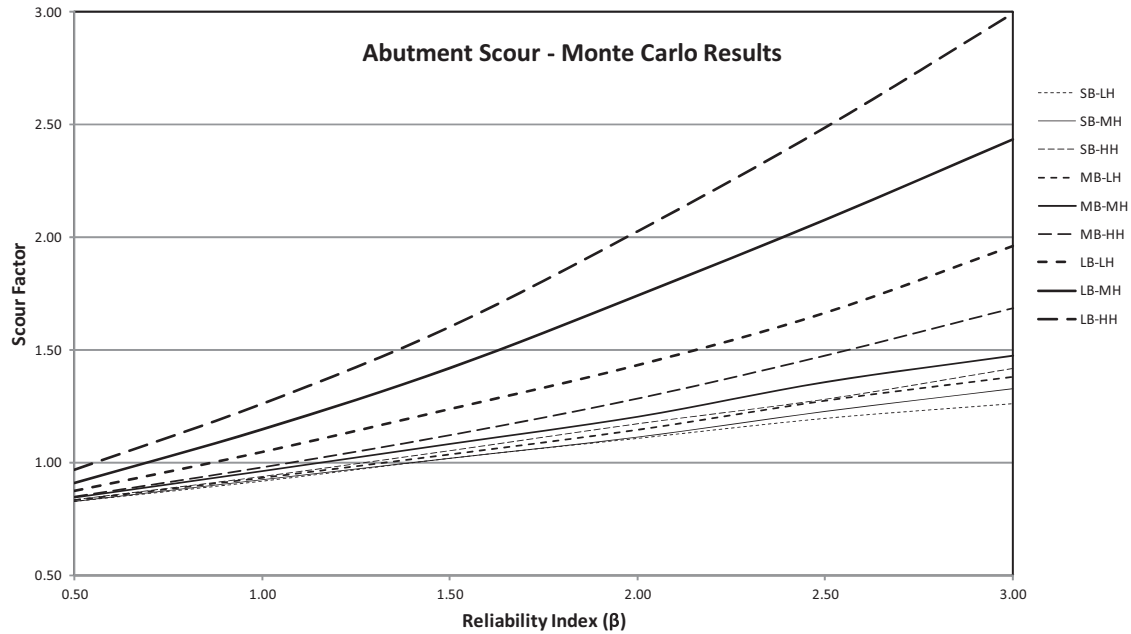
(a)
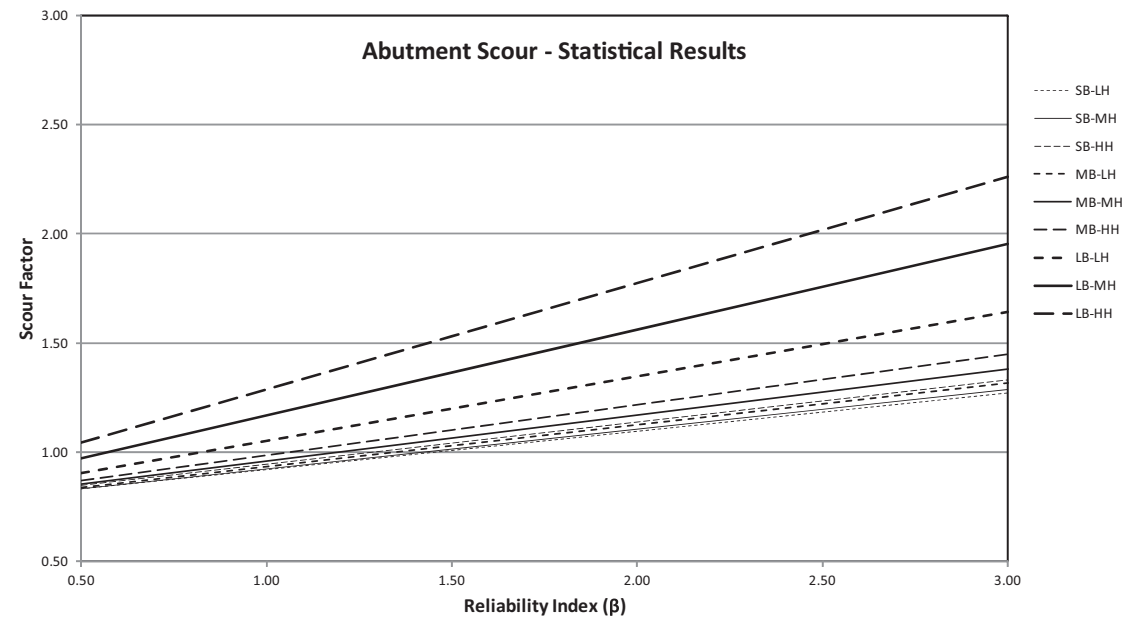
(b)

Figure 5.4.   Scour factors for NCHRP abutment scour equation.

Table 5.8.   Abutment scour bias and COV.

		Abutment Scour Bias Bridge Size			Abutment Scour COV Bridge Size		
		Small	Medium	Large	Small	Medium	Large
Hydrologic uncertainty	Low	0.74	0.74	0.76	0.24	0.26	0.39
	Medium	0.74	0.75	0.78	0.24	0.28	0.51
	High	0.75	0.75	0.80	0.26	0.31	0.61
Laboratory data		0.74			0.23		

5.4.1 Step-by-Step Procedure for Level II Analysis

A Level II analysis involves developing the statistical distribution of each scour component and total scour at a particular bridge site. This type of analysis may be required if the site conditions differ significantly from the conditions used to develop the Level I tables presented in Appendix B. A Level II analysis is useful if (1) the bridge has hydrologic or hydraulic uncertainties that are not reasonably represented by the range of Level I conditions; (2) site conditions require the use of other scour equations than were tested in Chapter 4; or (3) the bridge is considered to be significantly important and warrants a more detailed, site-specific analysis. Not all the steps outlined in this section would necessarily be required for every Level II analysis. For example, if the standard scour equations apply at the bridge site, then the model (equation) bias and COV developed in Chapter 4 would apply.

The Level II steps follow the approach used in Sections 5.2 and 5.3 to develop the Level I scour factors. Therefore, familiarity with the rest of this document is useful if a Level II analysis is to be performed. For many of the steps, a prior or subsequent chapter or section in this reference guide can serve as reference material. Steps are provided to determine the statistical distribution of scour for a specific event, such as the 100-year event, and therefore address conditional probabilities. A Monte Carlo simulation can be run for other events (as described in Chapter 6) to evaluate scour exceedance over the life of the bridge (unconditional probability). The steps of the Level II procedure are as follows:

Step 1. Develop a site-specific hydraulic model.

a. Develop a four cross-section HEC-RAS hydraulic model of the bridge site (see Section 3.4.1). The Monte Carlo analysis was developed for a four cross-section HEC-RAS model. If a large-extent model is required, then modification of the Monte Carlo software (e.g., rasTool©) would be required.

b. Make best estimates of Manning n for the channel and overbank areas. Because the Monte Carlo analysis will vary Manning n around the starting estimate, it is important to *not* use conservative values (high or low) of Manning n, as doing so will bias the results. Calibrated values should be used if observed water surface data are available.

c. Make a best estimate of the starting water surface boundary condition. It is recommended that the energy slope boundary condition be used, as doing so will vary the starting water surface for the various discharge values that will be applied in the Monte Carlo analysis. As with Manning n, a best estimate of the boundary condition should be used rather than a conservatively high or low value.

d. Evaluate site-specific hydrologic uncertainty (see Section 3.5.2). The Level I analysis uses a range of hydrologic uncertainties for each bridge size. For a Level II analysis, the best estimate of hydrologic uncertainty should be developed and applied. The preferred approach is to perform gage analysis and apply Bulletin 17B (Log-Pearson Type III) procedures to determine the target discharge and confidence limits.

   Notes: (1) When applying the HEC-RAS model to a wide range of conditions it may be necessary to limit road overtopping to produce more stable models. If the model is stable for road overtopping conditions, it is recommended that road overtopping be allowed, as doing so will provide more representative contraction scour results. (2) As described in Step 3 (perform Monte Carlo analysis), the model results should be evaluated to determine that the variability of water surface is reasonable for the site conditions.

Step 2. Determine scour equation (model) uncertainty (bias and COV).

a. If the standard scour equations are used (i.e., HEC-18 pier scour, Florida DOT pier scour, HEC-18 live-bed or clear-water contraction scour, or NCHRP Project 24-20 abutment scour),

then the model uncertainties (bias and COV) from the laboratory data analysis presented in Chapter 4 should be used.

b. If another scour equation is used (e.g., vertical contraction scour, coarse-bed pier scour, scour in cohesive or erodible rock materials, etc.), then the model uncertainties (bias and COV) from these alternative equations should be developed following the procedure in Chapter 4. The laboratory data for developing these equations should be used as they are from controlled conditions. HEC-18 (Arneson et al. 2012) includes references to research reports describing the development of several alternative equations.

Step 3. Perform Monte Carlo analysis.

a. Test the Monte Carlo simulation software for the bridge site (see Section 3.5) using the target (best estimate) values of discharge, channel and overbank Manning n, and starting energy slope and the uncertainties (COV) associated with these three input parameters. Determine the COV of the discharge using Equation (3.1) through Equation (3.5). The COV for Manning n should be 0.015, and uncertainty related to Manning n should be determined using Equation (3.9) through Equation (3.11). The COV of starting slope should be 0.10. However, as described in Section 3.5.3, the hydraulic results of the simulations should be reviewed to determine if the results are representative for the site. The tests should include holding discharge constant and varying only Manning n, only starting slope, and both variables. If the water surface varies much more or less than is expected and reasonable, then adjust the COV for Manning n and starting slope to better represent the site conditions. Do not adjust the discharge COV, as this was determined through statistical analysis.

b. Run the Monte Carlo simulation software using the target values of discharge, Manning n, and starting slope and the appropriate values of COV for these input variables. The number of cycles should be large enough to fully represent the range of possible hydraulic results. Because HEC-RAS executes quickly, a 10,000-cycle simulation can be achieved in less than 2 hours and should be sufficient.

Notes: (1) The rasTool© used with the Monte Carlo simulation software developed for this project is a research tool. It was not developed for distribution, nor is it thoroughly documented or supported for general use. It is, however, considered robust and could be applied to a range of bridge and/or open-channel applications. (2) If a different hydraulic model will be used, then a specific software tool will need to be developed to control the random number generation for the input parameters and to run the number of required cycles in the Monte Carlo simulation. Given the relatively longer simulation times for 2-D models, it is unlikely that the number of cycles could be large enough for their application with standard office computers, and high-performance (supercomputer) technology would need to be used.

Step 4. Compute component scour and total scour.

a. The output from the Monte Carlo simulation software is a text file table that includes the number of requested cycles of the hydraulic variables needed to perform scour calculations. This table is intended to be imported into a spreadsheet for calculating scour components and total scour. Alternatively, the results could be read by other software to calculate scour.

b. For each scour component, the computed scour should be determined by directly applying the appropriate equation. This scour value includes any level of conservatism (bias) included in the development of the equation. The variability of scour results in this step is based on the variability of the hydraulic results. (See the pier scour example and Figure 5.5 in Section 5.4.2.)

c. The computed scour from Step 4(b) is then adjusted to determine expected scour distribution by multiplying the computed scour by a random number with mean equal to the model bias (0.68 in the case of HEC-18 pier scour) and standard deviation (SD) equal to the model bias times COV (0.16 in the case of HEC-18 pier scour, resulting in a standard deviation of

0.68 x 0.16 = 0.109). The Monte Carlo simulation software includes four normally distributed random numbers (R) of mean equal to zero and standard deviation equal to 1.0, so the desired random number set for a specific scour equation is (R x SD) + Bias. The results of the component scour (pier, contraction, and abutment) are then multiplied by the random number to provide the component scour distribution. (See the pier scour example and Figure 5.6 in Section 5.4.2.)

d. At a pier, total scour is contraction plus local scour. The distribution of total scour is computed by adding the individual contraction and pier scour values including the bias and COV adjustments from Step 4(c). For abutment scour using the NCHRP Project 24-20 method, the result is total scour at the abutment. If a different scour equation is used, the evaluation of total scour must be consistent with the development of the equation.

e. Based on the distribution of total scour, the designer selects the level of scour that achieves the desired probability of scour exceedance.

The results of Step 4 are the distributions of scour for a given return period event (conditional probability). Steps 3 and 4 can be repeated for several events to evaluate the unconditional probability of scour exceedance over the life of a bridge. As described in Chapter 6, performing the Monte Carlo analysis for the 50-year, 100-year, and 500-year events and combining the scour results will provide data to evaluate scour reliability for a 75-year bridge life. Notice that the 50-year hydrologic uncertainty would be less than the 100-year hydrologic uncertainty because the 90% confidence limits would be closer to the expected value for the smaller event. Conversely, the uncertainty would be greater for the 500-year return period event. As described in Chapter 6, other sets of events would need to be evaluated for other bridge design lives.

The Level II process is illustrated in the following sections using the same Sacramento River bridge that was used to validate the HEC-RAS/Monte Carlo software in Section 3.5.3. The Level I application for this bridge is illustrated in Chapter 7 (Section 7.4, Example Bridge No. 3).

5.4.2 HEC-RAS/Monte Carlo Simulation Results for Pier Scour

The HEC-RAS model for the Sacramento River bridge was run for 20,000 cycles to evaluate the range of hydraulic conditions and scour that result from the parameter uncertainty as described in Section 3.5.3. For this application, 20,000 cycles were run to fully test the Monte Carlo application and to produce results at the extremes of the input parameters. Subsequent evaluations revealed that 10,000 Monte Carlo simulation cycles provide virtually identical probability distributions. Pier scour was evaluated using both the HEC-18 and Florida DOT procedures as described in Section 4.2.

The design condition of Q = 140,000 cfs, channel Manning n of 0.025, floodplain Manning n of 0.09, and starting energy slope of 0.00035 produced a design depth and velocity at the bridge of 24.5 ft and 12.1 ft/s. The computed HEC-18 scour for the 6 ft diameter circular pier was 13.7 ft, and the Florida DOT equation resulted in 11.2 ft of scour for a 2.0-mm bed material size. The sediment transport condition is live-bed for these conditions.

In the 20,000-cycle Monte Carlo simulation, discharge ranged from 87,000 cfs to 245,000 cfs and dominated the hydraulic conditions at the bridge. Energy slope, which ranged from 0.00022 to 0.00049, had the smallest impact on hydraulic conditions. Manning n ranged from 0.021 to 0.030 for the channel and from 0.074 to 0.108 for the floodplain. At the bridge, the design depth ranged from 19.5 ft to 30.2 ft, and design velocity ranged from 9.4 ft/s to 16.4 ft/s.

The results for pier scour in the Monte Carlo simulation are summarized in Table 5.9. Although the simulated discharge varied by more than a factor of 2.5 and velocity varied
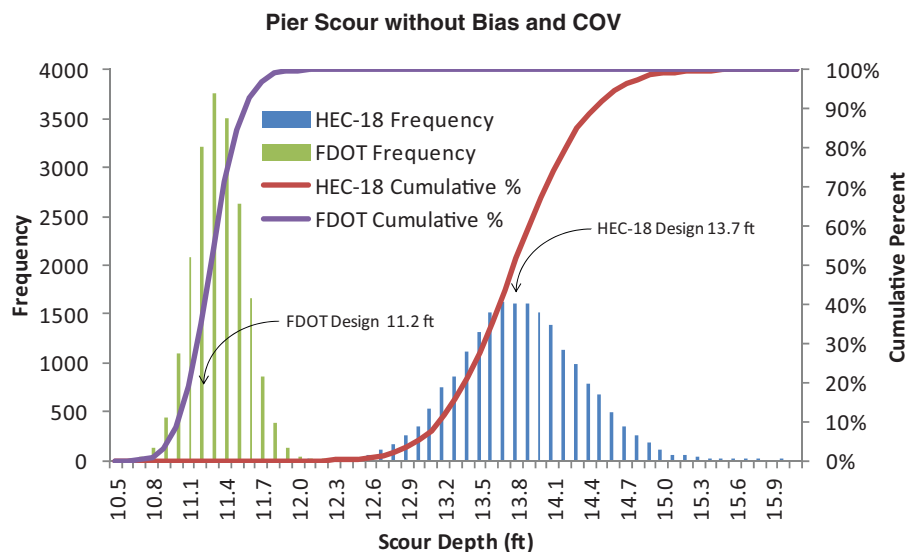
Figure 5.5.   *Direct pier scour results from HEC-RAS Monte Carlo simulations.*

significantly, the computed range of pier scour was 4 ft for the HEC-18 equation and was only 1.6 ft for the Florida DOT equation. For this range of hydraulic conditions, the range of computed scour from the Florida DOT equation is very small, indicating that the Florida DOT equation is less sensitive to hydraulic conditions. Notice that the maximum computed scour from the HEC-18 equation exceeds 2.4 times the pier width, which is an expected upper limit based on a circular pier and Froude number less than 0.8.

The pier scour results are also shown in Figure 5.5 and Figure 5.6. In Figure 5.5, the direct results of the Florida DOT and HEC-18 equations are shown for the computed velocity and depth from the HEC-RAS models. The design value for each of these equations is shown, and
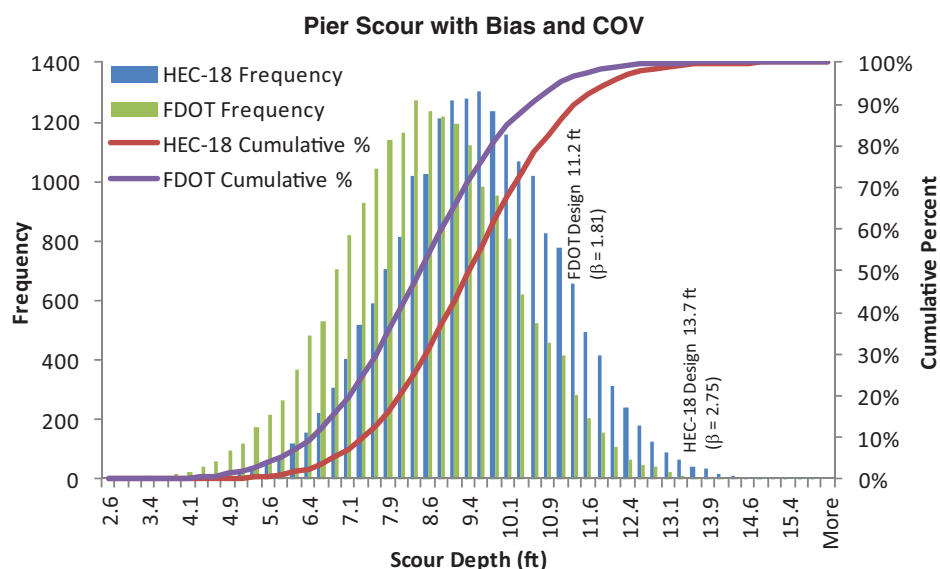
Figure 5.6.   *Pier scour results from HEC-RAS Monte Carlo simulations after including equation bias and COV.*

Table 5.9.   Pier scour results from 20,000-cycle Sacramento River bridge HEC-RAS.

Variable	HEC-18 Equation	Florida DOT Equation
Design scour (ft)	13.7	11.2
Mean scour (ft)	13.8	11.3
SD (ft)	0.49	0.21
COV	0.036	0.019
Minimum computed scour (ft)	12.1	10.6
Maximum computed scour (ft)	16.0*	12.2
Results After Applying Bias and COV		
Mean scour (ft)	9.4	8.5
SD (ft)	1.56	1.59
COV	0.166	0.189
Minimum computed scour (ft)	3.5	2.6
Maximum computed scour (ft)	15.8*	14.1
β (design result)	2.75	1.81
Scour factor for β = 3.0	1.04	1.17
Scour required for β = 3.0 (ft)	14.2	13.1

*Computed scour greater than 2.4 times the circular pier width.

in each case the design value is very close to the mean of the calculated values. This is expected because in the Monte Carlo simulation velocity and depth are distributed around the base-model results. Figure 5.5 illustrates that for this particular bridge hydraulic condition, the Florida DOT equation and the HEC-18 equation have no overlap, although the actual magnitude of scour is not significantly different. The Florida DOT equation is less sensitive to the hydraulic conditions, resulting in a spread of only 1.6 ft versus a spread of 4 ft for the HEC-18 equation.

Figure 5.6 shows the results after each equation's bias and COV are introduced. From the analysis of laboratory pier sour data, the bias and COV of the observed versus computed scour is 0.68 and 0.16 for the HEC-18 equation and 0.75 and 0.18 for the Florida DOT equation.

Assuming a normal distribution, these values result in an estimated conditional reliability (β) of 2.92 and 1.78 for the HEC-18 and Florida DOT equations (see Section 2.5.2 for a discussion of the reliability index as a measure of structural safety). The computed scour was then multiplied by normally distributed random values with mean equal to the bias, and SD based on the COV for each equation. As shown in Figure 5.6, because the HEC-18 equation has a smaller bias and COV than the Florida DOT equation, the resulting distributions are similar with only a small offset. From these results the value of β can be determined for each equation. The computed values of β from the Monte Carlo analysis (the HEC-18 β = 2.75 and the Florida DOT β = 1.81) are essentially the same as those originally estimated from the live-bed laboratory data bias and COV, assuming a normal distribution, which indicates that the implementation of the Monte Carlo simulation is reliable. If a target β of 2.5 is desired, then the Florida DOT design value of 11.2 ft would need to be increased to 12.4 ft (multiplied by a factor of 1.11) and the HEC-18 equation design value of 13.7 ft would need to be decreased to 13.4 ft (multiplied by a factor of 0.98).

Table 5.9 also shows the pier scour results after applying the bias and COV for each equation based on live-bed laboratory data. For this 100-year flow condition, the HEC-18 equation provides a β of 2.75, whereas the Florida DOT equation yields results that would need to be increased to provide the same level of reliability. The scour factors to achieve a β of 3.0 are shown, and in this case both equations would require greater design scour to achieve this level of reliability. Use of the Florida DOT equation for this bridge and hydraulic condition does

result in less required scour (11.2 x 1.17 = 13.1 ft) to achieve the same reliability as the HEC-18 equation (13.7 x 1.04 = 14.2 ft), as shown in Table 5.9 for a β of 3.0. This is due primarily to the fact that the Florida DOT equation is less sensitive over a wide range of velocity and depth.

5.4.3 HEC-RAS/Monte Carlo Simulation Results for Contraction Scour

Contraction scour is caused by a change in flow distribution from upstream of the bridge (approach cross section) to the bridge. At the approach, flow is distributed throughout the overall cross section among the channel, left, and right floodplains based on the conveyance of these sub-areas. At the bridge, flow is concentrated in the bridge opening entirely in the channel if the abutments are set at the channel bank or into the channel. If the abutments are set back from the channel banks, then some of the flow is conveyed in the setback areas between the channel banks and the abutments. The Monte Carlo simulations vary discharge, starting energy slope (downstream boundary condition), and channel and overbank Manning n values. Each of these parameters affects flow distribution at the approach and at the bridge. As with pier scour, contraction scour was computed for the 20,000-cycle simulation of the Sacramento River bridge to fully accommodate the extremes of the input parameters.

The design condition produced a design contraction scour of 5.3 ft. Although the largest computed contraction scour was generated from the highest discharges, other combinations of conditions also produced significantly more (or less) contraction scour than the design value. For example, if the channel Manning n value is high and the floodplain Manning n is low, then more flow is conveyed in the floodplain. This condition results in a much greater amount of flow constriction and much greater contraction scour. Conversely, a low channel Manning n combined with a high floodplain Manning n concentrates flow in the channel, resulting in less flow constriction at the bridge and much less contraction scour. The range of computed contraction scour was from 0.55 ft to 14.0 ft.

Another process that affects contraction scour is road overtopping. It has been standard practice to limit scour analyses to flow up to the point of road overtopping (Arneson et al. 2012). The rationale is that once road overtopping commences, flow through the bridge will not increase because of the significant amount of relief provided by the weir flow over the road. To keep the HEC-RAS model stable over the full range of flow and other input parameters, road overtopping was eliminated from the model and all flow was conveyed through the bridge opening. It is also better to exclude road overtopping for the general Monte Carlo analyses because the elevation where road overtopping initiates will be specific to the bridge. In the spreadsheet used to compute scour, however, adjustments were made to assess the impacts of road overtopping for the Sacramento River bridge. To develop Figure 5.7, the road elevation was set at a reasonable height relative to the design water surface elevation. The lower limit of computed contraction scour was, of course, unchanged. The upper limit was 9.2 ft and occurred with slight road overtopping flow (3,000 cfs of a total 181,000 cfs in that run).

A comparison of contraction scour estimates with and without road overtopping is shown in Figure 5.7. The majority of the simulations (16,907 cycles) did not generate road overtopping flow. The remaining simulations (3,093 cycles) generated up to 77,400 cfs of road overtopping flow. In Figure 5.7, the computed contraction scour is plotted versus the road overtopping discharge whether or not road overtopping was considered. This illustrates that for small amounts of road overtopping the scour is relatively unaffected by the relief flow, but that for the largest amounts road overtopping, scour can be minimal (2 ft versus 14 ft). Generally, road overtopping is undesirable, but from this analysis it is clear that it can greatly reduce contraction scour potential.

Contraction scour results from the Monte Carlo simulation are shown in Figure 5.8 and Figure 5.9. Figure 5.8 shows the contraction scour computed directly from the hydraulic results
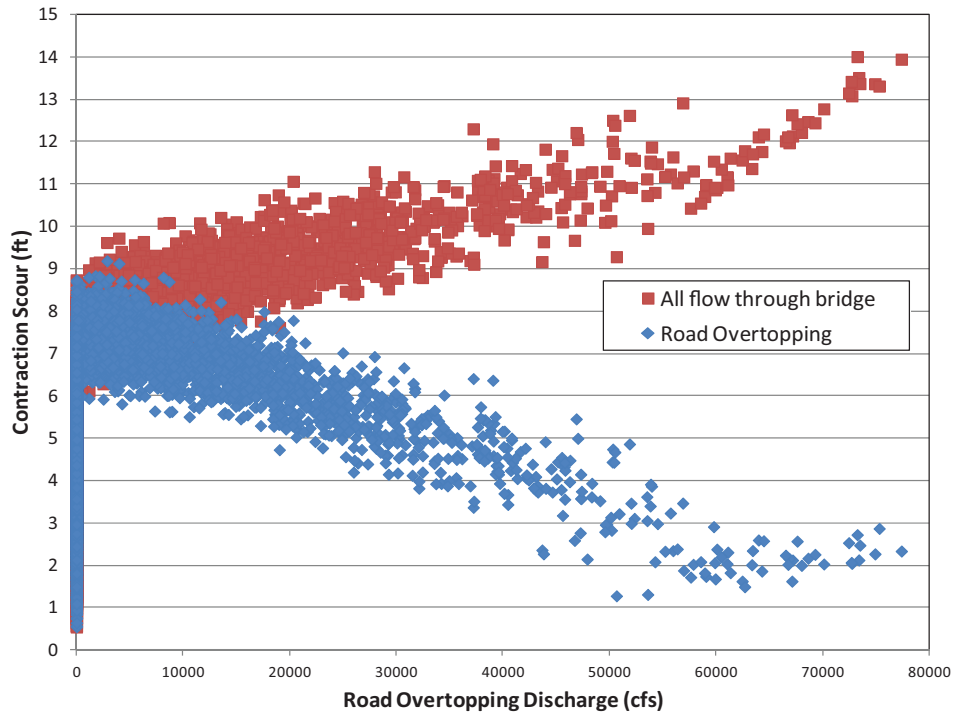
Figure 5.7. *Contraction scour with and without road overtopping.*
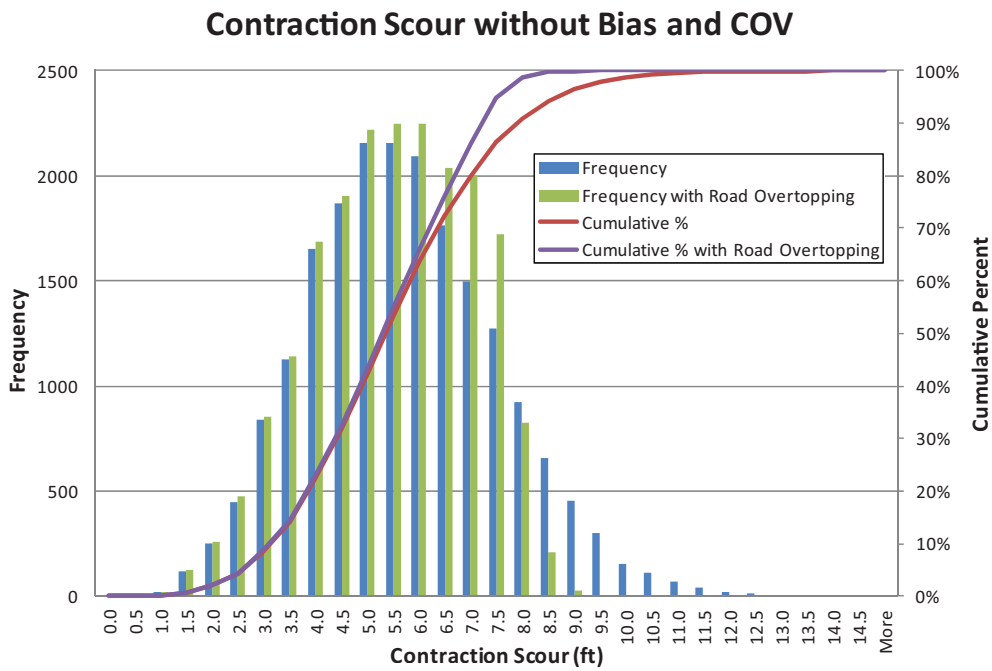
Figure 5.8. *Computed live-bed contraction scour results from HEC-RAS Monte Carlo simulations.*

Contraction Scour with Bias and COV
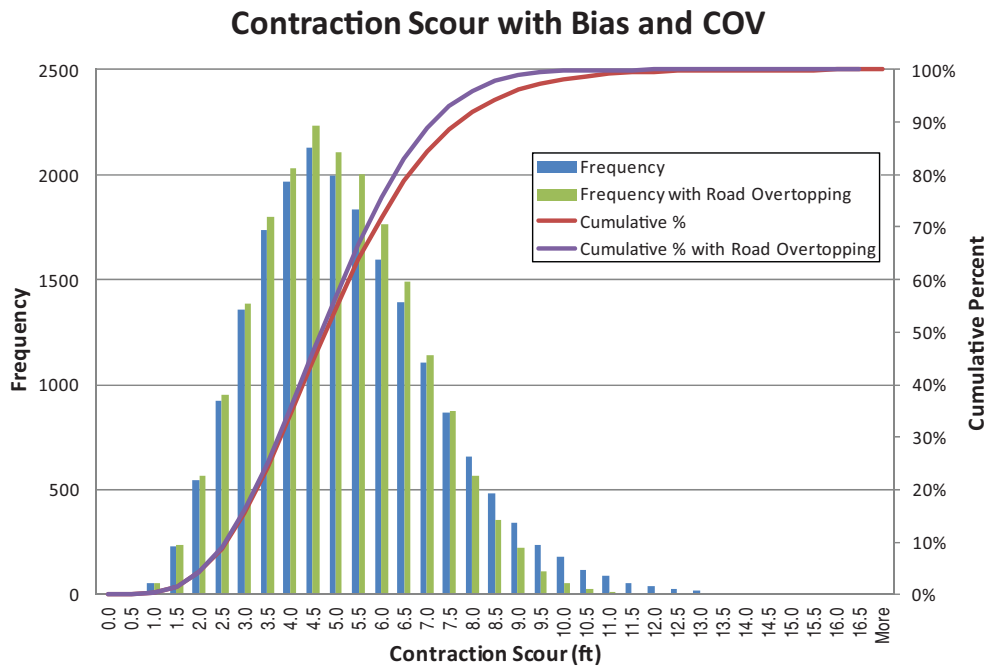
Figure 5.9.   Live-bed contraction scour results from HEC-RAS Monte Carlo simulations after including equation bias and COV.

with and without road overtopping flow. The design scour is 5.3 ft, which is centered within the distributions. Road overtopping shifts the most extreme amounts of contraction scour to lower values.

Unlike the HEC-18 and Florida DOT equations, the contraction scour equations are predictive and do not include conservative factors for design. The clear-water contraction scour equation is developed from sediment incipient motion criteria and the live-bed contraction scour equation is developed from sediment transport relationships. The HEC-18 and Florida DOT pier scour equations have bias values of 0.68 and 0.75 based on comparisons to the laboratory data, which indicates a level of conservatism. The clear-water contraction scour equation has a bias of 0.92 based on comparisons with laboratory data (see Chapter 4), which indicates very little bias (i.e., no built-in conservatism as expected in a predictive equation). Contraction scour laboratory data has a higher COV than pier scour (0.16 for HEC-18 and 0.18 for Florida DOT). This indicates greater variability in contraction scour. Although the bias and COV are for clear-water conditions, these values were applied to the live-bed equation to produce Figure 5.9. Both equations are derived based on sediment transport relationships and are predictive, so this is justifiable though not ideal. From a practical standpoint, there is insufficient live-bed data to develop independent bias and COV for the live-bed equation. Therefore, clear-water values were applied to the live-bed results.

With bias close to 1.0, the contraction scour equation has very low reliability, with β close to zero. As shown in Figure 5.9, for the larger COV the range of computed contraction scour increases significantly as compared to Figure 5.8, though the mean scour is relatively unchanged from the design value of 5.3 ft. It also made relatively little difference whether road overtopping was included.

Table 5.10 summarizes results from this set of bridge-specific simulations. Based on these results, scour factors are shown for various target levels of reliability. For example, a β of 2

Table 5.10.   Contraction scour results from 20,000-cycle Sacramento River bridge HEC-RAS.

Variable	All Flow Through Bridge					Road Overtopping				
Design scour (ft)	5.4					5.3				
Mean scour (ft)	5.5					5.2				
SD (ft)	1.85					1.53				
COV	0.338					0.293				
Minimum computed scour (ft)	0.55					0.55				
Maximum computed scour (ft)	14.0					9.2				
Results After Applying Bias and COV										
Mean scour (ft)	5.00					4.78				
SD (ft)	2.02					1.74				
COV	0.404					0.364				
Minimum computed scour (ft)	0.41					0.41				
Maximum computed scour (ft)	16.3					11.7				
β (design scour)	0.26					0.33				
Target β	1	1.5	2	2.5	3	1	1.5	2	2.5	3
Scour factor for target β	1.3	1.6	1.8	2.1	2.4	1.2	1.4	1.6	1.0	2.0
Scour required for target β (ft)	7.0	8.3	9.7	11.3	12.9	6.6	7.5	8.5	9.4	10.4

would require that contraction scour be multiplied by a factor of 1.8, resulting in a design scour of 9.7 ft if road overtopping is not considered. With road overtopping at this bridge, a β of 2 would require multiplying contraction scour by 1.6, giving 8.5 ft of scour to be used for design. This is considerably greater than the 5.3 ft that would currently be used. The level of bias for the contraction scour equations is quite reasonable considering their origin.

5.4.4 HEC-RAS/Monte Carlo Simulation Results for Abutment Scour

As described in Section 4.4, abutment scour is both a contraction and local scour process. The constriction of flow in the bridge opening that produces contraction scour also concentrates flow at the abutments. Therefore, the starting point for abutment scour is a contraction scour calculation. The obstruction of the abutment produces vortices and turbulence that amplify the contraction scour. The equations and figures in Section 4.4 present this approach to computing abutment scour for various hydraulic and sediment conditions and abutment configurations (Ettema et al. 2010).

The 20,000-cycle Monte Carlo simulation results were used to compute abutment scour at the Sacramento River bridge. The computed abutment scour for the base condition was 11.0 ft, but ranged from less than 1.0 ft to more than 30 ft depending on the hydraulic conditions computed in HEC-RAS. This variability is similar to the variability of computed contraction scour. This was expected because of the similarities of the two scour processes. As with the other scour components, the abutment scour equation bias and COV were applied to the computed scour values to determine the reliability of the design scour amount. For abutment scour, the bias and COV values are 0.74 and 0.23 from the data analysis in Chapter 4. The bias is lower than the contraction scour bias because the amplification values were developed to envelop the laboratory results.

Figure 5.10 shows the distributions of computed abutment scour and abutment scour after including equation bias and COV. Table 5.11 summarizes the results and shows scour factors
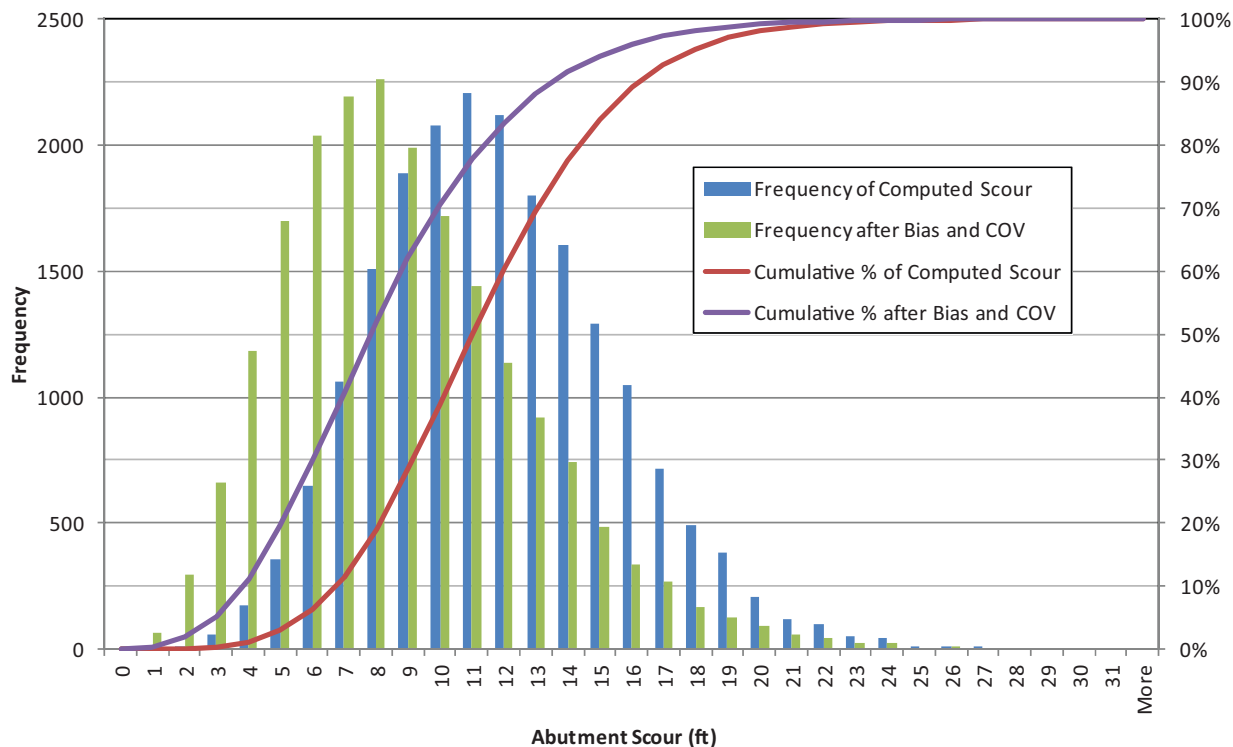
Figure 5.10.   Abutment scour results from the HEC-RAS Monte Carlo simulations.

needed to achieve various levels of reliability (β). For example, to achieve a target β value of 2.0, the design abutment scour of 11.0 ft (rounded from 10.94) would have to be increased by a factor of 1.6 to 17.5 ft. These results are based on the hydraulic variables computed without adjusting for road overtopping. As with contraction scour, it is expected that abutment scour potential would be reduced when road overtopping occurs.

Table 5.11.   Abutment scour results from 20,000-cycle Sacramento River bridge HEC-RAS.

Variable	Value				
Design scour (ft)	11.0				
Mean scour (ft)	11.3				
SD (ft)	3.7				
COV	0.33				
Minimum computed scour (ft)	0.35				
Maximum computed scour (ft)	30.4				
Results After Applying Bias and COV					
Mean scour (ft)	8.3				
SD (ft)	3.9				
COV	0.46				
Minimum computed scour (ft)	-1.4 (0.0)				
Maximum computed scour (ft)	30.4				
β (design scour)	0.78				
Target β	1.0	1.5	2.0	2.5	3.0
Scour factor for target β	1.1	1.3	1.6	1.9	2.2
Scour required for target β (ft)	12.1	14.6	17.5	20.9	24.0

CHAPTER 6

Calibration of Scour Factors for a Target Reliability

6.1 Approach

6.1.1 Background

The calculations performed for the probability-based scour estimates described in Chapter 5 are for a single discharge rate that corresponds to a design return period (e.g., the discharge rate having a return period of 100 years). Thus, the probability-based scour estimate obtained in Chapter 5 is a conditional probability of exceedance that is conditioned on the occurrence of the design discharge rate, which can be expressed symbolically as follows for a 100-year discharge rate:

$$P_{ex}/100 - yr\ rate \tag{6.1}$$

During its service life, T_n, a bridge might be exposed to a large range of possible discharge rates. Some of these discharge rates may exceed the one used for the design return period. Many others will be smaller, but they are still capable of causing scour at the bridge. Within the service life, each of these possible discharge rates will have a probability of occurrence, P_i. Therefore, the unconditional probability of exceedance should account for the probabilities of exceedance for all the possible discharge rates along with their probabilities of occurrence.

6.1.2 Reliability Analysis

Several methods can be used to calculate the unconditional probability of exceeding the design scour depth within a service life, T_n. One method consists of performing the conditional probability-based scour estimates described in Chapter 5 for a whole set of return periods and associating each conditional probability of exceedance with the probability of occurrence, P_i—that is, the probability that the maximum discharge rate within the service life will equal that of the selected return period, which is labeled as P_i. The final unconditional probability of exceedance will be the sum of the products of the probability of exceedance for each discharge rate times the probability of the occurrence of the discharge rate for which the probability of exceedance is calculated. This can be expressed as:

$$P_{ex}(T_n) = \sum_{all\ return\ years} (P_{ex}/i^{th} - yr\ rate) \times P_i \tag{6.2}$$

Where $P_{ex}(T_n)$ is the probability of exceeding the design scour within a service life period T_n, $(P_{ex}/i^{th} - yr\ rate)$ is the probability of exceeding the design scour given that the hydraulic event corresponds to that of a return period equal to i-years, and P_i is the probability that the maximum discharge rate within the service life of the bridge has a probability of occurrence equal to that of the discharge rate having the return period i-years corresponding to the ith hydraulic

event. Although there are an infinite number of hydraulic events, these can be combined into discrete segments where each segment has a probability of occurrence P_i. Note that the sum of all the hydraulic event probabilities, P_i, must add up to 1.0:

$$\sum_{\text{all return years}} P_i = 1.0 \tag{6.3}$$

It is common in the probabilistic evaluation of bridge safety to use the reliability index, β, as a measure of safety. The reliability index, β, is inversely related to the probability of scour depth exceedance through the normal cumulative distribution function (CDF), Φ:

$$P_{ex}(T_n) = \Phi(-\beta) \tag{6.4}$$

6.1.3 Reliability Calculation Process

The process for calculating the reliability for a given design scour depth can be summarized as follows:

Step 1. Find the design scour for a bridge using current methods.
Step 2. Divide the set of possible discharge rates that could occur within the service life, T_n, of the bridge into a limited number of representative discrete sets of discharge rates. These discharge rates can be identified based on the return period they are associated with.
Step 3. Find the probability of occurrence, P_i, that the maximum discharge expected to occur within the service life will equal each of the discharge rates, i, selected in Step 2.
Step 4. Use the approach described in Chapter 5 to find $P_{ex}/i^{th} - yr$, which gives the conditional probability of exceeding the design scour for each of the discharge rates, i, selected in Step 2.
Step 5. Multiply $P_{ex}/i^{th} - yr$ calculated in Step 4 by the probability P_i of Step 3.
Step 6. Repeat steps 3, 4, and 5 to cover the entire set of representative discharge rates.
Step 7. Add all the results from Step 6 to give $P_{ex}(T_n)$, which is the overall probability of exceedance in the service life T_n.
Step 8. Find the reliability index, β, using the normal CDF, Φ.

6.1.4 Calibration of Design Equations

A properly calibrated design scour methodology should provide a reliability index, β, that meets a target value as closely as possible for the range of applicable bridge geometries and channel conditions. If the current design methodology does not meet the target reliability level, adjustments to the scour design methodology must be made. One possible approach is to apply a scour factor on the results of the design scour calculations to ensure that the reliability levels obtained after adjustment meet the target reliability levels.

6.1.5 Simplified Example

In this section, an example set of calculations is performed and the probabilities are obtained as shown in Table 6.1. For this simplified example, it is assumed that the current design method will stipulate a design scour depth of 15 ft. The table illustrates the application of Equation (6.2) when the probability of exceedance for a service period $T_n = 1$ year is desired. The calculations assume that the entire range of hydraulic events can be divided into seven discrete segments (represented by the seven return periods $T_r = 5$ years, $T_r = 20$ years, $T_r = 50$ years, $T_r = 75$ years, $T_r = 100$ years, $T_r = 200$ years, and $T_r = 500$ years). The probability of occurrence, P_i, that corresponds to each segment is calculated to cover all the probabilities between the different return

Table 6.1.   Example calculations for determining probability of design scour exceedance within a 1-year period.

Return Period (T_r)	$P = 1/T_r$	Probability of Occurrence (P_i)	Conditional Probability of Exceeding Design Scour	Product of P_i Times Conditional Probability
5 years	0.2	0.875	6.82e-4	5.97e-4
20 years	0.05	0.09	5.06e-3	4.55e-4
50 years	0.02	0.0183	1.22e-2	2.24e-4
75 years	0.0133	0.005	1.65e-2	0.83e-4
100 years	0.01	0.00567	2.02e-2	1.14e-4
200 years	0.005	0.0035	3.14e-2	1.10e-4
500 years	0.002	0.0025	3.92e-2	0.98e-4
Sum		$\sum P_i = 1.0$		$P_{ex}(T_n = 1 - yr) = 1.681e\text{-}3$

periods. The probability of exceedance within a 1-year period is calculated to be $P_{ex}(T_n = 1 - yr) = 1.681e\text{-}3$. Notice that the return period, T_r, serves to specify the hydraulic event to be used. This is different from the service life, T_n, which defines the period for which the bridge will be in service.

Using a similar approach for the case when $T_n = 75$ years, the probability of exceedance within a 75-year design life is $P_{ex}(T_n = 75 - yr) = 12.1\%$. The reliability index, β, for the 75-year design life is found to be 1.18. To obtain a reliability index, β, of 1.5, the design scour depth will have to be increased by a scour factor, SC, of 1.10. In other words, the design scour must be increased from 15 ft to 16.5 ft.

The integration approach for calculating the reliability index as described in this section, based on Equation (6.2), Equation (6.3), and Equation (6.4), provides a simplified approach for calibrating scour factors for a target reliability consistent with LRFD procedures used by structural and geotechnical engineers as discussed in Section 2.5. The example in Table 6.1 uses seven return periods. Next, Section 6.2 presents a discussion of the number of return periods that can be used for the integration to obtain an optimum balance between accuracy and calculation efficiency.

6.2 Validation of the Simplified Procedure

6.2.1 Overview of the Procedure

This section describes an algorithm for the calculation of the reliability of design scour depth exceedance using a limited number of return periods. The validity of the proposed approach is verified by comparing the results from a full-fledged Monte Carlo simulation to those of the evaluation at discrete return periods. The comparison shows that it is sufficient to perform Monte Carlo simulations for five return periods or fewer to obtain good estimates of the mean and standard deviation (SD) of the actual scour depth. The statistics of the actual scour depth can subsequently be used to estimate the probability of exceeding the design scour depth. A list of suggested return periods to check for various service lives is provided in Table 6.2.

As mentioned earlier, several methods can be used to find the reliability of a bridge that may be subject to scour. The most basic approach consists of performing a Monte Carlo simulation to find the probability that the maximum scour depth around a bridge foundation will exceed the scour design depth at any time within the service life of the bridge. However, the full-fledged Monte Carlo simulation requires a heavy computational effort. As outlined in Section 6.1, a simplified approach was developed whereby the Monte Carlo simulation is executed at

Table 6.2.   Proposed return periods for use in estimating the scour reliability for different service lives.

Service Period (T$_n$)	Return Period 1	Return Period 2	Return Period 3	Return Period 4	Return Period 5
5 years	3 years	5 years	8 years	15 years	50 years
20 years	10 years	20 years	30 years	60 years	200 years
75 years	50 years	100 years	500 years		

only a limited number of discrete return periods and the results are integrated to obtain estimates of the reliability of the bridge over the entire service period.

The objective of the reliability analysis is to find the reliability index, β, which as defined in Equation (6.4) is related to the probability of design scour depth exceedance within a service period, $P_{ex}(T_n)$. This relationship also can be expressed as:

$$P_{ex}(T_n) = \Pr(y_{\text{max expected}} \geq y_{\text{sc design}}) = \Phi(-\beta) \tag{6.5}$$

where

$y_{\text{max expected}}$ = the expected maximum scour depth during the service life of the bridge,
$y_{\text{sc design}}$ = the design scour depth, and
Φ = the CDF for the normal distribution.

Notice also that $y_{\text{sc design}}$ is deterministic, computed from the HEC-18 equation (or any appropriate design equation) and $y_{\text{max expected}}$ is determined from the Monte Carlo simulation, based on uncertainty and the expected discharges occurring over the service life of the bridge.

The process of finding the probability of design scour depth exceedance and the reliability index, β, involves the following steps.

Step 1. Find the design scour for the bridge, $y_{\text{sc design}}$, from the as-built conditions or by using typical design equations such as the HEC-18 equations for the 100-year discharge rate.
Step 2. Use the discharge rate data to find the statistics of the maximum expected discharge rate within the remaining service life of the bridge. For example, knowing the probability distribution for the yearly discharge rate, $F_Q(x)$, the maximum flood discharge in a service period, T_n, has a cumulative probability distribution, $F_{QTn}(x)$, related to the probability distribution of the 1-year maximum discharge by:

$$F_{QTn}(x) = F_Q(x)^{Tn} \tag{6.6}$$

Step 3. Apply $F_{QTn}(x)$ and the bias and COV of the modeling variables into a Monte Carlo simulation to find the statistics of $y_{\text{max expected}}$ for different possible values of the scour within a service period, T_n.
Step 4. Determine the percentage of cases for which $y_{\text{max expected}}$ exceeds $y_{\text{sc design}}$ and find the reliability index from Equation (6.5).

Because of the numerical difficulties associated with covering the whole range of possible values of the cumulative distribution function, $F_{QTn}(x)$, a limited number of discharge rates were used to estimate the probability of scour depth exceedance. Through different comparisons between the full-fledged Monte Carlo simulation and simulations that used a limited number of discharge rates, it was determined that good accuracy can be achieved when the simulations are executed for five different return periods or fewer. The higher the service life, T_n, the lower the number of return periods that are needed for Q. This is because as T_n increases, QT_n evaluated from Equation (6.6)

will have a lower COV. Figure 6.1 provides a flow chart for evaluating the reliability index, β, using the simplified procedure.

6.2.2 Case Studies for Validation

To verify the validity of the simplified approach, several comparisons between the results obtained from the approach described in Figure 6.1 and a full-fledged Monte Carlo simulation were performed. To obtain realistic results for the effect of scour, different possible discharge rate data from a selected set of rivers are used and design scour depths are calculated for each of these river discharge rates. The simplified approach was shown to reproduce the full-fledged Monte Carlo simulation results quite well for the five rivers used to assess the procedure. The validation procedure is described in detail in the Contractor's Final Report for NCHRP Project 24-34, available at www.trb.org.

6.3 Implementation of Reliability Analysis for Sacramento River Bridge Data

In this section, the analysis procedure presented in Section 6.2 is implemented for a reliability analysis for the Sacramento River bridge that was analyzed in Chapters 3 and 5. This reliability analysis covers the following cases:

- Pier scour when the foundation is designed using the HEC-18 method.
- Pier scour when the foundation is designed using the Florida DOT method.
- Contraction scour using the HEC-18 equation.
- Combined pier scour and contraction scour when the foundation is designed using the HEC-18 method for the pier scour component.
- Combined pier scour and contraction scour when the foundation is designed using the Florida DOT method for the pier scour component.
- Abutment scour using the NCHRP Project 24-20 approach as recommended in the 5th edition of HEC-18.

A reliability analysis for the 75-year service life was executed in Section 6.1 using three return periods: $T_r = 45$ years, $T_r = 110$ years, and $T_r = 400$ years. However, during the implementation process it was decided to use the slightly modified set of typical return periods ($T_r = 50$ years, $T_r = 100$ years, and $T_r = 500$ years) because hydraulic engineers use these return periods on a regular basis and their values are more readily available. A sensitivity analysis on a random set of cases has shown that using the modified set of return periods does not lead to noticeable differences in the results.

6.3.1 Pier Scour Designed Using HEC-18 Method

As a first step, the simulations are executed to find the pier scour that would be obtained if no modeling bias is assumed (i.e., assuming that the HEC-18 equations give on the average good estimates of the actual pier scour depth). Figure 6.2 presents the results, assuming that the bridge is subjected to the hydraulic event that corresponds to each of the three return periods ($T_r = 50$ years, $T_r = 100$ years, and $T_r = 500$ years).

Given that the HEC-18 design scour for this bridge is 13.7 ft (see Section 5.4.2), the results show that if the 50-year event were to occur, the scour around the bridge pier would have a 27.64% probability of exceeding the 13.7 ft design scour, corresponding to a reliability index of β = 0.59. If the 100-year event were to occur, the scour around the bridge pier would have a 58.84% probability of exceeding the 13.7 ft design scour (β = −0.22); and if the 500-year event were to occur, the scour around the bridge pier would have a 93.73% probability of exceeding the 13.7 ft design scour (β = −1.5). Using the combined results from the 50-year, 100-year, and 500-year return periods, the
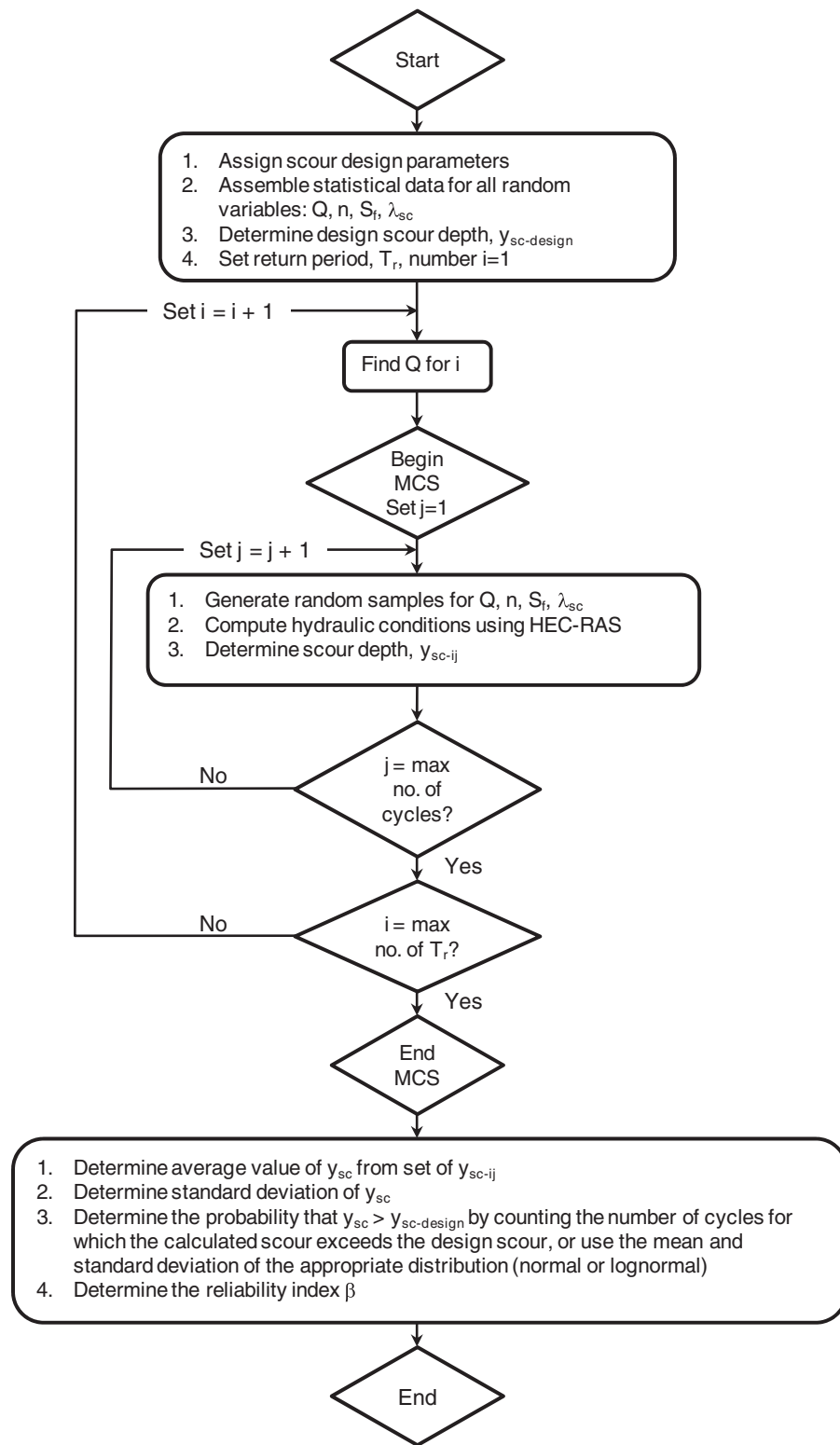
Figure 6.1.   Flow chart of simplified method for determining the reliability index, β, for scour depth exceedance.

HEC 18 Scour without Bias
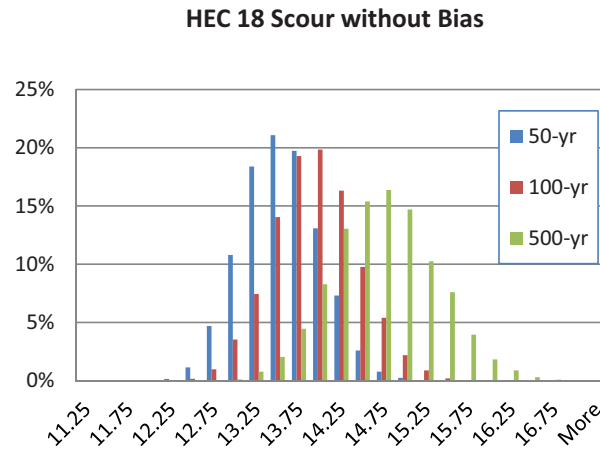
Figure 6.2.   Pier scour depth histogram without bias calculated based on HEC-18.

bridge would have a probability of 60.07% of exceeding the design scour within a 75-year service period ($\beta = -0.25$). Such reliability levels are certainly very low compared to acceptable levels.

Fortunately, as demonstrated in Chapter 4, the HEC-18 pier scour equation is **not** a predictive model of scour depth but instead contains on average some level of conservatism with an average bias of 0.68. In other words, based on laboratory and field data, the actual scour for a given hydraulic discharge rate is 0.68 times the scour depth predicted by the HEC-18 equation. On the other hand, Chapter 4 has shown a large level of variability in the bias around the 0.68 value, with a spread around the mean represented by a SD equal to 0.109 (COV = 16%). This spread around the bias offsets some of the conservatism of the HEC-18 equations by a level that can be evaluated using the simulation described in this section while accounting for the modeling bias and its COV.

The results of the simulation accounting for bias = 0.68 and the COV = 16% are presented in Figure 6.3. The results in Figure 6.3 demonstrate the dominance of the bias, which tends to pull the histograms for the three return periods closer together. The combination of the three histograms also is illustrated in Figure 6.3, which also shows that the maximum scour depth expected within the 75-year service life approaches that of a normal distribution. The effect of the bias leads to a significant increase in the reliability of the bridge design such that the probability that the actual scour will exceed the HEC-18 design scour depth of 13.7 ft is 0.38% with a reliability index of $\beta = 2.67$. This value is more in line with the reliability index that has been deemed acceptable for some bridges under extreme events such as earthquakes or for the rating of existing bridges under vehicular loading as discussed in Section 2.5.3.

HEC 18 Scour with Bias

Combined HEC 18 Scour with Bias
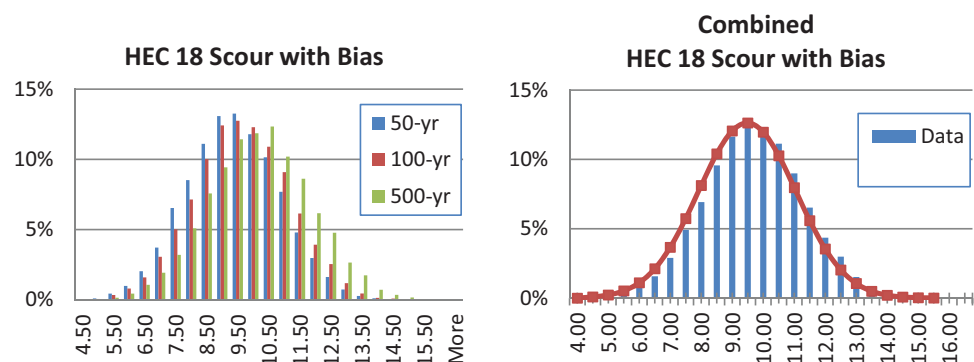
Figure 6.3.   Pier scour depth histogram with bias calculated based on HEC-18.

6.3.2 Pier Scour Designed Using Florida DOT Method

The approach was executed to find the pier scour that would be obtained if the bridge foundation is designed for the scour depth determined using the Florida DOT pier scour equation. The Florida DOT method leads to a design scour depth equal to 11.2 ft (see Section 5.4.2). For the Florida DOT equation, the average bias = 0.75 and the COV = 18%. The results of the simulation are presented in Figure 6.4. The results in Figure 6.4 show that the maximum scour depth expected within the bridge's 75-year service life approaches that of a normal distribution. The probability that the actual scour will exceed the Florida DOT design scour depth of 11.2 ft is 3.80% with a reliability index of $\beta = 1.77$. This value is somewhat on the low side compared to typical reliability indexes that have been deemed acceptable for bridges under extreme events.

6.3.3 Contraction Scour Designed Using HEC-18 Method

The approach was executed to find the contraction scour that would be obtained if the bridge foundation is designed for the scour depth determined using the HEC-18 method. The HEC-18 method leads to a contraction design scour depth equal to 5.3 ft (see Section 5.4.3). For the contraction scour, the average bias = 0.916 and the COV = 20.9%. This high bias reflects the fact that the HEC-18 contraction scour equations were developed to be predictive equations rather than more conservative design equations. This high bias, in combination with the high COV, will lead to low reliability levels. The results of the simulation presented in Figure 6.5 show that the maximum scour depth expected within the 75-year service life approaches that of a lognormal distribution. The probability that the actual scour will exceed the contraction design scour depth of 5.3 ft is 47.1% with a reliability index of $\beta = 0.07$. This value is very low compared to typical reliability indexes that have been deemed acceptable for bridges under extreme events.
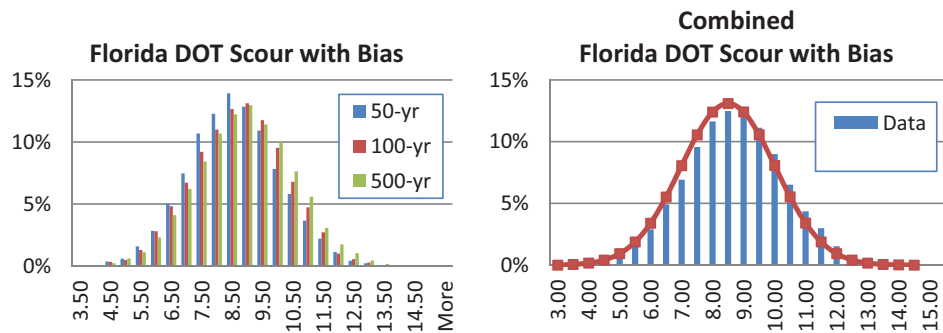
Figure 6.4.   Pier scour depth histogram with bias calculated based on Florida DOT method.
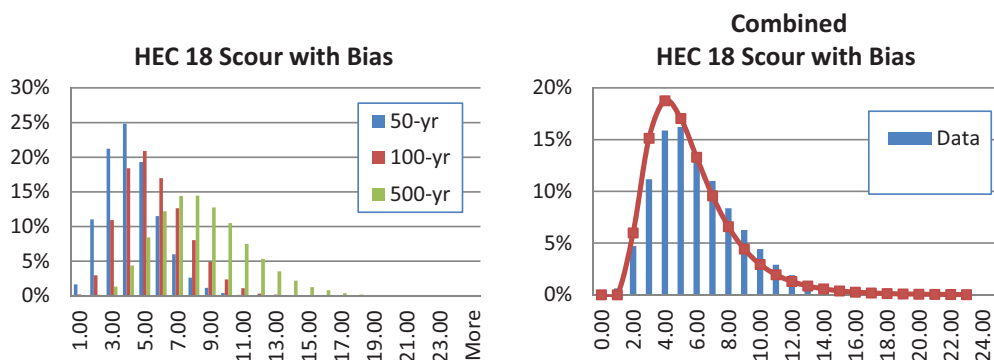
Figure 6.5.   Contraction scour depth histogram with bias calculated based on HEC-18.
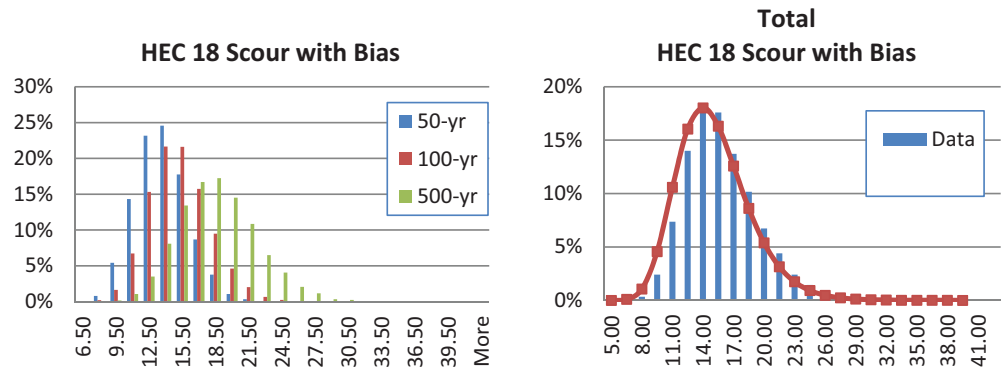
Figure 6.6. *Total pier and contraction scour depth histogram calculated using HEC-18.*

6.3.4 Total Pier and Contraction Scour Using HEC-18 Methods

The simulations were performed to find the combined (total) pier and contraction scour that would be obtained if the bridge foundation is designed for the scour depth determined using the HEC-18 methods for pier and contraction scour. The HEC-18 methods lead to a design total scour depth equal to 19 ft. The results of the simulation are presented in Figure 6.6, which shows that the maximum scour depth expected within the 75-year service life approaches that of a lognormal distribution but is not too different from a normal distribution. The probability that the actual scour will exceed the total design scour depth of 19 ft is 13.6% with a reliability index of $\beta = 1.10$. This value is low compared to typical reliability indexes that have been deemed acceptable for bridges under extreme events.

6.3.5 Total Pier and Contraction Scour Using Florida DOT Method

The simulations were performed to find the combined (total) pier and contraction scour that would be obtained if the bridge foundation were designed for the scour depth determined using the Florida DOT method for pier scour. Given that the Florida DOT method does not provide an equation for the contraction scour, the analysis looks at the design pier scour using the Florida DOT equation, whereas the contraction scour is obtained using the HEC-18 method. This leads to a design total scour depth equal to 16.5 ft. The results of the simulation presented in Figure 6.7 show that the maximum scour depth expected within the 75-year service life approaches that of a lognormal distribution. The probability that the actual scour will exceed the total design scour depth
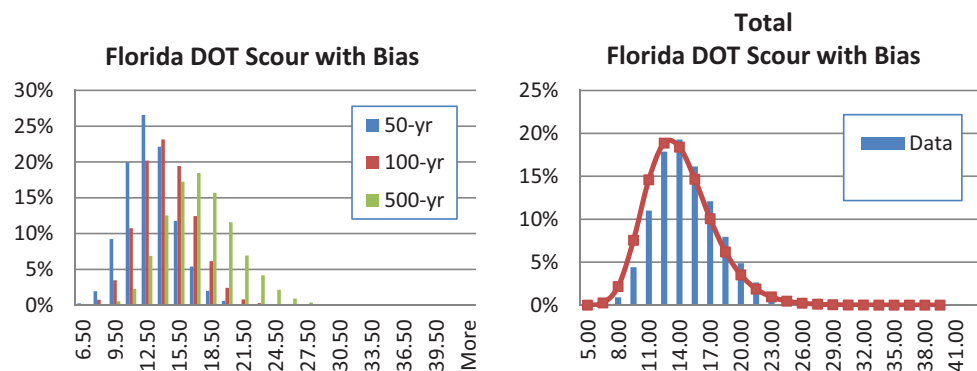
Figure 6.7. *Total pier and contraction scour depth histogram calculated using Florida DOT.*
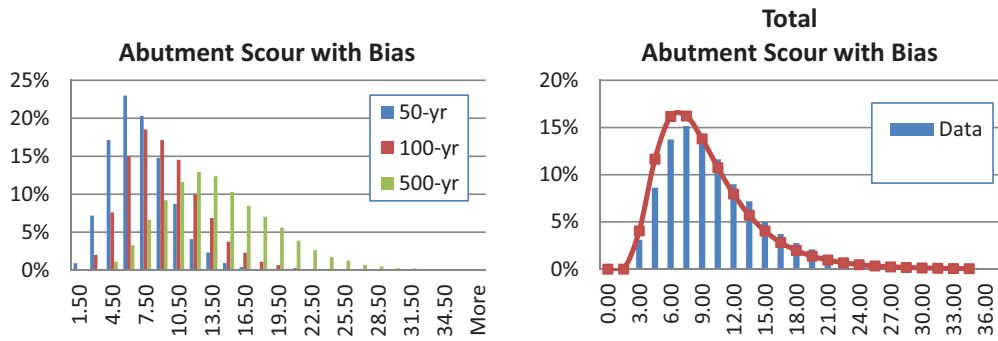
Figure 6.8. Total abutment scour depth histogram using NCHRP Project 24-20 method (HEC-18, 5th Ed.).

of 16.5 ft is 21.75% with a reliability index of $\beta = 0.78$. This value is very low compared to typical reliability indexes that have been deemed acceptable for bridges under extreme events.

6.3.6 Total Scour at an Abutment Using NCHRP Project 24-20 Method

This approach was executed to find the abutment scour that would be obtained if the bridge foundation were designed for the scour depth determined using the NCHRP Project 24-20 method as described and recommended in the latest edition of HEC-18. **Notice that this method includes both the effect of the abutment scour and the contraction scour at the end of the abutment, and therefore is an estimate of total scour at that location.** The method leads to a design abutment scour depth equal to 11 ft (see Section 5.4.4). For the abutment scour, the average bias $= 0.74$ and the COV $= 23\%$. The results of the simulation are presented in Figure 6.8 and show that the maximum scour depth expected within the 75-year service life approaches that of a lognormal distribution. The probability that the actual scour will exceed the abutment design scour depth of 11 ft is 30.58% with a reliability index of $\beta = 0.51$. This value is very low compared to typical reliability indexes that have been deemed acceptable for bridges under extreme events.

6.3.7 Summary

The results of the reliability analysis for a 75-year service life of the Sacramento River bridge are summarized in Table 6.3. The results demonstrate how the reliability index values vary considerably for the different types of scour and the different equations that can be used to determine the design scour depth. The results also demonstrate the dominant effect of the bias and

Table 6.3. Summary of reliability analysis results for 75-year service life based on Sacramento River bridge data.

Scour Type	Design Scour (ft)	Bias	COV	Probability of Exceedance	Reliability Index (β)
Pier scour (HEC-18)	13.7	0.68	16%	0.38%	2.67
Pier scour (Florida DOT)	11.2	0.75	18%	3.80%	1.77
Contraction scour	5.3	0.92	21%	47.1%	0.07
Combined HEC-18 pier and contraction scour	19	As shown in Section 6.3.4		13.6%	1.10
Combined Florida DOT pier and contraction scour	16.5	As shown in Section 6.3.5		21.8%	0.78
Abutment scour	11.0	0.74	23%	30.6%	0.51

its COV on the reliability index, which varies from an acceptable value of 2.67 (obtained when the HEC-18 pier scour equation is used to design the foundation) to the very low value of 0.07 (obtained when the HEC-18 equations are used for designing the foundation for contraction scour). These results are based on the bias and COV obtained by comparing the results from different equations to laboratory data. Results from the field may produce slightly different biases and COV; however, field data are generally considered less reliable because of the various difficulties discussed in Chapter 4.

6.4 Calibration of Scour Factors

The reliability analysis performed in Section 6.3 and summarized in Table 6.3 reveals large variations in the reliability levels obtained for the different types of scour. In most cases the reliability index obtained for the bridge is low compared to the level obtained for bridges designed for other extreme events. This low reliability is primarily due to the bias and COV of the existing contraction and abutment scour equations. Other causes for the variability include the hydrologic uncertainty of the discharge rates expected over the service life of the bridge, variability in soil and sediment properties, and the geometric and roughness conditions of the channel and overbank areas.

One approach that can be used to increase the reliability of existing scour equations is to apply a safety factor on the design scour calculated from current procedures so that bridges designed using the safety factor produce reliability levels that meet an acceptable target reliability index, β. The target reliability index must be set by the code-writing authorities and bridge owners to provide a balance between safety and cost. As indicated earlier, most current bridge LRFD specifications have used a target reliability level that varies between $\beta = 2.5$ and $\beta = 4.0$, depending on the types of loads, the consequences of exceeding the target reliability levels, the construction costs, and past histories of successful designs (see Section 2.5.3). In this section, a set of scour factors is calibrated to reach different reliability levels for each scour type. The final decision regarding which target reliability should be used must be made by the appropriate code-writing authorities. A trial-and-error process is used to find the scour factors required to reach different target reliability levels (see Table 6.4). The analyses performed in Table 6.4 are based on the scour depths generated directly from the Monte Carlo simulations for the Sacramento River bridge referenced in Section 6.3.

The calibration of the scour factors performed in this section assumes a 75-year service life, is based on the data for the Sacramento River bridge, and assumes that these data are representative of typical bridge conditions. Before actual implementation into a design code, similar analyses should be performed for numerous and varied bridges to confirm the consistency of the results.

Table 6.4.   Scour factors to meet different target reliability levels for 75-year service life based on Sacramento River bridge data.

Target Reliability Index (β)	Scour Factor					
	Pier Scour Using HEC-18	Pier Scour Using Florida DOT	Contraction Scour Using HEC-18	Total Scour Using HEC-18	Total Scour Using Florida DOT	Abutment Scour
1.50	N/A	N/A	1.95	1.10	1.18	1.60
2.00	N/A	1.03	2.35	1.23	1.33	1.95
2.50	N/A	1.10	2.77	1.37	1.47	2.31
3.00	1.04	1.15	3.20	1.50	1.60	2.75

For the case analyzed, the scour factors shown in Table 6.4 indicate that no additional safety factors would be required for the HEC-18 pier scour equation if the target reliability index is set at 2.50 or lower. A scour factor equal to 1.04 would be needed to reach a target reliability index of $\beta = 3.0$. Similarly, only modest scour factors need to be applied to the Florida DOT pier scour equation to achieve reasonable target reliabilities. Table 6.4 also shows that the current contraction scour equations would need significant additional safety factors to reach acceptable reliability levels. A modest target reliability index of $\beta = 1.50$ would require an additional safety factor equal to 1.95. Only slightly lower safety factors would be needed to improve the reliability of bridges designed using the NCHRP Project 24-20 abutment scour equation.

The safety factors obtained in Table 6.4 are quite modest for the HEC-18 and Florida DOT pier scour equations. However, larger factors are needed to offset the large variability observed between the scour depths measured in the laboratory compared to those predicted from the current contraction and abutment scour equations. Additional analyses are recommended to confirm the consistency of the results for different bridge and channel configurations and hydraulic conditions.

CHAPTER 7

Illustrative Examples

7.1 Overview

This chapter provides detailed illustrative examples to demonstrate the full range of applicability of the Level I probability-based scour estimates using the procedures presented in Chapter 5. Given the unique nature of any bridge-stream intersection, these examples illustrate application of the methodology for a wide variety of bridge-stream scenarios in a range of physiographic regions across the country. The five bridge sites selected cover a wide variety of situations, including bridges over navigable waterways where pier scour predominates, single-span bridges where contraction and/or abutment scour occur, and bridges where all three scour components are evident. **Although these are realistic examples using actual bridges, some conditions have been changed for purposes of illustration.**

7.2 Example Bridge No. 1: Maryland Piedmont Region

Location: Maryland
Physiographic region: Piedmont
Bridge length: Existing bridge: 44 ft; replacement bridge: 55 ft
No. spans: 1
ADT: 7,801
Main channel width: 33 ft
River planform: Meandering, moderately sinuous (1.06–1.25)
100-year discharge: 4,530 ft^3/sec
100-year depth: 7.5 ft approach flow depth in main channel
                               7.7 ft at upstream face, main channel
100-year velocity: 5.9 ft/sec approach velocity in main channel upstream
                               10.7 ft/sec at the upstream internal bridge section
Hydraulic model: 1-D (HEC-RAS)
Pier type/geometry: N/A
Bed material: Gravel
Abutment type/location: Vertical/South abutment set back 5 ft; North abutment in the low flow channel; replacement abutments will be wingwall configuration.
Purpose of study: Bridge replacement

Example Bridge No. 1 presents the Level I analysis method to provide probability values and scour factors for a bridge located in the Piedmont physiographic region of Maryland (see Figure 7.1). The site currently consists of a single-span, two-lane bridge with a history of
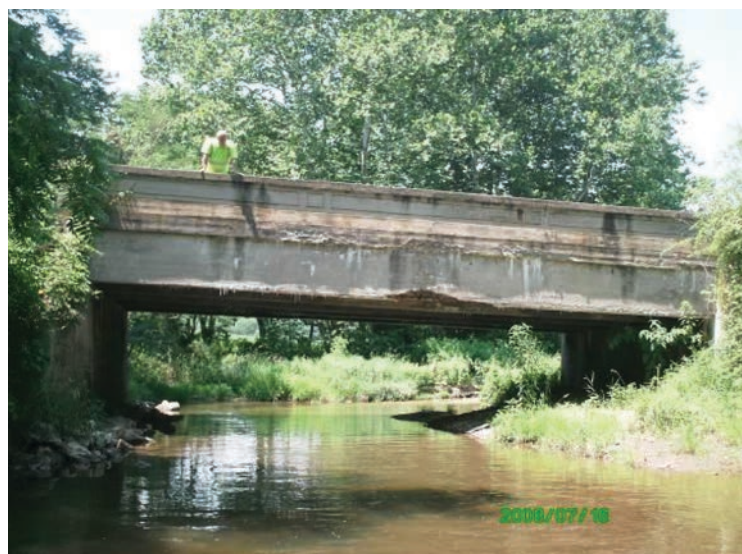
(a) Upstream channel   (b) Downstream face

Figure 7.1.   Example Bridge No. 1.

contraction and abutment scour. The bridge has been rated as scour critical, has scour countermeasures, and is scheduled for replacement. For the new bridge, no overtopping or pressure flow occurs in the 100-year design scour event. For the 100-year design scour event, a desired total scour reliability index, β, of 3.0 is assumed for this example. This β corresponds to a 99.86% probability of non-exceedance during the design event. The calculations presented in this example are for the proposed replacement bridge.

Step 1. Perform hydrologic, hydraulic, and design-equation scour computations using appropriate methods.

a. Hydrologic analysis: USGS regional regression relationships for the Maryland Piedmont and Blue Ridge regions were used to develop the estimate of the 100-year design flood. For the 100-year event, the regression equation is:

$$Q_{100} = 1,471.1(DA)^{0.617}(LIME+1)^{-0.154}(FOR+1)^{-0.045}$$

where:

Q_{100} = Estimate of 100-year flood discharge (cfs)
DA = Watershed drainage area (sq. mi.)
$LIME$ = Percentage of carbonate/limestone rock in watershed
FOR = Percentage of forest cover in watershed

Using the USGS regression equation and the watershed characteristics upstream of the bridge, the 100-year design discharge at this site is estimated to be 4,530 ft³/sec.

b. Compute abutment scour: The NCHRP Project 24-20 live-bed approach for estimating total scour at the abutment was used to determine a scour depth of 8.6 ft. The NCHRP approach includes contraction scour plus the local scour at the abutment toe. Because both abutments of the new bridge will be in close proximity to the channel banks, the total scour depth is approximately the same for the left and right sides.

c. Compute pier and contraction scour: The replacement bridge will be a single-span structure, so there are no pier scour or contraction scour components (other than the contraction scour at the abutments) to calculate at this site.

d. Summarize scour calculations (see Table 7.1):

Table 7.1.   100-year design scour depths, Example Bridge No. 1.

Pier Scour (ft)		Contraction Scour (ft)	Total Scour (ft)		Abutment Total Scour (ft)	
HEC-18	Florida DOT		HEC-18	Florida DOT	Left	Right
n/a	n/a	n/a	n/a	n/a	8.6	8.6

Step 2. Determine the appropriate bridge size, hydrologic uncertainty, and pier size corresponding to standard scour factor table values.

a. Bridge size: The bridge's length is 55 ft. From the guidance presented in Section 5.2.3, this bridge is considered a small bridge.

b. Hydrologic uncertainty: The USGS regional regression equation for the 100-year flood for the Maryland Piedmont and Blue Ridge regions has a standard error of 37.5%. From the guidance presented in Section 3.5.2, standard errors greater than 30% are considered to have high hydrologic uncertainty.

c. Pier size: Not applicable—the replacement bridge will be a single-span structure similar to the existing bridge.

Step 3. Determine scour factors.

Once the bridge has been classified, the practitioner can look in Appendix B, Table B.7 to determine appropriate bias and scour factors as a function of the desired β.

Table 7.2 corresponds to a small bridge, high hydrologic uncertainty, small pier configuration; however, note that pier size is not applicable for this example.

Table 7.2.   Scour factors for $\beta = 3.0$ (using Monte Carlo results), Example Bridge No. 1.

	Pier Scour		Contraction Scour	Abutment Total Scour	
	HEC-18	Florida DOT		Left	Right
Bias	n/a	n/a	n/a	0.75	0.75
Scour factor	n/a	n/a	n/a	1.42	1.42

Step 4. Apply the bias and scour factors and determine total design scour.

Applying the recommended bias and scour factors for $\beta = 3.0$ for all components produces the results shown in Table 7.3. The individual scour component design scour values are multiplied by the applicable bias to determine the expected scour. The component scour for $\beta = 3.0$ is the design scour times the scour factor. By definition for $\beta = 3.0$, the difference between the component scour and the expected scour is 3.0 standard deviations (SDs) from the expected scour. The total scour for the target β is the expected scour plus the difference.

Table 7.3.   100-year scour results for β = 3.0 (using Monte Carlo results), Example Bridge No. 1.

	Pier Scour		Contraction Scour	Total Scour		Abutment Total Scour	
	HEC-18	Florida DOT		HEC-18	Florida DOT	Left	Right
Design scour (ft)	n/a	n/a	n/a	n/a	n/a	8.6	8.6
Bias						0.75	0.75
Expected scour (ft)						6.5	6.5
Scour factor						1.42	1.42
Component scour for β = 3.0 (ft)						12.2	12.2
Difference from expected (ft)						5.7	5.7
Total scour for β = 3.0 (ft)						12.2	12.2

7.3 Example Bridge No. 2: Nevada Great Basin Subregion

Location:	Nevada
Physiographic region:	Intermontane basins and plateaus; Great Basin Subregion
Bridge length:	210 ft
No. spans:	3
ADT:	1,300 (2001)
Main channel width:	208 ft
River planform:	Sinuous (1.06–1.25)
100-year discharge:	31,150 ft³/s
100-year depth:	19.6 ft
100-year velocity:	11.7 ft/s
Hydraulic model:	1-D (HEC-RAS)
Pier type/geometry:	1.7 ft wide by 44 ft long concrete wall piers on 19 ft wide pile caps (exposed)
Bed material:	Sand with gravel
Abutment type/location:	Spill-through abutments at channel banks
Purpose of study:	Scour evaluation and countermeasure selection for a plan of action

Example Bridge No. 2 presents the Level I analysis method to provide probability values and scour factors for a bridge located in the Great Basin physiographic region of Nevada (see Figure 7.2). The example bridge is 210 ft long with two concrete wall piers on spread

Figure 7.2.   Example Bridge No. 2 (looking downstream).

footings. Because of long-term degradation at this site, the spread footings are now exposed above the stream bed. The abutments are of spill-through configuration located at the channel banks. No overtopping or pressure flow occurs in the 100-year design scour event. For the 100-year design scour event, a desired total scour reliability index, β, of 2.5 is assumed for this example. This β corresponds to a 99.38% probability of non-exceedance during the design event.

Step 1. Perform hydrologic, hydraulic, and design-equation scour computations using appropriate methods.

a. Hydrologic analysis: Bulletin 17B methods were used to determine the design scour event discharge, the expected value of the natural logarithm transform of discharge, and the SD of the uncertainty about that expected value for a given recurrence interval. The resulting discharges and summary statistics are presented in Table 7.4.

Table 7.4.   Hydrologic data from Bulletin 17B analysis of bridge site (n = 17 years), Example Bridge No. 2.

Annual Exceedance		Discharge (cfs)		
			95% Confidence Limits	
		Bulletin 17B		
p(X > x)	T (years)	Estimate	Lower	Upper
0.1	10	10,400	6,720	18,530
0.04	25	17,300	10,560	34,110
0.02	50	23,690	13,910	49,970
0.01	100	31,150	17,630	69,810
0.005	200	39,720	21,740	94,050
0.002	500	52,810	27,750	133,500

b. Design-equation scour computations using the HEC-18 method for pier scour, the HEC-18 method for contraction scour, and the NCHRP Project 24-20 method as presented in HEC-18 for abutment scour were computed for this example. Table 7.5 presents the results of these computations.

Table 7.5.   100-year design scour depths, Example Bridge No. 2.

Pier Scour (ft)	Contraction Scour (ft)	Total Scour (ft)	Abutment Total Scour (ft)	
			Left	Right
28.9	1.7	30.6	2.4	3.3

Step 2. Determine the appropriate bridge size, hydrologic uncertainty, and pier size corresponding to standard scour factor table values.

a. Bridge size: The example bridge's length is 210 ft. From the guidance presented in Section 5.2.3, this bridge is best represented as a medium bridge.

b. Hydrologic uncertainty: To establish the relative hydrologic uncertainty of this bridge, it is necessary to estimate the COV associated with the uncertainty of the discharge estimate for the design scour event.

   1. The lognormal distribution of hydrologic uncertainty is determined from the 95% confidence limit discharge values as follows. The hydrologic uncertainty of a given Bulletin 17B

discharge estimate is assumed to be lognormally distributed. Consequently, given the 95% upper and 95% lower confidence limits (see Section 3.5.2),

$$\mu = \frac{\ln(Q_{upper}) + \ln(Q_{lower})}{2}$$

$$\sigma = \frac{\ln(Q_{upper}) - \ln(Q_{lower})}{2Z_c}$$

$$COV = \frac{\sigma}{\mu}$$

2. For a 95% confidence limit, $Z_c = 1.645$ (see Appendix A). From the hydrologic analysis, the upper and lower 95% confidence limits for the 1% exceedance probability event (i.e., the 100-year flood) are:

$Q_{upper} = 69,810$ cfs,

$Q_{lower} = 17,360$ cfs, and

$Z_c = 1.645$

3. Substituting values for Q_{upper}, Q_{lower}, and Z_c into these equations,

$$\mu = \frac{\ln(69,810) + \ln(17,360)}{2} = 10.46$$

$$\sigma = \frac{\ln(69,810) - \ln(17,360)}{2(1.645)} = 0.423$$

$$COV = \frac{0.423}{10.46} = 0.0404$$

Compare the computed COV with Table 7.6 (reproduced from Table 3.4) for the 1% exceedance probability event:

Table 7.6.   Hydrologic uncertainty as function of annual exceedance probability (reproduced from Table 3.4), Example Bridge No. 2.

Annual Exceedance		Discharge COV (lognormal)		
p(X > x)	T (years)	Low	Medium	High
0.04	25	0.009	0.014	0.018
0.02	50	0.010	0.015	0.019
0.01	**100**	0.011	0.016	**0.021***
0.005	200	0.012	0.017	0.022
0.002	500	0.013	0.018	0.023

*Bolding shows where the COV for Example Bridge No. 2 falls within the table. These numbers indicate Example Bridge No. 2 has high hydrologic uncertainty.

This bridge has high hydrologic uncertainty.

c. Pier size: Because the pile caps are exposed above the stream bed, their width (19 ft) is compared to the values in Table 7.7 (reproduced from Table 5.1). This bridge has large piers for a bridge of its type.

Table 7.7.   Representative bridge pier size as a function of bridge type (reproduced from Table 5.1), Example Bridge No. 2.

Bridge Type	Pier Size (ft)		
	Small	Medium	Large
Small	1	2	3
Medium	1.5	3	4.5*
Large	3	6	9

*Bolding shows where the pier size for Example Bridge No. 2 falls within the table. This medium-size bridge has a large pier size.

Consequently, this bridge is best classified as a medium bridge with high hydrologic uncertainty and large pier size for the Level I analysis. However, the 19 ft wide pile cap is significantly larger than the 4.5 ft large pier assumed for a medium bridge, suggesting that this bridge may be a candidate for a Level II analysis.

Step 3.   Determine scour factors.

Once the bridge has been classified, the practitioner can look in Appendix B, Table B.18 to determine appropriate bias and scour factors as a function of the desired β.

Table 7.8 corresponds to a medium bridge with high hydrologic uncertainty and large pier size.

Table 7.8.   Scour factors for $\beta = 2.5$ (using Monte Carlo results), Example Bridge No. 2.

	Pier Scour	Contraction Scour	Abutment Total Scour	
			Left	Right
Bias	0.68	0.92	0.75	0.75
Scour factor	0.97	2.21	1.48	1.48

Step 4.   Apply the bias and scour factors and determine total design scour.

Applying the recommended bias and scour factors for $\beta = 2.5$ for all components produces the results shown in Table 7.9. The individual scour component design scour values are multiplied by the applicable bias to determine the expected scour. Total expected scour is the sum of expected pier and contraction scour. The component scour for $\beta = 2.5$ is the design scour times the scour factor. By definition for $\beta = 2.5$, the difference between the component scour and the expected scour is 2.5 standard deviations from the expected scour.

Table 7.9.   100-year scour results for $\beta = 2.5$ (using Monte Carlo results), Example Bridge No. 2.

	Pier Scour	Contraction Scour	Total Scour	Abutment Total Scour	
				Left	Right
Design scour (ft)	28.9	1.7	30.6	2.4	3.3
Bias	0.68	0.92		0.75	0.75
Expected scour (ft)	19.7	1.6	21.3	1.8	2.5
Scour factor	0.97	2.21		1.48	1.48
Component scour for $\beta = 2.5$ (ft)	28.0	3.8		3.6	4.9
Difference from expected (ft)	8.3	2.2	8.6	1.8	2.4
Total scour for $\beta = 2.5$ (ft)			29.9	3.6	4.9

The total scour difference from expected is the square root of the sum of the squares of the component scour differences (pier and contraction scour). The total scour for the target β is the expected plus the difference as shown in Table 7.9.

7.4 Example Bridge No. 3: California Pacific Mountains Subregion

Location:	California
Physiographic region:	Pacific mountains; Great Valley Subregion
Bridge length:	1,200 ft
No. spans:	10
ADT:	11,800 (2009)
Main channel width:	607 ft
River planform:	Meandering, highly sinuous (>1.26)
100-year discharge:	140,000 ft³/s
100-year depth:	24 ft
100-year velocity:	12.04 ft/s
Hydraulic model:	1-D (HEC-RAS)
Pier type/geometry:	2 column bents, 6-foot diameter columns @ 24 ft OC
Bed material:	Fine to coarse sand
Abutment type/location:	Spill-through abutments set back on floodplain
Purpose of study:	Scour evaluation

Example Bridge No. 3 presents the Level I analysis method to provide probability values and scour factors for a bridge located in the Pacific Mountain physiographic region of California (see Figure 7.3). The example bridge is a 1,200 ft long bridge with 6 ft diameter drilled shaft interior bents and set back, spill-through type abutments. No overtopping or pressure flow occurs in the 100-year design scour event. For the 100-year design scour event, a desired total scour reliability index, β, of 2.5 is assumed for this example. This β corresponds to a 99.38% probability of non-exceedance during the design event.

Note: For illustrative purposes, in this example pier scour is calculated using both the HEC-18 and Florida DOT methods.

Step 1. Perform hydrologic, hydraulic, and design-equation scour computations using appropriate methods.

a. Hydrologic analysis: Bulletin 17B methods were used to determine the design scour event discharge, the expected value of the natural logarithm transform of discharge, and the SD of the

Figure 7.3.   Example Bridge No. 3 (looking upstream).

uncertainty about that expected value for a given recurrence interval. The resulting discharges and summary statistics are presented in Table 7.10.

Table 7.10. Hydrologic data from Bulletin 17B analysis of bridge site (n = 49 years), Example Bridge No. 3.

Annual Exceedance		Discharge (cfs)		
			95% Confidence Limits	
		Bulletin 17B Estimate		
p(X > x)	T (years)		Lower	Upper
0.1	10	92,050	79,470	110,600
0.04	25	112,000	94,920	138,700
0.02	50	126,300	105,700	159,500
0.01	100	140,000	115,800	179,900
0.005	200	153,300	125,500	200,200
0.002	500	170,300	137,700	226,600

b. Design-equation scour computations using the HEC-18 and Florida DOT methods for pier scour, the HEC-18 method for contraction scour, and the NCHRP Project 24-20 method as presented in HEC-18 for abutment scour were computed for this example. Table 7.11 presents the results of these computations.

Table 7.11. 100-year design scour depths, Example Bridge No. 3.

Pier Scour (ft)			Total Scour (ft)		Abutment Total Scour (ft)	
HEC-18	Florida DOT	Contraction Scour (ft)	HEC-18	Florida DOT	Left	Right
13.7	11.2	5.3	19.0	16.5	11.0	6.7

Step 2. Determine the appropriate bridge size, hydrologic uncertainty, and pier size corresponding to standard scour factor table values.

a. Bridge size: The example bridge's length is 1,200 ft. From the guidance presented in Section 5.2.3, this bridge is best represented as a large bridge.
b. Hydrologic uncertainty: To establish the relative hydrologic uncertainty of this bridge it is necessary to estimate the COV associated with the uncertainty of the discharge estimate for the design scour event.
  1. The lognormal distribution of hydrologic uncertainty is determined from the 95% confidence limit discharge values as follows. The hydrologic uncertainty of a given Bulletin 17B discharge estimate is assumed to be lognormally distributed. Consequently, given the 95% upper and 95% lower confidence limits (see Section 3.5.2),

$$\mu = \frac{\ln(Q_{upper}) + \ln(Q_{lower})}{2}$$

$$\sigma = \frac{\ln(Q_{upper}) - \ln(Q_{lower})}{2Z_c}$$

$$COV = \frac{\sigma}{\mu}$$

2. For a 95% confidence limit, $Z_c = 1.645$ (see Appendix A). From the hydrologic analysis, the upper and lower 95% confidence limits for the 1% exceedance probability event (i.e., the 100-year flood) are:

$Q_{upper} = 179,900$ cfs;

$Q_{lower} = 115,800$ cfs; and

$Z_c = 1.645$

3. Substituting values for Q_{upper}, Q_{lower}, and Z_c into these equations,

$$\mu = \frac{\ln(179,900) + \ln(115,800)}{2} = 11.88$$

$$\sigma = \frac{\ln(179,900) - \ln(115,800)}{2(1.645)} = 0.1339$$

$$COV = \frac{0.1339}{11.88} = 0.0113$$

Compare the computed COV with Table 7.12 (reproduced from Table 3.4) for the 1% exceedance probability event:

Table 7.12. Hydrologic uncertainty as a function of annual exceedance probability (reproduced from Table 3.4), Example Bridge No. 3.

Annual Exceedance		Discharge COV (Lognormal)		
p(X > x)	T (years)	Low	Medium	High
0.04	25	0.009	0.014	0.018
0.02	50	0.010	0.015	0.019
0.01	**100**	**0.011***	0.016	0.021
0.005	200	0.012	0.017	0.022
0.002	500	0.013	0.018	0.023

*Bolding shows where the COV for Example Bridge No. 3 falls within the table. These numbers indicate that Example Bridge No. 3 has low hydrologic uncertainty.

This bridge has low hydrologic uncertainty.

c. Pier size: Compare the bridge pier size (6 ft diameter) to Table 7.13 (reproduced from Table 5.1). This bridge has medium piers for a bridge of its type.

Table 7.13. Representative bridge pier size as a function of bridge type (reproduced from Table 5.1), Example Bridge No. 3.

Bridge Type	Pier Size (ft)		
	Small	Medium	Large
Small	1	2	3
Medium	1.5	3	4.5
Large	3	6*	9

*Bolding shows where the pier size for Example Bridge No. 3 falls within the table. This large bridge has a medium pier size.

Consequently, this bridge is best classified as a large bridge with low hydrologic uncertainty and medium pier size for the Level I analysis.

Step 3. Determine scour factors.

Once the bridge has been classified, the practitioner can look in Appendix B, Table B.20 to determine appropriate bias and scour factors as a function of the desired β.

Table 7.14 corresponds to a large bridge with low hydrologic uncertainty and medium pier size.

Table 7.14.   Scour factors for β = 2.5 (using Monte Carlo results), Example Bridge No. 3.

	Pier Scour		Contraction Scour	Abutment Total Scour	
	HEC-18	Florida DOT		Left	Right
Bias	0.68	0.75	0.93	0.76	0.76
Scour factor	0.95	1.08	2.04	1.66	1.66

Step 4. Apply the bias and scour factors and determine total design scour.

Applying the recommended bias and scour factors for β = 2.5 for all components produces the results shown in Table 7.15. The individual scour component design scour values are multiplied by the applicable bias to determine the expected scour. Total expected scour is the sum of expected pier and contraction scour. The component scour for β = 2.5 is the design scour times the scour factor. By definition for β = 2.5, the difference between the component scour and the expected scour is 2.5 standard deviations from the expected scour.

Table 7.15.   100-year scour results for β = 2.5 (using Monte Carlo results), Example Bridge No. 3.

	Pier Scour		Contraction Scour	Total Scour		Abutment Total Scour	
	HEC-18	Florida DOT		HEC-18	Florida DOT	Left	Right
Design scour (ft)	13.7	11.2	5.3	19.0	16.5	11.0	6.7
Bias	0.68	0.75	0.93			0.76	0.76
Expected scour (ft)	9.3	8.4	4.9	14.2	13.3	8.4	5.1
Scour factor	0.95	1.08	2.04			1.66	1.66
Component scour for β = 2.5 (ft)	13.0	12.1	10.8			18.3	11.1
Difference from expected (ft)	3.7	3.7	5.9	7.0	7.0	9.9	6.0
Total scour for β = 2.5 (ft)				21.2	20.3	18.3	11.1

The total scour difference from expected is the square root of the sum of the squares of the component scour differences (pier and contraction scour). The total scour for the target β is the expected plus the difference, as shown in Table 7.15.

7.5 Example Bridge No. 4: Missouri Interior Lowlands Subregion

Location: Missouri
Physiographic region: Interior lowlands; Dissected Till Plains Subregion
Bridge length: 1,715 ft

No. spans:	7
ADT:	94,470 (2006)
Main channel width:	1013 ft
River planform:	sinuous (>1.25)
100-year discharge:	401,000 ft^3/s
100-year depth:	55.1 ft
100-year velocity:	9.8 ft/s (avg. channel)
Hydraulic model:	1-D (HEC-RAS)
Pier type/geometry:	Proposed bridge: 11 ft diameter drilled shafts with cap
Bed material:	Poorly graded sand (SP)
Abutment type/location:	Spill-through abutments on floodplain
Purpose of study:	New bridge

Example Bridge No. 4 presents the Level I analysis method to provide probability values and scour factors for a new bridge located in the interior lowlands, Dissected Till Plains physiographic subregion of Missouri (see Figure 7.4). The bridge will be a 1,715 ft long cable-stayed bridge with a large pylon in the main channel and approach bents on the overbanks. The abutments are of spill-through configuration set well back from the main channel. No overtopping or pressure flow occurs during the 100-year design flood. For the 100-year design scour event, a desired total scour reliability index, β, of 3.0 is assumed for this example. This β corresponds to a 99.86% probability of non-exceedance.

Step 1. Perform hydrologic, hydraulic, and design-equation scour computations using appropriate methods.

a. Hydrologic analysis: The Missouri River and its major tributaries are highly regulated by a large number of water supply, flood control, and navigation projects constructed over the last century and operated by various state and federal agencies. In 2004, the USACE completed the *Upper Mississippi River System Flow Frequency Study* (USACE 2004). That study developed methodologies to allow the USACE to reconstruct a 100-year period of annual peak flows at selected locations in the system as if all the currently-existing projects were in place and operating since the year 1898.

The USACE study used data from numerous gages, reservoir operation rules, reservoir routing, and unsteady channel flow routing procedures to develop an annual peak flow series at the bridge. Appendix E, Kansas City District Hydrology and Hydraulics of that study provides the reconstructed flow series for the Missouri River at Kansas City for the 100-year period from 1898 through 1997.

Figure 7.4.   Example Bridge No. 4 (looking upstream).

For this special study, site-specific methods were used to determine the flood frequency relationships for floods of various return periods. The 100-year discharges and summary statistics are presented in Table 7.16.

Table 7.16.   Hydrologic data from site-specific analysis of bridge site (n = 100 years), Example Bridge No. 4.

Annual Exceedance		Discharge (cfs)		
		Special Study Estimate	95% Confidence Limits	
p(X > x)	T (years)		Lower	Upper
0.01	100	401,000	350,000	458,000

b. Design-equation scour computations using the HEC-18 method for pier scour, the HEC-18 method for contraction scour, and the NCHRP Project 24-20 method as presented in HEC-18 for abutment scour were computed for the 100-year scour design flood in this example. The pier scour calculations are calculated for the large pylon in the main channel. Both left and right abutments are located outside the existing levees; therefore, no abutment scour is anticipated. Table 7.17 presents the results of these computations.

Table 7.17.   100-year design scour depths, Example Bridge No. 4.

Pier Scour (ft)	Contraction Scour (ft)	Total Scour (ft)	Abutment Total Scour (ft)	
			Left	Right
44.1	2.3	46.4	0.0	0.0

Step 2. Determine the appropriate bridge size, hydrologic uncertainty, and pier size corresponding to standard scour factor table values.

a. Bridge size: The example bridge's length is 1,715 ft. From the guidance presented in Section 5.2.3, this bridge is best represented as a large bridge.
b. Hydrologic uncertainty: To establish the relative hydrologic uncertainty of this bridge, it is necessary to estimate the COV associated with the uncertainty of the discharge estimate for the design flood event.
   1. The lognormal distribution of hydrologic uncertainty is determined from the 95% confidence limit discharge values as follows. The hydrologic uncertainty of a given discharge estimate (in this case, from a special study which does not correspond to a strict Bulletin 17B analysis) is assumed to be lognormally distributed. Consequently, given the 95% upper and 95% lower confidence limits (see Section 3.5.2),

$$\mu = \frac{\ln(Q_{upper}) + \ln(Q_{lower})}{2}$$

$$\sigma = \frac{\ln(Q_{upper}) - \ln(Q_{lower})}{2Z_c}$$

$$COV = \frac{\sigma}{\mu}$$

2. For a 95% confidence limit, $Z_c = 1.645$ (see Appendix A). From the hydrologic analysis, the upper and lower 95% confidence limits for the 1% exceedance probability event (i.e., the 100-year design flood) are:

$Q_{upper} = 458,000$ cfs;

$Q_{lower} = 350,000$; and

$Z_c = 1.645$

3. Substituting values for Q_{upper}, Q_{lower}, and Z_c into these equations,

$$\mu = \frac{\ln(458,000) + \ln(350,000)}{2} = 12.90$$

$$\sigma = \frac{\ln(458,000) - \ln(350,000)}{2(1.645)} = 0.082$$

$$COV = \frac{0.082}{12.90} = 0.0064$$

Compare the computed COV with Table 7.18 (reproduced from Table 3.4) for the 1.0% exceedance probability event:

Table 7.18.   Hydrologic uncertainty as a function of annual exceedance probability (reproduced from Table 3.4), Example Bridge No. 4.

Annual Exceedance		Discharge COV (lognormal)		
p(X > x)	T (years)	Low	Medium	High
0.04	25	0.009	0.014	0.018
0.02	50	0.010	0.015	0.019
0.01	**100**	**0.011***	0.016	0.021
0.005	200	0.012	0.017	0.022
0.002	500	0.013	0.018	0.023

*Bolding shows where the COV for Example Bridge No. 4 falls within the table. These numbers indicate that Example Bridge No. 4 has low hydrologic uncertainty.

This bridge has low hydrologic uncertainty.

c. Pier size: The 11 ft width of the drilled shaft piles beneath the main channel pylon is compared to the values in Table 7.19 (reproduced from Table 5.1). This bridge has large piers for a bridge of its type.

Table 7.19.   Representative bridge pier size as a function of bridge type (reproduced from Table 5.1), Example Bridge No. 4.

Bridge Type	Pier Size (ft)		
	Small	Medium	Large
Small	1	2	3
Medium	1.5	3	4.5
Large	3	6	9*

*Bolding shows where the pier size for Example Bridge No. 4 falls within the table. This large bridge has a large pier size.

Consequently, this bridge is best classified as a large bridge with low hydrologic uncertainty and large pier size for the Level I analysis.

Step 3. Determine scour factors.

Once the bridge has been classified, the practitioner can look in Appendix B, Table B.21 to determine appropriate bias and scour factors as a function of the desired β.

Table 7.20 corresponds to a large bridge with low hydrologic uncertainty and large pier size.

Table 7.20.   Scour factors for β = 3.0 (using Monte Carlo results), Example Bridge No. 4.

	Pier Scour	Contraction Scour	Abutment Total Scour	
			Left	Right
Bias	0.68	0.93	0.76	0.76
Scour factor	0.99	2.37	1.96	1.96

Step 4. Apply the bias and scour factors and determine total design scour.

Applying the recommended bias and scour factors for β = 3.0 for all components produces the results shown in Table 7.21. The individual scour component design scour values are multiplied by the applicable bias to determine the expected scour. Total expected scour is the sum of expected pier and contraction scour. The component scour for β = 3.0 is the design scour times the scour factor. By definition for β = 3.0, the difference between the component scour and the expected scour is 3.0 standard deviations from the expected scour.

Table 7.21.   100-year scour results for β = 3.0 (using Monte Carlo results).

	Pier Scour	Contraction Scour	Total Scour	Abutment Total Scour	
				Left	Right
Design scour (ft)	44.1	2.3	46.4	0.0	0.0
Bias	0.68	0.93			
Expected scour (ft)	30.0	2.1	32.1		
Scour factor	0.99	2.37			
Component scour for β = 3.0 (ft)	43.7	5.5			
Difference from expected (ft)	13.7	3.4	14.1		
Total scour for β = 3.0 (ft)			46.2		

The total scour difference from expected is the square root of the sum of the squares of the component scour differences (pier and contraction scour). The total scour for the target β is the expected plus the difference as shown in Table 7.21.

7.6 Example Bridge No. 5: South Carolina Atlantic Coastal Plain Subregion

Location: South Carolina
Physiographic region: Atlantic coastal plain; Sandhills subregion
Bridge lengths: Main channel: 1,950 ft; west relief: 520 ft; east relief: 520 ft
No. spans: 13, 8, 8
ADT: 7,450 (2009)
Main channel width: 320 ft

Figure 7.5.   Example Bridge No. 5 (main channel looking upstream).

River planform:	Meandering, low sinuosity (< 1.06)
100-year discharge:	249,100 ft³/s total (181,900 ft³/s main channel, 36,000 ft³/s west relief, and 31,200 ft³/s east relief)
100-year depth:	54 ft maximum
100-year velocity:	3.3 ft/s average in main channel bridge opening
Hydraulic model:	2-D (FESWMS FST-2DH)
Pier type/geometry:	Existing bridge: Drilled shafts with webwalls
	Proposed replacement bridge: 7 ft diameter drilled shafts main channel and 20 in. columns at the two relief bridges
Bed material:	Sandy clay (CL) and sandy silt (ML)
Abutment type/location:	Spill-through abutments set back on floodplains
Purpose of study:	Bridge replacement

Example Bridge No. 5 presents the Level I analysis method to provide probability values and scour factors for a bridge located in the Atlantic coastal plain physiographic region of the Sandhills subregion of South Carolina (see Figure 7.5). The site includes a main channel bridge and two relief bridges. No overtopping or pressure flow occurs in the 100-year design event. For the 100-year design scour event, a desired total scour reliability index, β, of 2.0 is assumed for this example. This β corresponds to a 97.72% probability of non-exceedance during the design event. Figure 7.6 illustrates the velocity contours from a 2-D hydraulic model of the 100-year flood at this site, showing the main bridge and the two relief bridges.

Step 1. Perform hydrologic, hydraulic, and design-equation scour computations using appropriate methods.

a. Hydrologic analysis: Bulletin 17B methods were used to determine the design scour event discharge, the expected value of the natural logarithm transform of discharge, and the SD of the uncertainty about that expected value for a given recurrence interval. The resulting discharges and summary statistics are presented in Table 7.22.

Table 7.22.   Hydrologic data from Bulletin 17B analysis of bridge site (N = 75 years), Example Bridge No. 5.

Annual Exceedance		Discharge (cfs)		
		Bulletin 17B Estimate	95% Confidence Limits	
p(X > x)	T (years)		Lower	Upper
0.1	10	139,000	125,000	157,000
0.04	25	178,800	159,000	206,000
0.02	50	212,400	185,000	252,000
0.01	100	249,100	214,000	301,000
0.005	200	287,800	244,000	354,000
0.002	500	351,800	293,000	443,000
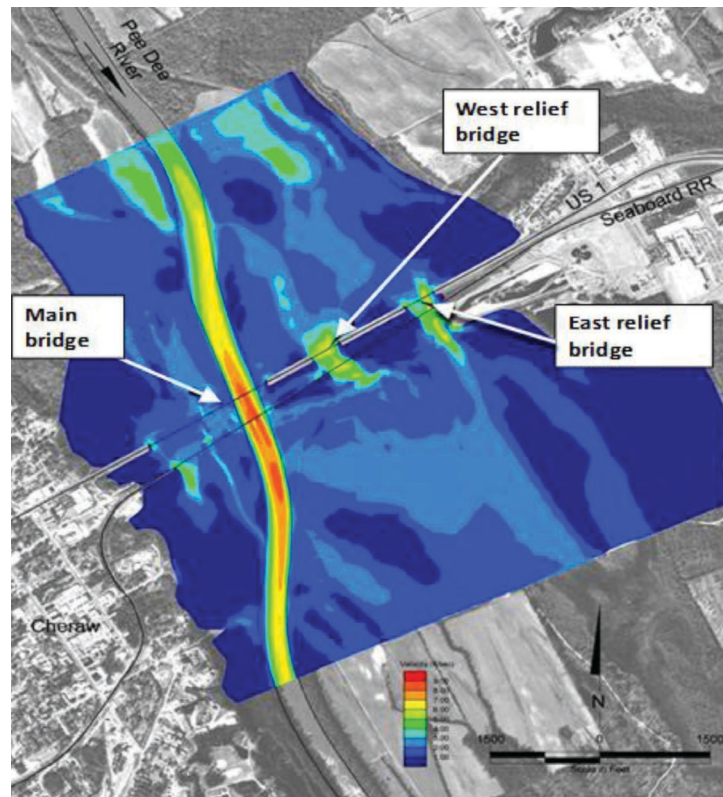
Figure 7.6.   2-D model of bridge site (velocity contours shown), Example Bridge No. 5.

b. Design-equation scour computations using the HEC-18 method for pier scour, the HEC-18 method for contraction scour, and the NCHRP Project 24-20 method as presented in HEC-18 for abutment scour were computed for this example. Table 7.23 presents the results of these computations.

Table 7.23.   100-year design scour depths, Example Bridge No. 5.

Bridge	Pier Scour (ft)	Contraction Scour (ft)	Total Scour (ft)	Abutment Total Scour (ft)	
				Left	Right
Main	9.9	3.4	13.3	4.6	8.8
West relief	5.4	3.7	9.1	14.5	9.8
East relief	5.8	4.5	10.3	12.8	15.5

Step 2. Determine the appropriate bridge size, hydrologic uncertainty, and pier size corresponding to standard scour factor table values.

a. Bridge size: The example bridges are 1,200 ft, 520 ft, and 520 ft long. From the guidance presented in Section 5.2.3, each bridge is best represented as a large bridge.

b. Hydrologic uncertainty: To establish the relative hydrologic uncertainty of this bridge example, it is necessary to estimate the COV associated with the uncertainty of the discharge estimate for the design scour event.

1. The lognormal distribution of hydrologic uncertainty is determined from the 95% confidence limit discharge values as follows. The hydrologic uncertainty of a given Bulletin 17B

discharge estimate is assumed to be lognormally distributed. Consequently, given the 95% upper and 95% lower confidence limits (see Section 3.5.2),

$$\mu = \frac{\ln(Q_{upper}) + \ln(Q_{lower})}{2}$$

$$\sigma = \frac{\ln(Q_{upper}) - \ln(Q_{lower})}{2Z_c}$$

$$COV = \frac{\sigma}{\mu}$$

2. For a 95% confidence limit, $Z_c = 1.645$ (see Appendix A). From the hydrologic analysis, the upper and lower 95% confidence limits for the 1% exceedance probability event are:

$Q_{upper} = 301,000$ cfs;

$Q_{lower} = 214,000$ cfs; and

$Z_c = 1.645$

3. Substituting values for Q_{upper}, Q_{lower}, and Z_c into these equations,

$$\mu = \frac{\ln(301,000) + \ln(214,000)}{2} = 12.4443$$

$$\sigma = \frac{\ln(301,000) - \ln(214,000)}{2(1.645)} = 0.103688$$

$$COV = \frac{0.103688}{12.4443} = 0.0083$$

Compare the computed COV with Table 7.24 (reproduced from Table 3.4) for the 1% exceedance probability event:

Table 7.24.   Hydrologic uncertainty as function of annual exceedance probability (reproduced from Table 3.4), Example Bridge No. 5.

Annual Exceedance		Discharge COV (lognormal)		
p(X > x)	T (years)	Low	Medium	High
0.04	25	0.009	0.014	0.018
0.02	50	0.010	0.015	0.019
0.01	**100**	**0.011***	0.016	0.021
0.005	200	0.012	0.017	0.022
0.002	500	0.013	0.018	0.023

*Bolding shows where the COV for Example Bridge No. 5 falls within the table. These numbers indicate that Example Bridge No. 5 has low hydrologic uncertainty.

This bridge has low hydrologic uncertainty.

c. Compare the bridge pier size (7 ft diameter and 20 inch diameter) to Table 7.25 (reproduced from Table 5.1). The main channel bridge has medium piers and the two relief bridges have small piers.

Table 7.25.   Representative bridge pier size as a function of bridge type (reproduced from Table 5.1), Example Bridge No. 5.

Bridge Type	Pier Size (ft)		
	Small	Medium	Large
Small	1	2	3
Medium	1.5	3	4.5
Large	3	6*	9

*Bolding shows where the pier sizes for Example Bridge No. 5 fall within the table. The main channel bridge in this example has medium piers, and the two relief bridges have small piers.

Consequently, the main channel bridge is best classified as a large bridge, low hydrologic uncertainty, medium pier size, and the two relief bridges are best classified as large bridge, low hydrologic uncertainty, small pier size for the Level I analysis.

Step 3. Determine scour factors.

Once the bridge has been classified, the practitioner can look in Appendix B, Table B.19 and Table B.20, to determine appropriate bias and scour factors as a function of the desired β.

Table 7.26 provides bias and scour factors corresponding to a large bridge with low hydrologic uncertainty and medium pier size (for the main bridge) and also for a large bridge with low hydrologic uncertainty and small pier size (for the relief bridges).

Table 7.26.   Scour factors for $\beta = 2.0$ (using Monte Carlo results), Example Bridge No. 5.

	HEC-18 Pier Scour		Contraction Scour	Abutment Total Scour	
	LB, LH, MP	LB, LH, SP		Left	Right
Bias	0.68	0.68	0.93	0.76	0.76
Scour factor	0.90	0.89	1.77	1.43	1.43

Step 4. Apply the bias and scour factors and determine total design scour.

Applying the recommended bias and scour factors for $\beta = 2.0$ for all components produces the results shown in Tables 7.27, 7.28, and 7.29 for the specific bridges. The individual scour component design scour values are multiplied by the applicable bias to determine the expected scour. Total expected scour is the sum of expected pier and contraction scour. The component scour for $\beta = 2.0$ is the design scour times the scour factor. By definition for $\beta = 2.0$, the difference between the component scour and the expected scour is 2.0 SDs from the expected scour.

The total scour difference from expected is the square root of the sum of the squares of the component scour differences (pier and contraction scour). The total scour for the target β is the expected scour plus the difference as shown in the tables.

Table 7.27.   100-year scour results for main channel bridge and β = 2.0, Example Bridge No. 5.

	HEC-18 Pier Scour	Contraction Scour	Total Scour	Abutment Total Scour	
				Left	Right
Design scour (ft)	9.9	3.4	13.3	4.6	8.8
Bias	0.68	0.93		0.76	0.76
Expected scour (ft)	6.7	3.2	9.9	3.5	6.7
Scour factor for target β	0.90	1.77		1.43	1.43
Component scour for target β (ft)	8.9	6.0		6.6	12.6
Difference from expected (ft)	2.2	2.8	3.6	3.1	5.9
Total scour for target β (ft)			13.5	6.6	12.6

Table 7.28.   100-year scour results for west relief bridge and β = 2.0, Example Bridge No. 5.

	HEC-18 Pier Scour	Contraction Scour	Total Scour	Abutment Total Scour	
				Left	Right
Design scour (ft)	5.4	3.7	9.1	14.5	9.8
Bias	0.68	0.93		0.76	0.76
Expected scour (ft)	3.7	3.4	7.1	11.0	7.5
Scour factor for target β	0.89	1.77		1.43	1.43
Component scour for target β (ft)	4.8	6.6		20.7	14.0
Difference from expected (ft)	1.1	3.2	3.4	9.7	6.5
Total scour for target β (ft)			10.5	20.7	14.0

Table 7.29.   100-year scour results for east relief bridge and β = 2.0, Example Bridge No. 5.

	HEC-18 Pier Scour	Contraction Scour	Total Scour	Abutment Total Scour	
				Left	Right
Design scour (ft)	5.8	4.5	10.3	12.8	15.5
Bias	0.68	0.93		0.76	0.76
Expected scour (ft)	3.9	4.2	8.1	9.7	11.8
Scour factor for target β	0.89	1.77		1.43	1.43
Component scour for target β (ft)	5.2	8.0		18.3	22.2
Difference from expected (ft)	1.2	3.8	4.0	8.6	10.4
Total scour for target β (ft)			12.1	18.3	22.2

CHAPTER 8

Conclusions and Observations

8.1 Conclusions

This reference guide is based on research conducted for NCHRP Project 24-34, "Risk-Based Approach for Bridge Scour Prediction." The research accomplished its basic objective of developing a risk and reliability-based methodology that can be used in calculating bridge pier, abutment, contraction, and total scour at waterway crossings so that scour estimates can be linked to a probability. The developed probabilistic procedures are consistent with LRFD approaches used by structural and geotechnical engineers.

There is widespread belief within the bridge engineering community that unaccounted-for biases and input parameter and hydraulic modeling uncertainty lead to overly conservative estimates of scour depths. The perception has been that this results in the design and construction of costly and unnecessarily deep foundations. This reference guide provides risk and reliability-based confidence bands for bridge scour estimates that align the hydraulic design approach with the design procedures currently used by structural and geotechnical engineers. Consequently, hydraulic engineers now have the option and ability to perform scour calculations that incorporate probabilistic methods into the hydraulic design of bridges.

The research project developed and implemented a work plan that produced significant results of practical use to the bridge engineering community. The project led to the development of two approaches that can be used by hydraulic engineers to more efficiently predict bridge scour. The Level I approach makes use of a set of tables of probability values or scour factors to associate an estimated scour depth provided by the hydraulic engineer with a probability of exceedance for simple pier and abutment geometries. For complex foundation systems and channel conditions or for cases requiring special consideration, the Level II approach is necessary. A Level II approach also is necessary if the unconditional probability of exceeding design scour depths to meet a target reliability over the life of a bridge is desired.

To develop the probability-based estimates or scour factor tables for each scour component and to develop the Level II approach, the project included an examination of the uncertainties associated with the prediction of individual scour components. These uncertainties were incorporated into a reliability analysis framework to estimate the probability of scour level exceedance for the service life of a bridge. The reliability analysis for scour is consistent with the reliability analysis procedures developed and implemented by AASHTO LRFD/LRFR for calibrating load and resistance factors for bridge structural components and bridge structural systems as well as foundations.

The Level I approach to determine the conditional probability of exceedance of design scour depth for a 100-year design event can be applied using the 27-element matrix presented in

Appendix B if a bridge fits the criteria of one of the 27 bridge categories reasonably well. In total, more than 300,000 HEC-RAS/Monte Carlo simulations were required to produce the statistics on which the 27 tables in Appendix B are based. In addition, more than 300,000 scour calculations were completed off-line for each of the scour equations (resulting in more than 1.2 million off-line scour calculations).

The Level II approach consists of a step-by-step procedure that hydraulic engineers can follow to provide probability-based estimates of site-specific scour factors. Conducting a Level II analysis implies that the design engineer must implement a HEC-RAS/Monte Carlo simulation using software similar to the rasTool© developed for NCHRP Project 24-34. The rasTool© software used in preparing this reference guide is a research-level software engine that requires considerable insight on the part of the user for application of the processes for Level II conditional and unconditional probability analyses. Specifically, the Monte Carlo simulation software was not developed for distribution, nor is it thoroughly documented or supported for general use. It is, however, considered robust and could be applied to a range of bridge and/or open-channel applications. Development of user-friendly HEC-RAS/Monte Carlo simulation software is listed as a research need in the Contractor's Final Report for NCHRP Project 24-34, which can be found at www.trb.org.

It bears repeating that the primary purpose of NCHRP Project 24-34 was to analyze the probability of scour depth exceedance, **not** the probability of bridge failure. The latter requires advanced analyses of the weakened foundation under the effects of the expected applied loads, which was beyond the scope of the research for this project.

8.2 Observations

During the course of NCHRP Project 24-34 a number of issues, considerations, and results were encountered that merit further discussion.

8.2.1 Data Analysis Issues

8.2.1.1 Pier Scour

There exists a plethora of data on pier scour from many sources, including both laboratory and field studies. The data sets used in the research that led to this reference guide included both clear-water and live-bed conditions. Both the HEC-18 and Florida DOT pier scour equations were developed as design equations, not best-fit prediction equations, and thus have a degree of conservatism built in. As such, the equations do not underpredict observed scour very often, and the reliability indexes for pier scour compare favorably with those used by structural and geotechnical engineers in LRFD applications for bridges.

8.2.1.2 Contraction Scour

In contrast with the pier scour equations, the HEC-18 contraction scour equations are essentially predictive, given that they are derived from sediment transport principles and theory. Therefore, underpredictions of observed scour are much more common, and the resulting reliability is very low compared to typical target values used in LRFD applications. Only studies that used long-contracted sections were analyzed, because short contractions include an abutment scour effect. Available data were limited to the clear-water condition.

8.2.1.3 Abutment Scour

The Contractor's Final Report for NCHRP Project 24-20, "Estimation of Scour Depth at Bridge Abutments" (Ettema et al. 2010) was published as this study was beginning. The results

of that research have been formally incorporated into the 5th edition of HEC-18 (Arneson et al. 2012).

Many data sets in the literature deal with abutment scour. Unfortunately, most of those data sets do not contain sufficient information regarding the distribution of flow between the main channel and the overbank area to allow analysis using the NCHRP Project 24-20 approach. The equations for live-bed abutment scour (Scour Condition A) and clear-water abutment scour (Scour Condition B) both use a calculation for contraction scour and then apply an amplification factor to account for the additional scour caused by local effects at the tip of the abutment. Therefore the scour predicted by this method is the total scour at the abutment.

Because the amplification factors were developed as envelope curves to the observed scour depths, the equations are considered to be design equations and therefore have a degree of built-in conservatism. The reliability of the abutment scour equations was found to be intermediate between those of the pier scour and contraction scour equations.

8.2.2 Importance of Hydrologic and Hydraulic Uncertainty

The HEC-RAS/Monte Carlo simulations proved to be very enlightening with respect to quantifying the effect that hydrologic and hydraulic uncertainties have on scour estimates. Using standard Water Resources Council Bulletin 17-B methodology, the uncertainty in the design discharge is easily quantified using the upper and lower 95% confidence limits. Risk increases—and the confidence interval decreases—with increasing periods of record. Using the confidence limits from flood frequency analyses showed that hydrologic uncertainty can have a major influence on scour variability.

Given any particular discharge, a hydraulic model (such as HEC-RAS) is necessary to develop hydraulic conditions such as depth and velocity, which are then used as input to the scour equations. A striking result of the research for NCHRP Project 24-34 was the effect of the Manning n resistance coefficient on the distribution of flow between the main channel and the overbank areas, and the resulting effect on the different types of scour. For pier scour, both the HEC-18 and Florida DOT equations were shown to be relatively insensitive to changes in flow distribution. In contrast, the contraction and abutment scour equations were very sensitive to this effect. Calibrating a hydraulic model to high water marks observed for various floods is crucial to reducing hydraulic uncertainty and thus reducing uncertainty in contraction and abutment scour depths.

8.2.3 Roadway Overtopping

When roadway overtopping is incorporated in the hydraulic model, contraction scour is considerably reduced. Roadway overtopping results in road closure and often results in damage to the approach embankments and possibly to the road surface. However, the bridge itself benefits from the relief of flow afforded by the overtopping condition. This effect has important implications for the design of new bridges as well as the analysis of existing bridges. Where overtopping is likely, the hydraulic model should reflect this as accurately as possible because of the benefit it provides in reducing contraction scour. For developing the scour factors used in Chapter 5 and the service life target reliability analysis used in Chapter 6 of this reference guide, however, the effects of roadway overtopping were not included. The total discharge was routed through the bridge opening in all the Monte Carlo simulation runs.

8.2.4 Total Scour

The combined effect of pier scour plus contraction scour was investigated to develop reliability indexes for the probability that the total design scour would be exceeded during the design life of the bridge. As first noted in Chapter 4, the NCHRP Project 24-20 abutment scour equations predict total scour at the abutment. NCHRP Project 24-37, currently underway, will examine whether total scour can be accurately estimated as simply a superposition of the individual components. Presumably, that study will include examination of the accuracy of estimates when a pier is within the abutment scour zone. The results of NCHRP Project 24-37 will have implications for the probability-based total scour procedures presented in this reference guide.

References

AASHTO (2005). *Guide Manual for Condition Evaluation and Load and Resistance Factor Rating (LRFR) of Highway Bridges, 1st Edition with 2005 Interim Revisions.* American Association of State Highway and Transportation Officials, Washington, D.C.

AASHTO (2007). *AASHTO LRFD Bridge Design Specifications: Customary U.S. Units,* 4th Edition, American Association of State Highway and Transportation Officials, Washington, D.C.

AASHTO (2008). *AASHTO Manual for Bridge Evaluation,* 1st Ed. (MBE 1-M), American Association of State Highway and Transportation Officials, Washington, D.C.

AASHTO (2009). "*Guide Specification and Commentary for Vessel Collision Design of Highway Bridges*" 2nd Ed., American Association of State Highway and Transportation Officials, Washington, D.C.

Arneson, L. A., L. W. Zevenbergen, P. F. Lagasse, and P. E. Clopper (2012). *Evaluating Scour at Bridges,* 5th Ed., Federal Highway Administration, Report FHWA-HIF-12-003, Hydraulic Engineering Circular No. 18, U.S. Department of Transportation, Washington, D.C.

ASCE (2010). *Minimum Design Loads for Buildings and Other Structures,* ASCE 7-10, American Society of Civil Engineers, Reston, VA.

ATC/MCEER Joint Venture (2002). *NCHRP Report 472: Comprehensive Specifications for the Seismic Design of Bridges,* Transportation Research Board of the National Academies, Washington D.C.

Ayyub, B. M. (2003). *Risk Analysis in Engineering and Economics,* Chapman and Hall/CRC, Boca Raton, FL.

Ayyub, B. M. and R. McCuen (2003). *Probability, Statistics, and Reliability for Engineers and Scientists,* 2nd Ed., Chapman and Hall/CRC, Boca Raton, FL.

Ballio, F., A. Terruzi, and A. Radice, (2009). Constriction Effects in Clear-Water Scour at Abutments, *Journal of Hydraulic Engineering,* Vol. 135, No. 2 (February), American Society of Civil Engineers, Reston, VA, pp. 140–145.

Cesare, M. A. (1991). First-order Analysis of Open-channel Flow, *Journal of Hydraulic Engineering,* Vol. 117, No. 2, pp. 242–247.

Dey, S. and R. V. Raikar (2005). Scour in Long Contractions, *Journal of Hydraulic Engineering,* Vol. 131, No. 12, American Society of Civil Engineers, Reston, VA, pp. 1035–1049.

Ettema, R., T. Nakato, and M. Muste (2010). Estimation of Scour Depth at Bridge Abutments, Draft/Final report, NCHRP Project 24-20, Transportation Research Board of the National Academies, Washington D.C.

Flynn, K. M., W. H. Kirby, and P. R. Hummel (2006). User's Manual for Program Peak FQ, Annual Flood-Frequency Analysis Using Bulletin 17B Guidelines, Techniques and Methods, Book 4, Chapter B4, U.S. Department of the Interior, U.S. Geological Survey, Reston, VA.

Froehlich, D. C. (2003). Finite Element Surface-Water Modeling System: Two-Dimensional Flow in a Horizontal Plane, In *FESWMS-2DH, Version 2, User's Manual,* U.S. Department of Transportation, Federal Highway Administration, Research, Development, and Technology, Turner-Fairbank Highway Research Center, McLean, VA.

Ghosn, M. and F. Moses (1998). *NCHRP Report 406: Redundancy in Highway Bridge Superstructures,* TRB, National Research Council, Washington, D.C.

Ghosn, M., F. Moses, and J. Wang (2003). *NCHRP Report 489: Design of Highway Bridges for Extreme Events,* Transportation Research Board of the National Academies, Washington, D.C.

Gill, M. A. (1981). "Bed Erosion in Rectangular Long Contraction." *Journal of Hydraulic Engineering,* Vol. 107, No. 3, American Society of Civil Engineers, Reston, VA, pp. 273–84.

Helsel, D. R. and R. M. Hirsch (1992). *Statistical Methods in Water Resources,* Elsevier Science B.V., New York, NY.

Hydrologic Engineering Center (1986). Accuracy of Computed Water Surface Profiles, U.S. Army Corps of Engineers, Davis, CA.

Imbsen, R. (2007). AASHTO Guide Specifications for LRFD Seismic Bridge Design, Report to AASHTO T3 Subcommittee, Washington, D.C.

Johnson, P. A. (1991). Advancing Bridge Pier Scour Engineering, *Journal of Professional Issues in Engineering Education and Practice,* Vol. 117, No. 1, American Society of Civil Engineers, New York, NY, pp. 48–55.

Johnson, P. A. and B. M. Ayyub (1992). Probability of Bridge Failure Due to Pier Scour, in *Proc. of the Water Resources Sessions at Water Forum '92,* August 2–6, 1992, Baltimore, MD, p. 690.

Johnson, P. A. (1996). Uncertainty of Hydraulic Parameters, *Journal of Hydraulic Engineering,* Vol. 122, No. 2, American Society of Civil Engineers, Reston, VA, pp. 112–115.

Johnson, P. A. and D. A. Dock (1998). Probabilistic Bridge Scour Estimates, *Journal of Hydraulic Engineering,* Vol. 124, No. 7, July 1998, American Society of Civil Engineers, Reston, VA, pp. 750-754. DOI 10.1061/ (ASCE)0733-9429(1998)124:7(750).

Jones, J. S. (1984). Comparison of Prediction Equations for Bridge Pier and Abutment Scour, *Transportation Research Record: Journal of the Transportation Research Board, No. 950,* Vol. 2, Second Bridge Engineering Conference, Transportation Research Board of the National Academies, Washington, D.C.

Keaton, J. R., S. K. Mishra, and P. E. Clopper (2012). *NCHRP Report 717: Scour at Bridge Foundations on Rock,* Transportation Research Board of the National Academies, Washington, D.C.

Komura, S. (1966). Equilibrium Depth of Scour in Long Constrictions. *Journal of the Hydraulics Division,* Vol. 92, No. 5, American Society of Civil Engineers, New York, NY.

Kulicki, J. M., D. R. Mertz, and A. S. Nowak (2007). Updating the Calibration Report for AASHTO LRFD Code, Draft/Final report, NCHRP Project 20-7/186, Transportation Research Board of the National Academies, Washington, D.C.

Lagasse, P. F., W. J. Spitz, L. W. Zevenbergen, and D. W. Zachmann (2004). *NCHRP Report 533: Handbook for Predicting Stream Meander Migration,* Transportation Research Board of the National Academies, Washington, D.C.

Lagasse, P. F., P. E. Clopper, L. W. Zevenbergen, W. J. Spitz, and L. G. Girard (2010). *NCHRP Report 653: Effects of Debris on Bridge Pier Scour,* Transportation Research Board of the National Academies, Washington, D.C.

Lagasse, P. F., L. W. Zevenbergen, W. J. Spitz, and L. A. Arneson (2012). Stream Stability at Highway Structures, Hydraulic Engineering Circular No. 20, 4th Ed., Federal Highway Administration, HIF-FHWA-12-004, Washington, D.C.

Lagasse, P. F., M. Ghosn, P. A. Johnson, L. W. Zevenbergen, and P. E. Clopper (2013). Risk-Based Approach for Bridge Scour Prediction, Final report, NCHRP Project 24-34, Transportation Research Board of the National Academies, Washington, D.C.

Lim, S. Y. (1993). Clear Water Scour in Long Contractions, in *Water and Maritime Engineering: Proceedings of the Institution of Civil Engineers, Vol. 101* (June), London.

Liu, D., M. Ghosn, F. Moses, and A. Neuenhoffer (2001). *NCHRP Report 458: Redundancy in Highway Bridge Substructures,* TRB, National Research Council, Washington, D.C.

Mays, L. W. and Y. K. Tung (1992). *Hydrosystems Engineering and Management,* McGraw-Hill, Inc., New York, NY.

Melchers, R. E. (1999). *Structural Reliability: Analysis and Prediction,* 2nd Ed., John Wiley & Sons, New York, NY.

Military Engineer (2012). National Levee Database and Its Asset Management Application, Technology News, *The Military Engineer,* Vol. 104, No. 679, Society of American Military Engineers, Alexandria, VA.

Moses, F. (2001). *NCHRP Report 454: Calibration of Load Factors for LRFR Bridge Evaluation,* TRB, National Research Council, Washington, D.C.

Nowak. A. S. (1999). *NCHRP Report 368: Calibration of LRFD Bridge Design Code,* TRB, National Research Council, Washington, D.C.

Nowak, A. S. and K. R. Collins (2000). *Reliability of Structures,* McGraw-Hill, Inc., New York, NY.

Oben-Nyarko, K. and R. Ettema (2011). Pier and Abutment Scour Interaction, *Journal of Hydraulic Engineering,* Vol. 137, No. 12, American Society of Civil Engineers, Reston, VA, pp. 1598–1605.

Raikar, R. (2004). *Local and General Scour of Gravel Beds.* PhD thesis, Department of Civil Engineering, Indian Institute of Technology, Kharagpur, India.

Ries, K. G. (2007). The National Streamflow Statistics Program: A Computer Program for Estimating Streamflow Statistics for Ungaged Sites, U.S. Geological Survey Techniques and Methods 4-A6, Reston, VA.

Richardson, E. V., D. B. Simons, and P. F. Lagasse (2001). River Engineering for Highway Encroachments: Highways in the River Environment, Report No. FHWA NHI 01-004, Hydraulic Design Series No. 6, Federal Highway Administration, Washington, D.C.

Sheppard, D. M., B. W. Melville, and H. Deamir (2011). *NCHRP Report 682: Scour at Wide Piers and Long Skewed Piers,* Transportation Research Board of the National Academies, Washington, D.C.

Sturm, T. W., R. Ettema, and B. W. Melville (2011). *NCHRP Web-Only Document 181: Evaluation of Bridge-Scour Research: Abutment and Contraction Scour Processes and Prediction,* Transportation Research Board of the National Academies, Washington D.C.

Thoft-Christensen, P. and M. J. Baker (1982). *Structural Reliability Theory and Its Applications,* Springer Verlag, Berlin.

Tung, Y. K. (1990). Mellin Transform Applied to Uncertainty Analysis in Hydrology/Hydraulics, *Journal of Hydraulic Engineering,* Vol. 116, No. 5, American Society of Civil Engineers, New York, NY, pp. 659–674.

U.S. Army Corps of Engineers (1986). Accuracy of Computed Water Surface Profiles, Research Document No. 26 (M. Burnham and D. W. Davis), 198 p.

U.S. Army Corps of Engineers (1992). Reliability Assessment of Navigation Structures, Department of the Army, Engineer Technical Letter No. 1110-2-532.

U.S. Army Corps of Engineers (2004). Upper Mississippi: River System Flow Frequency Study—Final Report: Appendix E, Kansas City District, Missouri River Hydrology and Hydraulic Analysis, November 2003, U.S. Army Corps of Engineers, Rock Island District, Rock Island, IL.

U.S. Army Corps of Engineers (2010). HEC-RAS Version 4.1, USACE Hydrologic Engineering Center, Davis, CA.

U.S. Geological Survey (1981). Guidelines for Determining Flood Flow Frequency, Bulletin 17B of the Hydrology Subcommittee, Interagency Advisory Committee on Water Data, Reston, VA.

Webby, M. G. (1984). General Scour at a Contraction, *RRU Bulletin 73,* National Roads Board, Bridge Design and Research Seminar, New Zealand.

Wu, B. and A. Molinas (2005). Energy Losses and Threshold Conditions for Choking in Channel Contractions, *Journal of Hydraulic Research,* Vol. 43, No. 2, International Association for Hydro-Environment Engineering and Research (IAHR), pp. 139–148.

Yeh, K. C. and Y. K. Tung (1993). Uncertainty and Sensitivity Analyses of Pit-Migration Model, *Journal of Hydraulic Engineering,* Vol. 119, No. 2, American Society of Civil Engineers, New York, NY, pp. 262–283.

Yevjevich, V. (1972). *Probability and Statistics in Hydrology,* Water Resources Publications, Fort Collins, CO.

APPENDIX A

Glossary

I. Hydrologic, Hydraulic, and Geomorphic Terms*

Aggradation:	General and progressive buildup of the longitudinal profile of a channel bed due to sediment deposition.
Alluvial Channel:	Channel wholly in alluvium; no bedrock is exposed in channel at low flow or likely to be exposed by erosion.
Alluvial Stream:	A stream which has formed its channel in cohesive or noncohesive materials that have been and can be transported by the stream.
Alluvium:	Unconsolidated material deposited by a stream in a channel, floodplain, alluvial fan, or delta.
Annual Flood:	The maximum flow in one year (may be daily or instantaneous).
Average Velocity:	Velocity at a given cross section determined by dividing discharge by cross-sectional area.
Backwater:	The increase in water surface elevation relative to the elevation occurring under natural channel and floodplain conditions. It is induced by a bridge or other structure that obstructs or constricts the free flow of water in a channel.
Backwater Area:	The low-lying lands adjacent to a stream that may become flooded due to backwater.
Bank:	The sides of a channel between which the flow is normally confined.
Bank, Left (Right):	The side of a channel as viewed in a downstream direction.
Bankfull Discharge:	Discharge that, on the average, fills a channel to the point of overflowing.

*Many of the entries in Part I of this Glossary are from HEC-18 (Arneson et al. 2012).

A-1

Base Floodplain:	Floodplain associated with the flood with a 100-year recurrence interval.
Bed:	Bottom of a channel bounded by banks.
Bed Form:	A recognizable relief feature on the bed of a channel, such as a ripple, dune, plane bed, antidune, or bar. Bed forms are a consequence of the interaction between hydraulic forces (boundary shear stress) and the bed sediment.
Bed Material:	Material found in and on the bed of a stream (may be transported as bed load or in suspension).
Bed Shear (Tractive Force):	The force per unit area exerted by a fluid flowing past a stationary boundary.
Boulder:	A rock fragment whose diameter is greater than 250 mm.
Boundary Condition (Model):	A specified hydraulic condition such as a water surface elevation or energy slope used as a starting point for a hydraulic model simulation.
Bridge Opening:	The cross-sectional area beneath a bridge that is available for conveyance of water.
Bridge Substructure:	Structural elements supporting a bridge in contact with the stream or channel bed, including bridge abutments, piers, and footings.
Bridge Waterway:	The area of a bridge opening available for flow, as measured below a specified stage and normal to the principal direction of flow.
Catchment:	See Drainage Basin.
Channel:	The bed and banks that confine the surface flow of a stream.
Channel Pattern:	The aspect of a stream channel in plan view, with particular reference to the degree of sinuosity, braiding, and anabranching.
Channel Process:	Behavior of a channel with respect to shifting, erosion, and sedimentation.
Choking (of flow):	Excessive constriction of flow which may cause severe backwater effect.
Clay (Mineral):	A particle whose diameter is in the range of 0.00024 to 0.004 mm.

Clear-Water Scour:	Scour at a pier or abutment (or contraction scour) when there is no movement of the bed material upstream of the bridge crossing at the flow causing bridge scour.
Constriction:	A natural or artificial control section, such as a bridge crossing, channel reach or dam, with limited flow capacity in which the upstream water surface elevation is related to discharge.
Contraction:	The effect of channel or bridge constriction on flow streamlines.
Contraction Scour:	Contraction scour, in a natural channel or at a bridge crossing, involves the removal of material from the bed and banks across all or most of the channel width. This component of scour results from a contraction of the flow area at the bridge which causes an increase in velocity and shear stress on the bed at the bridge. The contraction can be caused by the bridge or from a natural narrowing of the stream channel.
Conveyance:	A measure of the carrying capacity of a channel section. In the Manning equation, conveyance K is:

$$K = \frac{1.486}{n} AR^{2/3} = \frac{Q}{\sqrt{S}}$$

Critical Shear Stress:	The minimum amount of shear stress required to initiate soil particle motion.
Critical Velocity (Particle Motion):	The velocity required to initiate motion of a particle of a specified size and weight.
Cross Section:	A section normal to the trend of a channel or flow.
Daily Discharge:	Discharge averaged over one day (24 hours).
Debris:	Floating or submerged material, such as logs, vegetation, or trash, transported by a stream (Drift).
Degradation (Bed):	A general and progressive (long-term) lowering of the channel bed due to erosion, over a relatively long channel length.
Depth of Scour:	The vertical distance a streambed is lowered by scour below a reference elevation.
Design Flow (Design Flood):	The discharge that is selected as the basis for the design or evaluation of a hydraulic structure including a hydraulic design flood, scour design flood, and scour design check flood.

Discharge:	Volume of water passing through a channel during a given time.
Drainage Basin:	An area confined by drainage divides, often having only one outlet for discharge (Catchment, Watershed).
Drift:	Alternative term for vegetative debris.
Energy (Friction) Slope:	Rate of energy loss with distance in the downstream flow direction: $S_f = dH/dL$ where H is total energy and L is streamwise distance.
Ephemeral Stream:	A stream or reach of stream that does not flow for parts of the year. As used here, the term includes intermittent streams with flow less than perennial.
Erosion:	Displacement of soil particles due to water or wind action.
FESWMS:	A 2-dimensional open-channel flow model called the Finite Element Surface Water Modeling System developed and supported by the Federal Highway Administration (also referred to as FST-2DH).
Fill Slope:	Side or end slope of an earth-fill embankment. Where a fill-slope forms the streamward face of a spill-through abutment, it is regarded as part of the abutment.
Flood:	Large volumetric rate of discharge in a river or stream that occurs infrequently and is usually associated with inundation and economic damage.
Flood Exceedance Probability:	The statistical chance that a specified discharge rate will be equaled or exceeded in a given year.
Flood Frequency:	The average interval between floods exceeding a given magnitude. For example, a flood having an annual probability of exceedance of 1 percent has a $1/(0.01) =$ 100-year frequency of recurrence; a flood of this magnitude would be expected to occur on average about once every 100 years.
Flood-Frequency Curve:	A graph indicating the probability that the annual flood discharge will exceed a given magnitude, or the recurrence interval corresponding to a given magnitude.
Floodplain:	A nearly flat, alluvial lowland bordering a stream, which is subject to frequent inundation by floods.
Flood Return Period/Recurrence Interval:	See Flood Frequency.
Flow Skew:	The angle of incidence of flow on a rectangular or long wall pier. Flow aligned with the long axis of a structure has a skew of zero degrees.

Fluvial Geomorphology:	The science dealing with the morphology (form) and dynamics of streams and rivers.
Fluvial System:	The natural river system consisting of (1) the drainage basin, watershed, or sediment source area, (2) tributary and mainstem river channels or sediment transfer zone, and (3) alluvial fans, valley fills and deltas, or the sediment deposition zone.
Freeboard:	The vertical distance above a design stage that is allowed for waves, surges, drift, and other contingencies.
Froude Number:	A dimensionless number that represents the ratio of inertial to gravitational forces in open-channel flow.
Gabion:	A basket or compartmented rectangular container made of wire mesh. When filled with cobbles or other rock of suitable size, the gabion becomes a flexible and permeable unit with which flow- and erosion-control structures can be built.
Gaging Station:	Instrumentation on a stream or river that is used for measuring the volumetric rate of flow. Gaging stations exhibit a unique relationship between water surface elevation and flow rate which is periodically calibrated.
Geomorphology/Morphology:	That science that deals with the form of the Earth, the general configuration of its surface, and the changes that take place due to erosion and deposition.
Graded Stream:	A geomorphic term used for streams that have apparently achieved a state of equilibrium between the rate of sediment transport and the rate of sediment supply throughout long reaches.
Gravel:	A rock fragment whose diameter ranges from 2 to 64 mm.
HEC-RAS:	A 1-dimensional open-channel flow model developed and supported by the U.S. Army Corps of Engineers - Hydrologic Engineering Center.
Headcutting:	Channel degradation associated with abrupt changes in the bed elevation (headcut) that generally migrates in an upstream direction.
Hydraulics:	The applied science concerned with the behavior and flow of liquids, especially in pipes, channels, structures, and the ground.
Hydraulic Model:	A small-scale physical (or mathematical) representation of a flow situation.
Hydrograph:	The graph of stage or discharge against time.

Hydrology:	The science concerned with the occurrence, distribution, and circulation of water on the earth.
Incised Reach:	A stretch of stream with an incised channel that only rarely overflows its banks.
Incised Stream:	A stream which has deepened its channel through the bed of the valley floor, so that the floodplain is a terrace.
Ineffective Flow:	An area of flow where water is not being conveyed in a downstream direction (e.g., ponding above or below an embankment).
Instantaneous Discharge/Peak:	The volumetric rate of flow passing a given cross section on a stream or river at a specific point in time.
Invert:	The lowest point in the channel cross section or at flow control devices such as weirs, culverts, or dams.
Lateral Erosion (Migration):	Erosion in which the removal of material is extended horizontally as contrasted with degradation and scour in a vertical direction.
Live-Bed Scour:	Scour at a pier or abutment (or contraction scour) when the bed material in the channel upstream of the bridge is moving at the flow causing bridge scour.
Live Flow:	Area of flow where water is actively conveyed in a downstream direction (e.g., channel flow and unobstructed floodplain flow).
Local Scour:	Removal of material from around piers, abutments, spurs, and embankments caused by an acceleration of flow and resulting vortices induced by obstructions to the flow.
Longitudinal Profile:	The profile of a stream or channel drawn along the length of its centerline. In drawing the profile, elevations of the water surface or the thalweg are plotted against distance as measured from the mouth or from an arbitrary initial point.
Manning Equation:	Relationship between discharge, channel geometry, and roughness: $$Q = \frac{1.486}{n} AR^{2/3} S_f^{1/2}$$
Manning Roughness Coefficient (n):	Parameter of the Manning equation that is a measure of the resistance to flow caused by the channel boundary.
Mathematical Model:	A numerical representation of a flow situation using mathematical equations (also computer model).
Meandering Stream:	A stream having a sinuosity greater than some arbitrary value. The term also implies a moderate degree of pattern

	symmetry, imparted by regularity of size and repetition of meander loops. The channel generally exhibits a characteristic process of bank erosion and point bar deposition associated with systematically shifting migrating meanders.
Median Diameter:	The particle diameter of the 50th percentile point on a size distribution curve such that half of the particles (by weight, number, or volume) are larger and half are smaller ($D_{50.}$)
Migration:	Change in position of a channel by lateral erosion of one bank and simultaneous accretion of the opposite bank.
Nonalluvial Channel:	A channel whose boundary is in bedrock or non-erodible material.
Normal Stage:	The water stage prevailing during the greater part of the year.
Obstructed Flow Area:	Portion of the waterway and/or floodplain blocked by a structure such as a bridge pier or approach roadway embankment.
Overbank Flow:	Water movement that overtops the bank either due to stream stage or to overland surface water runoff.
Overtopping Flow:	Portion of the flood discharge that flows over a roadway embankment or bridge deck.
Perennial Stream:	A stream or reach of a stream that flows continuously for all or most of the year.
Pile:	An elongated member, usually made of timber, concrete, or steel, which serves as a structural component of a river-training structure or bridge.
Pressure Flow/Scour:	See Vertical Contraction Scour.
Probable Maximum Flood:	A very rare flood discharge value computed by hydro-meteorological methods, usually in connection with major hydraulic structures.
Probability Distribution (Log-Pearson Type III):	Statistical probability distribution used to estimate flood frequency characteristics, typically using historical flood peak flows from gaging station records.
Reach:	A segment of stream length that is arbitrarily bounded for purposes of study.
Recurrence Interval:	The reciprocal of the annual probability of exceedance of a hydrologic event (also return period, exceedance interval).

Regression Relationship (Regional):	A method for estimating the magnitude and frequency of floods using watershed characteristics such as drainage area, percent impervious surface, percent forest cover, etc.
Relief Bridge:	An opening in an embankment on a floodplain to permit passage of overbank flow.
Riparian:	Pertaining to anything connected with or adjacent to the banks of a stream (corridor, vegetation, zone, etc.).
Riprap:	Layer or facing of rock or broken concrete dumped or placed to protect a structure or embankment from erosion; also the rock or broken concrete suitable for such use. Riprap has also been applied to almost all kinds of armor, including wire-enclosed riprap, grouted riprap, sacked concrete, and concrete slabs.
Roughness Coefficient:	Numerical measure of the frictional resistance to flow in a channel, as in the Manning or Chezy's formulas.
Sand:	A rock fragment whose diameter is in the range of 0.062 to 2.0 mm.
Scour:	Erosion of streambed or bank material due to flowing water; often considered as being localized (see local scour, contraction scour, total scour).
Scour Prism:	Total volume of streambed material removed by scour in the bridge reach for design flood conditions.
Sediment or Fluvial Sediment:	Fragmental material transported, suspended, or deposited by water.
Sediment Concentration:	Weight or volume of sediment relative to the quantity of transporting (or suspending) fluid.
Sediment Discharge:	The quantity of sediment that is carried past any cross section of a stream in a unit of time. Discharge may be limited to certain sizes of sediment or to a specific part of the cross section.
Sediment Load (Transport):	Amount of sediment being moved (transported) by a stream.
Sediment Yield:	The total sediment outflow from a watershed or a drainage area at a point of reference and in a specified time period. This outflow is equal to the sediment discharge from the drainage area.
Sediment Size (Median Diameter):	The particle diameter of the 50th percentile point on a size distribution curve such that half of the particles (by weight, number, or volume) are larger and half are smaller (D_{50}).

Shear Stress:	See Unit Shear Force.
Silt:	A particle whose diameter is in the range of 0.004 to 0.062 mm.
Sinuosity:	The ratio between the thalweg length and the valley length of a stream.
Slope (of Channel or Stream):	Fall per unit length along the channel centerline or thalweg.
Slope-Area Method:	A method of estimating unmeasured flood discharges in a uniform channel reach using observed high-water levels.
Spill-Through Abutment:	A bridge abutment having a fill slope on the streamward side. The term originally referred to the "spill-through" of fill at an open abutment but is now applied to any abutment having such a slope.
Spread Footing:	A pier or abutment footing that transfers load directly to the earth.
Stability:	A condition of a channel when, though it may change slightly at different times of the year as the result of varying conditions of flow and sediment charge, there is no appreciable change from year to year; that is, accretion balances erosion over the years.
Stable Channel:	A condition that exists when a stream has a bed slope and cross section which allows its channel to transport the water and sediment delivered from the upstream watershed without aggradation, degradation, or bank erosion (a graded stream).
Stage:	Water-surface elevation of a stream with respect to a reference elevation.
Stream:	A body of water that may range in size from a large river to a small rill flowing in a channel. By extension, the term is sometimes applied to a natural channel or drainage course formed by flowing water whether it is occupied by water or not.
Subcritical, Supercritical Flow:	Open-channel flow conditions with Froude Number less than and greater than unity, respectively.
Thalweg:	The line extending down a channel that follows the lowest elevation of the bed.
Toe of Bank:	That portion of a stream cross section where the lower bank terminates and the channel bottom or the opposite lower bank begins.

Total Scour:	The sum of long-term degradation, contraction scour, and local scour.
Tractive Force:	The drag or shear on a streambed or bank caused by passing water which tends to move soil particles along with the streamflow.
Turbulence:	Motion of fluids in which local velocities and pressures fluctuate irregularly in a random manner as opposed to laminar flow where all particles of the fluid move in distinct and separate lines.
Ultimate Scour:	The maximum depth of scour attained for a given flow condition. May require multiple flow events and in cemented or cohesive soils may be achieved over a long time period.
Uniform Flow:	Flow of constant cross section and velocity through a reach of channel at a given time. Both the energy slope and the water slope are equal to the bed slope under conditions of uniform flow.
Unit Discharge:	Discharge per unit width (may be average over a cross section, or local at a point).
Unit Shear Force (Shear Stress):	The force or drag developed at the channel bed by flowing water. For uniform flow, this force is equal to a component of the gravity force acting in a direction parallel to the channel bed on a unit wetted area. Usually in units of stress, Pa (N/m^2) or (lb/ft^2).
Unsteady Flow:	Flow of variable discharge and velocity through a cross section with respect to time.
Velocity:	The time rate of flow usually expressed in m/s (ft/sec). The average velocity is the velocity at a given cross section determined by dividing discharge by cross-sectional area.
Vertical Contraction Scour:	Scour resulting from flow impinging on bridge superstructure elements (e.g., low chord).
Vortex:	Turbulent eddy in the flow generally caused by an obstruction such as a bridge pier or abutment (e.g., horseshoe vortex).
Watershed:	See Drainage Basin.
Waterway Opening Width (Area):	Width (area) of bridge opening at (below) a specified stage, measured normal to the principal direction of flow.

II. Probability and Statistical Terms

Bias:	A statistical measure of systematic difference between a predicted value and the population parameter of interest, typically showing as the symbol λ; a measure of consistent overprediction or underprediction.
Box-Muller Transform:	A method for generating independent standard normally distributed random numbers given a source of uniformly distributed random numbers.
Chi-Squared Test:	A statistical test commonly used to compare observed data with data one would expect to obtain according to a specific hypothesis.
Coefficient of Variation (COV):	A measure of the dispersion of a probability distribution defined as the standard deviation divided by the mean:

$$COV = \frac{\sigma}{\mu}$$

Confidence Limit:	An interval estimator of a population parameter used to assess the reliability of an estimate, typically shown as the symbol Z_c. For example, there is a 90% probability that the true value lies between the Upper and Lower 95% confidence limits.

Confidence Limit	Z_c
90%	1.281
95%	1.645
98%	2.054

Cumulative Distribution (Density) Function (CDF):	A mathematical expression that quantifies the likelihood (or percent chance) that a quantity will be exceeded.
Data Set Outlier:	An observation that is numerically distant from the rest of the data in a sample. Outliers are sometimes considered to be faulty data and are removed from the data set.
Design Life (of Bridge):	The useful life over which a structure is planned to perform its intended function without becoming damaged or obsolete. Typically this term refers to new structures.
Deterministic Factor:	A parameter which is not variable for a given structure; for example the width of a bridge pier.
Equation (Design):	A mathematical relationship that envelopes the observed data in such a way that the results are conservative in nature.
Equation (Predictive):	A mathematical relationship that tends to fit through the cloud of observed data points in such a way that overprediction and underprediction occur with relatively equal magnitude and frequency.

Gaussian Distribution:	The Standard Normal or "bell-shaped" probability distribution function.
Kolmogorov-Smirnov Test:	A nonparametric goodness-of-fit test that compares a probability distribution obtained from a sample to a reference cumulative distribution function, or to a distribution from a second sample.
Latin Hypercube Simulation (LHS):	A statistical method of generating a sample using equally probable intervals, often used in uncertainty analysis.
Level I Analysis/Approach:	A method for accounting for uncertainty in bridge scour estimates that multiplies a scour estimate by a "scour factor" to achieve a desired level of reliability that the resulting scour depth will not be exceeded during a design flood event.
Level II Analysis/Approach:	A method for accounting for uncertainty in bridge scour estimates that uses Monte Carlo simulation to develop scour estimates for a specific bridge using its unique characteristics.
Load and Resistance Factor Design (LRFD):	A structural design method that uses calibrated load factors and prescribed code values to achieve a desired level of reliability against structural failure.
Load and Resistance Factor Rating (LRFR):	A structural rating system used to evaluate bridges based upon calibrated load factors using principles of structural reliability.
Log-Transform:	The natural logarithms of a data series.
Mean:	The average value of a sample or a population, typically shown as the symbol μ.
Monte Carlo Realization:	One simulation out of many where certain variables are allowed to vary within prescribed limits in accordance with specified probability distributions.
Monte Carlo Simulation (MCS):	The net result of performing many individual realizations in order to obtain statistical information about the process or phenomenon being modeled.
Poisson Process:	A stochastic process which counts the number of events and the time that these events occur within a given time interval.
Probability:	A measure or estimate of the likelihood (or percent chance) that an event will occur or that a statement is true ranging from 0 (0% chance or will not happen) to 1 (100% chance, or will happen). Typically, P symbolizes probability (e.g., the term P_F is the probability of failure).

Probability (Conditional):   The likelihood (percent chance) that a quantity will be exceeded given the condition that another event has occurred or will occur.

Probability Distribution (Density) Function (PDF):   A mathematical expression that quantifies the likelihood that an event will occur or that a quantity will take on a value or fall within a range of values.

Probability Distribution (Log-Normal):   A mathematical expression of the Gaussian or "bell-shaped" probability curve that fits the logarithms of the data points.

Probability Distribution (Normal):   A mathematical expression of the Gaussian or "bell-shaped" probability curve that fits the values of the data points.

Probability of Exceedance: The likelihood (percent chance) that a quantity will exceed a specified value, typically shown as P_N for N years or P_a for annual probability of exceedance.

Probability of Non-Exceedance: The likelihood (percent chance) that a quantity will not exceed a specified value.

Probability (Unconditional):   The likelihood (percent chance) that a design value will be exceeded over the entire remaining service life of a structure.

Random Factor: A factor is random when the quantities under study are part of a larger population and the goal of the study is to make a statement or conclusion regarding the larger population.

Random Number Generator (RNG):   A computational or physical device designed to generate a sequence of numbers or symbols that lack any pattern.

rasTool$^©$:   The name given to the computer program which links the HEC-RAS hydraulic model to Monte Carlo simulation software.

Reliability: A branch of statistics which seeks to quantify the ability of a system or component to perform its required functions under stated conditions for a specified period of time.

Reliability Index: The probability of non-exceedance expressed as the number of standard deviations from the mean, typically shown as the symbol β. For example, the standard Normal distribution has a probability of non-exceedance of 84.13% at $\beta = 1.0$, 97.73% at $\beta = 2.0$, and 99.87% at $\beta = 3.0$.

Risk:	The potential that a chosen action or activity (including the choice of inaction) will lead to a loss (an undesirable outcome). In economic terms, risk is often defined as the product of probability of failure times the cost of failure, and is measured in dollars, typically shown as the symbol R.
Scour Factor:	A safety factor which multiplies a scour estimate to achieve a desired target Reliability Index β.
Service Life (of Bridge):	Similar to Design Life. Refers to the remaining planned life of an existing structure. Typically this term refers to existing structures.
Skew (Distribution):	A measure of the asymmetry of a probability distribution.
Standard Deviation (SD):	In probability and statistics, a measure of the spread or dispersion that exists from the average value, typically shown as the symbol σ.
Standard Error (SE):	A measure of the accuracy of predictions. In hydrology, SE is often reported as the accuracy, in percent, of a discharge estimate developed using regional regression equations.
Stochastic:	A non-deterministic system or process which is characterized both by the system's predictable actions and by a random element.
Target Reliability:	The desired level of probability of non-exceedance. See Reliability Index.
Uncertainty (Aleatory):	Sources of uncertainty which reflect the natural randomness of a process and which cannot be suppressed by making more accurate measurements. Also referred to as statistical uncertainty.
Uncertainty (Epistemic):	Sources of uncertainty that reflect the inaccuracies in the modeling of a process. Also referred to as modeling uncertainty.
Z Limit:	The number of standard deviations from the mean.

Summary of Scour Factors in Tabular and Graphical Form

Table B.1	Small Bridge—Low Hydrologic Uncertainty—Small Pier (1 ft)					
	Pier Scour (HEC-18)	Pier Scour (FDOT)	Contraction Scour	Total Scour (HEC-18)	Total Scour (FDOT)	Abutment Scour
Design scour (ft)	2.40	2.13	1.70	4.10	3.82	4.02
Expected scour (ft)	1.63	1.60	1.55	3.19	3.15	2.99
Bias	0.68	0.75	0.92	0.78	0.82	0.74
Std. dev. (ft)	0.26	0.28	0.41	0.49	0.50	0.71
COV	0.16	0.18	0.26	0.15	0.16	0.24
Design scour β	2.96	1.87	0.35	1.87	1.35	1.46
Non-exceedance	0.9985	0.9696	0.6356	0.9690	0.9110	0.9281
Scour Non-exceedance (ft) Based on Monte Carlo Results						
β = 0.5 (0.6915)	1.76	1.74	1.73	3.41	3.39	3.32
β = 1.0 (0.8413)	1.89	1.88	1.96	3.67	3.65	3.69
β = 1.5 (0.9332)	2.02	2.03	2.21	3.94	3.93	4.09
β = 2.0 (0.9772)	2.15	2.17	2.45	4.22	4.22	4.45
β = 2.5 (0.9938)	2.28	2.31	2.70	4.51	4.49	4.81
β = 3.0 (0.9987)	2.35	2.39	2.98	4.81	4.84	5.07
Scour Factors Based on Monte Carlo Results						
β = 0.5 (0.6915)	0.73	0.82	1.02	0.83	0.89	0.83
β = 1.0 (0.8413)	0.79	0.89	1.16	0.90	0.95	0.92
β = 1.5 (0.9332)	0.84	0.95	1.30	0.96	1.03	1.02
β = 2.0 (0.9772)	0.90	1.02	1.44	1.03	1.10	1.11
β = 2.5 (0.9938)	0.95	1.08	1.59	1.10	1.17	1.20
β = 3.0 (0.9987)	0.98	1.13	1.76	1.17	1.27	1.26
Scour Non-exceedance (ft) Based on Scour Mean and Standard Deviation						
β = 0.5 (0.6915)	1.76	1.74	1.76	3.43	3.40	3.34
β = 1.0 (0.8413)	1.89	1.88	1.96	3.67	3.65	3.69
β = 1.5 (0.9332)	2.02	2.02	2.17	3.92	3.90	4.04
β = 2.0 (0.9772)	2.15	2.16	2.37	4.16	4.15	4.40
β = 2.5 (0.9938)	2.28	2.30	2.58	4.41	4.40	4.75
β = 3.0 (0.9987)	2.41	2.44	2.78	4.65	4.65	5.10
Scour Factors Based on Scour Mean and Standard Deviation						
β = 0.5 (0.6915)	0.73	0.82	1.04	0.84	0.89	0.83
β = 1.0 (0.8413)	0.79	0.88	1.16	0.90	0.95	0.92
β = 1.5 (0.9332)	0.84	0.95	1.28	0.96	1.02	1.01
β = 2.0 (0.9772)	0.90	1.02	1.40	1.02	1.09	1.09
β = 2.5 (0.9938)	0.95	1.08	1.52	1.08	1.15	1.18
β = 3.0 (0.9987)	1.00	1.15	1.64	1.14	1.22	1.27

Table B.2	Small Bridge—Low Hydrologic Uncertainty—Medium Pier (2 ft)					
	Pier Scour (HEC-18)	Pier Scour (FDOT)	Contraction Scour	Total Scour (HEC-18)	Total Scour (FDOT)	Abutment Scour
Design scour (ft)	4.66	3.78	1.70	6.35	5.47	4.02
Expected scour (ft)	3.16	2.84	1.55	4.72	4.39	2.99
Bias	0.68	0.75	0.92	0.74	0.80	0.74
Std. dev. (ft)	0.51	0.50	0.41	0.67	0.65	0.71
COV	0.16	0.18	0.26	0.14	0.15	0.24
Design scour β	2.95	1.87	0.35	2.46	1.66	1.46
Non-exceedance	0.9984	0.9696	0.6356	0.9930	0.9517	0.9281
Scour Non-exceedance (ft) Based on Monte Carlo Results						
β = 0.5 (0.6915)	3.42	3.08	1.73	5.04	4.71	3.32
β = 1.0 (0.8413)	3.68	3.35	1.96	5.38	5.04	3.69
β = 1.5 (0.9332)	3.92	3.60	2.21	5.73	5.39	4.09
β = 2.0 (0.9772)	4.17	3.84	2.45	6.09	5.75	4.45
β = 2.5 (0.9938)	4.44	4.10	2.70	6.46	6.09	4.81
β = 3.0 (0.9987)	4.57	4.25	2.98	6.81	6.48	5.07
Scour Factors Based on Monte Carlo Results						
β = 0.5 (0.6915)	0.73	0.82	1.02	0.79	0.86	0.83
β = 1.0 (0.8413)	0.79	0.89	1.16	0.85	0.92	0.92
β = 1.5 (0.9332)	0.84	0.95	1.30	0.90	0.99	1.02
β = 2.0 (0.9772)	0.89	1.02	1.44	0.96	1.05	1.11
β = 2.5 (0.9938)	0.95	1.09	1.59	1.02	1.11	1.20
β = 3.0 (0.9987)	0.98	1.13	1.76	1.07	1.18	1.26
Scour Non-exceedance (ft) Based on Scour Mean and Standard Deviation						
β = 0.5 (0.6915)	3.42	3.09	1.76	5.05	4.72	3.34
β = 1.0 (0.8413)	3.67	3.34	1.96	5.38	5.04	3.69
β = 1.5 (0.9332)	3.92	3.59	2.17	5.72	5.37	4.04
β = 2.0 (0.9772)	4.17	3.84	2.37	6.05	5.69	4.40
β = 2.5 (0.9938)	4.43	4.09	2.58	6.38	6.02	4.75
β = 3.0 (0.9987)	4.68	4.34	2.78	6.71	6.35	5.10
Scour Factors Based on Scour Mean and Standard Deviation						
β = 0.5 (0.6915)	0.73	0.82	1.04	0.79	0.86	0.83
β = 1.0 (0.8413)	0.79	0.88	1.16	0.85	0.92	0.92
β = 1.5 (0.9332)	0.84	0.95	1.28	0.90	0.98	1.01
β = 2.0 (0.9772)	0.90	1.02	1.40	0.95	1.04	1.09
β = 2.5 (0.9938)	0.95	1.08	1.52	1.00	1.10	1.18
β = 3.0 (0.9987)	1.00	1.15	1.64	1.06	1.16	1.27

Table B.3	Small Bridge—Low Hydrologic Uncertainty—Large Pier (3 ft)					
	Pier Scour (HEC-18)	Pier Scour (FDOT)	Contraction Scour	Total Scour (HEC-18)	Total Scour (FDOT)	Abutment Scour
Design scour (ft)	6.06	5.17	1.70	7.76	6.87	4.02
Expected scour (ft)	4.12	3.89	1.55	5.67	5.44	2.99
Bias	0.68	0.75	0.92	0.73	0.79	0.74
Std. dev. (ft)	0.66	0.69	0.41	0.79	0.81	0.71
COV	0.16	0.18	0.26	0.14	0.15	0.24
Design scour β	2.95	1.87	0.35	2.63	1.77	1.46
Non-exceedance	0.9984	0.9695	0.6356	0.9958	0.9619	0.9281
Scour Non-exceedance (ft) Based on Monte Carlo Results						
β = 0.5 (0.6915)	4.45	4.22	1.73	6.06	5.83	3.32
β = 1.0 (0.8413)	4.79	4.58	1.96	6.47	6.24	3.69
β = 1.5 (0.9332)	5.10	4.93	2.21	6.86	6.67	4.09
β = 2.0 (0.9772)	5.42	5.27	2.45	7.29	7.09	4.45
β = 2.5 (0.9938)	5.77	5.61	2.70	7.70	7.51	4.81
β = 3.0 (0.9987)	5.96	5.82	2.98	8.12	7.82	5.07
Scour Factors Based on Monte Carlo Results						
β = 0.5 (0.6915)	0.73	0.82	1.02	0.78	0.85	0.83
β = 1.0 (0.8413)	0.79	0.89	1.16	0.83	0.91	0.92
β = 1.5 (0.9332)	0.84	0.95	1.30	0.89	0.97	1.02
β = 2.0 (0.9772)	0.90	1.02	1.44	0.94	1.03	1.11
β = 2.5 (0.9938)	0.95	1.09	1.59	0.99	1.09	1.20
β = 3.0 (0.9987)	0.98	1.12	1.76	1.05	1.14	1.26
Scour Non-exceedance (ft) Based on Scour Mean and Standard Deviation						
β = 0.5 (0.6915)	4.45	4.23	1.76	6.07	5.84	3.34
β = 1.0 (0.8413)	4.78	4.57	1.96	6.46	6.25	3.69
β = 1.5 (0.9332)	5.10	4.92	2.17	6.86	6.65	4.04
β = 2.0 (0.9772)	5.43	5.26	2.37	7.26	7.05	4.40
β = 2.5 (0.9938)	5.76	5.60	2.58	7.65	7.46	4.75
β = 3.0 (0.9987)	6.09	5.95	2.78	8.05	7.86	5.10
Scour Factors Based on Scour Mean and Standard Deviation						
β = 0.5 (0.6915)	0.73	0.82	1.04	0.78	0.85	0.83
β = 1.0 (0.8413)	0.79	0.88	1.16	0.83	0.91	0.92
β = 1.5 (0.9332)	0.84	0.95	1.28	0.88	0.97	1.01
β = 2.0 (0.9772)	0.90	1.02	1.40	0.94	1.03	1.09
β = 2.5 (0.9938)	0.95	1.08	1.52	0.99	1.09	1.18
β = 3.0 (0.9987)	1.01	1.15	1.64	1.04	1.14	1.27

Table B.4	Small Bridge—Medium Hydrologic Uncertainty—Small Pier (1 ft)					
	Pier Scour (HEC-18)	Pier Scour (FDOT)	Contraction Scour	Total Scour (HEC-18)	Total Scour (FDOT)	Abutment Scour
Design scour (ft)	2.40	2.13	1.70	4.10	3.82	4.02
Expected scour (ft)	1.63	1.60	1.58	3.21	3.17	2.99
Bias	0.68	0.75	0.93	0.78	0.83	0.74
Std. dev. (ft)	0.26	0.29	0.46	0.53	0.55	0.73
COV	0.16	0.18	0.29	0.17	0.17	0.24
Design scour β	2.96	1.84	0.26	1.67	1.18	1.42
Non-exceedance	0.9985	0.9674	0.6020	0.9525	0.8819	0.9217
Scour Non-exceedance (ft) Based on Monte Carlo Results						
β = 0.5 (0.6915)	1.77	1.74	1.78	3.45	3.42	3.33
β = 1.0 (0.8413)	1.90	1.89	2.04	3.74	3.72	3.72
β = 1.5 (0.9332)	2.02	2.03	2.32	4.04	4.04	4.10
β = 2.0 (0.9772)	2.14	2.18	2.63	4.37	4.35	4.48
β = 2.5 (0.9938)	2.26	2.31	2.95	4.68	4.68	4.94
β = 3.0 (0.9987)	2.35	2.40	3.29	4.94	5.02	5.34
Scour Factors Based on Monte Carlo Results						
β = 0.5 (0.6915)	0.74	0.82	1.05	0.84	0.90	0.83
β = 1.0 (0.8413)	0.79	0.89	1.20	0.91	0.97	0.93
β = 1.5 (0.9332)	0.84	0.95	1.37	0.99	1.06	1.02
β = 2.0 (0.9772)	0.89	1.02	1.55	1.07	1.14	1.11
β = 2.5 (0.9938)	0.94	1.09	1.74	1.14	1.22	1.23
β = 3.0 (0.9987)	0.98	1.13	1.94	1.21	1.31	1.33
Scour Non-exceedance (ft) Based on Scour Mean and Standard Deviation						
β = 0.5 (0.6915)	1.76	1.74	1.81	3.47	3.45	3.35
β = 1.0 (0.8413)	1.89	1.88	2.04	3.74	3.72	3.72
β = 1.5 (0.9332)	2.02	2.03	2.27	4.01	4.00	4.08
β = 2.0 (0.9772)	2.15	2.17	2.50	4.27	4.27	4.44
β = 2.5 (0.9938)	2.28	2.32	2.74	4.54	4.54	4.81
β = 3.0 (0.9987)	2.41	2.46	2.97	4.80	4.82	5.17
Scour Factors Based on Scour Mean and Standard Deviation						
β = 0.5 (0.6915)	0.73	0.82	1.07	0.85	0.90	0.83
β = 1.0 (0.8413)	0.79	0.89	1.20	0.91	0.97	0.92
β = 1.5 (0.9332)	0.84	0.95	1.34	0.98	1.05	1.02
β = 2.0 (0.9772)	0.90	1.02	1.48	1.04	1.12	1.11
β = 2.5 (0.9938)	0.95	1.09	1.61	1.11	1.19	1.20
β = 3.0 (0.9987)	1.00	1.16	1.75	1.17	1.26	1.29

Table B.5	Small Bridge—Medium Hydrologic Uncertainty—Medium Pier (2 ft)					
	Pier Scour (HEC-18)	Pier Scour (FDOT)	Contraction Scour	Total Scour (HEC-18)	Total Scour (FDOT)	Abutment Scour
Design scour (ft)	4.66	3.78	1.70	6.35	5.47	4.02
Expected scour (ft)	3.16	2.84	1.58	4.74	4.41	2.99
Bias	0.68	0.75	0.93	0.75	0.81	0.74
Std. dev. (ft)	0.51	0.51	0.46	0.71	0.70	0.73
COV	0.16	0.18	0.29	0.15	0.16	0.24
Design scour β	2.95	1.84	0.26	2.27	1.52	1.42
Non-exceedance	0.9984	0.9673	0.6020	0.9884	0.9352	0.9217
Scour Non-exceedance (ft) Based on Monte Carlo Results						
β = 0.5 (0.6915)	3.42	3.10	1.78	5.08	4.75	3.33
β = 1.0 (0.8413)	3.68	3.35	2.04	5.45	5.12	3.72
β = 1.5 (0.9332)	3.93	3.61	2.32	5.84	5.50	4.10
β = 2.0 (0.9772)	4.16	3.87	2.63	6.22	5.87	4.48
β = 2.5 (0.9938)	4.37	4.11	2.95	6.58	6.22	4.94
β = 3.0 (0.9987)	4.57	4.27	3.29	6.91	6.65	5.34
Scour Factors Based on Monte Carlo Results						
β = 0.5 (0.6915)	0.73	0.82	1.05	0.80	0.87	0.83
β = 1.0 (0.8413)	0.79	0.89	1.20	0.86	0.93	0.93
β = 1.5 (0.9332)	0.84	0.95	1.37	0.92	1.01	1.02
β = 2.0 (0.9772)	0.89	1.02	1.55	0.98	1.07	1.11
β = 2.5 (0.9938)	0.94	1.09	1.74	1.04	1.14	1.23
β = 3.0 (0.9987)	0.98	1.13	1.94	1.09	1.21	1.33
Scour Non-exceedance (ft) Based on Scour Mean and Standard Deviation						
β = 0.5 (0.6915)	3.42	3.09	1.81	5.09	4.76	3.35
β = 1.0 (0.8413)	3.67	3.35	2.04	5.45	5.11	3.72
β = 1.5 (0.9332)	3.92	3.60	2.27	5.80	5.46	4.08
β = 2.0 (0.9772)	4.18	3.86	2.50	6.16	5.81	4.44
β = 2.5 (0.9938)	4.43	4.11	2.74	6.52	6.16	4.81
β = 3.0 (0.9987)	4.68	4.37	2.97	6.87	6.51	5.17
Scour Factors Based on Scour Mean and Standard Deviation						
β = 0.5 (0.6915)	0.73	0.82	1.07	0.80	0.87	0.83
β = 1.0 (0.8413)	0.79	0.89	1.20	0.86	0.93	0.92
β = 1.5 (0.9332)	0.84	0.95	1.34	0.91	1.00	1.02
β = 2.0 (0.9772)	0.90	1.02	1.48	0.97	1.06	1.11
β = 2.5 (0.9938)	0.95	1.09	1.61	1.03	1.13	1.20
β = 3.0 (0.9987)	1.01	1.16	1.75	1.08	1.19	1.29

Table B.6	Small Bridge—Medium Hydrologic Uncertainty—Large Pier (3 ft)					
	Pier Scour (HEC-18)	Pier Scour (FDOT)	Contraction Scour	Total Scour (HEC-18)	Total Scour (FDOT)	Abutment Scour
Design scour (ft)	6.06	5.17	1.70	7.76	6.87	4.02
Expected scour (ft)	4.12	3.88	1.58	5.70	5.46	2.99
Bias	0.68	0.75	0.93	0.73	0.79	0.74
Std. dev. (ft)	0.66	0.70	0.46	0.84	0.86	0.73
COV	0.16	0.18	0.29	0.15	0.16	0.24
Design scour β	2.94	1.84	0.26	2.47	1.65	1.42
Non-exceedance	0.9983	0.9672	0.6020	0.9932	0.9500	0.9217
Scour Non-exceedance (ft) Based on Monte Carlo Results						
β = 0.5 (0.6915)	4.46	4.24	1.78	6.10	5.88	3.33
β = 1.0 (0.8413)	4.79	4.59	2.04	6.53	6.32	3.72
β = 1.5 (0.9332)	5.12	4.94	2.32	6.98	6.77	4.10
β = 2.0 (0.9772)	5.42	5.31	2.63	7.42	7.19	4.48
β = 2.5 (0.9938)	5.70	5.62	2.95	7.84	7.68	4.94
β = 3.0 (0.9987)	5.96	5.84	3.29	8.28	8.09	5.34
Scour Factors Based on Monte Carlo Results						
β = 0.5 (0.6915)	0.74	0.82	1.05	0.79	0.86	0.83
β = 1.0 (0.8413)	0.79	0.89	1.20	0.84	0.92	0.93
β = 1.5 (0.9332)	0.85	0.95	1.37	0.90	0.99	1.02
β = 2.0 (0.9772)	0.89	1.03	1.55	0.96	1.05	1.11
β = 2.5 (0.9938)	0.94	1.09	1.74	1.01	1.12	1.23
β = 3.0 (0.9987)	0.98	1.13	1.94	1.07	1.18	1.33
Scour Non-exceedance (ft) Based on Scour Mean and Standard Deviation						
β = 0.5 (0.6915)	4.45	4.23	1.81	6.11	5.89	3.35
β = 1.0 (0.8413)	4.78	4.58	2.04	6.53	6.32	3.72
β = 1.5 (0.9332)	5.11	4.93	2.27	6.95	6.74	4.08
β = 2.0 (0.9772)	5.44	5.28	2.50	7.37	7.17	4.44
β = 2.5 (0.9938)	5.77	5.63	2.74	7.79	7.60	4.81
β = 3.0 (0.9987)	6.10	5.98	2.97	8.20	8.03	5.17
Scour Factors Based on Scour Mean and Standard Deviation						
β = 0.5 (0.6915)	0.73	0.82	1.07	0.79	0.86	0.83
β = 1.0 (0.8413)	0.79	0.89	1.20	0.84	0.92	0.92
β = 1.5 (0.9332)	0.84	0.95	1.34	0.90	0.98	1.02
β = 2.0 (0.9772)	0.90	1.02	1.48	0.95	1.04	1.11
β = 2.5 (0.9938)	0.95	1.09	1.61	1.00	1.11	1.20
β = 3.0 (0.9987)	1.01	1.16	1.75	1.06	1.17	1.29

Table B.7	Small Bridge—High Hydrologic Uncertainty—Small Pier (1 ft)					
	Pier Scour (HEC-18)	Pier Scour (FDOT)	Contraction Scour	Total Scour (HEC-18)	Total Scour (FDOT)	Abutment Scour
Design scour (ft)	2.40	2.13	1.70	4.10	3.82	4.02
Expected scour (ft)	1.63	1.60	1.58	3.21	3.18	3.01
Bias	0.68	0.75	0.93	0.78	0.83	0.75
Std. dev. (ft)	0.26	0.28	0.55	0.61	0.63	0.78
COV	0.16	0.18	0.35	0.19	0.20	0.26
Design scour β	2.99	1.87	0.20	1.45	1.03	1.29
Non-exceedance	0.9986	0.9690	0.5806	0.9259	0.8481	0.9013
Scour Non-exceedance (ft) Based on Monte Carlo Results						
β = 0.5 (0.6915)	1.76	1.74	1.80	3.47	3.44	3.37
β = 1.0 (0.8413)	1.89	1.88	2.12	3.81	3.80	3.78
β = 1.5 (0.9332)	2.02	2.03	2.47	4.20	4.17	4.23
β = 2.0 (0.9772)	2.14	2.16	2.89	4.57	4.58	4.71
β = 2.5 (0.9938)	2.26	2.30	3.30	5.04	5.05	5.15
β = 3.0 (0.9987)	2.35	2.41	3.82	5.53	5.56	5.69
Scour Factors Based on Monte Carlo Results						
β = 0.5 (0.6915)	0.73	0.82	1.06	0.85	0.90	0.84
β = 1.0 (0.8413)	0.79	0.89	1.25	0.93	0.99	0.94
β = 1.5 (0.9332)	0.84	0.96	1.46	1.02	1.09	1.05
β = 2.0 (0.9772)	0.89	1.02	1.70	1.11	1.20	1.17
β = 2.5 (0.9938)	0.94	1.08	1.95	1.23	1.32	1.28
β = 3.0 (0.9987)	0.98	1.13	2.25	1.35	1.45	1.42
Scour Non-exceedance (ft) Based on Scour Mean and Standard Deviation						
β = 0.5 (0.6915)	1.76	1.74	1.86	3.52	3.49	3.40
β = 1.0 (0.8413)	1.89	1.88	2.13	3.82	3.81	3.79
β = 1.5 (0.9332)	2.02	2.02	2.41	4.13	4.12	4.18
β = 2.0 (0.9772)	2.15	2.16	2.68	4.43	4.43	4.57
β = 2.5 (0.9938)	2.27	2.31	2.96	4.74	4.74	4.96
β = 3.0 (0.9987)	2.40	2.45	3.24	5.04	5.06	5.35
Scour Factors Based on Scour Mean and Standard Deviation						
β = 0.5 (0.6915)	0.73	0.82	1.10	0.86	0.91	0.85
β = 1.0 (0.8413)	0.79	0.88	1.26	0.93	1.00	0.94
β = 1.5 (0.9332)	0.84	0.95	1.42	1.01	1.08	1.04
β = 2.0 (0.9772)	0.89	1.02	1.58	1.08	1.16	1.14
β = 2.5 (0.9938)	0.95	1.08	1.75	1.16	1.24	1.24
β = 3.0 (0.9987)	1.00	1.15	1.91	1.23	1.32	1.33

Table B.8	Small Bridge—High Hydrologic Uncertainty—Medium Pier (2 ft)					
	Pier Scour (HEC-18)	Pier Scour (FDOT)	Contraction Scour	Total Scour (HEC-18)	Total Scour (FDOT)	Abutment Scour
Design scour (ft)	4.66	3.78	1.70	6.35	5.47	4.02
Expected scour (ft)	3.16	2.83	1.58	4.74	4.42	3.01
Bias	0.68	0.75	0.93	0.75	0.81	0.75
Std. dev. (ft)	0.51	0.51	0.55	0.79	0.77	0.78
COV	0.16	0.18	0.35	0.17	0.17	0.26
Design scour β	2.97	1.86	0.20	2.05	1.38	1.29
Non-exceedance	0.9985	0.9688	0.5806	0.9797	0.9154	0.9013
Scour Non-exceedance (ft) Based on Monte Carlo Results						
β = 0.5 (0.6915)	3.41	3.09	1.80	5.10	4.77	3.37
β = 1.0 (0.8413)	3.67	3.35	2.12	5.52	5.17	3.78
β = 1.5 (0.9332)	3.93	3.61	2.47	5.98	5.62	4.23
β = 2.0 (0.9772)	4.17	3.86	2.89	6.41	6.07	4.71
β = 2.5 (0.9938)	4.40	4.09	3.30	6.94	6.53	5.15
β = 3.0 (0.9987)	4.61	4.27	3.82	7.49	7.15	5.69
Scour Factors Based on Monte Carlo Results						
β = 0.5 (0.6915)	0.73	0.82	1.06	0.80	0.87	0.84
β = 1.0 (0.8413)	0.79	0.89	1.25	0.87	0.95	0.94
β = 1.5 (0.9332)	0.84	0.96	1.46	0.94	1.03	1.05
β = 2.0 (0.9772)	0.90	1.02	1.70	1.01	1.11	1.17
β = 2.5 (0.9938)	0.95	1.08	1.95	1.09	1.19	1.28
β = 3.0 (0.9987)	0.99	1.13	2.25	1.18	1.31	1.42
Scour Non-exceedance (ft) Based on Scour Mean and Standard Deviation						
β = 0.5 (0.6915)	3.41	3.09	1.86	5.13	4.80	3.40
β = 1.0 (0.8413)	3.66	3.34	2.13	5.53	5.19	3.79
β = 1.5 (0.9332)	3.91	3.59	2.41	5.92	5.57	4.18
β = 2.0 (0.9772)	4.17	3.85	2.68	6.32	5.95	4.57
β = 2.5 (0.9938)	4.42	4.10	2.96	6.71	6.34	4.96
β = 3.0 (0.9987)	4.67	4.35	3.24	7.10	6.72	5.35
Scour Factors Based on Scour Mean and Standard Deviation						
β = 0.5 (0.6915)	0.73	0.82	1.10	0.81	0.88	0.85
β = 1.0 (0.8413)	0.79	0.88	1.26	0.87	0.95	0.94
β = 1.5 (0.9332)	0.84	0.95	1.42	0.93	1.02	1.04
β = 2.0 (0.9772)	0.89	1.02	1.58	0.99	1.09	1.14
β = 2.5 (0.9938)	0.95	1.09	1.75	1.06	1.16	1.24
β = 3.0 (0.9987)	1.00	1.15	1.91	1.12	1.23	1.33

Table B.9	Small Bridge—High Hydrologic Uncertainty—Large Pier (3 ft)					
	Pier Scour (HEC-18)	Pier Scour (FDOT)	Contraction Scour	Total Scour (HEC-18)	Total Scour (FDOT)	Abutment Scour
Design scour (ft)	6.06	5.17	1.70	7.76	6.87	4.02
Expected scour (ft)	4.12	3.88	1.58	5.70	5.46	3.01
Bias	0.68	0.75	0.93	0.73	0.80	0.75
Std. dev. (ft)	0.66	0.70	0.55	0.91	0.92	0.78
COV	0.16	0.18	0.35	0.16	0.17	0.26
Design scour β	2.94	1.86	0.20	2.25	1.53	1.29
Non-exceedance	0.9983	0.9684	0.5806	0.9878	0.9369	0.9013
Scour Non-exceedance (ft) Based on Monte Carlo Results						
β = 0.5 (0.6915)	4.45	4.23	1.80	6.12	5.90	3.37
β = 1.0 (0.8413)	4.78	4.58	2.12	6.61	6.38	3.78
β = 1.5 (0.9332)	5.13	4.94	2.47	7.12	6.88	4.23
β = 2.0 (0.9772)	5.44	5.29	2.89	7.64	7.38	4.71
β = 2.5 (0.9938)	5.76	5.61	3.30	8.24	7.93	5.15
β = 3.0 (0.9987)	6.02	5.85	3.82	8.85	8.55	5.69
Scour Factors Based on Monte Carlo Results						
β = 0.5 (0.6915)	0.73	0.82	1.06	0.79	0.86	0.84
β = 1.0 (0.8413)	0.79	0.89	1.25	0.85	0.93	0.94
β = 1.5 (0.9332)	0.85	0.96	1.46	0.92	1.00	1.05
β = 2.0 (0.9772)	0.90	1.02	1.70	0.98	1.07	1.17
β = 2.5 (0.9938)	0.95	1.09	1.95	1.06	1.15	1.28
β = 3.0 (0.9987)	0.99	1.13	2.25	1.14	1.24	1.42
Scour Non-exceedance (ft) Based on Scour Mean and Standard Deviation						
β = 0.5 (0.6915)	4.45	4.23	1.86	6.16	5.92	3.40
β = 1.0 (0.8413)	4.78	4.58	2.13	6.61	6.38	3.79
β = 1.5 (0.9332)	5.11	4.92	2.41	7.07	6.84	4.18
β = 2.0 (0.9772)	5.44	5.27	2.68	7.53	7.30	4.57
β = 2.5 (0.9938)	5.77	5.62	2.96	7.98	7.76	4.96
β = 3.0 (0.9987)	6.10	5.97	3.24	8.44	8.22	5.35
Scour Factors Based on Scour Mean and Standard Deviation						
β = 0.5 (0.6915)	0.73	0.82	1.10	0.79	0.86	0.85
β = 1.0 (0.8413)	0.79	0.88	1.26	0.85	0.93	0.94
β = 1.5 (0.9332)	0.84	0.95	1.42	0.91	1.00	1.04
β = 2.0 (0.9772)	0.90	1.02	1.58	0.97	1.06	1.14
β = 2.5 (0.9938)	0.95	1.09	1.75	1.03	1.13	1.24
β = 3.0 (0.9987)	1.01	1.15	1.91	1.09	1.20	1.33

Table B.10	Medium Bridge—Low Hydrologic Uncertainty—Small Pier (1.5 ft)					
	Pier Scour (HEC-18)	**Pier Scour (FDOT)**	**Contraction Scour**	**Total Scour (HEC-18)**	**Total Scour (FDOT)**	**Abutment Scour**
Design scour (ft)	3.60	3.19	8.02	11.62	11.21	15.12
Expected scour (ft)	2.45	2.39	7.36	9.81	9.75	11.23
Bias	0.68	0.75	0.92	0.84	0.87	0.74
Std. dev. (ft)	0.39	0.43	2.21	2.25	2.26	2.88
COV	0.16	0.18	0.30	0.23	0.23	0.26
Design scour β	2.95	1.85	0.30	0.81	0.65	1.35
Non-exceedance	0.9984	0.9676	0.6170	0.7897	0.7406	0.9113
Scour Non-exceedance (ft) Based on Monte Carlo Results						
β = 0.5 (0.6915)	2.65	2.61	8.34	10.80	10.78	12.58
β = 1.0 (0.8413)	2.84	2.84	9.59	12.10	12.01	14.09
β = 1.5 (0.9332)	3.04	3.04	10.84	13.31	13.28	15.66
β = 2.0 (0.9772)	3.23	3.26	12.30	14.75	14.76	17.31
β = 2.5 (0.9938)	3.43	3.46	13.65	16.17	16.15	19.27
β = 3.0 (0.9987)	3.54	3.61	15.15	17.50	17.65	20.87
Scour Factors Based on Monte Carlo Results						
β = 0.5 (0.6915)	0.73	0.82	1.04	0.93	0.96	0.83
β = 1.0 (0.8413)	0.79	0.89	1.20	1.04	1.07	0.93
β = 1.5 (0.9332)	0.85	0.95	1.35	1.15	1.18	1.04
β = 2.0 (0.9772)	0.90	1.02	1.53	1.27	1.32	1.15
β = 2.5 (0.9938)	0.95	1.08	1.70	1.39	1.44	1.27
β = 3.0 (0.9987)	0.98	1.13	1.89	1.51	1.57	1.38
Scour Non-exceedance (ft) Based on Scour Mean and Standard Deviation						
β = 0.5 (0.6915)	2.64	2.61	8.46	10.93	10.88	12.67
β = 1.0 (0.8413)	2.84	2.83	9.57	12.05	12.01	14.11
β = 1.5 (0.9332)	3.04	3.04	10.68	13.18	13.14	15.55
β = 2.0 (0.9772)	3.23	3.26	11.78	14.30	14.27	17.00
β = 2.5 (0.9938)	3.43	3.47	12.89	15.42	15.40	18.44
β = 3.0 (0.9987)	3.62	3.69	14.00	16.55	16.52	19.88
Scour Factors Based on Scour Mean and Standard Deviation						
β = 0.5 (0.6915)	0.73	0.82	1.06	0.94	0.97	0.84
β = 1.0 (0.8413)	0.79	0.89	1.19	1.04	1.07	0.93
β = 1.5 (0.9332)	0.84	0.95	1.33	1.13	1.17	1.03
β = 2.0 (0.9772)	0.90	1.02	1.47	1.23	1.27	1.12
β = 2.5 (0.9938)	0.95	1.09	1.61	1.33	1.37	1.22
β = 3.0 (0.9987)	1.01	1.16	1.75	1.42	1.47	1.32

Table B.11	Medium Bridge—Low Hydrologic Uncertainty—Medium Pier (3 ft)					
	Pier Scour (HEC-18)	Pier Scour (FDOT)	Contraction Scour	Total Scour (HEC-18)	Total Scour (FDOT)	Abutment Scour
Design scour (ft)	7.20	5.94	8.02	15.22	13.95	15.12
Expected scour (ft)	4.90	4.45	7.36	12.26	11.81	11.23
Bias	0.68	0.75	0.92	0.81	0.85	0.74
Std. dev. (ft)	0.78	0.81	2.21	2.34	2.37	2.88
COV	0.16	0.18	0.30	0.19	0.20	0.26
Design scour β	2.95	1.84	0.30	1.26	0.90	1.35
Non-exceedance	0.9984	0.9672	0.6170	0.8967	0.8168	0.9113
Scour Non-exceedance (ft) Based on Monte Carlo Results						
β = 0.5 (0.6915)	5.29	4.87	8.34	13.31	12.90	12.58
β = 1.0 (0.8413)	5.68	5.27	9.59	14.62	14.20	14.09
β = 1.5 (0.9332)	6.09	5.66	10.84	15.94	15.50	15.66
β = 2.0 (0.9772)	6.46	6.06	12.30	17.42	17.02	17.31
β = 2.5 (0.9938)	6.86	6.45	13.65	18.80	18.47	19.27
β = 3.0 (0.9987)	7.08	6.71	15.15	20.33	20.18	20.87
Scour Factors Based on Monte Carlo Results						
β = 0.5 (0.6915)	0.73	0.82	1.04	0.87	0.92	0.83
β = 1.0 (0.8413)	0.79	0.89	1.20	0.96	1.02	0.93
β = 1.5 (0.9332)	0.85	0.95	1.35	1.05	1.11	1.04
β = 2.0 (0.9772)	0.90	1.02	1.53	1.14	1.22	1.15
β = 2.5 (0.9938)	0.95	1.09	1.70	1.24	1.32	1.27
β = 3.0 (0.9987)	0.98	1.13	1.89	1.34	1.45	1.38
Scour Non-exceedance (ft) Based on Scour Mean and Standard Deviation						
β = 0.5 (0.6915)	5.29	4.86	8.46	13.43	12.99	12.67
β = 1.0 (0.8413)	5.68	5.26	9.57	14.60	14.18	14.11
β = 1.5 (0.9332)	6.07	5.66	10.68	15.77	15.37	15.55
β = 2.0 (0.9772)	6.46	6.06	11.78	16.94	16.55	17.00
β = 2.5 (0.9938)	6.85	6.47	12.89	18.12	17.74	18.44
β = 3.0 (0.9987)	7.24	6.87	14.00	19.29	18.93	19.88
Scour Factors Based on Scour Mean and Standard Deviation						
β = 0.5 (0.6915)	0.73	0.82	1.06	0.88	0.93	0.84
β = 1.0 (0.8413)	0.79	0.89	1.19	0.96	1.02	0.93
β = 1.5 (0.9332)	0.84	0.95	1.33	1.04	1.10	1.03
β = 2.0 (0.9772)	0.90	1.02	1.47	1.11	1.19	1.12
β = 2.5 (0.9938)	0.95	1.09	1.61	1.19	1.27	1.22
β = 3.0 (0.9987)	1.01	1.16	1.75	1.27	1.36	1.32

Table B.12	Medium Bridge—Low Hydrologic Uncertainty—Large Pier (4.5 ft)					
	Pier Scour (HEC-18)	Pier Scour (FDOT)	Contraction Scour	Total Scour (HEC-18)	Total Scour (FDOT)	Abutment Scour
Design scour (ft)	10.35	8.44	8.02	18.37	16.45	15.12
Expected scour (ft)	7.06	6.33	7.36	14.41	13.69	11.23
Bias	0.68	0.75	0.92	0.78	0.83	0.74
Std. dev. (ft)	1.14	1.15	2.21	2.57	2.53	2.88
COV	0.16	0.18	0.30	0.18	0.18	0.26
Design scour β	2.89	1.84	0.30	1.54	1.09	1.35
Non-exceedance	0.9981	0.9670	0.6170	0.9380	0.8632	0.9113
Scour Non-exceedance (ft) Based on Monte Carlo Results						
$\beta = 0.5$ (0.6915)	7.62	6.92	8.34	15.59	14.87	12.58
$\beta = 1.0$ (0.8413)	8.21	7.49	9.59	17.00	16.22	14.09
$\beta = 1.5$ (0.9332)	8.80	8.05	10.84	18.40	17.59	15.66
$\beta = 2.0$ (0.9772)	9.34	8.63	12.30	20.05	19.15	17.31
$\beta = 2.5$ (0.9938)	9.90	9.14	13.65	21.50	20.70	19.27
$\beta = 3.0$ (0.9987)	10.33	9.55	15.15	23.11	22.34	20.87
Scour Factors Based on Monte Carlo Results						
$\beta = 0.5$ (0.6915)	0.74	0.82	1.04	0.85	0.90	0.83
$\beta = 1.0$ (0.8413)	0.79	0.89	1.20	0.93	0.99	0.93
$\beta = 1.5$ (0.9332)	0.85	0.95	1.35	1.00	1.07	1.04
$\beta = 2.0$ (0.9772)	0.90	1.02	1.53	1.09	1.16	1.15
$\beta = 2.5$ (0.9938)	0.96	1.08	1.70	1.17	1.26	1.27
$\beta = 3.0$ (0.9987)	1.00	1.13	1.89	1.26	1.36	1.38
Scour Non-exceedance (ft) Based on Scour Mean and Standard Deviation						
$\beta = 0.5$ (0.6915)	7.63	6.90	8.46	15.70	14.95	12.67
$\beta = 1.0$ (0.8413)	8.20	7.48	9.57	16.98	16.21	14.11
$\beta = 1.5$ (0.9332)	8.77	8.05	10.68	18.27	17.48	15.55
$\beta = 2.0$ (0.9772)	9.34	8.62	11.78	19.56	18.74	17.00
$\beta = 2.5$ (0.9938)	9.91	9.20	12.89	20.84	20.00	18.44
$\beta = 3.0$ (0.9987)	10.48	9.77	14.00	22.13	21.27	19.88
Scour Factors Based on Scour Mean and Standard Deviation						
$\beta = 0.5$ (0.6915)	0.74	0.82	1.06	0.85	0.91	0.84
$\beta = 1.0$ (0.8413)	0.79	0.89	1.19	0.92	0.99	0.93
$\beta = 1.5$ (0.9332)	0.85	0.95	1.33	0.99	1.06	1.03
$\beta = 2.0$ (0.9772)	0.90	1.02	1.47	1.06	1.14	1.12
$\beta = 2.5$ (0.9938)	0.96	1.09	1.61	1.13	1.22	1.22
$\beta = 3.0$ (0.9987)	1.01	1.16	1.75	1.20	1.29	1.32

Table B.13	Medium Bridge—Medium Hydrologic Uncertainty—Small Pier (1.5 ft)					
	Pier Scour (HEC-18)	Pier Scour (FDOT)	Contraction Scour	Total Scour (HEC-18)	Total Scour (FDOT)	Abutment Scour
Design scour (ft)	3.60	3.19	8.02	11.62	11.21	15.12
Expected scour (ft)	2.45	2.39	7.42	9.87	9.81	11.35
Bias	0.68	0.75	0.93	0.85	0.88	0.75
Std. dev. (ft)	0.39	0.42	2.74	2.78	2.78	3.18
COV	0.16	0.18	0.37	0.28	0.28	0.28
Design scour β	2.99	1.90	0.22	0.63	0.50	1.18
Non-exceedance	0.9986	0.9713	0.5857	0.7353	0.6923	0.8818
Scour Non-exceedance (ft) Based on Monte Carlo Results						
β = 0.5 (0.6915)	2.64	2.60	8.60	11.07	11.02	12.77
β = 1.0 (0.8413)	2.84	2.82	10.17	12.66	12.61	14.55
β = 1.5 (0.9332)	3.03	3.03	11.89	14.36	14.31	16.38
β = 2.0 (0.9772)	3.22	3.23	13.56	16.08	16.04	18.21
β = 2.5 (0.9938)	3.37	3.41	15.50	18.02	17.89	20.54
β = 3.0 (0.9987)	3.48	3.56	17.24	19.79	19.79	22.31
Scour Factors Based on Monte Carlo Results						
β = 0.5 (0.6915)	0.73	0.82	1.07	0.95	0.98	0.84
β = 1.0 (0.8413)	0.79	0.88	1.27	1.09	1.13	0.96
β = 1.5 (0.9332)	0.84	0.95	1.48	1.24	1.28	1.08
β = 2.0 (0.9772)	0.89	1.01	1.69	1.38	1.43	1.20
β = 2.5 (0.9938)	0.94	1.07	1.93	1.55	1.60	1.36
β = 3.0 (0.9987)	0.97	1.12	2.15	1.70	1.77	1.48
Scour Non-exceedance (ft) Based on Scour Mean and Standard Deviation						
β = 0.5 (0.6915)	2.64	2.60	8.79	11.26	11.20	12.94
β = 1.0 (0.8413)	2.83	2.81	10.16	12.65	12.59	14.53
β = 1.5 (0.9332)	3.02	3.02	11.53	14.03	13.98	16.12
β = 2.0 (0.9772)	3.22	3.23	12.91	15.42	15.37	17.72
β = 2.5 (0.9938)	3.41	3.45	14.28	16.81	16.76	19.31
β = 3.0 (0.9987)	3.60	3.66	15.65	18.20	18.15	20.90
Scour Factors Based on Scour Mean and Standard Deviation						
β = 0.5 (0.6915)	0.73	0.81	1.10	0.97	1.00	0.86
β = 1.0 (0.8413)	0.79	0.88	1.27	1.09	1.12	0.96
β = 1.5 (0.9332)	0.84	0.95	1.44	1.21	1.25	1.07
β = 2.0 (0.9772)	0.89	1.01	1.61	1.33	1.37	1.17
β = 2.5 (0.9938)	0.95	1.08	1.78	1.45	1.50	1.28
β = 3.0 (0.9987)	1.00	1.15	1.95	1.57	1.62	1.38

Table B.14	Medium Bridge—Medium Hydrologic Uncertainty—Medium Pier (3 ft)					
	Pier Scour (HEC-18)	Pier Scour (FDOT)	Contraction Scour	Total Scour (HEC-18)	Total Scour (FDOT)	Abutment Scour
Design scour (ft)	7.20	5.94	8.02	15.22	13.95	15.12
Expected scour (ft)	4.89	4.45	7.42	12.31	11.87	11.35
Bias	0.68	0.75	0.93	0.81	0.85	0.75
Std. dev. (ft)	0.77	0.79	2.74	2.86	2.89	3.18
COV	0.16	0.18	0.37	0.23	0.24	0.28
Design scour β	2.99	1.89	0.22	1.01	0.72	1.18
Non-exceedance	0.9986	0.9706	0.5857	0.8444	0.7648	0.8818
Scour Non-exceedance (ft) Based on Monte Carlo Results						
β = 0.5 (0.6915)	5.29	4.85	8.60	13.58	13.13	12.77
β = 1.0 (0.8413)	5.68	5.24	10.17	15.18	14.76	14.55
β = 1.5 (0.9332)	6.05	5.63	11.89	16.90	16.47	16.38
β = 2.0 (0.9772)	6.44	6.01	13.56	18.69	18.28	18.21
β = 2.5 (0.9938)	6.73	6.37	15.50	20.73	20.21	20.54
β = 3.0 (0.9987)	6.96	6.62	17.24	22.54	22.19	22.31
Scour Factors Based on Monte Carlo Results						
β = 0.5 (0.6915)	0.73	0.82	1.07	0.89	0.94	0.84
β = 1.0 (0.8413)	0.79	0.88	1.27	1.00	1.06	0.96
β = 1.5 (0.9332)	0.84	0.95	1.48	1.11	1.18	1.08
β = 2.0 (0.9772)	0.89	1.01	1.69	1.23	1.31	1.20
β = 2.5 (0.9938)	0.94	1.07	1.93	1.36	1.45	1.36
β = 3.0 (0.9987)	0.97	1.11	2.15	1.48	1.59	1.48
Scour Non-exceedance (ft) Based on Scour Mean and Standard Deviation						
β = 0.5 (0.6915)	5.28	4.84	8.79	13.75	13.31	12.94
β = 1.0 (0.8413)	5.66	5.23	10.16	15.18	14.75	14.53
β = 1.5 (0.9332)	6.05	5.63	11.53	16.61	16.20	16.12
β = 2.0 (0.9772)	6.43	6.02	12.91	18.04	17.64	17.72
β = 2.5 (0.9938)	6.82	6.42	14.28	19.48	19.08	19.31
β = 3.0 (0.9987)	7.20	6.81	15.65	20.91	20.53	20.90
Scour Factors Based on Scour Mean and Standard Deviation						
β = 0.5 (0.6915)	0.73	0.82	1.10	0.90	0.95	0.86
β = 1.0 (0.8413)	0.79	0.88	1.27	1.00	1.06	0.96
β = 1.5 (0.9332)	0.84	0.95	1.44	1.09	1.16	1.07
β = 2.0 (0.9772)	0.89	1.01	1.61	1.19	1.26	1.17
β = 2.5 (0.9938)	0.95	1.08	1.78	1.28	1.37	1.28
β = 3.0 (0.9987)	1.00	1.15	1.95	1.37	1.47	1.38

Table B.15	Medium Bridge—Medium Hydrologic Uncertainty—Large Pier (4.5 ft)					
	Pier Scour (HEC-18)	Pier Scour (FDOT)	Contraction Scour	Total Scour (HEC-18)	Total Scour (FDOT)	Abutment Scour
Design scour (ft)	10.35	8.44	8.02	18.37	16.45	15.12
Expected scour (ft)	7.05	6.32	7.42	14.47	13.74	11.35
Bias	0.68	0.75	0.93	0.79	0.84	0.75
Std. dev. (ft)	1.13	1.12	2.74	3.13	3.03	3.18
COV	0.16	0.18	0.37	0.22	0.22	0.28
Design scour β	2.91	1.88	0.22	1.25	0.89	1.18
Non-exceedance	0.9982	0.9701	0.5857	0.8935	0.8143	0.8818
Scour Non-exceedance (ft) Based on Monte Carlo Results						
β = 0.5 (0.6915)	7.64	6.90	8.60	15.86	15.09	12.77
β = 1.0 (0.8413)	8.19	7.46	10.17	17.65	16.79	14.55
β = 1.5 (0.9332)	8.77	8.00	11.89	19.43	18.56	16.38
β = 2.0 (0.9772)	9.34	8.55	13.56	21.32	20.40	18.21
β = 2.5 (0.9938)	9.79	9.06	15.50	23.34	22.41	20.54
β = 3.0 (0.9987)	10.26	9.44	17.24	25.29	24.82	22.31
Scour Factors Based on Monte Carlo Results						
β = 0.5 (0.6915)	0.74	0.82	1.07	0.86	0.92	0.84
β = 1.0 (0.8413)	0.79	0.88	1.27	0.96	1.02	0.96
β = 1.5 (0.9332)	0.85	0.95	1.48	1.06	1.13	1.08
β = 2.0 (0.9772)	0.90	1.01	1.69	1.16	1.24	1.20
β = 2.5 (0.9938)	0.95	1.07	1.93	1.27	1.36	1.36
β = 3.0 (0.9987)	0.99	1.12	2.15	1.38	1.51	1.48
Scour Non-exceedance (ft) Based on Scour Mean and Standard Deviation						
β = 0.5 (0.6915)	7.62	6.88	8.79	16.04	15.26	12.94
β = 1.0 (0.8413)	8.18	7.45	10.16	17.60	16.77	14.53
β = 1.5 (0.9332)	8.75	8.01	11.53	19.16	18.29	16.12
β = 2.0 (0.9772)	9.32	8.57	12.91	20.73	19.80	17.72
β = 2.5 (0.9938)	9.89	9.13	14.28	22.29	21.32	19.31
β = 3.0 (0.9987)	10.45	9.69	15.65	23.86	22.84	20.90
Scour Factors Based on Scour Mean and Standard Deviation						
β = 0.5 (0.6915)	0.74	0.82	1.10	0.87	0.93	0.86
β = 1.0 (0.8413)	0.79	0.88	1.27	0.96	1.02	0.96
β = 1.5 (0.9332)	0.85	0.95	1.44	1.04	1.11	1.07
β = 2.0 (0.9772)	0.90	1.02	1.61	1.13	1.20	1.17
β = 2.5 (0.9938)	0.96	1.08	1.78	1.21	1.30	1.28
β = 3.0 (0.9987)	1.01	1.15	1.95	1.30	1.39	1.38

Table B.16	Medium Bridge—High Hydrologic Uncertainty—Small Pier (1.5 ft)					
	Pier Scour (HEC-18)	Pier Scour (FDOT)	Contraction Scour	Total Scour (HEC-18)	Total Scour (FDOT)	Abutment Scour
Design scour (ft)	3.60	3.19	8.02	11.62	11.21	15.12
Expected scour (ft)	2.46	2.40	7.40	9.85	9.80	11.40
Bias	0.68	0.75	0.92	0.85	0.87	0.75
Std. dev. (ft)	0.39	0.43	3.26	3.28	3.30	3.51
COV	0.16	0.18	0.44	0.33	0.34	0.31
Design scour β	2.94	1.85	0.19	0.54	0.43	1.06
Non-exceedance	0.9984	0.9679	0.5754	0.7046	0.6656	0.8553
Scour Non-exceedance (ft) Based on Monte Carlo Results						
β = 0.5 (0.6915)	2.65	2.61	8.77	11.22	11.18	12.87
β = 1.0 (0.8413)	2.84	2.83	10.60	13.10	13.05	14.83
β = 1.5 (0.9332)	3.04	3.05	12.52	15.04	15.03	16.99
β = 2.0 (0.9772)	3.24	3.27	14.84	17.33	17.33	19.44
β = 2.5 (0.9938)	3.43	3.47	17.67	20.00	20.00	22.33
β = 3.0 (0.9987)	3.56	3.58	19.84	22.36	22.32	25.51
Scour Factors Based on Monte Carlo Results						
β = 0.5 (0.6915)	0.74	0.82	1.09	0.97	1.00	0.85
β = 1.0 (0.8413)	0.79	0.89	1.32	1.13	1.16	0.98
β = 1.5 (0.9332)	0.84	0.96	1.56	1.29	1.34	1.12
β = 2.0 (0.9772)	0.90	1.02	1.85	1.49	1.55	1.29
β = 2.5 (0.9938)	0.95	1.09	2.21	1.72	1.78	1.48
β = 3.0 (0.9987)	0.99	1.12	2.47	1.93	1.99	1.69
Scour Non-exceedance (ft) Based on Scour Mean and Standard Deviation						
β = 0.5 (0.6915)	2.65	2.61	9.02	11.49	11.45	13.16
β = 1.0 (0.8413)	2.84	2.83	10.65	13.13	13.09	14.91
β = 1.5 (0.9332)	3.04	3.04	12.28	14.77	14.74	16.67
β = 2.0 (0.9772)	3.23	3.25	13.91	16.42	16.39	18.42
β = 2.5 (0.9938)	3.43	3.47	15.54	18.06	18.04	20.18
β = 3.0 (0.9987)	3.62	3.68	17.17	19.70	19.69	21.93
Scour Factors Based on Scour Mean and Standard Deviation						
β = 0.5 (0.6915)	0.74	0.82	1.13	0.99	1.02	0.87
β = 1.0 (0.8413)	0.79	0.89	1.33	1.13	1.17	0.99
β = 1.5 (0.9332)	0.84	0.95	1.53	1.27	1.32	1.10
β = 2.0 (0.9772)	0.90	1.02	1.74	1.41	1.46	1.22
β = 2.5 (0.9938)	0.95	1.09	1.94	1.55	1.61	1.33
β = 3.0 (0.9987)	1.01	1.15	2.14	1.70	1.76	1.45

Table B.17	Medium Bridge—High Hydrologic Uncertainty—Medium Pier (3 ft)					
	Pier Scour (HEC-18)	Pier Scour (FDOT)	Contraction Scour	Total Scour (HEC-18)	Total Scour (FDOT)	Abutment Scour
Design scour (ft)	7.20	5.94	8.02	15.22	13.95	15.12
Expected scour (ft)	4.91	4.47	7.40	12.31	11.87	11.40
Bias	0.68	0.75	0.92	0.81	0.85	0.75
Std. dev. (ft)	0.78	0.80	3.26	3.35	3.41	3.51
COV	0.16	0.18	0.44	0.27	0.29	0.31
Design scour β	2.94	1.83	0.19	0.87	0.61	1.06
Non-exceedance	0.9984	0.9667	0.5754	0.8073	0.7295	0.8553
Scour Non-exceedance (ft) Based on Monte Carlo Results						
$\beta = 0.5$ (0.6915)	5.30	4.86	8.77	13.74	13.32	12.87
$\beta = 1.0$ (0.8413)	5.69	5.27	10.60	15.63	15.25	14.83
$\beta = 1.5$ (0.9332)	6.07	5.69	12.52	17.62	17.25	16.99
$\beta = 2.0$ (0.9772)	6.47	6.09	14.84	19.93	19.60	19.44
$\beta = 2.5$ (0.9938)	6.85	6.50	17.67	22.53	22.32	22.33
$\beta = 3.0$ (0.9987)	7.13	6.73	19.84	24.89	24.68	25.51
Scour Factors Based on Monte Carlo Results						
$\beta = 0.5$ (0.6915)	0.74	0.82	1.09	0.90	0.95	0.85
$\beta = 1.0$ (0.8413)	0.79	0.89	1.32	1.03	1.09	0.98
$\beta = 1.5$ (0.9332)	0.84	0.96	1.56	1.16	1.24	1.12
$\beta = 2.0$ (0.9772)	0.90	1.03	1.85	1.31	1.41	1.29
$\beta = 2.5$ (0.9938)	0.95	1.09	2.21	1.48	1.60	1.48
$\beta = 3.0$ (0.9987)	0.99	1.13	2.47	1.64	1.77	1.69
Scour Non-exceedance (ft) Based on Scour Mean and Standard Deviation						
$\beta = 0.5$ (0.6915)	5.30	4.87	9.02	13.98	13.57	13.16
$\beta = 1.0$ (0.8413)	5.69	5.27	10.65	15.66	15.28	14.91
$\beta = 1.5$ (0.9332)	6.08	5.67	12.28	17.33	16.98	16.67
$\beta = 2.0$ (0.9772)	6.47	6.07	13.91	19.01	18.69	18.42
$\beta = 2.5$ (0.9938)	6.86	6.47	15.54	20.69	20.40	20.18
$\beta = 3.0$ (0.9987)	7.25	6.87	17.17	22.36	22.10	21.93
Scour Factors Based on Scour Mean and Standard Deviation						
$\beta = 0.5$ (0.6915)	0.74	0.82	1.13	0.92	0.97	0.87
$\beta = 1.0$ (0.8413)	0.79	0.89	1.33	1.03	1.10	0.99
$\beta = 1.5$ (0.9332)	0.84	0.95	1.53	1.14	1.22	1.10
$\beta = 2.0$ (0.9772)	0.90	1.02	1.74	1.25	1.34	1.22
$\beta = 2.5$ (0.9938)	0.95	1.09	1.94	1.36	1.46	1.33
$\beta = 3.0$ (0.9987)	1.01	1.16	2.14	1.47	1.58	1.45

Table B.18	Medium Bridge—High Hydrologic Uncertainty—Large Pier (4.5 ft)					
	Pier Scour (HEC-18)	Pier Scour (FDOT)	Contraction Scour	Total Scour (HEC-18)	Total Scour (FDOT)	Abutment Scour
Design scour (ft)	10.35	8.44	8.02	18.37	16.45	15.12
Expected scour (ft)	7.06	6.36	7.40	14.46	13.75	11.40
Bias	0.68	0.75	0.92	0.79	0.84	0.75
Std. dev. (ft)	1.15	1.14	3.26	3.64	3.56	3.51
COV	0.16	0.18	0.44	0.25	0.26	0.31
Design scour β	2.87	1.82	0.19	1.08	0.76	1.06
Non-exceedance	0.9979	0.9658	0.5754	0.8589	0.7756	0.8553
Scour Non-exceedance (ft) Based on Monte Carlo Results						
$\beta = 0.5$ (0.6915)	7.64	6.92	8.77	16.06	15.30	12.87
$\beta = 1.0$ (0.8413)	8.23	7.51	10.60	18.08	17.27	14.83
$\beta = 1.5$ (0.9332)	8.78	8.10	12.52	20.21	19.30	16.99
$\beta = 2.0$ (0.9772)	9.39	8.69	14.84	22.54	21.72	19.44
$\beta = 2.5$ (0.9938)	10.03	9.25	17.67	25.07	24.58	22.33
$\beta = 3.0$ (0.9987)	10.45	9.64	19.84	27.20	27.00	25.51
Scour Factors Based on Monte Carlo Results						
$\beta = 0.5$ (0.6915)	0.74	0.82	1.09	0.87	0.93	0.85
$\beta = 1.0$ (0.8413)	0.79	0.89	1.32	0.98	1.05	0.98
$\beta = 1.5$ (0.9332)	0.85	0.96	1.56	1.10	1.17	1.12
$\beta = 2.0$ (0.9772)	0.91	1.03	1.85	1.23	1.32	1.29
$\beta = 2.5$ (0.9938)	0.97	1.10	2.21	1.36	1.49	1.48
$\beta = 3.0$ (0.9987)	1.01	1.14	2.47	1.48	1.64	1.69
Scour Non-exceedance (ft) Based on Scour Mean and Standard Deviation						
$\beta = 0.5$ (0.6915)	7.63	6.93	9.02	16.27	15.53	13.16
$\beta = 1.0$ (0.8413)	8.21	7.50	10.65	18.09	17.32	14.91
$\beta = 1.5$ (0.9332)	8.78	8.07	12.28	19.91	19.10	16.67
$\beta = 2.0$ (0.9772)	9.36	8.64	13.91	21.73	20.88	18.42
$\beta = 2.5$ (0.9938)	9.93	9.21	15.54	23.55	22.66	20.18
$\beta = 3.0$ (0.9987)	10.51	9.78	17.17	25.37	24.44	21.93
Scour Factors Based on Scour Mean and Standard Deviation						
$\beta = 0.5$ (0.6915)	0.74	0.82	1.13	0.89	0.94	0.87
$\beta = 1.0$ (0.8413)	0.79	0.89	1.33	0.99	1.05	0.99
$\beta = 1.5$ (0.9332)	0.85	0.96	1.53	1.08	1.16	1.10
$\beta = 2.0$ (0.9772)	0.90	1.02	1.74	1.18	1.27	1.22
$\beta = 2.5$ (0.9938)	0.96	1.09	1.94	1.28	1.38	1.33
$\beta = 3.0$ (0.9987)	1.01	1.16	2.14	1.38	1.49	1.45

Table B.19	Large Bridge—Low Hydrologic Uncertainty—Small Pier (3 ft)					
	Pier Scour (HEC-18)	Pier Scour (FDOT)	Contraction Scour	Total Scour (HEC-18)	Total Scour (FDOT)	Abutment Scour
Design scour (ft)	7.20	6.10	5.29	12.49	11.39	10.96
Expected scour (ft)	4.90	4.56	4.95	9.85	9.51	8.28
Bias	0.68	0.75	0.93	0.79	0.83	0.76
Std. dev. (ft)	0.78	0.81	1.93	2.08	2.11	3.24
COV	0.16	0.18	0.39	0.21	0.22	0.39
Design scour β	2.97	1.90	0.18	1.28	0.89	0.83
Non-exceedance	0.9985	0.9712	0.5711	0.8990	0.8140	0.7961
Scour Non-exceedance (ft) Based on Monte Carlo Results						
β = 0.5 (0.6915)	5.29	4.96	5.74	10.74	10.42	9.57
β = 1.0 (0.8413)	5.69	5.38	6.86	11.89	11.59	11.47
β = 1.5 (0.9332)	6.07	5.76	8.05	13.16	12.84	13.56
β = 2.0 (0.9772)	6.44	6.19	9.35	14.46	14.21	15.70
β = 2.5 (0.9938)	6.79	6.60	10.79	15.87	15.65	18.25
β = 3.0 (0.9987)	7.10	6.85	12.55	17.68	17.62	21.51
Scour Factors Based on Monte Carlo Results						
β = 0.5 (0.6915)	0.73	0.81	1.08	0.86	0.91	0.87
β = 1.0 (0.8413)	0.79	0.88	1.30	0.95	1.02	1.05
β = 1.5 (0.9332)	0.84	0.95	1.52	1.05	1.13	1.24
β = 2.0 (0.9772)	0.89	1.02	1.77	1.16	1.25	1.43
β = 2.5 (0.9938)	0.94	1.08	2.04	1.27	1.37	1.66
β = 3.0 (0.9987)	0.99	1.12	2.37	1.41	1.55	1.96
Scour Non-exceedance (ft) Based on Scour Mean and Standard Deviation						
β = 0.5 (0.6915)	5.28	4.96	5.91	10.88	10.56	9.90
β = 1.0 (0.8413)	5.67	5.37	6.88	11.92	11.62	11.52
β = 1.5 (0.9332)	6.06	5.77	7.84	12.96	12.67	13.14
β = 2.0 (0.9772)	6.45	6.18	8.80	14.00	13.73	14.76
β = 2.5 (0.9938)	6.84	6.58	9.76	15.04	14.78	16.39
β = 3.0 (0.9987)	7.22	6.99	10.73	16.07	15.84	18.01
Scour Factors Based on Scour Mean and Standard Deviation						
β = 0.5 (0.6915)	0.73	0.81	1.12	0.87	0.93	0.90
β = 1.0 (0.8413)	0.79	0.88	1.30	0.95	1.02	1.05
β = 1.5 (0.9332)	0.84	0.95	1.48	1.04	1.11	1.20
β = 2.0 (0.9772)	0.90	1.01	1.66	1.12	1.21	1.35
β = 2.5 (0.9938)	0.95	1.08	1.84	1.20	1.30	1.49
β = 3.0 (0.9987)	1.00	1.15	2.03	1.29	1.39	1.64

Table B.20	Large Bridge—Low Hydrologic Uncertainty—Medium Pier (6 ft)					
	Pier Scour (HEC-18)	Pier Scour (FDOT)	Contraction Scour	Total Scour (HEC-18)	Total Scour (FDOT)	Abutment Scour
Design scour (ft)	13.77	11.28	5.29	19.07	16.57	10.96
Expected scour (ft)	9.35	8.43	4.95	14.30	13.38	8.28
Bias	0.68	0.75	0.93	0.75	0.81	0.76
Std. dev. (ft)	1.51	1.50	1.93	2.58	2.50	3.24
COV	0.16	0.18	0.39	0.18	0.19	0.39
Design scour β	2.94	1.89	0.18	1.85	1.28	0.83
Non-exceedance	0.9983	0.9707	0.5711	0.9677	0.8990	0.7961
Scour Non-exceedance (ft) Based on Monte Carlo Results						
β = 0.5 (0.6915)	10.11	9.18	5.74	15.50	14.56	9.57
β = 1.0 (0.8413)	10.88	9.95	6.86	16.88	15.87	11.47
β = 1.5 (0.9332)	11.62	10.68	8.05	18.30	17.26	13.56
β = 2.0 (0.9772)	12.33	11.47	9.35	19.82	18.81	15.70
β = 2.5 (0.9938)	13.03	12.21	10.79	21.28	20.34	18.25
β = 3.0 (0.9987)	13.57	12.73	12.55	22.99	22.31	21.51
Scour Factors Based on Monte Carlo Results						
β = 0.5 (0.6915)	0.73	0.81	1.08	0.81	0.88	0.87
β = 1.0 (0.8413)	0.79	0.88	1.30	0.89	0.96	1.05
β = 1.5 (0.9332)	0.84	0.95	1.52	0.96	1.04	1.24
β = 2.0 (0.9772)	0.90	1.02	1.77	1.04	1.13	1.43
β = 2.5 (0.9938)	0.95	1.08	2.04	1.12	1.23	1.66
β = 3.0 (0.9987)	0.99	1.13	2.37	1.21	1.35	1.96
Scour Non-exceedance (ft) Based on Scour Mean and Standard Deviation						
β = 0.5 (0.6915)	10.10	9.19	5.91	15.59	14.63	9.90
β = 1.0 (0.8413)	10.86	9.94	6.88	16.88	15.88	11.52
β = 1.5 (0.9332)	11.61	10.69	7.84	18.17	17.13	13.14
β = 2.0 (0.9772)	12.36	11.44	8.80	19.46	18.38	14.76
β = 2.5 (0.9938)	13.12	12.19	9.76	20.75	19.63	16.39
β = 3.0 (0.9987)	13.87	12.94	10.73	22.04	20.88	18.01
Scour Factors Based on Scour Mean and Standard Deviation						
β = 0.5 (0.6915)	0.73	0.81	1.12	0.82	0.88	0.90
β = 1.0 (0.8413)	0.79	0.88	1.30	0.89	0.96	1.05
β = 1.5 (0.9332)	0.84	0.95	1.48	0.95	1.03	1.20
β = 2.0 (0.9772)	0.90	1.01	1.66	1.02	1.11	1.35
β = 2.5 (0.9938)	0.95	1.08	1.84	1.09	1.18	1.49
β = 3.0 (0.9987)	1.01	1.15	2.03	1.16	1.26	1.64

Table B.21	Large Bridge—Low Hydrologic Uncertainty—Large Pier (9 ft)					
	Pier Scour (HEC-18)	Pier Scour (FDOT)	Contraction Scour	Total Scour (HEC-18)	Total Scour (FDOT)	Abutment Scour
Design scour (ft)	17.93	15.90	5.29	23.22	21.19	10.96
Expected scour (ft)	12.19	11.89	4.95	17.14	16.84	8.28
Bias	0.68	0.75	0.93	0.74	0.79	0.76
Std. dev. (ft)	1.97	2.13	1.93	2.93	2.96	3.24
COV	0.16	0.18	0.39	0.17	0.18	0.39
Design scour β	2.91	1.89	0.18	2.08	1.47	0.83
Non-exceedance	0.9982	0.9704	0.5711	0.9811	0.9296	0.7961
Scour Non-exceedance (ft) Based on Monte Carlo Results						
β = 0.5 (0.6915)	13.18	12.95	5.74	18.55	18.27	9.57
β = 1.0 (0.8413)	14.19	14.03	6.86	20.07	19.79	11.47
β = 1.5 (0.9332)	15.16	15.08	8.05	21.62	21.32	13.56
β = 2.0 (0.9772)	16.11	16.20	9.35	23.31	23.08	15.70
β = 2.5 (0.9938)	17.00	17.21	10.79	25.16	24.93	18.25
β = 3.0 (0.9987)	17.72	17.95	12.55	26.86	26.66	21.51
Scour Factors Based on Monte Carlo Results						
β = 0.5 (0.6915)	0.74	0.81	1.08	0.80	0.86	0.87
β = 1.0 (0.8413)	0.79	0.88	1.30	0.86	0.93	1.05
β = 1.5 (0.9332)	0.85	0.95	1.52	0.93	1.01	1.24
β = 2.0 (0.9772)	0.90	1.02	1.77	1.00	1.09	1.43
β = 2.5 (0.9938)	0.95	1.08	2.04	1.08	1.18	1.66
β = 3.0 (0.9987)	0.99	1.13	2.37	1.16	1.26	1.96
Scour Non-exceedance (ft) Based on Scour Mean and Standard Deviation						
β = 0.5 (0.6915)	13.18	12.95	5.91	18.60	18.32	9.90
β = 1.0 (0.8413)	14.16	14.02	6.88	20.07	19.80	11.52
β = 1.5 (0.9332)	15.15	15.08	7.84	21.53	21.27	13.14
β = 2.0 (0.9772)	16.13	16.14	8.80	23.00	22.75	14.76
β = 2.5 (0.9938)	17.12	17.20	9.76	24.46	24.23	16.39
β = 3.0 (0.9987)	18.10	18.27	10.73	25.93	25.71	18.01
Scour Factors Based on Scour Mean and Standard Deviation						
β = 0.5 (0.6915)	0.73	0.81	1.12	0.80	0.86	0.90
β = 1.0 (0.8413)	0.79	0.88	1.30	0.86	0.93	1.05
β = 1.5 (0.9332)	0.84	0.95	1.48	0.93	1.00	1.20
β = 2.0 (0.9772)	0.90	1.02	1.66	0.99	1.07	1.35
β = 2.5 (0.9938)	0.95	1.08	1.84	1.05	1.14	1.49
β = 3.0 (0.9987)	1.01	1.15	2.03	1.12	1.21	1.64

Table B.22	Large Bridge—Medium Hydrologic Uncertainty—Small Pier (3 ft)					
	Pier Scour (HEC-18)	Pier Scour (FDOT)	Contraction Scour	Total Scour (HEC-18)	Total Scour (FDOT)	Abutment Scour
Design scour (ft)	7.20	6.10	5.29	12.49	11.39	10.96
Expected scour (ft)	4.89	4.57	5.09	9.98	9.66	8.50
Bias	0.68	0.75	0.96	0.80	0.85	0.78
Std. dev. (ft)	0.77	0.82	2.56	2.67	2.72	4.30
COV	0.16	0.18	0.50	0.27	0.28	0.51
Design scour β	2.99	1.87	0.08	0.94	0.64	0.57
Non-exceedance	0.9986	0.9691	0.5322	0.8274	0.7379	0.7165
Scour Non-exceedance (ft) Based on Monte Carlo Results						
β = 0.5 (0.6915)	5.28	4.99	6.08	11.04	10.76	9.96
β = 1.0 (0.8413)	5.67	5.40	7.58	12.61	12.34	12.57
β = 1.5 (0.9332)	6.06	5.81	9.31	14.32	14.06	15.55
β = 2.0 (0.9772)	6.43	6.20	11.20	16.24	15.93	19.09
β = 2.5 (0.9938)	6.76	6.56	13.22	18.19	18.01	22.78
β = 3.0 (0.9987)	7.04	6.88	15.22	20.40	20.15	26.69
Scour Factors Based on Monte Carlo Results						
β = 0.5 (0.6915)	0.73	0.82	1.15	0.88	0.94	0.91
β = 1.0 (0.8413)	0.79	0.89	1.43	1.01	1.08	1.15
β = 1.5 (0.9332)	0.84	0.95	1.76	1.15	1.23	1.42
β = 2.0 (0.9772)	0.89	1.02	2.12	1.30	1.40	1.74
β = 2.5 (0.9938)	0.94	1.08	2.50	1.46	1.58	2.08
β = 3.0 (0.9987)	0.98	1.13	2.87	1.63	1.77	2.44
Scour Non-exceedance (ft) Based on Scour Mean and Standard Deviation						
β = 0.5 (0.6915)	5.28	4.98	6.37	11.31	11.02	10.65
β = 1.0 (0.8413)	5.66	5.39	7.64	12.64	12.38	12.80
β = 1.5 (0.9332)	6.05	5.80	8.92	13.98	13.74	14.95
β = 2.0 (0.9772)	6.44	6.21	10.20	15.31	15.10	17.10
β = 2.5 (0.9938)	6.82	6.61	11.48	16.64	16.46	19.25
β = 3.0 (0.9987)	7.21	7.02	12.76	17.98	17.82	21.40
Scour Factors Based on Scour Mean and Standard Deviation						
β = 0.5 (0.6915)	0.73	0.82	1.20	0.91	0.97	0.97
β = 1.0 (0.8413)	0.79	0.88	1.44	1.01	1.09	1.17
β = 1.5 (0.9332)	0.84	0.95	1.69	1.12	1.21	1.36
β = 2.0 (0.9772)	0.89	1.02	1.93	1.23	1.33	1.56
β = 2.5 (0.9938)	0.95	1.08	2.17	1.33	1.45	1.76
β = 3.0 (0.9987)	1.00	1.15	2.41	1.44	1.56	1.95

Table B.23	Large Bridge—Medium Hydrologic Uncertainty—Medium Pier (6 ft)					
	Pier Scour (HEC-18)	Pier Scour (FDOT)	Contraction Scour	Total Scour (HEC-18)	Total Scour (FDOT)	Abutment Scour
Design scour (ft)	13.77	11.28	5.29	19.07	16.57	10.96
Expected scour (ft)	9.32	8.46	5.09	14.41	13.54	8.50
Bias	0.68	0.75	0.96	0.76	0.82	0.78
Std. dev. (ft)	1.52	1.52	2.56	3.19	3.09	4.30
COV	0.16	0.18	0.50	0.22	0.23	0.51
Design scour β	2.93	1.85	0.08	1.46	0.98	0.57
Non-exceedance	0.9983	0.9681	0.5322	0.9278	0.8365	0.7165
Scour Non-exceedance (ft) Based on Monte Carlo Results						
β = 0.5 (0.6915)	10.08	9.23	6.08	15.82	14.87	9.96
β = 1.0 (0.8413)	10.85	10.00	7.58	17.61	16.59	12.57
β = 1.5 (0.9332)	11.63	10.78	9.31	19.50	18.42	15.55
β = 2.0 (0.9772)	12.41	11.48	11.20	21.47	20.44	19.09
β = 2.5 (0.9938)	13.05	12.16	13.22	23.59	22.77	22.78
β = 3.0 (0.9987)	13.76	12.84	15.22	25.70	24.97	26.69
Scour Factors Based on Monte Carlo Results						
β = 0.5 (0.6915)	0.73	0.82	1.15	0.83	0.90	0.91
β = 1.0 (0.8413)	0.79	0.89	1.43	0.92	1.00	1.15
β = 1.5 (0.9332)	0.84	0.96	1.76	1.02	1.11	1.42
β = 2.0 (0.9772)	0.90	1.02	2.12	1.13	1.23	1.74
β = 2.5 (0.9938)	0.95	1.08	2.50	1.24	1.37	2.08
β = 3.0 (0.9987)	1.00	1.14	2.87	1.35	1.51	2.44
Scour Non-exceedance (ft) Based on Scour Mean and Standard Deviation						
β = 0.5 (0.6915)	10.08	9.22	6.37	16.00	15.09	10.65
β = 1.0 (0.8413)	10.84	9.98	7.64	17.60	16.63	12.80
β = 1.5 (0.9332)	11.60	10.74	8.92	19.20	18.18	14.95
β = 2.0 (0.9772)	12.36	11.50	10.20	20.79	19.72	17.10
β = 2.5 (0.9938)	13.12	12.26	11.48	22.39	21.27	19.25
β = 3.0 (0.9987)	13.88	13.02	12.76	23.99	22.81	21.40
Scour Factors Based on Scour Mean and Standard Deviation						
β = 0.5 (0.6915)	0.73	0.82	1.20	0.84	0.91	0.97
β = 1.0 (0.8413)	0.79	0.88	1.44	0.92	1.00	1.17
β = 1.5 (0.9332)	0.84	0.95	1.69	1.01	1.10	1.36
β = 2.0 (0.9772)	0.90	1.02	1.93	1.09	1.19	1.56
β = 2.5 (0.9938)	0.95	1.09	2.17	1.17	1.28	1.76
β = 3.0 (0.9987)	1.01	1.15	2.41	1.26	1.38	1.95

Table B.24	Large Bridge—Medium Hydrologic Uncertainty—Large Pier (9 ft)					
	Pier Scour (HEC-18)	Pier Scour (FDOT)	Contraction Scour	Total Scour (HEC-18)	Total Scour (FDOT)	Abutment Scour
Design scour (ft)	17.93	15.90	5.29	23.22	21.19	10.96
Expected scour (ft)	12.20	11.92	5.09	17.28	17.01	8.50
Bias	0.68	0.75	0.96	0.74	0.80	0.78
Std. dev. (ft)	2.02	2.16	2.56	3.59	3.53	4.30
COV	0.17	0.18	0.50	0.21	0.21	0.51
Design scour β	2.84	1.84	0.08	1.66	1.18	0.57
Non-exceedance	0.9977	0.9672	0.5322	0.9510	0.8819	0.7165
Scour Non-exceedance (ft) Based on Monte Carlo Results						
$\beta = 0.5$ (0.6915)	13.20	13.01	6.08	18.85	18.60	9.96
$\beta = 1.0$ (0.8413)	14.23	14.10	7.58	20.84	20.50	12.57
$\beta = 1.5$ (0.9332)	15.26	15.25	9.31	22.99	22.53	15.55
$\beta = 2.0$ (0.9772)	16.32	16.23	11.20	25.27	24.68	19.09
$\beta = 2.5$ (0.9938)	17.26	17.27	13.22	27.52	27.32	22.78
$\beta = 3.0$ (0.9987)	18.28	18.24	15.22	29.85	29.60	26.69
Scour Factors Based on Monte Carlo Results						
$\beta = 0.5$ (0.6915)	0.74	0.82	1.15	0.81	0.88	0.91
$\beta = 1.0$ (0.8413)	0.79	0.89	1.43	0.90	0.97	1.15
$\beta = 1.5$ (0.9332)	0.85	0.96	1.76	0.99	1.06	1.42
$\beta = 2.0$ (0.9772)	0.91	1.02	2.12	1.09	1.16	1.74
$\beta = 2.5$ (0.9938)	0.96	1.09	2.50	1.18	1.29	2.08
$\beta = 3.0$ (0.9987)	1.02	1.15	2.87	1.29	1.40	2.44
Scour Non-exceedance (ft) Based on Scour Mean and Standard Deviation						
$\beta = 0.5$ (0.6915)	13.21	13.00	6.37	19.08	18.78	10.65
$\beta = 1.0$ (0.8413)	14.22	14.08	7.64	20.87	20.54	12.80
$\beta = 1.5$ (0.9332)	15.23	15.16	8.92	22.67	22.31	14.95
$\beta = 2.0$ (0.9772)	16.24	16.24	10.20	24.46	24.07	17.10
$\beta = 2.5$ (0.9938)	17.25	17.32	11.48	26.25	25.84	19.25
$\beta = 3.0$ (0.9987)	18.26	18.40	12.76	28.05	27.60	21.40
Scour Factors Based on Scour Mean and Standard Deviation						
$\beta = 0.5$ (0.6915)	0.74	0.82	1.20	0.82	0.89	0.97
$\beta = 1.0$ (0.8413)	0.79	0.89	1.44	0.90	0.97	1.17
$\beta = 1.5$ (0.9332)	0.85	0.95	1.69	0.98	1.05	1.36
$\beta = 2.0$ (0.9772)	0.91	1.02	1.93	1.05	1.14	1.56
$\beta = 2.5$ (0.9938)	0.96	1.09	2.17	1.13	1.22	1.76
$\beta = 3.0$ (0.9987)	1.02	1.16	2.41	1.21	1.30	1.95

Table B.25	Large Bridge—High Hydrologic Uncertainty—Small Pier (3 ft)					
	Pier Scour (HEC-18)	Pier Scour (FDOT)	Contraction Scour	Total Scour (HEC-18)	Total Scour (FDOT)	Abutment Scour
Design scour (ft)	7.20	6.10	5.29	12.49	11.39	10.96
Expected scour (ft)	4.90	4.58	5.26	10.16	9.84	8.79
Bias	0.68	0.75	0.99	0.81	0.86	0.80
Std. dev. (ft)	0.77	0.81	3.16	3.24	3.32	5.33
COV	0.16	0.18	0.60	0.32	0.34	0.61
Design scour β	2.99	1.86	0.01	0.72	0.47	0.41
Non-exceedance	0.9986	0.9686	0.5039	0.7642	0.6796	0.6582
Scour Non-exceedance (ft) Based on Monte Carlo Results						
β = 0.5 (0.6915)	5.29	5.00	6.45	11.38	11.16	10.63
β = 1.0 (0.8413)	5.67	5.40	8.35	13.30	13.09	13.83
β = 1.5 (0.9332)	6.06	5.80	10.48	15.49	15.28	17.57
β = 2.0 (0.9772)	6.45	6.20	12.99	17.95	17.77	22.21
β = 2.5 (0.9938)	6.82	6.60	15.76	20.66	20.41	27.26
β = 3.0 (0.9987)	7.08	6.81	18.06	23.13	23.10	32.80
Scour Factors Based on Monte Carlo Results						
β = 0.5 (0.6915)	0.73	0.82	1.22	0.91	0.98	0.97
β = 1.0 (0.8413)	0.79	0.89	1.58	1.06	1.15	1.26
β = 1.5 (0.9332)	0.84	0.95	1.98	1.24	1.34	1.60
β = 2.0 (0.9772)	0.90	1.02	2.45	1.44	1.56	2.03
β = 2.5 (0.9938)	0.95	1.08	2.98	1.65	1.79	2.49
β = 3.0 (0.9987)	0.98	1.12	3.41	1.85	2.03	2.99
Scour Non-exceedance (ft) Based on Scour Mean and Standard Deviation						
β = 0.5 (0.6915)	5.28	4.99	6.84	11.78	11.50	11.45
β = 1.0 (0.8413)	5.67	5.40	8.42	13.40	13.16	14.12
β = 1.5 (0.9332)	6.05	5.80	10.00	15.02	14.82	16.79
β = 2.0 (0.9772)	6.44	6.21	11.58	16.65	16.48	19.45
β = 2.5 (0.9938)	6.82	6.62	13.16	18.27	18.13	22.12
β = 3.0 (0.9987)	7.21	7.02	14.74	19.89	19.79	24.78
Scour Factors Based on Scour Mean and Standard Deviation						
β = 0.5 (0.6915)	0.73	0.82	1.29	0.94	1.01	1.04
β = 1.0 (0.8413)	0.79	0.88	1.59	1.07	1.16	1.29
β = 1.5 (0.9332)	0.84	0.95	1.89	1.20	1.30	1.53
β = 2.0 (0.9772)	0.89	1.02	2.19	1.33	1.45	1.77
β = 2.5 (0.9938)	0.95	1.09	2.48	1.46	1.59	2.02
β = 3.0 (0.9987)	1.00	1.15	2.78	1.59	1.74	2.26

Table B.26	Large Bridge—High Hydrologic Uncertainty—Medium Pier (6 ft)					
	Pier Scour (HEC-18)	Pier Scour (FDOT)	Contraction Scour	Total Scour (HEC-18)	Total Scour (FDOT)	Abutment Scour
Design scour (ft)	13.77	11.28	5.29	19.07	16.57	10.96
Expected scour (ft)	9.31	8.48	5.26	14.57	13.74	8.79
Bias	0.68	0.75	0.99	0.76	0.83	0.80
Std. dev. (ft)	1.53	1.52	3.16	3.79	3.68	5.33
COV	0.16	0.18	0.60	0.26	0.27	0.61
Design scour β	2.92	1.84	0.01	1.19	0.77	0.41
Non-exceedance	0.9983	0.9672	0.5039	0.8826	0.7796	0.6582
Scour Non-exceedance (ft) Based on Monte Carlo Results						
β = 0.5 (0.6915)	10.05	9.24	6.45	16.16	15.29	10.63
β = 1.0 (0.8413)	10.84	10.02	8.35	18.24	17.28	13.83
β = 1.5 (0.9332)	11.63	10.78	10.48	20.62	19.72	17.57
β = 2.0 (0.9772)	12.43	11.53	12.99	23.32	22.25	22.21
β = 2.5 (0.9938)	13.26	12.28	15.76	25.83	24.94	27.26
β = 3.0 (0.9987)	13.79	12.70	18.06	28.62	27.83	32.80
Scour Factors Based on Monte Carlo Results						
β = 0.5 (0.6915)	0.73	0.82	1.22	0.85	0.92	0.97
β = 1.0 (0.8413)	0.79	0.89	1.58	0.96	1.04	1.26
β = 1.5 (0.9332)	0.84	0.96	1.98	1.08	1.19	1.60
β = 2.0 (0.9772)	0.90	1.02	2.45	1.22	1.34	2.03
β = 2.5 (0.9938)	0.96	1.09	2.98	1.35	1.51	2.49
β = 3.0 (0.9987)	1.00	1.13	3.41	1.50	1.68	2.99
Scour Non-exceedance (ft) Based on Scour Mean and Standard Deviation						
β = 0.5 (0.6915)	10.07	9.24	6.84	16.46	15.58	11.45
β = 1.0 (0.8413)	10.84	10.00	8.42	18.36	17.42	14.12
β = 1.5 (0.9332)	11.60	10.76	10.00	20.25	19.25	16.79
β = 2.0 (0.9772)	12.36	11.52	11.58	22.14	21.09	19.45
β = 2.5 (0.9938)	13.13	12.28	13.16	24.03	22.93	22.12
β = 3.0 (0.9987)	13.89	13.04	14.74	25.93	24.77	24.78
Scour Factors Based on Scour Mean and Standard Deviation						
β = 0.5 (0.6915)	0.73	0.82	1.29	0.86	0.94	1.04
β = 1.0 (0.8413)	0.79	0.89	1.59	0.96	1.05	1.29
β = 1.5 (0.9332)	0.84	0.95	1.89	1.06	1.16	1.53
β = 2.0 (0.9772)	0.90	1.02	2.19	1.16	1.27	1.77
β = 2.5 (0.9938)	0.95	1.09	2.48	1.26	1.38	2.02
β = 3.0 (0.9987)	1.01	1.16	2.78	1.36	1.49	2.26

| Table B.27	Large Bridge—High Hydrologic Uncertainty—Large Pier (9 ft)					
	Pier Scour (HEC-18)	Pier Scour (FDOT)	Contraction Scour	Total Scour (HEC-18)	Total Scour (FDOT)	Abutment Scour
Design scour (ft)	17.93	15.90	5.29	23.22	21.19	10.96
Expected scour (ft)	12.23	11.95	5.26	17.49	17.22	8.79
Bias	0.68	0.75	0.99	0.75	0.81	0.80
Std. dev. (ft)	2.06	2.16	3.16	4.25	4.11	5.33
COV	0.17	0.18	0.60	0.24	0.24	0.61
Design scour β	2.76	1.82	0.01	1.35	0.97	0.41
Non-exceedance	0.9971	0.9658	0.5039	0.9113	0.8335	0.6582
Scour Non-exceedance (ft) Based on Monte Carlo Results						
β = 0.5 (0.6915)	13.23	13.03	6.45	19.25	19.02	10.63
β = 1.0 (0.8413)	14.27	14.15	8.35	21.59	21.20	13.83
β = 1.5 (0.9332)	15.35	15.27	10.48	24.36	23.76	17.57
β = 2.0 (0.9772)	16.55	16.27	12.99	27.29	26.54	22.21
β = 2.5 (0.9938)	17.73	17.36	15.76	30.43	29.62	27.26
β = 3.0 (0.9987)	18.69	17.99	18.06	33.56	32.75	32.80
Scour Factors Based on Monte Carlo Results						
β = 0.5 (0.6915)	0.74	0.82	1.22	0.83	0.90	0.97
β = 1.0 (0.8413)	0.80	0.89	1.58	0.93	1.00	1.26
β = 1.5 (0.9332)	0.86	0.96	1.98	1.05	1.12	1.60
β = 2.0 (0.9772)	0.92	1.02	2.45	1.18	1.25	2.03
β = 2.5 (0.9938)	0.99	1.09	2.98	1.31	1.40	2.49
β = 3.0 (0.9987)	1.04	1.13	3.41	1.44	1.55	2.99
Scour Non-exceedance (ft) Based on Scour Mean and Standard Deviation						
β = 0.5 (0.6915)	13.26	13.03	6.84	19.62	19.27	11.45
β = 1.0 (0.8413)	14.29	14.12	8.42	21.74	21.32	14.12
β = 1.5 (0.9332)	15.33	15.20	10.00	23.87	23.38	16.79
β = 2.0 (0.9772)	16.36	16.28	11.58	25.99	25.43	19.45
β = 2.5 (0.9938)	17.39	17.36	13.16	28.11	27.49	22.12
β = 3.0 (0.9987)	18.42	18.45	14.74	30.24	29.54	24.78
Scour Factors Based on Scour Mean and Standard Deviation						
β = 0.5 (0.6915)	0.74	0.82	1.29	0.84	0.91	1.04
β = 1.0 (0.8413)	0.80	0.89	1.59	0.94	1.01	1.29
β = 1.5 (0.9332)	0.85	0.96	1.89	1.03	1.10	1.53
β = 2.0 (0.9772)	0.91	1.02	2.19	1.12	1.20	1.77
β = 2.5 (0.9938)	0.97	1.09	2.48	1.21	1.30	2.02
β = 3.0 (0.9987)	1.03	1.16	2.78	1.30	1.39	2.26
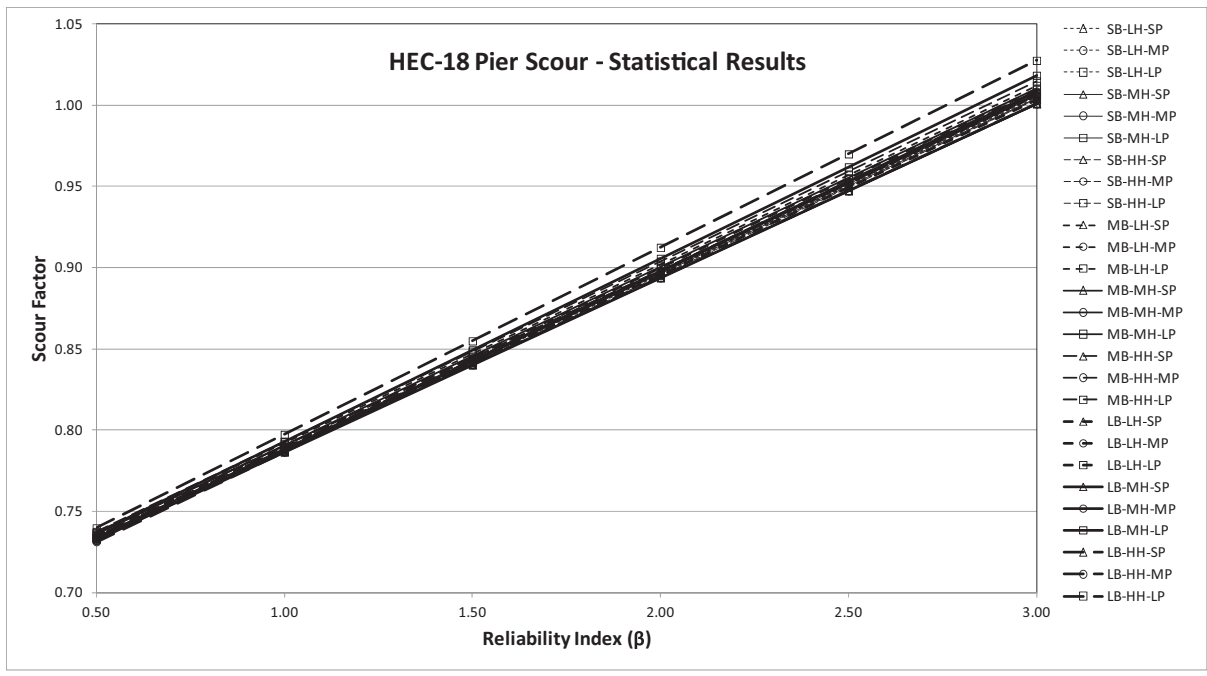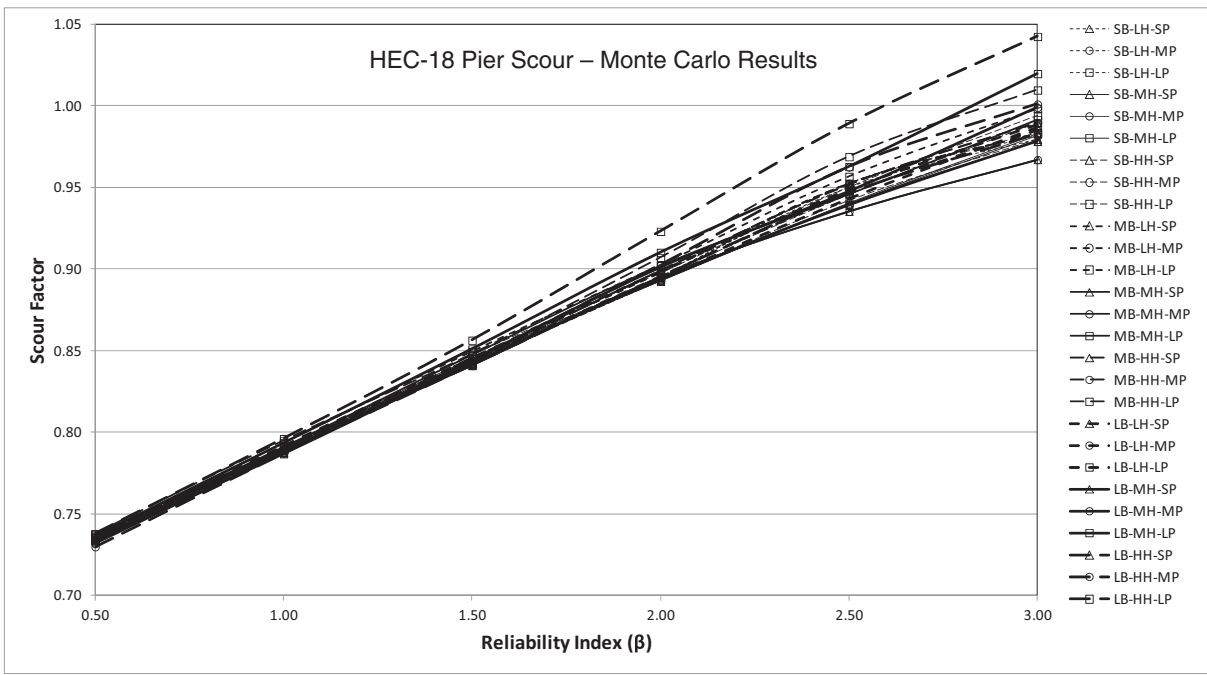
Figure B.1. Scour factors for the HEC-18 pier scour equation.
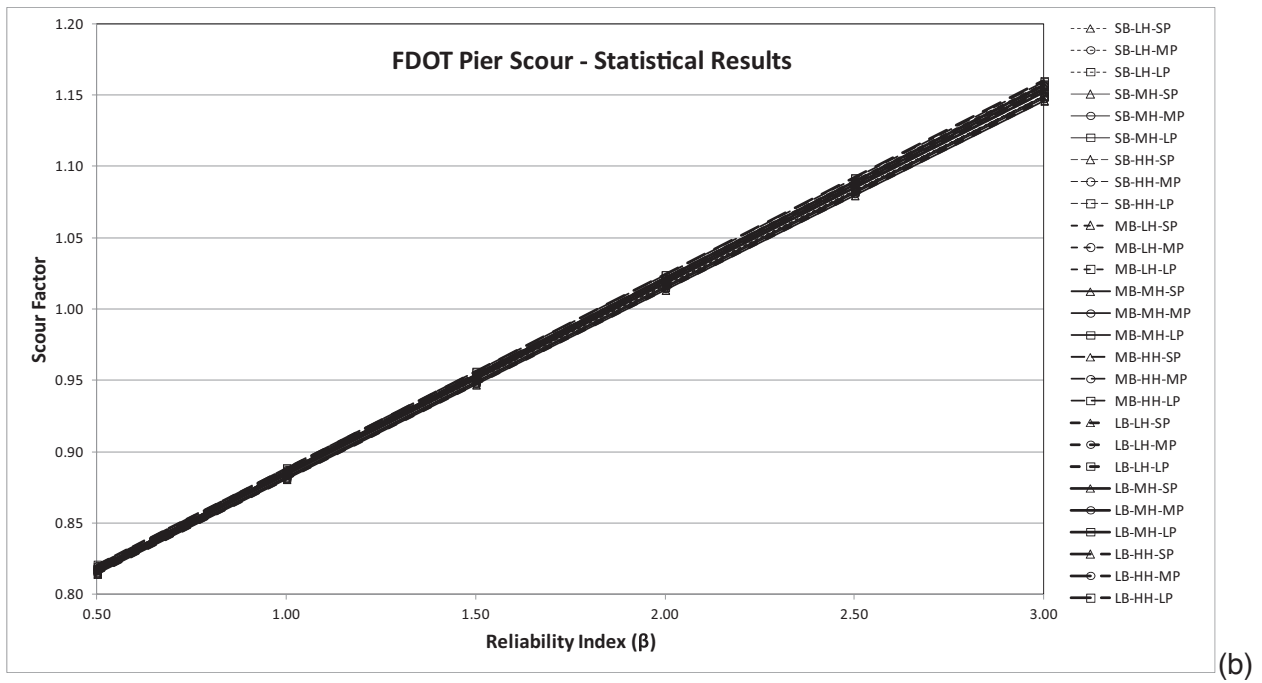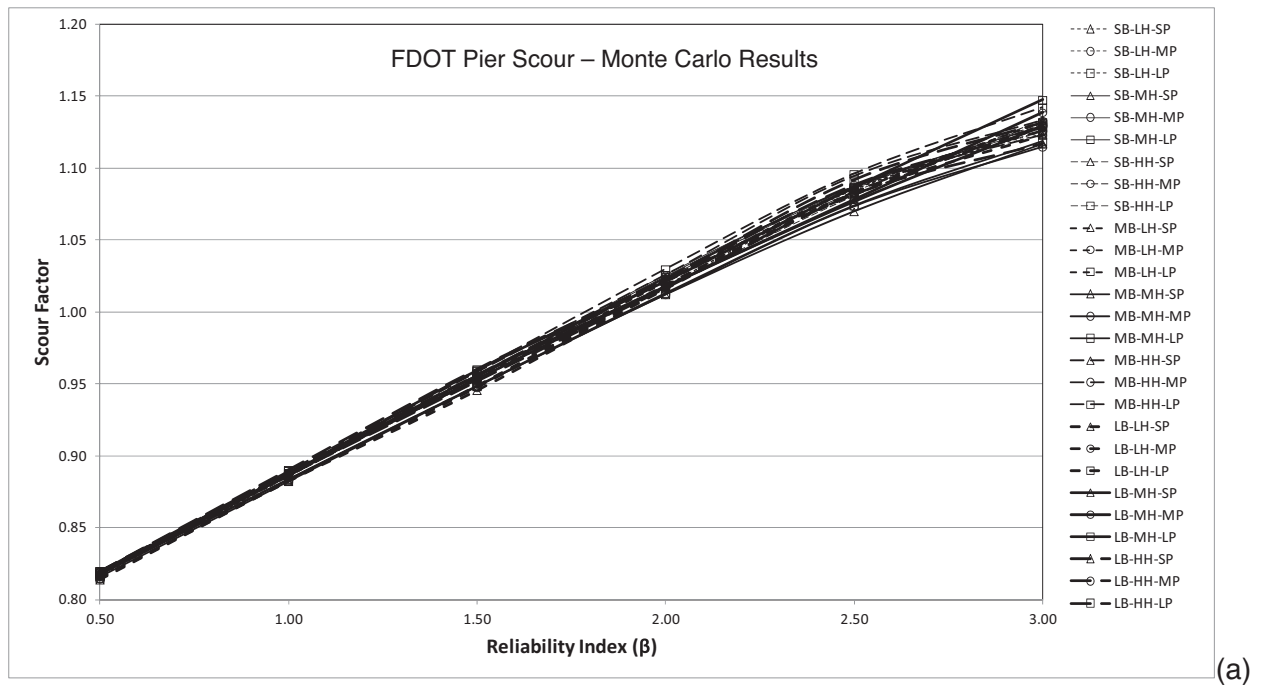
Figure B.2. Scour factors for the Florida DOT (FDOT) pier scour equation.
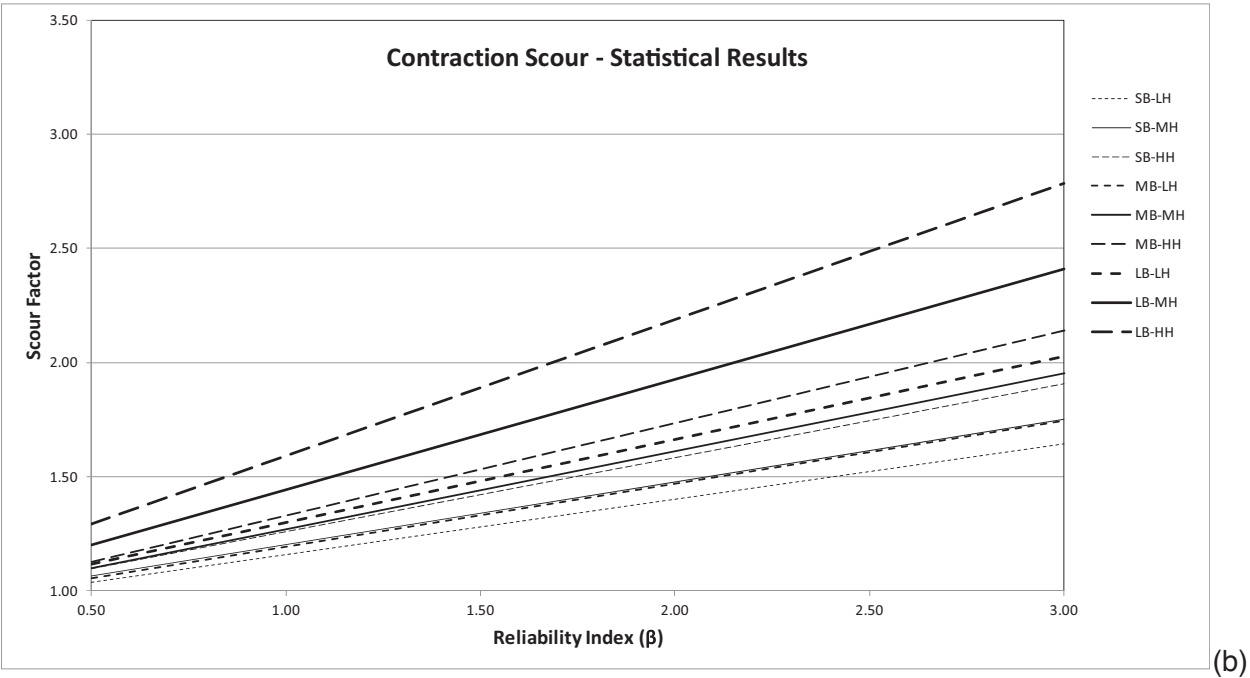
Figure B.3. Scour factors for contraction scour.
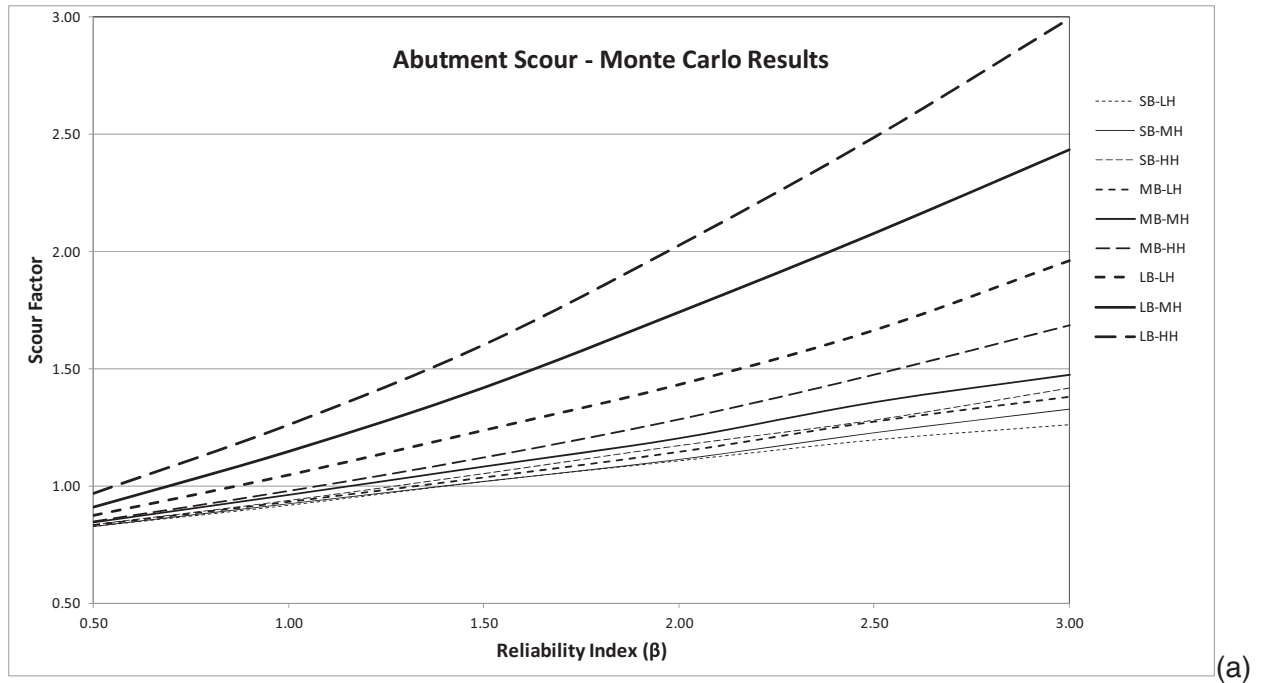
(a)
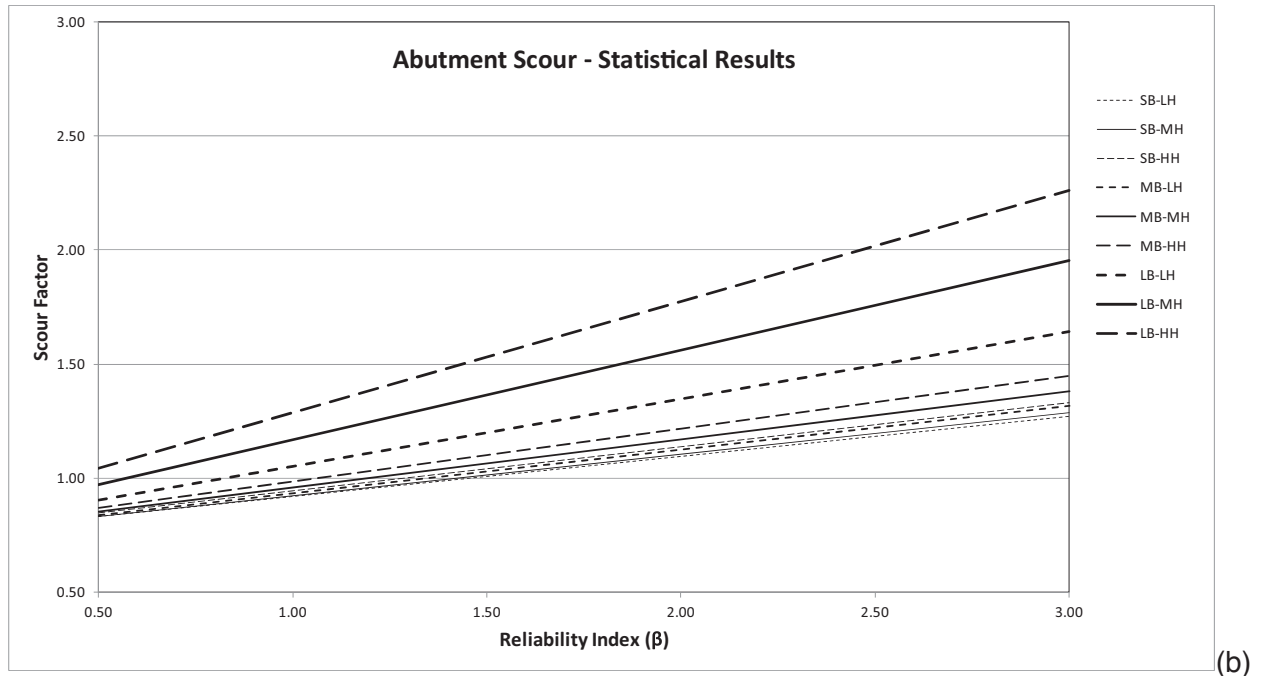
(b)

Figure B.4. Scour factors for the NCHRP Project 24-20 abutment scour equation.

Abbreviations and acronyms used without definitions in TRB publications:

A4A	Airlines for America
AAAE	American Association of Airport Executives
AASHO	American Association of State Highway Officials
AASHTO	American Association of State Highway and Transportation Officials
ACI–NA	Airports Council International–North America
ACRP	Airport Cooperative Research Program
ADA	Americans with Disabilities Act
APTA	American Public Transportation Association
ASCE	American Society of Civil Engineers
ASME	American Society of Mechanical Engineers
ASTM	American Society for Testing and Materials
ATA	American Trucking Associations
CTAA	Community Transportation Association of America
CTBSSP	Commercial Truck and Bus Safety Synthesis Program
DHS	Department of Homeland Security
DOE	Department of Energy
EPA	Environmental Protection Agency
FAA	Federal Aviation Administration
FHWA	Federal Highway Administration
FMCSA	Federal Motor Carrier Safety Administration
FRA	Federal Railroad Administration
FTA	Federal Transit Administration
HMCRP	Hazardous Materials Cooperative Research Program
IEEE	Institute of Electrical and Electronics Engineers
ISTEA	Intermodal Surface Transportation Efficiency Act of 1991
ITE	Institute of Transportation Engineers
MAP-21	Moving Ahead for Progress in the 21st Century Act (2012)
NASA	National Aeronautics and Space Administration
NASAO	National Association of State Aviation Officials
NCFRP	National Cooperative Freight Research Program
NCHRP	National Cooperative Highway Research Program
NHTSA	National Highway Traffic Safety Administration
NTSB	National Transportation Safety Board
PHMSA	Pipeline and Hazardous Materials Safety Administration
RITA	Research and Innovative Technology Administration
SAE	Society of Automotive Engineers
SAFETEA-LU	Safe, Accountable, Flexible, Efficient Transportation Equity Act: A Legacy for Users (2005)
TCRP	Transit Cooperative Research Program
TEA-21	Transportation Equity Act for the 21st Century (1998)
TRB	Transportation Research Board
TSA	Transportation Security Administration
U.S.DOT	United States Department of Transportation